

**Regulation of lysophosphatidate-induced mechanisms of  
chemo-resistance**

by

Ganesh Venkatraman

A thesis submitted in partial fulfillment of the requirements for the degree of

Doctor of Philosophy

Department of Biochemistry  
University of Alberta

© Ganesh Venkatraman, 2015

## ABSTRACT

Systemic chemotherapy in combination with local intervention through surgery and radiotherapy are effective treatments for breast cancers. Chemotherapy is often used in patients with early signs of disease to effectively shrink the tumor and prevent metastasis before surgical excision of the tumor. However, relapse occurs in some of these patients due to the presence of remnant cancer cells that are resistant to chemotherapy. These cancer cells may acquire additional resistance mechanisms resulting in multi-drug resistance and treatment failure. Aggressive tumors show inherently poor sensitivity to chemotherapeutics. Studies primarily based on cell culture models have identified mechanisms of chemo-resistance. These mechanisms include alterations in drug accumulation, increased drug metabolism, altered DNA damage response, evasion of cell-death and decreased ceramide accumulation. In animal models of cancer, additional complexity arises from signaling cross-talk among the cancer cells, stroma, extracellular matrix and the vasculature in the tumor microenvironment that contribute to the development of multi-drug resistance. Cytokines, chemokines and growth factors secreted into the tumor microenvironment represent a hurdle to successful chemotherapy by making the tumors inherently resistant and contributing to development of additional resistance.

We examined the mechanism by which extracellular lysophosphatidate (LPA), which is produced by the secreted enzyme, autotaxin (ATX), contributes to multi-drug resistance using breast, thyroid, liver and lung cancer cells. LPA acts

through its G-protein coupled receptor, LPA<sub>1-6</sub>, to promote survival and proliferation in cancers. We discovered that LPA increased the stability and nuclear localization of the transcription factor Nuclear Factor, Erythroid 2-Like 2 or Nrf2. Nrf2, a master regulator of the antioxidant response, promotes resistance to chemotherapeutics through increased metabolism, conjugation and export of drugs from the cell. We showed that LPA, through the activation of LPA<sub>1</sub> receptors and phosphatidylinositol 3-kinase (PI3K), increased Nrf2 stabilization and the expression of multi-drug resistance transporters (MDRT) and antioxidant genes. LPA increased the efflux of substrates of the MDRT, which includes chemotherapeutics such as doxorubicin. Consequentially, LPA protected cancer cells from doxorubicin- and etoposide-induced apoptosis. We tested these results *in vivo* using a syngeneic 4T1 breast cancer model. Blocking LPA production with ONO-8430506, a competitive ATX inhibitor, decreased the expression of Nrf2 and Nrf2-regulated genes in breast tumors. Combining 4 mg/kg doxorubicin every third day with 10 mg/kg ONO-8430506 every day decreased tumor growth and metastasis to lungs and liver by >70%, whereas doxorubicin alone had no significant effect on tumor growth. Additionally, we show increased expression of Nrf2 in the primary tumors of breast cancer patients, who have a recurrence following surgery and chemotherapy. We also demonstrate a novel concept of chemotherapy-induced increases in inflammation and ATX production as a mediator of resistance to oxidative damage in the 4T1 tumors. Increased expression of Nrf2 and its targets were also observed in

tamoxifen-treated breast cancer cells and tumors. Inhibition of ATX overcomes this vicious cycle of inflammation, LPA production and resistance to oxidative damage.

Finally, we examined another aspect of LPA signaling that contributes to increased resistance to chemotherapeutics. This involves increased activation and expression of sphingosine kinase 1 (SK1), which results in formation of sphingosine 1-phosphate (S1P) in the cells. LPA-induced translocation of SK1 to membranes, which constitutes an activation step, is higher in doxorubicin-resistant cancer cells when compared to their isogenic controls. Additionally, the doxorubicin-resistant cancer cells have increased expression of the MDRT and S1P receptors. We propose that extracellular LPA coordinates S1P signaling in cancer cells. This is through activation of SK1, secretion of S1P through the MDRT and increased signaling of secreted S1P through the S1P receptors.

Overall, our studies have demonstrated a potentially important role for LPA signaling in increasing resistance to chemotherapies and development of multi-drug resistance. This is through the increased expression of Nrf2 and transcription of antioxidant and MDRT genes. Our study also provides a practical strategy for targeting LPA signaling in cancers by blocking LPA production with ATX inhibitors. There are no ATX inhibitors in the clinic. Inhibition of ATX could be a useful strategy in improving the efficacy of existing cancer therapies and to prevent the development of chemo-resistance in patients.

## PREFACE

This thesis is an original work by Ganesh Venkatraman. Animal procedures were performed in accordance with the Canadian Council of Animal Care as approved by the University of Alberta Animal Welfare Committee (Animal User Protocol 226). Human samples were obtained with approval of University of Alberta Health Research Ethics Board (“Mechanisms of Lymph Node Metastases”, ID Pro00018758, 01/15/2011).

**Author contributions** - I performed all of the original work, data collection, analysis and manuscript preparation. Matthew Benesch and Xiaoyun Tang originally established the 4T1 tumor models and helped with the animal experiments, data collection and analysis. Experiments on tamoxifen resistance were done jointly with Raie Bekele. Plasma ATX activity assays were done jointly with Zelei Yang. Jay Dewald provided significant technical help with all the animal experiments. Todd McMullen provided the patient samples and helped with the clinical data interpretation. David Brindley supervised the project.

Some sections of the thesis are partly based on previously published work:

**Venkatraman G**, Benesch MGK, Tang X, Dewald J, McMullen TPW and Brindley DN. (2015) Lysophosphatidate signaling stabilizes and increases the expression of genes involved in drug resistance and oxidative stress response: implications to cancer chemotherapy. *FASEB J* 29, 772-785.

**Venkatraman, G.**, and Brindley, D. N. (2013) Lipid Phosphate Phosphatases and Signaling by Lysophospholipid Receptors, In *Lysophospholipid Receptors*, pp 201-227, John Wiley & Sons, Inc.

Kok, B. P., **Venkatraman, G.**, Capatos, D., and Brindley, D. N. (2012) Unlike two peas in a pod: lipid phosphate phosphatases and phosphatidate phosphatases, *Chem Rev 112*, 5121-5146.

Samadi, N., Bekele, R., Capatos, D., **Venkatraman, G.**, Sariahmetoglu, M., and Brindley, D. N. (2011) Regulation of lysophosphatidate signaling by ATX and lipid phosphate phosphatases with respect to tumor progression, angiogenesis, metastasis and chemo-resistance. *Biochimie 93*, 61-70.

*"And when all the wars are over, a butterfly will still be beautiful."*

Ruskin Bond

## ACKNOWLEDGMENTS

I want to thank my supervisor, Dr. David Brindley, for everything he has done for me during my time in graduate school. He has been an excellent guide and a role model. I want to extend my gratitude and appreciation to my committee members, Dr. Luis Schang and Dr. Luc Berthiaume. They have improved the quality of my research and technical writing immensely. I would also like to thank Dr. Todd McMullen for his continued involvement in my project, career mentorship and clinical expertise. I want to acknowledge my external examiners - Dr. Vishwanathan Natarajan, University of Illinois at Chicago and Dr. David Murray, University of Alberta - for their time and commitment.

I want to thank all the members of my laboratory who made this time memorable. I want to thank Matthew Benesch, Xiaoyun Tang and Raie Bekele for their ideas and help with experiments; Meltem Sariahmetoglu, Bernard Kok and Jay Dewald who trained me in laboratory skills; Sabina Isgandarova, Nasser Samadi, Dora Capatos, Nancy Ling, Le Luong, Tete Li, Hannah Pena, Betty Chang and Zelei Yang from the Brindley laboratory, members of the McMullen laboratory and members of the Signal Transduction Research Group.

I want to acknowledge all our collaborators who have generously provided us with research tools including Dr. John Mackey, Dr. Amadeo Parissenti, Dr. Sylvain Bourgoin, Dr. Webster Santos, Dr. Guangwei Du and ONO Pharmaceuticals; I would like to thank the funding agencies for personal and travel support: Alberta Innovates - Health Solutions, Women and Children's Health Research Institute,



Faculty of Medicine and Dentistry and the Graduate Student Association. I also thank Dr. Charles Holmes, Dr. David Stuart and the Department of Biochemistry for their general guidance in all matters.

Finally, I want to thank my family and friends for their support, understanding, encouragement and love.

## TABLE OF CONTENTS

|   |           |
|---|-----------|
| <b>CHAPTER 1 – INTRODUCTION .....</b>   | <b>1</b>  |
| <b>1.1. Overview of resistance to chemotherapies in cancer .....</b>                | <b>2</b>  |
| 1.1.1. Uptake and efflux of chemotherapeutic drugs .....                            | 3         |
| 1.1.2. Drug metabolism in cancer cells .....  | 8         |
| 1.1.3. DNA damage response .....  | 10        |
| 1.1.4. Evasion of cell death .....  | 11        |
| 1.1.5. Tumor microenvironment.....  | 12        |
| 1.1.6. Cancer stem cell paradigm .....  | 14        |
| 1.1.7. Targeted therapies .....   | 15        |
| 1.1.8. Summary .....  | 16        |
| <b>1.2. Overview of ATX/LPA signaling.....</b>                                      | <b>17</b> |
| 1.2.1. Historical perspective .....   | 17        |
| 1.2.2. LPA mediated G-protein coupled receptor signaling .....                      | 18        |
| 1.2.3. ATX and circulating LPA levels .....   | 20        |
| 1.2.4. Other LPA biosynthetic pathways.....   | 21        |
| 1.2.5. Structure studies of ATX and model for generation of LPA .....               | 21        |
| 1.2.6. ATX/LPA signaling in disease – wound healing, inflammation and cancer.....   | 23        |
| 1.2.7. Degradation of extracellular LPA by lipid phosphate phosphatases .....       | 25        |
| <b>1.3. ATX/LPA signaling in tumor progression and metastasis.....</b>              | <b>27</b> |
| 1.3.1. Expression of ATX and LPA receptors in various cancers.....                  | 28        |
| 1.3.2. ATX/LPA signaling in mice models of cancer .....                             | 30        |
| 1.3.3. Role for ATX and LPA signaling in protection against cancer therapies.....   | 33        |
| 1.3.4. ATX/ LPA targeted therapies.....   | 34        |
| <b>1.4. Sphingosine kinase in development of resistance to chemotherapies .....</b> | <b>39</b> |
| 1.4.1. Bioactive sphingolipids in cellular signaling .....                          | 39        |
| 1.4.2. Sphingolipid pathway.....  | 41        |
| 1.4.3. SK1 structure, catalysis and S1P formation .....                             | 43        |

|   |           |
|---|-----------|
| 1.4.4. Agonist activation of SK1 .....  | 44        |
| 1.4.5. Phosphatidate and SK1 activation .....   | 46        |
| 1.4.6. S1P function, trafficking and inside out signaling .....                       | 48        |
| 1.4.7. Role for S1P in disease and development of S1P-modulating drugs                | 50        |
| 1.4.7.1. Inflammatory disorders .....   | 50        |
| 1.4.7.2. Cancer .....   | 52        |
| 1.4.8. S1P and ceramide rheostat .....  | 54        |
| 1.4.9. SK1 activation and resistance to therapy .....                                 | 55        |
| 1.4.10. Alternate sphingolipid pathways in drug resistance .....                      | 57        |
| 1.4.10.1. Ceramide synthesis by de novo pathway .....                                 | 58        |
| 1.4.10.2. Sphingomyelinases .....   | 58        |
| 1.4.10.3. Glycosylation of ceramides.....   | 58        |
| <b>1.5. Summary and thesis objectives.....</b>  | <b>59</b> |
| <br>  |           |
| <b>CHAPTER 2 – MATERIALS AND METHODS .....</b>  | <b>61</b> |
| <b>2.1. Reagents .....</b>  | <b>62</b> |
| <b>2.2. Cell culture .....</b>  | <b>64</b> |
| 2.2.1. Cell lines .....   | 64        |
| 2.2.2. Transient transfection of cultured cells with plasmids .....                   | 66        |
| 2.2.3. siRNA knockdown of LPA <sub>1/2/3</sub> and Nrf2 .....                         | 68        |
| 2.2.4. Preparation of charcoal-treated serum.....                                     | 70        |
| 2.2.5. Adenoviral inoculation of cells .....  | 70        |
| 2.2.6. shRNA knockdown of PLD1/2 in cancer cells .....                                | 71        |
| 2.2.7. Plasmids, lentiviral production and stable expression in cancer cells<br>..... | 72        |
| 2.2.8. Transfection of PA probes.....   | 74        |
| <b>2.3. Measurement of doxorubicin sensitivity and accumulation .....</b>             | <b>75</b> |
| 2.3.1. Cell viability assays.....   | 75        |
| 2.3.2. Caspase 3/7 activity assays.....   | 75        |
| 2.3.3. Doxorubicin fluorescence analysis .....  | 76        |
| 2.3.4. [ <sup>14</sup> C]doxorubicin and Fluo3-AM efflux .....                        | 77        |

|              |   |            |
|--------------|---|------------|
| <b>2.4.</b>  | <b>Measurement of gene expression</b> .....                                     | <b>78</b>  |
| 2.4.1.       | RNA isolation .....   | 78         |
| 2.4.2.       | Quantitative real time PCR .....  | 79         |
| 2.4.3.       | Pathway gene expression array .....   | 80         |
| 2.4.4.       | Tissue microarray data from breast cancer patients .....                        | 81         |
| <b>2.5.</b>  | <b>SDS-PAGE gel electrophoresis</b> .....                                       | <b>85</b>  |
| 2.5.1.       | Nuclear fractionation .....   | 86         |
| <b>2.6.</b>  | <b>Immunocytochemistry</b> .....  | <b>87</b>  |
| <b>2.7.</b>  | <b>Mouse model of breast cancer</b> .....                                       | <b>88</b>  |
| 2.7.1.       | Preparation and administration of drug .....                                    | 88         |
| 2.7.2.       | Measurement of spontaneous and experimental metastasis.....                     | 90         |
| 2.7.3.       | Immunohistochemistry analysis .....   | 90         |
| 2.7.4.       | Glutathione (GSH) measurements.....   | 91         |
| 2.7.5.       | Leukocyte counts.....   | 93         |
| 2.7.6.       | Enzyme-linked immunosorbent assay (ELISA) .....                                 | 93         |
| 2.7.6.1.     | Multiplex cytokine/chemokine arrays.....  | 93         |
| 2.7.6.2.     | ATX sandwich ELISA.....   | 94         |
| 2.7.7.       | ATX activity assay .....  | 95         |
| <b>2.8.</b>  | <b>Measurement of SK1 activity</b> .....  | <b>96</b>  |
| 2.8.1.       | Separation of cytosol from cell ghost by digitonin lysis .....                  | 96         |
| <b>2.9.</b>  | <b>Sphingosine labeling and S1P secretion</b> .....                             | <b>99</b>  |
| <b>2.10.</b> | <b>Measurement of PLD activity by formation of phosphatidylbutanol</b><br>..... | <b>100</b> |
| <b>2.11.</b> | <b>Statistical Analysis</b> .....   | <b>101</b> |
| <b>2.12.</b> | <b>Ethics approval</b> .....  | <b>101</b> |

**CHAPTER 3 - LYSOPHOSPHATIDATE SIGNALING REGULATES THE EXPRESSION OF MDRT AND ANTIOXIDANT GENES THROUGH INCREASED NRF2 EXPRESSION.....102**

**3.1. INTRODUCTION .....103**

**3.2. RESULTS .....104**

3.2.1. LPA protects cancer cells from doxorubicin-induced apoptosis.....104

3.2.2. Doxorubicin accumulation in cancer cells .....108

3.2.3. Expression of MDRT in breast cancers.....114

3.2.4. LPA increases the expression of MDRT through increased LPA<sub>1</sub>-dependent transcription .....116

3.2.5. Nrf2 is stabilized by LPA-LPA<sub>1</sub> receptor signaling .....122

3.2.6. Nrf2 is nuclear localized and increases antioxidant-response element (ARE) activity by PI3K signaling .....126

**3.3. DISCUSSION .....131**

**CHAPTER 4 – INHIBITION OF ATX/LPA SIGNALING DECREASES NRF2 EXPRESSION AND SENSITIZES CANCER CELLS TO DOXORUBICIN-INDUCED KILLING IN A MOUSE MODEL OF BREAST CANCER .....135**

**4.1. INTRODUCTION .....136**

**4.2. RESULTS .....139**

4.2.1. Attenuation of LPA signaling decreases Nrf2 expression in a mice model of breast cancer.....139

4.2.2. ATX inhibition combined with doxorubicin decreased tumor formation and improved treatment outcome .....141

4.2.3. Combination of doxorubicin and ATX inhibition decreased metastases in orthotopic and tail-vein 4T1 models... .....144

4.2.4. Analysis of tumors treated with combination therapy show increase caspase-3 activation, decreased proliferation and decreased GSH 145

4.2.5. Analysis of banked patient samples .....149

4.2.6. Doxorubicin increases inflammation and ATX production in the tumor-adjacent mammary fat pad.....150

4.2.7. Nrf2 and RALBP1 in tamoxifen-resistance .....156

**4.3. DISCUSSION .....163**

|   |            |
|---|------------|
| <b>CHAPTER 5 – LPA INCREASES SK1 TRANSLOCATION IN DOXORUBICIN RESISTANT CELLS THROUGH PHOSPHOLIPASE D2 ACTIVITY .....</b> | <b>170</b> |
| <b>5.1. INTRODUCTION .....</b>  | <b>171</b> |
| <b>5.2. RESULTS .....</b>   | <b>172</b> |
| 5.2.1. Characterization of isogenic, doxorubicin-resistant cancer cells ...   | 172        |
| 5.2.2. Expression of the specific S1P transporter, Spns2, in cancer cells .   | 176        |
| 5.2.3. LPA increases SK1 translocation to the membranes .....   | 177        |
| 5.2.4. Phospholipase D2 pathway mediates SK1 translocation and activity .....   | 180        |
| 5.2.5. LPA increases SK1 activity and S1P <sub>1/3</sub> mRNA expression .....  | 182        |
| <b>5.3. DISCUSSION AND FUTURE DIRECTIONS.....</b>   | <b>185</b> |
| <br><b>CHAPTER 6 – GENERAL DISCUSSION AND FUTURE DIRECTIONS.....</b>  | <b>192</b> |
| <b>6.1 General discussion and future directions .....</b>   | <b>193</b> |
| 6.1.1 Cancer-associated inflammation and ATX production drive resistance to doxorubicin therapy in tumors .....           | 201        |
| 6.1.2 Nrf2 activation and tamoxifen-resistance .....  | 205        |
| 6.1.3 Regulation of RALBP1 expression by ATX/LPA signaling .....  | 206        |
| 6.1.4 LPA activates SK1 autocrine/paracrine signaling in doxorubicin-resistant cells .....                                | 209        |
| <b>6.2 SUMMARY .....</b>  | <b>209</b> |
| <br><b>BIBLIOGRAPHY .....</b>   | <b>210</b> |
| <br><b>APPENDIX – EFFECTS OF LIPID PHOSPHATE PHOSPHATASES ON PROTEIN PRENYLATION .....</b>                                | <b>272</b> |

## LIST OF FIGURES

### CHAPTER 1

|                 |  |           |
|-----------------|--|-----------|
| <b>Fig. 1.1</b> | Topological structure of the ABC transporters : ABCB1, ABCC1 and ABCG2 .....                                   | <b>5</b>  |
| <b>Fig. 1.2</b> | Illustration of ATX mediated LPA receptor signaling.....   | <b>19</b> |
| <b>Fig. 1.3</b> | Illustration of proposed model for LPA formation and degradation in cancer cells .....                         | <b>26</b> |
| <b>Fig. 1.4</b> | Illustration of autocrine and paracrine models for inflammation-driven ATX production in tumors.....           | <b>28</b> |
| <b>Fig. 1.5</b> | Illustration of sphingolipid backbone.....   | <b>41</b> |
| <b>Fig. 1.6</b> | Sphingolipid metabolism and the role of SK1 in doxorubicin-mediated killing and survival of cancer cells ..... | <b>43</b> |
| <b>Fig. 1.7</b> | Recruitment of the cytosolic protein SK1 by PA formation to sphingosine-rich regions of the membrane .....     | <b>48</b> |
| <b>Fig. 1.8</b> | Functions of SK1-derived S1P from various cell sources in the tumor microenvironment .....                     | <b>54</b> |

### CHAPTER 2

|                 |   |           |
|-----------------|---|-----------|
| <b>Fig. 2.1</b> | Adenoviral overexpression of phospholipase D in cancer cells.....                                       | <b>71</b> |
| <b>Fig. 2.2</b> | shRNA knockdown of phospholipase D in cancer cells .....  | <b>72</b> |
| <b>Fig. 2.3</b> | Lentiviral expression and selection of SK1 and SK2 expressing cell lines .....                          | <b>74</b> |
| <b>Fig. 2.4</b> | Measurement of reduced and total glutathione from standards .....                                       | <b>92</b> |
| <b>Fig. 2.5</b> | Optimization of SK1 assay conditions .....  | <b>98</b> |
| <b>Fig. 2.6</b> | TLC separation of [ <sup>3</sup> H]S1P and [ <sup>3</sup> H]sphingosine by differential extraction..... | <b>99</b> |

### **CHAPTER 3**

|                  |  |            |
|------------------|--|------------|
| <b>Fig. 3.1</b>  | Increased cell-viability to drugs in LPA-treated MDA-MB-231 breast cancer cells .....  | <b>106</b> |
| <b>Fig. 3.2</b>  | Decreased PARP cleavage and apoptosis in breast cancer cells treated with LPA .....  | <b>107</b> |
| <b>Fig. 3.3</b>  | LPA did not affect the predominant nuclear localization of doxorubicin but increased its expulsion in breast cancer cells..... | <b>110</b> |
| <b>Fig. 3.4</b>  | LPA does not affect the uptake of [ <sup>14</sup> C]doxorubicin.....   | <b>112</b> |
| <b>Fig. 3.5</b>  | LPA increases the efflux activity of the MDRT.....   | <b>113</b> |
| <b>Fig. 3.6</b>  | Expression of MDRT in breast cancer cell lines.....  | <b>115</b> |
| <b>Fig. 3.7</b>  | LPA increases the MDRT – ABCC1 and ABCG2 levels in breast cancer cells: .....  | <b>117</b> |
| <b>Fig. 3.8</b>  | LPA-LPA <sub>1</sub> signaling increases transcription of the ABC transporters .....   | <b>118</b> |
| <b>Fig. 3.9</b>  | LPA-LPA <sub>1</sub> -G <sub>i</sub> -PI3K signaling increases ABCC1 and ABCG2 mRNA levels.....                                | <b>120</b> |
| <b>Fig. 3.10</b> | Characterization of Nrf2 protein levels in breast, liver and lung carcinoma .....  | <b>121</b> |
| <b>Fig. 3.11</b> | LPA increases Nrf2 expression and transcription of its targets in MDA-MB-231 cells .....                                       | <b>124</b> |
| <b>Fig. 3.12</b> | LPA increases Nrf2 expression and transcription of its targets in different cancer cells .....                                 | <b>125</b> |
| <b>Fig. 3.13</b> | LPA does not affect Nrf2 mRNA levels .....   | <b>126</b> |
| <b>Fig. 3.14</b> | LPA-LPA <sub>1</sub> signaling increases basal and t-BHQ-induced Nrf2 expression.....  | <b>127</b> |
| <b>Fig. 3.15</b> | LPA increases nuclear localization of EGFP-Nrf2 .....  | <b>128</b> |
| <b>Fig. 3.16</b> | LPA increases Nrf2 nuclear localization and ARE activity.....  | <b>129</b> |



## **CHAPTER 4**

|                  |   |            |
|------------------|---|------------|
| <b>Fig. 4.1</b>  | The ATX inhibitor, ONO-8430506, decreased Nrf2 expression and the transcription of antioxidant genes and MDRT in 4T1 breast tumors..... | <b>140</b> |
| <b>Fig. 4.2</b>  | Stable or doxycycline induced LPP1 overexpression in cancers from a xenograft tumor model decreased Nrf2 expression.....                | <b>141</b> |
| <b>Fig. 4.3</b>  | Combination of ATX inhibition with doxorubicin treatment in decreasing breast tumor growth in mice.....                                 | <b>143</b> |
| <b>Fig. 4.4</b>  | Blood leukocyte count.....  | <b>144</b> |
| <b>Fig. 4.5</b>  | ATX inhibition combined with doxorubicin decreased spontaneous and experimental metastasis in mice.....                                 | <b>146</b> |
| <b>Fig. 4.6</b>  | Combination of ATX inhibition with doxorubicin decreases the concentration of GSH in the breast tumors.....                             | <b>147</b> |
| <b>Fig. 4.7</b>  | Combination of ATX inhibition with doxorubicin decreases cell division and increases apoptosis in the breast tumors.....                | <b>148</b> |
| <b>Fig. 4.8</b>  | Expression Nrf2 and NQO1 is increased in tumors from patients with recurrent breast cancer.....   | <b>149</b> |
| <b>Fig. 4.9</b>  | Doxorubicin increases inflammation in the tumor-adjacent but not contralateral mammary fat pad.....                                     | <b>152</b> |
| <b>Fig. 4.10</b> | Doxorubicin increases ATX production in the tumor-adjacent but not contralateral mammary fat pad.....                                   | <b>153</b> |
| <b>Fig. 4.11</b> | Doxorubicin increase cytokine/chemokine mRNA in LPA-treated MCF-7 breast cancer cells.....  | <b>154</b> |
| <b>Fig. 4.12</b> | MCF-7 cells selected for doxorubicin-resistance express higher levels of cytokine/chemokine mRNA.....                                   | <b>155</b> |
| <b>Fig. 4.13</b> | Doxorubicin and ONO-8430506 had no effect on the cytokine/chemokine levels in 4T1 tumors.....   | <b>156</b> |
| <b>Fig. 4.14</b> | 4-HT increases Nrf2 expression, nuclear localization and ARE activity in breast cancer cells.....                                       | <b>159</b> |

|                  |  |            |
|------------------|--|------------|
| <b>Fig. 4.15</b> | Nrf2 knockdown in 4T1 cells decreases the expression of antioxidant genes and MDRT but not RALBP1 .....          | <b>160</b> |
| <b>Fig. 4.16</b> | Nrf2 expression is higher in tamoxifen-treated 4T1 tumors .....  | <b>161</b> |
| <b>Fig. 4.17</b> | RALBP1 is upregulated in breast cancer patients and is decreased by in 4T1 tumors treated with ONO-8430506 ..... | <b>162</b> |
| <b>Fig. 4.18</b> | Proposed mechanism for the role of ATX/LPA signaling in resistance to chemotherapy through Nrf2 activation ..... | <b>166</b> |

## **CHAPTER 5**

|                 |  |            |
|-----------------|--|------------|
| <b>Fig. 5.1</b> | Increased protein levels of ABCC1 and ABCG2 in doxorubicin-resistant MCF-7 cells.....  | <b>173</b> |
| <b>Fig. 5.2</b> | The presence of LPA/S1P in the medium was enough to maintain the resistance phenotype of doxorubicin-resistant MCF-7 cells ..... | <b>174</b> |
| <b>Fig. 5.3</b> | Expression of LPA and S1P receptors in doxorubicin-resistant and control MCF-7 cells.....  | <b>175</b> |
| <b>Fig. 5.4</b> | Expression of the S1P transporter, Spns2 in various cancer and normal cell lines .....   | <b>176</b> |
| <b>Fig. 5.5</b> | LPA increases the membrane translocation of SK1 in doxorubicin resistant MCF-7 cells.....  | <b>179</b> |
| <b>Fig. 5.6</b> | LPA increases PLD2-dependent SK1 activity and intracellular S1P formation .....  | <b>181</b> |
| <b>Fig. 5.7</b> | Visualization of LPA-induced PLD activation in the cell by PA biosensors .....   | <b>183</b> |
| <b>Fig. 5.8</b> | LPA increases the transcription of SK1 and S1P <sub>1,3</sub> .....  | <b>184</b> |
| <b>Fig. 5.9</b> | Proposed model for modulation of SK1 signaling in cancer cells by LPA .....  | <b>189</b> |

## LIST OF TABLES

|                |   |           |
|----------------|---|-----------|
| <b>TABLE 1</b> | List of chemotherapeutic MDRT substrates .....  | <b>6</b>  |
| <b>TABLE 2</b> | LPA agonists and antagonists used in the study .....  | <b>38</b> |
| <b>TABLE 3</b> | Pharmacological activators/inhibitors used in the study.....  | <b>63</b> |
| <b>TABLE 4</b> | List of cell lines used in the study.....   | <b>65</b> |
| <b>TABLE 5</b> | Comparison of Antioxidant Response Element (ARE) for Nrf2-<br>regulated genes used in this study..... | <b>66</b> |
| <b>TABLE 6</b> | Nrf2 DsiRNA sequences.....  | <b>69</b> |
| <b>TABLE 7</b> | Primer sequences used in the study .....  | <b>82</b> |
| <b>TABLE 8</b> | Antibodies used in the study .....  | <b>84</b> |

## LIST OF ABBREVIATIONS

ABC – ATP-binding cassette  
ABCB1 – ATP-binding cassette family B member 1; also MDR1  
ABCC1 – ATP-binding cassette family C member 1; Also MRP1  
ABCG2 – ATP-binding cassette family G member 2; Also BCRP  
ARE – Antioxidant response element  
ATP – Adenosine triphosphate  
ATP7 A/B –ATPase, Cu<sup>2+</sup> transporting  
ATX/ENPP2 – Autotaxin  
Bax – Bcl2-associated X protein  
Bcl2 – B cell lymphoma 2  
BSA – Bovine serum albumin  
C1P – Ceramide 1-phosphate  
CERT – Ceramide transfer protein  
DAG – Diacylglycerol  
DMS – Dimethylsphingosine  
DsiRNA – Dicer-substrate siRNA  
EDG – Endothelial differentiation gene  
EGF – Epidermal growth factor  
EF hand – Helix loop helix structural motif  
ER – Endoplasmic reticulum  
ERK1/2 – Extracellular regulated kinase; Also MAPK1/2  
EMT – Epithelial mesenchymal transition  
ENPP – Ectonucleotide pyrophosphatase/phosphodiesterase  
FBS- Fetal bovine serum  
FTY-720 – Fingolimoid  
G<sub>i</sub>, G<sub>q</sub>, G<sub>12/13</sub>, G<sub>s</sub> – Guanine-nucleotide binding proteins  
GPAT – Glycerol-3-phosphate acyltransferase

GPCR – G-protein coupled receptor  
GPX – Glutathione peroxidase  
GRB2 – Growth factor receptor-bound protein 2  
GSH- Glutathione  
GST – Glutathione transferase  
GSK3 $\beta$  – Glycogen synthase kinase 3 beta  
4-HT – 4-hydroxytamoxifen  
4-HNE – 4-hydroxynonenal  
HDL – High-density lipoprotein  
HIF1 – Hypoxia inducible factor 1  
HO-1 – Hemeoxygenase 1  
KEAP1 – Kelch-like ECH-associated protein 1  
LCAT – Lecithin-cholesterol acyltransferase  
LDL – Low-density lipoprotein  
LPA – Lysophosphatidic acid/ Lysophosphatidate  
LPA<sub>1-6</sub> – LPA receptors; gene – LPAR1-6  
LPAATs – Lysophosphatidate acyltransferase  
LPC – Lysophosphatidylcholine  
LPP1/2/3 – Lipid phosphate phosphatases; PPAP2  
MAPK1/2 – Mitogen activated protein kinase; ERK1/2  
MCS – Multiple cloning site  
MDR/MDRT – Multi-drug resistance/Multi-drug resistant transporters  
MEFs – Mouse embryonic fibroblasts  
MMPs – Matrix metalloproteinases  
MMTV – Mouse mammary tumor virus  
MMTV-LTR – MMTV long-terminal repeat  
ND – Not detected  
neu/ERBB2/HER2 – V-Erb-B2 avian erythroblastic leukemia viral oncogene;  
Human epidermal growth factor receptor 2

NF $\kappa$ B – Nuclear factor kappa-light-chain-enhancer of activated B cell  
NRF2 – Nuclear Factor, Erythroid 2-Like 2; NFE2L2  
NQO1 –NADPH quinone oxidoreductase  
PA – Phosphatidate  
PARP – Poly-ADP ribose polymerase  
PDGF – Platelet-derived growth factor  
p53 – Tumor protein p53  
PI3K – Phosphoinositide-3-kinase  
PLA2 – Phospholipase A2; also iPLA2, cPLA2, sPLA2  
PLC – Phospholipase C  
PLD1/2 - Phospholipase D  
PKC- Protein kinase C  
PP1 – Protein phosphatase 1  
PS – Phosphatidylserine  
PyMT – Polyoma middle T antigen  
RALBP1 – RalA binding protein 1  
SHP2 – Protein tyrosine phosphatases, non-receptor type 11 ; PTPN11  
siRNA – Small interfering RNA  
SK1/2 – Sphingosine kinase 1/2; gene - SPHK1/2  
SOS1/2 – Son of sevenless homolog 1/2  
S1P – Sphingosine-1-Phosphate  
STAT3 –Signal transducer and activator of transcription 3  
t-BHQ – Tert-butylhydroquinone  
TGF $\beta$  –Transforming growth factor beta  
TNF- $\alpha$  – Tumor necrosis factor alpha  
VEGF – Vascular endothelial growth factor  
WNT – Wingless-type MMTV integration site family

## **CHAPTER 1 – INTRODUCTION**

## **1.1 Overview of resistance to chemotherapies in cancer**

A major challenge in cancer treatment is to prevent metastasis and the development of resistance to existing therapies. Chemotherapy is often used in combination with other treatment options including surgery, radiotherapy, hormonal therapy and targeted therapies. Systemic chemotherapy is the primary treatment in patients diagnosed with late stages of locally invasive and metastatic cancers. However, resistance to chemotherapeutics occurs frequently. The progressive development of resistance to multiple chemotherapeutics is termed multi-drug resistance (MDR) and results in treatment failure, relapse and death (reviewed in (1-3)). MDR has been studied in the laboratory through cell culture and animal models (4). Investigations using cell culture and animal models have offered mechanistic insights into the diverse signaling pathways that are altered, leading to resistance to chemotherapeutics.

In this work, I have investigated the role of extracellular LPA in promoting chemo-resistance in cell culture and animal models. The common mechanisms of chemo-resistance in cancer cells include 1. Decreased drug accumulation; 2. Increased drug metabolism; 3. Decreased DNA damage response; 4. Evasion of cell-death; and 5. Decreased ceramide accumulation (2, 3, 5). These aspects will be described in more detail in the following section. The role of LPA in promoting resistance to therapies is discussed in Section 1.3. The role of sphingolipids, including ceramides, in promoting resistance to chemotherapies (6, 7) is discussed in Section 1.4.



### **1.1.1 Uptake and efflux of chemotherapeutic drugs**

The accumulation of drugs in cancer cells at the level of plasma membrane is controlled by uptake and efflux mechanisms. Once the drug has crossed the plasma membrane, additional mechanisms exist to decrease cell drug concentrations in the cell through increased compartmentalization, metabolism and finally efflux of the drug and its metabolites. Increased efflux activity through ATP-binding cassette (ABC) drug transporters is the most frequently cited mechanism of drug resistance (8). ABC transporters are membrane proteins that regulate the efflux of drugs against their concentration gradient in an ATP-dependent manner. The ABC superfamily includes 48 functional ABC transporters encoded by the human genome and these are further divided into 7 sub-families - A through G. ABCB1 (9), ABCC1 (10) and ABCG2 (11) are best characterized for their role in multidrug resistance.

The clinical importance of the MDRT are still under investigation (4). Increased ABCB1 expression has been clinically correlated to poor prognosis and chemotherapy response in adult leukemia (12). ABCC1 is expressed in many solid tumors such as breast, ovarian, lung and prostate cancers as well as in hematological malignancies. However, the clinical association between ABCC1 expression and treatment outcomes are not clear (13). High ABCG2 expression has been reported in drug-resistant cells that do not express ABCB1 or ABCC1. ABCG2 expression has been linked to poor chemotherapy response in many solid tumors and leukemia (13). A comprehensive gene signature using overlapping MDRT genes has been suggested

as an alternative approach for predicting survival and chemotherapy responses in clinics (14).

ABCB1 was the first identified MDRT. It consists of two transmembrane domains (TMD) and 2 nucleotide-binding domains (NBD), which is typical for the ABC superfamily (Figure 1.1). ABCC1 contains an additional transmembrane domain (TMD<sub>0</sub>) at the N-terminus. ABCG2 is a half-transporter and is thought to homodimerize to function as a full transporter (2, 8). The mechanism of drug transport in human MDRT is still under investigation. However, it is thought to be a two-step cycle of ATP hydrolysis coupled to substrate transport across the membrane based on homology models from bacterial transporters (13).

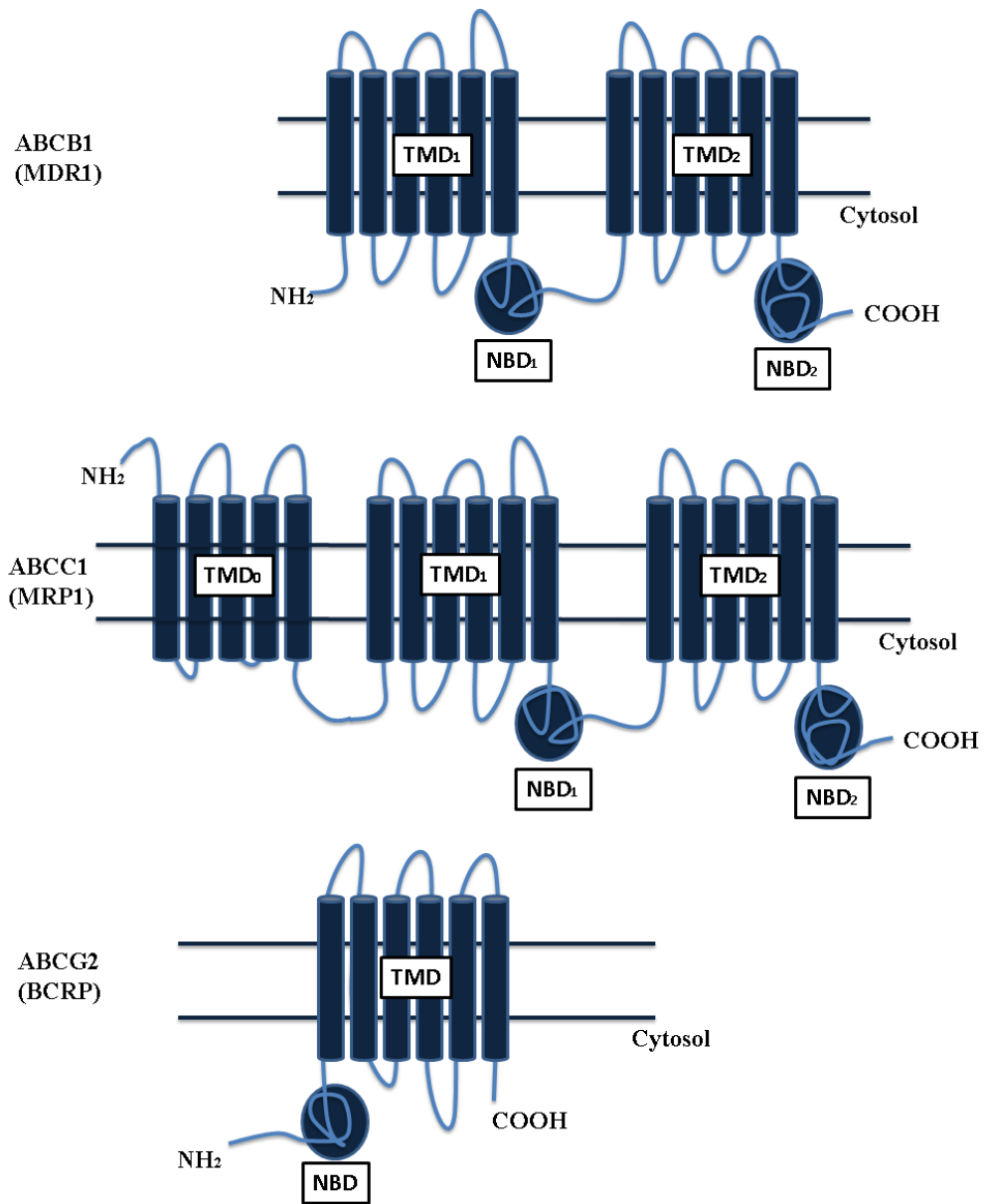


**FIGURE 1.1- Topological structure of the ABC transporters: ABCB1, ABCC1 and ABCG2** – ABCB1, ABCC4, ABCC5 have two TMD domains, which is typical for the ABC-family. ABCC1 has an extra TMD (TMD<sub>0</sub>), which is also seen in ABCC -2, -3, -6 and -7. ABCG2 is a half-transporter. NBD: Nucleotide binding domain; TMD: Transmembrane domain.

**TABLE 1: List of chemotherapeutic MDRT substrates (13).**

| <b>ABCB1</b>  | <b>ABCC1</b>   | <b>ABCG2</b>   |
|---|--|--|
| <b>Vinca alkaloids</b><br>(Vincristine, Vinblastine)<br><b>Anthracyclines</b><br>(Doxorubicin, Daunorubicin)<br><b>Epipodophyllotoxins</b><br>(Etoposide, Teniposide)<br><b>Camptothecins</b><br>(Topotecan, Irinotecan)<br><b>Taxanes</b><br><b>Anthracenes</b><br>(Bisantrene and Mitoxantrone) | <b>Vinca alkaloids</b><br>(Vincristine, Vinblastine)<br><b>Anthracyclines</b><br>(Doxorubicin, Daunorubicin)<br><b>Epipodophyllotoxins</b><br>(Etoposide, Teniposide)<br><b>Camptothecins</b><br>(Topotecan, Irinotecan)<br><b>Methotrexate</b><br><br><b>Drug Conjugates</b><br>(Doxorubicin-SG, Cyclophosphamide-SG, Melphalan-SG, Etoposide-glucuronide, SN-38-glucuronide) | <b>Vinca alkaloids</b><br>(Vincristine, Vinblastine)<br><b>Anthracyclines</b><br>(Doxorubicin, Daunorubicin)<br><b>Epipodophyllotoxins</b><br>(Etoposide, Teniposide)<br><b>Camptothecins</b><br>(Topotecan, Irinotecan)<br><b>Methotrexate</b><br><b>Anthracenes</b><br>(Bisantrene and Mitoxantrone) |

MDRT are highly expressed in pharmacologically relevant regions such as in blood-brain barrier, placenta, liver, gut and kidney. They play a physiological role in tissue defense and protection from xenobiotic-induced toxicity (15). Chemotherapeutics that are substrates for ABCB1, ABCC1 and ABCG2 are listed in the Table 1. In addition to chemotherapeutics, several toxins, carcinogens, pesticides, metal/metalloids and lipid peroxidation products are amongst their substrates (8, 15, 16). The ABCC- (MRP) family can also transport organic anions and by-products that are conjugated with glutathione, sulfate or glucuronides (2, 8).

Other members of the ABCC family, such as ABCC2 confer resistance to drugs such as taxanes (17) or platins (18). As many as 31 members of the 48 member ABC transporter superfamily decrease the sensitivity of cancer cells to chemotherapeutics (19). Non-ABC transporters have also been implicated in drug resistance (20, 21). RALBP1 (22), a GTPase activating protein, increases the efflux of doxorubicin and glutathione conjugates in an ATP-dependent manner. Significantly, RALBP1 accounted for the export of 80% of total conjugated 4-hydroxynonenal (4-HNE), a major lipid peroxidation metabolite formed as a result of increased oxidative stress. 4-HNE glutathione conjugates are also effluxed by ABCC1 (23-25). Several clinically relevant drugs such as antibiotics, tyrosine kinase inhibitors and statins are substrates for the MDRT. Hence, new drug candidates are often pre-screened for their interaction with ABC-transporters (13).

The mechanism of uptake for many chemotherapeutics by cancer cells is poorly understood (16). The solute carrier superfamily (SLC) of transporters (~360 members) includes ion-coupled transporters, exchangers and passive transporters. They are localized to the plasma membrane and also to intracellular organelles such as the mitochondria (26). They also facilitate passive diffusion, co-transport or ion-exchange across the concentration gradient. The SLC families that have been previously linked with uptake of chemotherapy drugs include organic cation transporters (SLC22A1-3), organic cation/carnitine transporter (SLC22A4-5), organic anion transporters (SLC22A6-8), organic anion-transporting polypeptides (SLCOs) and copper transporters (CTR). For example, the solute carrier SLCO1B3

was shown to take up paclitaxel (27). Overexpression of another solute carrier, SLC22A4, confers increased sensitivity to doxorubicin (28). The folate transporters, SLC19A1 and SLC46A1, have been implicated in resistance to methotrexate (29). In addition to their role in chemotherapeutic drug uptake, certain SLC family members may influence the survival of tumors by increased uptake of nutrients (29).

### **1.1.2 Drug metabolism in cancer cells**

Drugs that have crossed the plasma membrane encounter cell defense mechanisms, which decrease their effectiveness. Chemotherapeutic drugs such as doxorubicin and cisplatin are compartmentalized to lysosomes, Golgi and melanosomes leading to decreased DNA damage, increased efflux and acquisition of chemoresistance (21, 30-33). Cancer cells isolated from doxorubicin-resistant tumors also show nuclear exclusion of doxorubicin and increased expression of ABCB1 (34).

Cells respond to xenobiotics, including drugs, by making them less toxic, more water-soluble and more easily excreted. The coordinated regulation of the enzymes involved in drug metabolism and export can be broadly divided into 3 phases (35). Phase I reactions are mainly oxidation, reduction and hydrolysis reactions. The hepatic cytochrome P450 complex is the primary Phase I oxidation system against xenobiotics and is localized to the endoplasmic reticulum. The overall result of Phase I is conversion of lipophilic drugs into more polar metabolites. The Phase II biotransformation reactions involve conjugation reactions such as glucoronidation,

sulfonation and acetylation (36-38). Phase II reactions result in detoxification of xenobiotics through formation of conjugated-metabolites. The resulting metabolites are more readily excreted by the cell in the next phase. Phase III detoxification involves efflux of the conjugated metabolites outside the cell by the ABC transporters. Many of these Phase I, II and III gene products are also expressed outside the liver where they play a similar role in cell detoxification and antioxidant defense.

It is now well documented that expression of many of these Phase I, II, III genes are coordinately regulated by transcription factors (35) such as Nrf2 (Nuclear Factor, Erythroid 2-Like 2). This battery of coordinately-regulated enzymes plays an important role in cellular defense against xenobiotics. For example,  $\gamma$ -glutamyl-cysteine synthetase ( $\gamma$ -GCS) and ABCC1 were initially discovered to be coordinately induced by toxic agents such as arsenite (39), by cisplatin through generation of ROS (40) and by the pro-oxidant *tert*-butylhydroquinone (t-BHQ) (41). Nrf2 is activated as an adaptive response to oxidative stress induced by xenobiotics and it is the master regulator of the antioxidant response (42). Induction of drug metabolizing enzymes by Nrf2 requires a *cis*-acting element, the antioxidant response element (ARE) (Table 5), leading to increased detoxification and elimination of exogenous and some endogenous chemicals. Hence, it is not surprising that several of these enzymes are overexpressed in cancers and linked to efficient antioxidant system and increased drug resistance (35, 43). For example, the commonly cited Nrf2-target and redox enzyme NADPH quinone oxidoreductase 1 (NQO1) is involved in the

conversion of doxorubicin to its semiquinone and 7-deoxyglycone metabolites (44). Increased NQO1 expression has been linked to resistance to doxorubicin and other chemotherapeutics and overall poor prognosis in breast and lung cancer patients (45, 46).

### **1.1.3 DNA damage response**

Cancer cells are constantly dealing with DNA damage, which occurs from increased metabolism, replication stress, reactive oxygen species and inflammation (47). A variety of chemotherapeutic agents target DNA, at the level of synthesis or they trigger single- or double-strand breaks. For example, doxorubicin-treatment induces double strand breaks and ROS generation resulting in activation of the DNA damage response pathway (48). Hence, the efficient activation of DNA repair mechanisms is a necessary step in survival of cancer cells and resistance to chemotherapeutics (49). The repair pathways are regulated by genes that are frequently mutated in cancers such as p53 and BRCA1/2 (2). The cell-dependent DNA damage response involves a complex mechanism that can be divided into the following steps: 1. DNA lesions are detected, 2. Cell cycle checkpoint kinases and repair signaling pathways are activated and 3. DNA is repaired successfully. When DNA repair is not successful, the regulators of DNA damage response alternatively activate programmed cell death pathways (50). The DNA damage response pathway can promote resistance to radiation (51), platinum drugs (52), anti-metabolites (53), alkylating agents (54) and topoisomerase poisons (55).



#### **1.1.4 Evasion of cell death**

Resisting cell death is one of the hallmarks of cancer cell (56). Overcoming this resistance to cell death remains the overall objective of a cancer therapy. Chemotherapeutics such as doxorubicin induce more than one form of cell death. Cell death can occur in the form of apoptosis, necrosis, mitotic catastrophe, senescence and autophagy (57). Both apoptotic and non-apoptotic mechanisms can contribute to the drug-resistant phenotype seen in cancer cells (57, 58). The mitochondrial Bcl2 family members (~30) have been mainly implicated in chemoresistance associated with evasion of apoptosis (59). In cancers, frequent mutations are found in the Bcl2 family members resulting in suppression of pro-apoptotic proteins like Bax and overexpression of anti-apoptotic proteins like Bcl2. Such mutations in apoptotic pathway can lead to escape from apoptosis and drug resistance. Yet clinical validation on the predictive value of the expression of the Bcl2 family members and other apoptotic pathways on chemotherapy response has not been clear (60-62). A causal link between ABC-transporter efflux activity and resistance to caspase-dependent apoptosis has been demonstrated (63-65). These studies suggest that regulation of apoptosis can also contribute towards the development of multi-drug resistance.

Alterations in the cell-cycle represent another factor that contributes to multidrug resistance. Activation of apoptotic pathways by chemotherapeutics have been reported to be both cell-cycle dependent and independent. An example of a

cell-cycle-specific chemotherapeutics would be the taxanes, which enhance microtubule stabilization to induce a G2/M arrest and G1-S arrest to a lesser extent (66). Other mechanisms such as Bcl2 hyperphosphorylation have also been suggested for taxane-induced killing (66). Similar to taxanes, cisplatin is maximally sensitive at the G1-phase even though it can induce killing in other phases of cell cycle (66). Signal transduction pathways are frequently altered in cancers to favor growth and suppress programmed cell death. Activation of receptor tyrosine kinases contribute to multidrug resistance through negative regulation of cell death pathways and increasing growth and proliferation (67). For example, acquired resistance to PI3K inhibition correlated with increased expression of the insulin growth factor receptor. Targeting the insulin growth factor receptor pathway led to sensitization of the resistant cells to the PI3K inhibitor (68). Activation of other signal transduction pathways such as WNT- and integrin-signaling pathways can also increase cancer cell survival and proliferation. Thus activation of alternate survival pathways can additionally contribute to MDR.

#### **1.1.5 Tumor microenvironment**

The tumor microenvironment presents additional complexity to the mechanisms of resistance already discussed (56). Solid tumors are heterogeneous structures made of cancer cells, stromal cells, extracellular matrix and vasculature (69). When compared to normal tissue, the tumor stroma is made up of increased numbers of fibroblasts, which play an important role in tumor progression,

metastasis and sensitivity to chemotherapy (69, 70). In another example, the concerted action of tumor-associated macrophages and cancer cells was shown to facilitate proliferation and metastasis in an experimental breast cancer model (71). How this complex environment influences the drug sensitivity of the tumor through secretion of several factors is an active area of investigation (72). The tumor microenvironment contributes to increased secretion of cytokines, chemokines, growth factors and adhesion molecules. Immune cells, cancer-associated fibroblasts, adipocytes and cancer cells themselves are sources of these secreted factors. These secreted factors represent a hurdle to successful chemotherapy by making the cancers inherently resistant and contributing to development of acquired resistance mechanisms (56, 73). For example, integrins can protect lung cancers from DNA damage-induced apoptosis (74). Several groups have reported similar effects of integrins on increasing resistance to chemotherapies (72). This has led to testing of integrin inhibitors to overcome chemo- and radio-resistance (75). The association between tumor microenvironment and drug resistance has been demonstrated in metastatic breast cancers that are inherently resistant to therapy (76, 77). Here the disseminated cancer cells must establish a stromal relationship by secreting growth factors and extracellular matrix fragments in the invaded tissue. For example, hematopoietic progenitor cells are recruited early by the cancer cells to the site of metastasis resulting in the formation of a so called “pre-metastatic niche” (78). Thus cytokines, chemokines, growth and matrix factors derived from micro-environment

play a major role in determining sensitivity to chemotherapy both at the primary tumor and metastatic sites.

#### **1.1.6 Cancer stem cell paradigm**

Another active area of investigation is the cancer stem cell paradigm and its role in drug resistance (56). The cancer stem cell is a “*small subset of cancer cells within a cancer that constitute a reservoir of self-sustaining cells with the exclusive ability to self-renew and to cause the heterogeneous lineages of cancer cells that comprise the tumor*” (79). Cancer stem cells are identified by markers associated with the stem cell phenotype since no unique marker has yet been identified for them. High expression of the ABC transporters has been reported both in stem cells and cancer stem cells (80). For example, ABCG2 has been used to identify both stem cell (81) and cancer stem cell populations (82-84) in a flow cytometry sorting assay.

The implication of the cancer stem cell phenotype to drug resistance is that success to chemotherapy depends mainly on the cancer stem cell sensitivity (85). Several recent studies support the hypothesis, also called ‘dandelion hypothesis’, that a tumor subpopulation is intrinsically less sensitive to chemotherapy and gives rise to drug-resistant tumors. Breast cancer patients treated with neo-adjuvant chemotherapy such as docetaxel and doxorubicin display an enhanced cancer stem cell signature in the residual tumors (86, 87). The survival and maintenance of cancer stem cells in a tumor are dependent on the microenvironment, which is also

called a “niche”. Here again, the stromal fibroblasts are thought to play a major role in maintaining the cancer stem cells and protecting them from chemotherapy (88).

### **1.1.7 Targeted therapies**

To improve efficacy and prevent toxicity associated with cytotoxic chemotherapeutics discussed above, a new line of cancer-targeted therapies (or targeted therapies) were developed. Tamoxifen is widely regarded as the first targeted therapy in breast cancer. It is prescribed as an adjuvant therapy in estrogen-receptor alpha (ER- $\alpha$ ) positive patients, who represent more than half of total breast cancer patients (89-92). Active tamoxifen metabolites processed by the hepatic cytochrome P450 complex, such as 4-hydroxytamoxifen and 4-hydroxy-N-desmethyltamoxifen, show strong affinity to the estrogen receptors and prevent estrogen-receptor dependent growth signaling in breast cancer (93, 94). However, resistance frequently develops to tamoxifen and also other anti-hormonal therapies (90, 95). Tamoxifen and its metabolites can build up to  $\mu\text{M}$  concentrations in breast cancer tissue (96, 97). Higher dosage tamoxifen is also used as adjuvant therapy in glioblastoma and melanoma based on its inhibitory effects on protein kinase C (PKC) activity. At higher concentrations, tamoxifen can induce oxidative stress independently of ER status (98, 99). Increased antioxidant response has been linked to tamoxifen resistance in MCF-7 xenografts (100). ABCB1 efflux activity was linked to decreased accumulation of tamoxifen metabolites in the brain but not in the circulation (101, 102). However, a role of ABCB1 in tamoxifen resistance is not

clear since the transporter is not usually expressed in breast cancers. Tamoxifen-resistant MCF-7 cells also show higher ABCG2-expression and a cancer stem cell-like phenotype (103). Phase II glucurodination and sulfation reactions decrease the activity of tamoxifen metabolites (104) and is associated with poor tamoxifen-response in breast cancer patients (105). Similarly, several drug metabolizing enzymes have been linked to poor tamoxifen response in patients (104). The ABCC-family of transporters primarily mediate the transport of metabolites and conjugated drug-products. ABCC2 activity was linked to poor tamoxifen-response in breast cancer patients (104). Cells which are clonally selected in the presence of tamoxifen show increased expression of Nrf2, antioxidant genes and drug transporters (106) including ABCC2 (107). However, a direct link from tamoxifen and its metabolites to increased expression of Nrf2 and its transcriptional targets has not been established. The small molecule tyrosine kinase inhibitor, imatinib, is another widely used targeted therapy in leukemia. Imatinib is a substrate for the ABC transporters ABCB1 and ABCG2 (108, 109). Other small molecule tyrosine kinase inhibitors used in cancer therapy have also been shown to be substrates for the ABC transporters (8). Potential inhibitors are now routinely screened for their efflux activity by ABC-transporters at the drug-development stage (2).

### **1.1.8 Summary**

Multiple factors can promote resistance to chemotherapies. Growth factors, cytokines, chemokines and matrix factors secreted in the tumor microenvironment

coordinate these mechanisms and drive tumor progression, metastasis and resistance to therapy (56, 72). Genetic risk factors, such as gene polymorphisms and mutations, contribute towards resistance to therapies in certain patients (110). Pharmacological and pharmacokinetic factors additionally influence the sensitivity to chemotherapeutics in cancer patients.

## **1.2 Overview of ATX/LPA signaling**

Lysophosphatidate (LPA) is a bioactive lipid produced from lysophosphatidylcholine (LPC) by the secreted protein autotaxin (ATX/ENPP2). Much of what we know today about ATX/LPA signaling comes from the last 30 years of work. Here, I will discuss some of the literature on ATX/LPA signaling with relevance to their biological actions in cancer progression, metastasis and drug resistance.

### **1.2.1 Historical perspective**

LPA was initially discovered as an intermediate in the phospholipid metabolism pathway involved in the synthesis of glycerolipids (111). Tokumura and colleagues first described the signaling effects of plasma LPA in transient hypertension in rats and other species (112, 113). The lysophospholipase D activity leading to the formation of plasma LPA from LPC was not discovered until 1986 (114). Purification of this lysophospholipase D activity in 2002 identified that it was in fact the secreted enzyme, ATX, which produces LPA from LPC (115, 116). ATX

had been identified in the 1980s at the National Cancer Institute, NIH from the culture medium of malignant melanoma and named “autocrine motility factor”. It took almost a decade for the motility factor to be identified as ATX (117) and another decade to be linked to its lysophospholipase D activity (115, 116).

### **1.2.2 LPA mediated G protein-coupled receptor signaling**

Most biological actions of LPA are mediated by its binding to G-protein coupled receptors (111). However, this was not known until the identification of an orphan GPCR, endothelial differentiation gene 2 (EDG2) as the LPA receptor (LPA<sub>1</sub>) from the brain (118). Subsequently, several orphan GPCRs were also found to have high affinity for LPA with at least 6 identified as LPA receptors (LPA<sub>1-6</sub>) (111). The LPA<sub>1/2/3</sub> (EDG2/5/7) receptors are endothelial differentiation gene family members, which also includes S1P receptors (119). These receptors typically couple to the G-proteins G<sub>i</sub>, G<sub>q</sub> and G<sub>12/13</sub>. LPA<sub>4,6</sub> belongs to the purinergic family of GPCRs (119) and couple to G<sub>q</sub>, G<sub>12/13</sub> and G<sub>s</sub>. A variety of signaling effects have been attributed to LPA based on tissue receptor expression levels, coupling to different G-proteins and subsequent activation of signaling cascades. These include activation of MAPK (120), PI3K (121), PLC (122), Rho GTPase (123) and activation or inhibition of adenylyl cyclase (122) depending on their coupling to G<sub>s</sub> and G<sub>i</sub> respectively (Fig. 1.2). The biological effects of LPA in cancer, including wound healing, inflammatory response and tissue remodeling, promote cell growth, proliferation, chemokine secretion, differentiation, motility and survival (124-126).



LPA also transactivates other signaling pathways, such as through the EGF receptor (127) or PDGF receptor (128) to promote migration and invasion. The actions of ATX/LPA signaling on the various LPA receptors are summarized in Figure 1.2. There is redundancy in function observed among the various LPA receptors. Gene knockouts for each receptor have been generated in mice and investigated thoroughly (111). This has led to identification of several physiological and pathological roles for individual LPA receptors including LPA<sub>1</sub> in fibrosis (129) and neuropathic pain (130), LPA<sub>3</sub> in embryo implantation and spacing (131) and LPA<sub>6</sub> in maintenance of hair growth (132).

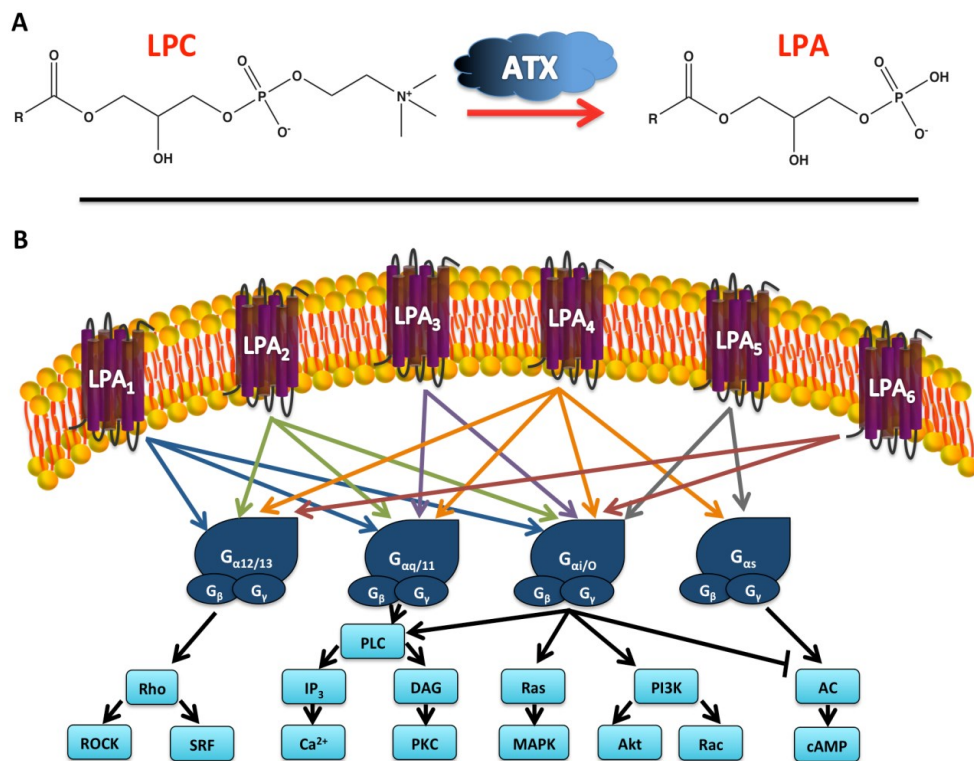


**Figure 1.2: Illustration of ATX mediated LPA receptor signaling** - Extracellular LPA formed by ATX (A) activates at least 6 different LPA receptors (LPA<sub>1-6</sub>) to activate G-protein coupled signaling pathways (B). Reproduced with permission from Benesch *et al.*,(133)

### 1.2.3 ATX and circulating LPA levels

ATX plays a major role in the regulation of circulating LPA levels from the abundant LPC. In addition to LPC other minor lysolipids such as lysophosphatidylserine and lysophosphatidylethanolamine have been proposed to be substrates for ATX. The concentration of saturated, mono- and poly-unsaturated LPC present in human blood is  $>200 \mu\text{M}$  (134). Unsaturated LPC is secreted directly by the liver and activated platelets (135). Additionally, lecithin-cholesterol acyltransferase (LCAT) contributes to formation of mainly saturated LPC from phosphatidylcholine (PC) in high-density lipoproteins (136).

The combined concentration of all the molecular species of LPA ( $\sim 0.1 \mu\text{M}$ ) in circulation is three orders of magnitude lower than LPC levels (137). A rapid turnover of circulating LPA ( $t_{1/2} < 180 \text{ s}$ ) has been reported by several studies (138-141). ATX inhibitors have been shown to decrease LPA levels in circulation, particularly the polyunsaturated LPA species (138, 140). Blocking LPA production during embryonic development by generation of ATX<sup>-/-</sup> knockout resulted in death due to defective vasculature and neural crest formation (142, 143). Similarly, heterozygous ATX<sup>+/-</sup> mice show 50% decrease in normal plasma LPA levels (143). Mice with liver-specific transgenic expression of ATX show 1.5-2-fold increase in the circulating LPA levels (144). Adipose-specific disruption of ATX decreased circulating LPA levels by 38%, suggesting that adipocytes are a major source of ATX activity (145). Plasma ATX activity and LPA levels are also increased in certain cancers such as follicular lymphoma and ovarian cancers (146).

#### 1.2.4 Other LPA biosynthetic pathways

LPA can be generated by other pathways besides the ATX pathway. This is mainly through hydrolysis of PA to generate LPA. Secretory phospholipase A<sub>2</sub> (sPLA<sub>2</sub>) generates extracellular LPA from phosphatidate (PA) in microvesicles that are shed during inflammation (147). The intracellular Ca<sup>2+</sup>-dependent and -independent PLA<sub>2</sub> (cPLA<sub>2</sub>, iPLA<sub>2</sub>) and possibly PLA<sub>1</sub> can also generate intracellular LPA from PA (147). Other intracellular synthetic pathways include glycerol-3-phosphate acyltransferase (GPAT) in ER and mitochondria and acylglycerolkinase in mitochondria. Thus ATX independent pathways could also be involved in tissue-level production and signaling by LPA.

#### 1.2.5 Structure studies of ATX and model for generation of LPA

ATX is a glycoprotein containing a signal peptide at its N-terminus, which is responsible for its secretion and autocrine signaling (148). ATX (ENPP2) was grouped into the ectonucleotide pyrophosphatase/phosphodiesterases (ENPP1-7) family, based on its sequence homology. Indeed, ATX has phosphodiesterase activity *in vitro*, a common feature in the ENPP family members. ATX additionally has lysophospholipase D activity. The physiologically significant lysophospholipase D activity was initially proposed based on the following evidence. First, ATX was secreted into the extracellular space where it can access LPC. Second, ATX shows increased affinity for LPC and LPA formation compared to its nucleotide

phosphodiesterase activity. Finally, the autocrine motility properties attributed to ATX are explained by increased LPA formation and not nucleotide recycling (133). The physiological lysophospholipase D activity was validated by evidence from mice models of ATX discussed earlier. In addition to its catalytic sites, ATX has a nuclease-like domain and two somatomedin-B-like domains. The somatomedin-B-like domain was suggested to mediate binding to integrins or heparan sulfate and thus bring ATX closer to the LPA receptors (149-151). The crystal structure of ATX revealed some interesting details on its catalytic mechanisms. The catalytic site is sandwiched between the somatomedin-B-like domains and nuclease domains. The lipid tail of LPA fits into the hydrophobic pocket, which accommodates the kinked unsaturated fatty acids, such as in 22:6-LPC and 18:1-LPC, while restricting access to saturated fatty acids, such as 18:0-LPC. Unsaturated LPA was also a binding partner for ATX, which suggests that ATX may have non-catalytic functions in delivering LPA to its receptor (152, 153). LPA was proposed to act as a natural competitive ATX inhibitor using low  $\mu\text{M}$  concentrations of a fluorescent substrate – FS-3. However, the competitive inhibition of ATX by LPA does not occur when physiological LPC concentrations ( $>200 \mu\text{M}$ ) are used (154). Instead, LPA-treatment inhibits ATX production and secretion. This normal feedback regulation is overcome by inflammatory mediators, which drive continuous ATX and LPA production (154). This explains why high levels of ATX and LPA concentrations co-exist in inflammatory conditions.

### **1.2.6 ATX/LPA signaling in disease – wound healing, inflammation and cancer**

One of the main roles for ATX/LPA signaling in adults is its function in the acute inflammatory process of wound healing and tissue remodeling (133). Platelet aggregation results in buildup of ATX/LPA levels in the blister fluid. Conversely, LPA itself increases aggregation of platelets and fibronectin assembly (144, 155, 156). Increased ATX/LPA levels leads to closure of the wound by formation of an epithelial cover in animal models of wound healing (157, 158). LPA promotes the growth and migration of fibroblasts, keratinocyte migration and new blood vessel formation (133). In chronically inflamed tissue, ATX/LPA signaling has additional roles in lymphocyte homing, mast cell activation, smooth muscle cell contraction and cytokine/chemokine production (159). LPA increases the production of inflammatory mediators by activating NF $\kappa$ B (160), AP1 (161), STAT3 (162), p38MAPK (163) and HIF-1 (164).

Increased LPA signaling through its receptors has been linked to a variety of pathological conditions. The role of ATX/LPA signaling in chronic inflammatory conditions like rheumatoid and osteo-arthritis, asthma, atherosclerosis, fibrosis, obesity and cancer has received a lot of attention recently (reviewed by Liu *et al.*, (165), Bourgoin *et al.*, (166), and Benesch *et al.*, (133)). For example, ATX activity and LPA levels were found to be increased in the bronchoalveolar lavage fluid of patients with lung fibrosis (129), in asthmatic patients (167, 168) and in synovial fluid of arthritic patients (169), where there is increased cytokine/chemokine

production. ATX and LPA signaling have also been linked to early and late formation of plaques during atherosclerosis. Here, LPA accumulates in thrombogenic cores of atherosclerotic plaque. This results in release of pro-inflammatory chemokines, cytokines and recruitment of leukocytes (144, 170, 171).

The link between inflammation and cancers was initially proposed based on observations that tumors occur in chronically inflamed regions and there is infiltration of immune cells in tumors (172). Patients with chronic inflammatory conditions are predisposed to certain cancers, such as in inflammatory bowel disease patients and colorectal cancer. An inflammatory component is seen in most cancers, including breast cancers (172). Increased inflammation is frequently studied by the presence of inflammatory mediators like cytokines, chemokines, growth factors and prostaglandins in the tumor microenvironment. In chronic conditions such as cancer, impaired wound healing and unresolved tissue damage results in further inflammation and disease progression. Thus, inflammation has been described as an enabling characteristic that promotes multiple hallmarks of cancers (56).

Direct and indirect roles in inflammation-driven initiation and progression of tumorigenesis have been proposed for ATX/LPA signaling (165). The indirect evidence includes the involvement of ATX/LPA in inflammatory processes and positive correlation between ATX/LPA levels and pro-inflammatory mediators in chronic inflammatory conditions including cancers. For example, hepatitis C infection, which induces chronic inflammation in the infected tissue, is a significant risk factor in hepatocellular carcinoma. ATX expression is elevated in hepatitis-

infected livers and hepatitis-infected liver carcinomas when compared to other liver carcinomas. Further, ATX expression is positively correlated to cirrhosis in all patient groups (173, 174). In another example, ATX levels were higher in the inflamed mucosa of patients suffering from inflammatory bowel disease, a risk factor in colorectal cancer (175). Our group recently discovered that ATX/LPA levels and inflammatory mediators were elevated in patients with malignant thyroid cancers (176). The direct evidence comes from mouse models of cancer, and inhibition of ATX/LPA signaling, which are discussed in Section 1.3. The role of ATX/LPA signaling in inflammation and cancers will also be considered in the Discussion Section. ATX/LPA signaling has been proposed to be a mediator of chronic inflammation in cancers, where inflammation in the tumor microenvironment increases ATX/LPA levels which in turn increased further inflammation through cytokine/chemokine production (176) (Fig 1.4).

### **1.2.7 Degradation of extracellular LPA by lipid phosphate phosphatases**

Lipid phosphate phosphatases (LPPs) consist of three related proteins named LPP1, LPP1a (a splice variant), LPP2 and LPP3. LPPs are broad specificity phosphatases, which dephosphorylate many lipid phosphates and lipid pyrophosphates. Their substrates include lysophosphatidate (LPA), sphingosine-1-phosphate (S1P), phosphatidate (PA), ceramide-1-phosphate (C1P), diacylglycerol pyrophosphate and N-oleoyl ethanolamine phosphatidate (177-179). LPPs are transmembrane proteins localized to the plasma membrane (180). This localization

allows for their catalytic site facing the extracellular space where LPPs can dephosphorylate extracellular bioactive lipids such as LPA and S1P (177).

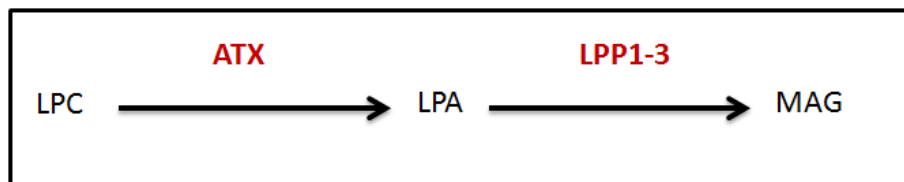


**Figure 1.3: Illustration of proposed model for LPA formation and degradation -** Extracellular LPA produced by ATX is normally degraded by LPP1-3 into monoacylglycerol and inorganic phosphate.

LPP1 expression is decreased in the majority of ovarian cancers and breast cancers, where extracellular LPA protects from apoptosis and increases proliferation (181, 182). Overexpression of LPP1/3 reverses many of these effects and can decrease tumor growth *in vivo* (181, 183, 184). Our group demonstrated that LPP1 overexpression in 4T1 breast cancer cells has intracellular effects independent of its *ecto*-phosphatase activity on LPA (183, 185). LPP1 overexpression attenuated breast cancer cell migration in the presence of LPP1-resistant LPA analog, wls31, and the protease-activated receptor-1 peptide. LPP1's effects on cell migration were due to decreased  $\text{Ca}^{2+}$  mobilization and Rho activation downstream of receptor activation. These results support previous observations that LPP1 can act downstream of LPA, S1P and thrombin activation by unknown mechanism (186, 187). LPPs hydrolyze intracellular lipids like PA (187) and S1P (188), which are increased downstream of GPCR activation by PLD1/2 and SK1/2 activities respectively. Additionally, some non-catalytic functions have been proposed for LPPs (189).



### **1.3 ATX/LPA signaling in tumor progression and metastasis**

ATX/LPA signaling is part of the chronic inflammatory response that supports multiple hallmark capabilities and drives tumor progression (56). ATX/LPA signaling sustains tumor proliferation together with oncogenes such as c-myc (190), helps cancer cells evade growth suppressors such as p53 (191, 192), activates tissue remodeling, invasion and metastasis (193-196), induces angiogenic signaling (197-200) and protects from the cytotoxic effects of chemotherapy (Section 1.3.3).

Our group proposed autocrine and paracrine models for ATX/LPA production in cancers leading to increased tumor growth, proliferation, metastasis and chemotherapy resistance (See Fig. 1.4). In breast cancers, ATX is mainly derived from the cancer-associated and peritumoral fibroblasts and mammary adipocytes. The growing tumor increases inflammation in the surrounding adipose tissue triggering a paracrine loop of ATX/LPA production. Increased LPA signaling in the tumor and surrounding tissue further increases the production of pro-inflammatory mediators. By contrast, cancers expressing higher ATX mRNA levels such as thyroid cancers, melanoma and glioblastoma, act through an autocrine feedback loop of increased inflammation and ATX/LPA production. Inhibition of ATX/LPA signaling blocks this vicious cycle of inflammation-driven tumor progression (133, 154, 176).

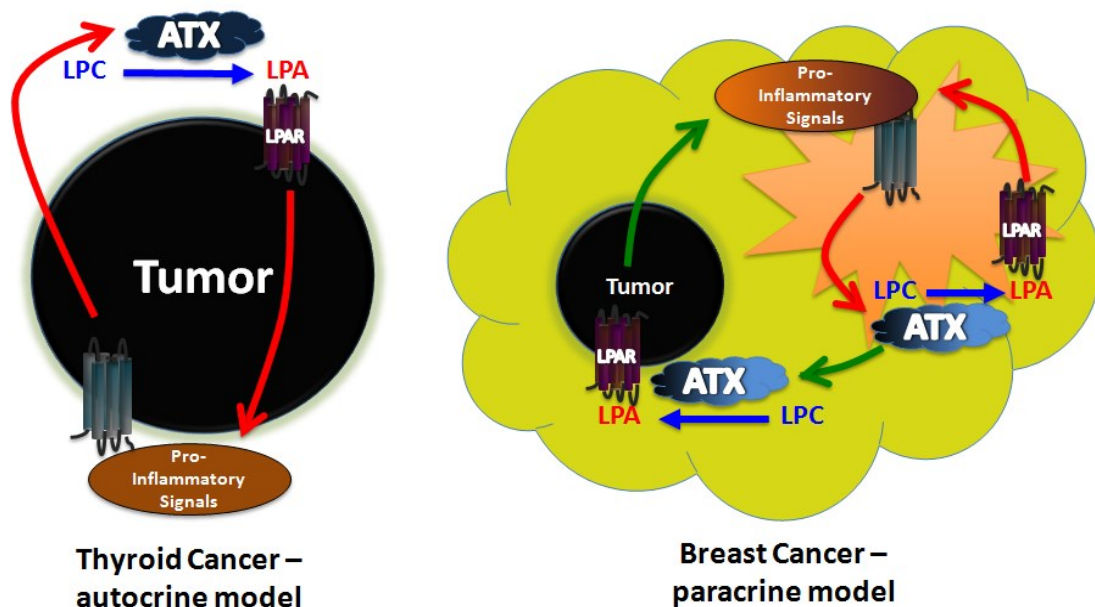


**Figure 1.4: Illustration of autocrine and paracrine models for inflammation-driven ATX production in tumors-** Tumor-promoting inflammation drives an autocrine feedback loop in cancer cells expressing high levels of ATX such as in glioblastoma, melanomas and thyroid cancer. In the autocrine model, pro-inflammatory mediators secreted by the growing tumor drives ATX/LPA production (red arrows). LPA further fuels inflammation by increasing the production of cytokines, chemokines and growth factors (blue arrows). In cancer cells expressing little or no ATX such as in breast cancer, fibroblasts and the surrounding mammary adipocytes contribute to ATX/LPA production. Here, pro-inflammatory mediators in the tumor microenvironment trigger a paracrine feedback loop of ATX production in the surrounding tissue (yellow). This vicious cycle of ATX/LPA production leads to increased tumor proliferation, metastasis and resistance to chemotherapy. Figure reproduced with permission from Benesch *et al* (133).

### 1.3.1 Expression of ATX and LPA receptors in various cancers

The role of ATX/LPA signaling in cancer progression is perhaps best understood in ovarian cancers, where a number of studies have been done on various aspects of tumor biology. Elevated levels of bioactive LPA have been shown in both plasma and ascites of ovarian cancer patients (201-203). LPA<sub>2/3</sub> receptors were also found to be upregulated in ovarian cancers (204, 205). LPP1 and LPP3 were

decreased in ovarian cancer patients resulting in overall increased LPA signaling (181, 184). LPA has been suggested as a potential biomarker for ovarian cancers along with LPC and S1P (206, 207). However, ATX alone was not useful as a biomarker in serum of ovarian cancer patients (208).

Even before the ATX-LPA link had been uncovered, LPA was shown to play a role in breast cancer invasion (203). Normal mammary epithelial cells express mainly LPA<sub>1</sub> and LPA<sub>2</sub>. Both LPA<sub>1</sub> and LPA<sub>2</sub> were implicated in LPA-induced chemotaxis of human breast cancer cells (209). Expression of LPA<sub>1</sub> was also implicated in MDA-MB-231 cell migration and bone metastasis (194). Increased expression of LPA<sub>2</sub> is commonly observed in ductal carcinomas of post-menopausal women (210). Our group previously reported the effects of ATX on migration and chemo-resistance of MCF-7, MDA-MB-231 breast cancer and MDA-MB-435 melanoma cells (211, 212). Mice that overexpress ATX or LPA<sub>1</sub>, LPA<sub>2</sub> or LPA<sub>3</sub> receptors in mammary epithelium show increased incidence of spontaneous tumors and metastasis (193). ATX was identified amongst the 40 most upregulated genes in metastatic cancers, suggesting increased ATX expression contributes to the metastatic phenotype (195). Increased expression of ATX in stromal cells and LPA<sub>3</sub> in epithelial cell has been correlated with aggressive breast carcinomas and higher clinical stage of disease (213).

Increased expression of ATX was also observed in other cancers such as glioblastoma and prostate cancer (214). In prostate cancer, LPA<sub>1</sub> signaling can mediate survival, migration and invasion (215-217). In glioblastoma, ATX-induced

LPA formation promotes cancer cell migration (218). In cervical cancers, knockdown of LPA<sub>2/3</sub> receptors in the cancer cells decreased tumor growth due to decreased angiogenesis and decreased expression of IL-8 (199, 219). In endometrial cancers, LPA increases invasion by stimulating the activity of tissue remodeling proteins such as MMPs (220, 221). ATX is increased in the serum of patients with hematological malignancies like Hodgkin's lymphoma and B-cell lymphoma, leading to efforts on developing it as a clinical biomarker (146). Thus ATX/LPA plays an important and diverse role in many cancers.

### **1.3.2 ATX/LPA signaling in mice models of cancer**

Nam *et al.*, (222) first established an autocrine model of ATX expression in tumor growth and metastases. They showed that subcutaneous injection of NIH3T3 fibroblasts transfected with ATX in nude mice gave rise to spontaneous, slow-growing sarcomas. Ras-transformed 3T3 fibroblasts overexpressing ATX produced rapidly growing solid tumors and increased incidence of experimental metastases compared to their ras-transformed controls. LPA<sub>1,2,4</sub> expression in c-myc expressing mouse embryonic fibroblasts (MEFs) induce tumor formation in nude mice (LPA<sub>1</sub>>LPA<sub>2</sub>>LPA<sub>4</sub>), whereas the control or LPA<sub>3</sub> expressing MEFs did not produce any tumors for over 75 days in this model (190).

To address the role of increased ATX and LPA receptor signaling in the development of breast cancers Liu *et al.*, (193) overexpressed ATX or LPA<sub>1</sub>, LPA<sub>2</sub> or LPA<sub>3</sub> under the control of MMTV-promoter in mouse mammary epithelium. These

conditions resulted in spontaneous development of late-stage tumors in these mice. Varying levels of metastases were observed ( $LPA_3 > LPA_1 > ATX > LPA_2$ ) in lung and lymph nodes. Chronic mastitis prior to development of tumors was observed in the mammary glands of these mice and there was increased expression of inflammatory markers in the tumors, suggesting a role for inflammation in breast tumor development.

Genetic ablation of  $LPA_2$  in C57BL/6 mice decreased tumor incidence and progression of intestinal cancers in an inflammatory mouse model of colitis (223). Similarly,  $LPA_2^{-/-}$  knockout decreased tumor progression in another cancer model of adenomatous polyposis coli (APC) gene point mutation resulting in multiple intestinal neoplasia in mice (224). Unlike the MMTV breast cancer model, transgenic overexpression of  $LPA_2$  in the gonads did not produce malignancy in the ovaries in C57BL/6 mice. However,  $LPA_2$  overexpression was found to amplify VEGF signaling through VEGF receptors 1 and 2, a growth factor linked to increased metastasis and angiogenesis (200).

Peyrchaud *et al.*, (225) reported the creation of a metastatic cell line MDA-BO2 cells from MDA-MB-231 breast cancer cells by repeated intracardial injections of the resulting bone metastases in nude mice. Boucharaba and colleagues (194, 226) intravenously injected an MDA-BO2 variant, which overexpresses  $LPA_1$ , to show increased bone metastases and tumor burden in these mice. Alternatively, silencing  $LPA_1$  decreased bone and soft tissue metastasis. Overexpression of ATX also increased tumor growth and bone metastasis (227). The likely source of ATX were

platelets (226), which were activated by the cancer cells in a  $\alpha_v\beta_3$  integrin-mediated process (228). It was concluded that the ATX/LPA-rich microenvironment supports LPA<sub>1</sub>-driven tumor progression, metastasis and bone resorption through secretion of pro-inflammatory mediators. The results described above on the effects of LPA<sub>1</sub> signaling on lung and liver metastasis were confirmed by another group. A 4T1 syngeneic model, which results in spontaneous lung and liver metastasis was used in these experiments (229). Alternatively, MDA-MB-231 was injected by tail-vein resulting in experimental lung metastasis. LPA<sub>1</sub> knockdown in cancer cells or LPA<sub>1</sub> inhibition by a small-molecule inhibitor decreased metastasis in both models (229).

Our group reported increased expression of ATX and inflammatory cytokines in the tumor-adjacent but not contralateral mammary fat-pads in the 4T1 syngeneic model. Since the 4T1 breast cancer cells themselves express very little ATX mRNA, it was concluded that the inflamed mammary fat pad bearing the tumor was the likely source of increased ATX activity (137). LPA production in the tumor microenvironment increases the production of pro-inflammatory cytokines/chemokines in the cancer cell and drive further tumor growth (Fig 1.4) (133). A recent study comparing LPA<sub>1,2,5</sub> knockout and wild-type animals showed that there were no differences in subcutaneous tumor formation when melanoma cells expressing LPA receptors were injected in these animals. This indicates that stromal LPA signaling does not influence tumor growth directly (230).

These results indicate that ATX/LPA/LPA receptor signaling may promote tumorigenesis, albeit indirectly by acting alongside primary oncogenic events that

drive proliferation. Additionally, LPA signaling may have a more prominent role in tissue remodeling and metastatic events.

### **1.3.3 Role for ATX/ LPA signaling in protection against cancer therapies**

Much of the information on the role of LPA signaling in chemo-resistance comes from earlier observations that LPA can protect cells from apoptosis and drive proliferation (214). LPA levels in plasma and ascites were increased in ovarian cancer patients (202, 231). Increased LPA signaling can protect ovarian cancers from cisplatin-induced killing. Cancer cells selected for cisplatin-resistance express higher levels of LPA<sub>1</sub> receptors (232, 233). In colon cancers, LPA protected against 5-fluorouracil and cisplatin-induced apoptosis in a PI3K-dependent manner (234).

ATX was identified amongst the highly upregulated genes in a screen of ovarian tumors, which were resistant to carboplatin/paclitaxel-therapy (235). Our group found that ATX/LPA signaling protects against paclitaxel-induced apoptosis in breast cancer cells by activation of PI3K-signaling and decreasing ceramide production (211). These results were confirmed by Vidot *et al.*, who also showed that ATX/LPA signaling can protect from paclitaxel- and carboplatin-induced apoptosis (236). The mechanism suggested for the protective effects of LPA was through reversing G2/M-arrest induced by paclitaxel (237). It is possible that these cancer cells acquire other adaptive resistance mechanisms.

LPA<sub>2</sub> receptor-dependent mechanism was shown to mediate resistance to radiotherapy (238). This was mainly through the C-terminal intracellular loop of

LPA<sub>2</sub> receptor, which acts as an interaction partner to recruit zinc-finger domain proteins. LPA<sub>2</sub> recruits the anti-apoptotic protein, Siva1, to prevent a p53 damage response induced by radiation (239). Another LPA<sub>2</sub> receptor-activated complex was shown to protect from radiation or doxorubicin-induced killing through increased PI3K-Akt, MAPK and NFκB signaling (240). The same group reported a decrease in various markers of apoptosis, which were induced by γ-radiation, by selective activation of LPA<sub>2</sub>-receptors (241).

Rat hepatoma cell lines stably overexpressing LPA<sub>3</sub> show increased survival to cisplatin or doxorubicin (242, 243). The authors also reported an increased expression of the ABCB1 gene (Mdr1a, Mdr1b) and glutathione transferase (Gstp1) in these cell lines when compared to the parental RH7777 cells. Inhibition of LPA<sub>1/3</sub> signaling was able to overcome resistance to the tyrosine kinase inhibitor, sunitinib, in renal carcinoma (244). Additionally, LPA<sub>5</sub> expression has been suggested to promote growth advantages in rat hepatomas (245). In summary, ATX/LPA/LPA receptor signaling has been shown to protect against chemotherapies in various cancers. The mechanisms of protection offered by LPA are not understood completely and these will be investigated in the thesis.

#### **1.3.4 ATX/ LPA signaling targeted therapies**

The pharmacological inhibition of the ATX/LPA/LPA receptor axis has generated considerable interest in the last decade (246). Most of the current inhibitors targeting LPA signaling are either lipid analogs or small molecule



inhibitors of LPA receptors. Lipid analogs tend to have poor pharmacokinetic profile and often lack the specificity to a particular LPA receptor. Small molecule inhibitors that decrease ATX activity *in vitro* have also been developed. Here, I will detail some of the LPA receptor antagonists and ATX inhibitors, which have been tested as a potential therapeutics in cancer.

A number of small molecule antagonists to LPA<sub>1-3</sub> have been reported (246). The LPA receptor agonists and antagonists used in our study are shown in Table 2. Most of these compounds were screened *in vitro* using a functional assay such as a Ca<sup>2+</sup> transient assay for the specific receptors, cell migration assays or using receptor activation assays like the GTP $\gamma$ -binding assay. Evidence from experiments *in vivo* is limited. The Kirin breweries compound, Ki16425 or its stereoisomer Debio0719 are perhaps the best studied of them. Ki16425 is a dual LPA<sub>1/3</sub> antagonist and it blocks bone metastasis formation in the MDA-BO2 xenograft model described earlier (194). Debio0719 decreased lung metastasis in a 4T1 breast tumor model (247). Several of the LPA antagonists such as Debio-0719 or BMS-986020 are either already in clinical trials or on their way to being tested (248).

Monoclonal antibodies against LPA and S1P (Lpath Inc) can be used to target extracellular lipid signaling (249-252). The effectiveness of the LPA monoclonal antibody has not yet been tested in cancers. However, they are in clinical trials to improve outcomes in traumatic brain injury and neuropathic pain (253). The anti-LPA, Lpathomab, decreased lesion volume and improved outcomes following traumatic brain injury and spinal cord injuries (251, 254).

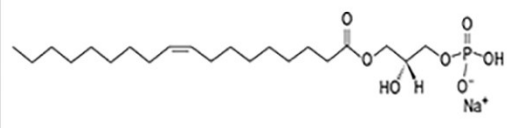
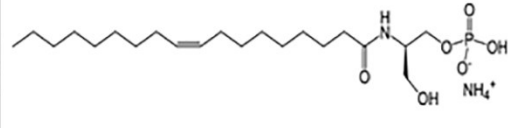
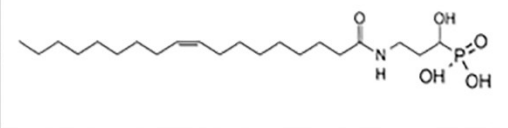
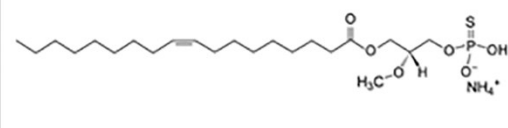
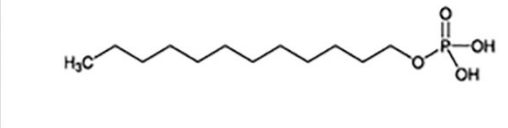
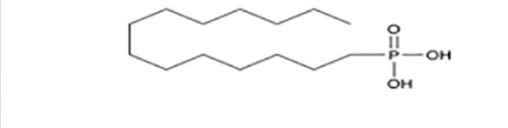
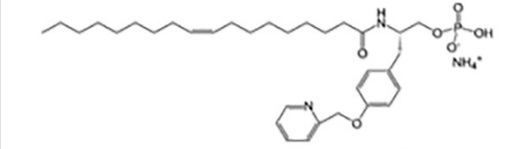
Currently there are no ATX inhibitors in the clinic. A phosphonate analog with pan-LPA receptor antagonist and ATX inhibitor activities, BrP-LPA (255), was shown to decrease tumor growth and angiogenesis in breast and lung cancer xenografts (197, 256). BrP-LPA also demonstrated radiosensitization effects in a subcutaneous model of glioma (257). BrP-LPA's protective effects were mediated by blocking fibroblast differentiation in a subcutaneous model of hepatocellular carcinoma (258). It is not clear if these effects of BrP-LPA were mediated by ATX inhibition and decreased LPA production.

Amongst the inhibitors, which target ATX, an analog of cyclic-phosphatidate (c-PA) was shown to reverse metastasis in an experimental model of lung metastasis using melanoma cells in C54BL/6 mice (259). PF8380, a competitive ATX inhibitor developed by Pfizer, had limited bioavailability *in vivo*. PF8380 was reported to reduce plasma LPA levels and LPA levels in sites of local inflammation after 4 h even though these decreases were not sustained (141). When PF8380 was combined with radiation in a mouse model of glioblastoma, a delay in tumor growth was reported (260). This was attributed to the effect of PF8380 on the tumor vasculature (260). PF8380 had very little effect on its own either on subcutaneous tumor growth or on the tumor vasculature (260).

ONO-8430506 (ONO pharmaceuticals, Osaka, Japan; USPTO reference number – 13807947 (261)) is an ATX inhibitor, which was able to suppress plasma ATX activity potently (262). Additionally, ONO-8430506 decreased plasma LPA levels in both regular and cancer bearing BALB/c mice at 24 h following

administration (137). ONO-8430506 decreased mainly the polyunsaturated LPA species. Furthermore, ONO-8430506 delayed tumor growth in a 4T1 orthotopic model and thyroid xenograft models in addition to its effect on metastasis (137, 176).

**TABLE 2: LPA agonists and antagonists used in the study**

| Compound    | Action  | Structure  |
|-------------|---|--|
| LPA 18:1    | Natural LPA receptor agonist  |    |
| VPC31143(R) | Synthetic LPA receptor agonist  |    |
| wls31       | LPA <sub>1/2</sub> agonist  |    |
| 2S-OMPT     | LPA <sub>3</sub> agonist<br>EC <sub>50</sub> – 68nM                     |   |
| LP105       | LPA <sub>2</sub> agonist<br>EC <sub>50</sub> – 3.1µM                    |  |
| TDP         | LPA <sub>1/2/3</sub> antagonist<br>IC <sub>50</sub> – 10, 5.5,<br>3.1µM |  |
| VPC32183    | LPA <sub>1/3</sub> antagonist<br>K <sub>i</sub> < 1µM                   |  |

## **1.4 Sphingosine kinase in development of resistance to chemotherapies**

Sphingosine 1-phosphate (S1P) is the sphingolipid equivalent of LPA with a wide variety of roles in cellular signaling. ATX has been proposed to generate extracellular S1P from sphingophosphorylcholine based on its catalytic activity (263). However, the concentration of sphingophosphorylcholine in plasma is very low compared to LPC and therefore sphingophosphorylcholine is unlikely to be an effective substrate *in vivo*. This statement is supported by evidence from ATX<sup>+/-</sup> heterozygous knockout mice, which demonstrates that extracellular LPA and not S1P is the major product of ATX (143). Also, inhibition of ATX did not alter S1P levels in the plasma or tumors of mice (137). Extracellular S1P is mainly produced inside cells by the two sphingosine kinases, SK1 and SK2, before being secreted outside the cell. SK1/2 account for most of the S1P produced in the developing mouse embryo (264). A large body of evidence points to a role for sphingolipid pathway in mediating resistance to chemotherapies (see Section 1.4.9). In this Section, I will introduce some concepts of sphingolipid metabolism, signaling and their relevance to disease. I will focus on mechanisms of activation of SK1 by external stimuli with relevance to LPA signaling. Finally, I will describe the current evidence linking SK1 to cancer progression, metastasis and resistance to therapies.

### **1.4.1 Bioactive sphingolipids in cellular signaling**

Extracellular signals activate various lipid kinases and phospholipases to generate bioactive lipid intermediates and activate signaling cascades in the cell.

These lipid intermediates can promote lipid-lipid interactions that affect the membrane bilayer or lipid-protein interactions that modulate the functions of proteins. Sphingolipids are enriched in 'lipid-rafts' or 'membrane-rafts', which are cholesterol-rich domains capable of acting as a signaling platform in the cell (265). Even complex sphingolipids like glycosphingolipids, which were initially thought of as structural lipids, have been found to play a major role in cellular signaling (7).

S1P is formed inside the cell by sphingosine kinases, SK1 and SK2, from sphingosine. SK1 and SK2 belong to the lipid kinase family, which also includes ceramide kinase and acylglycerolkinases (266). SK1 can be activated by many extracellular stimuli and it amplifies signaling cascades by production of S1P. S1P is involved in a variety of roles from regulating cell growth, migration, differentiation, proliferation, stress-response and angiogenesis through GPCR signaling (267). The sphingolipid backbone present in sphingosine and S1P is also shared by ceramides, glycosphingolipids and sphingomyelin. It consists of sphingosine base (long-chain aliphatic alcohol) to which a fatty acid is attached to the amine-group (Fig. 1.5). Ceramides have hydrogen in their R-group whereas sphingomyelin has phosphocholine and glycosphingolipids have complex sugar linked by a  $\beta$ -glycosidic bond.

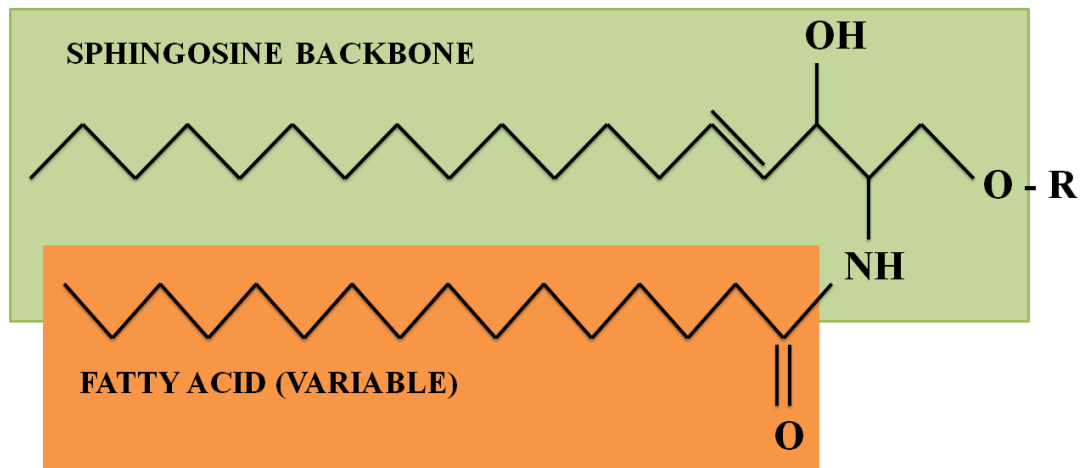


**Figure 1.5: Illustration of sphingolipid backbone** - All sphingolipids consist of sphingoid backbone and variable amide-linked fatty acid linkage and R-group.

#### 1.4.2 Sphingolipid pathway

Sphingolipids are tightly regulated in the cell and their synthesis pathway is highly conserved across eukaryotes (268, 269). Both simple and complex sphingolipids are synthesized by the *de novo* pathway, which results in formation of ceramide from serine and palmitoyl-coA as initial precursors (270). The *de novo* synthesis of sphingolipids takes place in ER and Golgi before transport to plasma membrane where they are retained as complex sphingolipids such as glycosphingolipids or sphingomyelin (271). In the alternative salvage pathway, complex sphingolipids are constantly taken up by endocytosis within acidic compartments where they can be recycled or degraded to ceramides from sphingomyelin or glycosphingolipids (272). Several lysosomal disorders arise from mutations in sphingolipid-modifying enzymes present in lysosomes (273). For example, Niemann-pick disease is characterized by mutations in acid

sphingomyelinase. In Farber disease, ceramide cannot be converted to sphingosine by acid ceramidases.

Ceramides are a diverse group of lipids with different signaling roles due to the differences in acyl species added to the sphingoid base resulting in >200 different species (274). In response to stimuli such as chemotherapeutics or irradiation, sphingomyelin and glycosylceramides can be converted to ceramides by the action of sphingomyelinases and  $\beta$ -glucosidases/galactosidases respectively, which can result in formation of S1P by the sequential action of ceramidases and SK1 (269).

The pathway for formation of various sphingolipids is shown in Figure 1.6. Ceramides are phosphorylated to the bioactive ceramide 1-phosphate by ceramide kinase and this action is reversed by LPPs (275). Ceramidases convert ceramides into sphingosine and non-esterified fatty acid. This is reversed by ceramide synthases that utilize fatty acids to N-acylate sphingoid bases. The sphingosine resulting from ceramidase action is rapidly converted to S1P in the presence of ATP by SK1 and SK2. S1P is hydrolyzed to sphingosine by the two specific S1P phosphatases (276) or the broad-specificity lipid phosphate phosphatases (277). The terminal products of S1P degradation result in the formation of hexadecenal and phosphoethanolamine and this reaction is catalyzed by S1P-lyase.



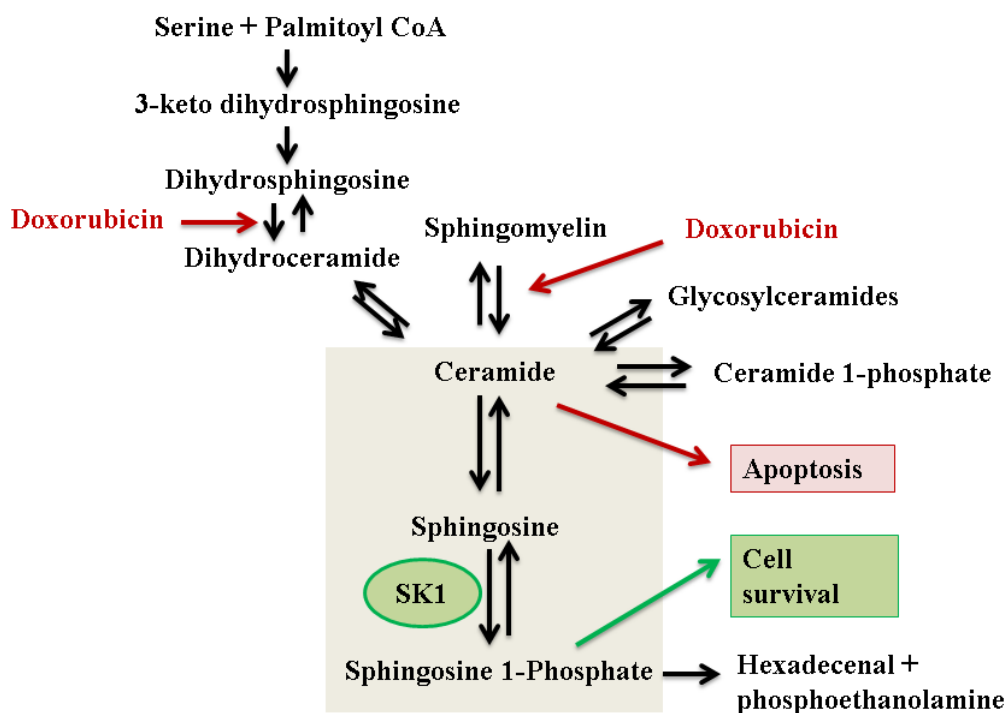


**Figure 1.6: Sphingolipid metabolism and the role of SK1 in doxorubicin-mediated killing and survival of cancer cells.**

### 1.4.3 SK1 structure, catalysis and S1P formation

Two mammalian isoforms of sphingosine kinase – SK1 and SK2- have been characterized. SK1 is expressed ubiquitously and is highly conserved across various species (278-280). SK1 is a predominantly cytosolic protein with a nuclear exclusion sequence motif, whereas SK2 is localized to the nucleus with a nuclear localization sequence motif. SK1 is activated by a variety of extracellular agonists, whereas SK2 does not respond to these stimuli. SK1 activity *in vitro* is enhanced by TritonX-100 and inhibited by high salt concentration (281). These properties can be used to differentiate between the two isoforms by supplying the sphingosine in mixed micelle Triton X-100 or in BSA-solution in 1 M KCl respectively. A single knockout

of SK1 or SK2 is viable in mice demonstrating that these enzymes can compensate for each other although they have different biochemical functions. However, a double knockout of SK1/2 result in embryonic lethality emphasizing the importance of S1P, while also suggesting that the roles of SK1 and SK2 during embryogenesis may be redundant (264).

The protein structure of SK1 contains two domain lobe similar to the DAG kinases and the phosphofructokinase superfamily (282). The ATP-binding lobe is conserved amongst the family members whereas the C-terminal lobe varies allowing for specific substrate recognition (*ie.* sphingosine for SK1). Mutation of SK1 in the ATP-binding lobe resulted in complete loss of catalytic activity or decreased ATP-binding and hydrolysis (283, 284). The basis for sphingosine recognition and binding into the lipid-binding pocket remains unclear from the crystal structure model (283). A recent study proposed that a C-terminal hydrophobic domain, which lines the cavity of the catalytic site, could be involved in substrate recognition and tunneling by direct interaction with the acidic phospholipids in the lipid bilayer (285).

#### **1.4.4 Agonist activation of SK1**

SK1 can be activated by a variety of stimuli. These include serum (286); growth factors and hormones like PDGF (287), TGF $\beta$  (288), nerve growth factor (289), EGF (290), VEGF (291), estrogens (292); cytokines like TNF- $\alpha$  (293); GPCR ligands like PAR1 (294), acetylcholine (295), LPA (296), SIP itself (297); phorbol

esters (298); other complex regulators like LDL (299) and vitamin D3 (300) have also been identified as SK1 activators.

The activation of SK1 is biphasic for many agonists such as phorbol esters (301), estrogen and prolactin (302). The first phase is a rapid increase in SK1 activity and S1P formation. This is followed by a transcriptional increase in SK1 protein expression and S1P-dependent signaling. EGF (290) and LPA through transactivation of EGFR (127) can also activate SK1 transcription in colon and breast cancer cells. AP-1 and SP-1 have been identified as transcription factors responsible for the action of some of these agonists (303, 304). The oncogene v-Src induces SK1 synthesis by increasing its mRNA stability rather than transcription (305).

External stimuli activate intracellular factors, like  $\text{Ca}^{2+}$  mobilization (295), protein kinases like PKC $\alpha$  or ERK1/2 (298, 306) and phospholipases like PLC $\gamma$  (307), leading to increased SK1 activation. This activation is thought to occur in plasma membrane (308) or endocytic vesicles (309), where the cytosolic SK1 can access its substrate, sphingosine. There is also some evidence that secreted SK1 can be directly activated outside the cell where it can form S1P and access S1P receptors (310, 311). However, the amount of S1P formed from secreted extracellular SK1 activity, in cells overexpressing SK1, is very low and its biological significance is not clear.

Multiple mechanisms have been suggested for increased agonist-induced activation of SK1 activity. These include 1) Reversible phosphorylation of SK1

(306, 312, 313), 2) Interaction with other proteins, which help in its membrane translocation (308, 314) and 3) Association with acidic phospholipids like phosphatidate (PA), phosphatidylserine (PS) and phosphatidylinositol (PI).

#### **1.4.5 Phosphatidate and SK1 activation**

Several studies have shown the involvement of negative charged phospholipids like PA in SK1 activation. An early report identified that acidic phospholipids like PA, PS, PI but not the neutral diacylglycerol can increase SK1 activity (315). The macrophage-specific receptor, Fc $\gamma$ RI, can activate SK1 through increased PA formation (316). Delon *et al.*, (317) showed that SK1 has a selective affinity for PA-rich regions of the plasma membrane. The C-terminal region of SK1 was implicated for this binding (Fig. 1.7). Stahelin *et al.*, (318) identified the more abundant PS as a selective lipid-binding partner for human SK1. Mutational analysis identified the conserved regions Thr54 and Asn89 to be essential for PS-binding. In plants, it appears that PA can bind to both SK1 and SK2 (319). The crystal structure of SK1 is now available (283) and a recent report has shed more light on the PA/PS lipid-interaction of SK1 (285). Shen *et al.*, (285) reported that membrane targeting of SK1 occurred by a direct interaction of the lipid-bilayer to a hydrophobic patch in SK1. The hydrophobic region of SK1 was shown to control movement of its substrate, sphingosine, into the interior of the protein. Mutations to key residues in the C-terminal hydrophobic region (L194Q and F197A/L198Q) reversed the acidic phospholipid binding and resulted in a diffuse cytosolic localization of SK1.

PS is synthesized in the ER from phosphatidylethanolamine and phosphatidylcholine and then transported to inner leaflet of the plasma membrane. In contrast, PA is a short-lived signaling lipid, which can be synthesized in the plasma membranes. A major role for PA is in membrane curvature, formation of vesicles and cytoskeletal reorganization (320). PA in the plasma membrane is generated by hydrolysis of phosphatidylcholine by phospholipase D (PLD) activity. Delon *et al.*, (317) demonstrated a co-localization of phospholipase D1 with SK1 upon its activation mostly to perinuclear membranes (Golgi, ER and late endosomes). Phospholipase D2 on the other hand is predominantly localized to the plasma membrane although it can localize to other compartments like Golgi (321). Diacylglycerol kinases can also translocate to membranes to produce PA from DAG (321). The LPAATs (lysophosphatidate-acyltransferases) synthesize the majority of PA in organelles where it is quickly converted to DAG by lipins for synthesis of more complex phospholipids (189). PA has also been shown to recruit other important signaling proteins such as SOS, RAF, GRB2, SHP2, PP1c, etc (Reviewed in (321)). It is likely from these results that PA is involved in retaining SK1 in acidic regions of membrane.

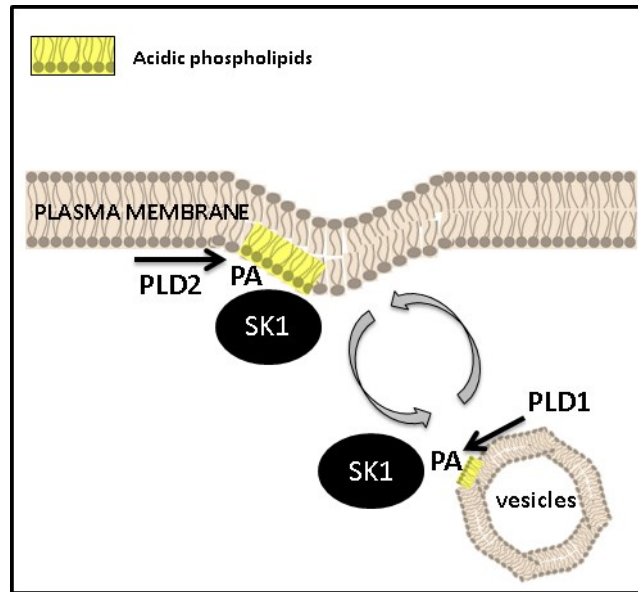


**Figure 1.7: Recruitment of the cytosolic protein SK1 by PA formation to sphingosine-rich regions of the membrane.**

#### 1.4.6 S1P function, trafficking and inside out signaling

Extracellular S1P signaling and function can vary depending on the localization, tissue expression of S1P receptors (S1P<sub>1-5</sub>) and S1P receptor coupling to different G-proteins. S1P<sub>1</sub> was initially identified in an angiogenesis screen as an orphan GPCR, *edg1* (endothelial differentiation gene -1) (322). S1P<sub>1</sub><sup>-/-</sup> mice die *in utero* due to vascular defects resulting in embryonic hemorrhaging (323). Although S1P<sub>2-5</sub><sup>-/-</sup> mice are viable, these receptors have been shown to be involved in various inflammatory processes, endothelial function and regulation of the immune system (324). SK1/2 double knockout mice are embryonic lethal due to major defects in neurogenesis and angiogenesis (264). A variety of pathways including ERK1/2 (325), p38MAPK (326), PI3K/Akt (327) and NFκB (293) have been shown to be activated by S1P receptor signaling.

The *de novo* synthesis of simple and complex sphingolipids in ER and Golgi was described earlier. The delivery of ceramides from ER to Golgi is thought to be directly facilitated by the ceramide transfer protein or CERT (328). However, the delivery of complex sphingolipids to the plasma membrane is mediated by exocytosis. Glycosphingolipids and sphingomyelin are degraded and recycled by the endosomal-lysosomal pathway. Intracellular S1P degradation is mainly controlled by S1P lyase and S1P phosphatases activities, which are localized mainly to ER with active sites facing the lumen and cytosol respectively (329, 330).

S1P can be transported outside the cell by the ABC transporters, ABCA1 (331), ABCC1 (332) and ABCG2 (333). However, only the newly identified spinster homolog 2 (Spns2) was both a specific and physiological S1P transporter (334-336). The source of plasma S1P (100 nM - 1  $\mu$ M) is unclear with studies suggesting they may arise from activated platelets (337), hematopoietic stem cells (338), erythrocytes (339) and vascular endothelium (340). It is likely more than one source contributes to its formation under various conditions. Outside the cell, where S1P is more abundant, it is carried by HDL and to a lesser extent it can bind to albumin and LDL (341). Lipoprotein-bound S1P is not degraded as easily as albumin-bound S1P by LPP activity localized to the plasma membrane (342). Additionally, erythrocytes were proposed to act as a buffer to store S1P (343). Most of the signaling functions of S1P are attributed to its secretion and inside-out signaling through its GPCRs (S1P<sub>1-5</sub>). However, intracellular second messenger roles for S1P have also been identified. For example, intracellular SK1 activity is required for ERK1/2 activation

downstream of the VEGF receptor (291). SK1 binds to TRAF2 (TNF receptor-associated factor 2), where S1P is a cofactor for TRAF2's E3 ubiquitin ligase activity (314, 344). Intracellular S1P is a direct binding partner for histone deacetylases linking it to gene regulation (345, 346).

#### **1.4.7 Role for S1P in disease and development of S1P-modulating drugs**

SK1 and its product S1P have important roles in immune cell trafficking, vascular development, cardiac function and inflammatory diseases besides its role in cancer. Several S1P modulators are currently in clinical trials for various disorders like multiple sclerosis, ulcerative colitis, cancer, rheumatoid arthritis, psoriasis, etc (Reviewed in (347)). Here, I will briefly discuss the role of S1P in inflammatory conditions and cancer.

##### **1.4.7.1 Inflammatory disorders**

Fingolimoid (FTY720), which was originally identified as an immunomodulator, is a S1P receptor regulator and a clinically approved treatment in multiple sclerosis (348). The FTY720 prodrug is phosphorylated by SK2 to FTY720-P, which can potently activate multiple S1P receptors and target them for proteosomal degradation (338, 349). Immune cells are desensitized to the effects of S1P due to degradation of S1P<sub>1</sub> receptor by FTY720 and remain in the lymphoid organs. Extensive work from Dr. Cyster's group has established the involvement of S1P-S1P receptor signaling in lymphocyte egress from lymphoid organs (339, 350-



352). FTY-720 can also stimulate S1P<sub>1</sub> receptor degradation in other cell types in the central nervous system and may have other therapeutic effects in multiple sclerosis patients.

S1P levels are increased in the synovial fluid of patients with rheumatoid arthritis. Inhibition of SK1 blocked the production of inflammatory cytokines and thus reduced disease incidence and progression in a mouse model of arthritis (353). Overexpression of SK1 was linked to diabetic nephropathy in an *ex vivo* model, where S1P increased the expression of glomerular extracellular matrix protein, fibronectin (354). S1P has also been linked to fibrotic diseases, where elevated S1P promotes EMT-like phenotype (355). Serum S1P levels were also elevated in systemic sclerosis patients (356).

Sphingosine kinase activity has been linked to ulcerative colitis using the dextranulfatesodium (DSS) model in SK1<sup>-/-</sup> mice and IHC analysis of SK1 on patient samples (357). Small molecule inhibitors of sphingosine kinases effectively targeted chemically-induced inflammatory cytokines and S1P production in the colon carcinoma model (358, 359). KRP-203, a synthetic immunomodulator structurally similar to FTY720 (360), suppressed colitis in IL10<sup>-/-</sup> model by decreasing the infiltration of lymphocytes and blocking cytokine production (360). SK1 activity has also been reported to be increased in colon cancer (361). SK1 increases the severity of chemically induced colitis in SK2<sup>-/-</sup> mice by persistent activation of the inflammatory mediators, NFκB and STAT3, thus linking colitis-associated cancer to chronic inflammation (362).

#### 1.4.7.2 Cancer

S1P's mitogenic and anti-apoptotic role prompted many investigators to work on its role in cancer. Overexpression of SK1 protected cancer cells from apoptosis. Xia and colleagues showed increased tumorigenesis in 3T3 fibroblasts-overexpressing SK1 (312, 363). Results from clinical studies show several cancers including thyroid (364), breast (365), glioblastoma (366) and lung cancers (367) are characterized by increased expression of SK1. Estimating S1P levels and SK1 expression have potential as a biomarker in breast (365) and prostate cancers (368). Mice with 4T1 orthotopic tumors have elevated S1P levels in circulation and an increase in SK1 expression was observed in the tumors (369).

The idea of tumor-derived S1P autocrine/paracrine signaling loop was challenged by a study recently (252). By injecting SK1-expressing cancer cells in a SK1<sup>-/-</sup> or wild type mice and the authors were able to differentiate between the effects of systemic and tumor-derived S1P. The authors showed that proliferating tumors induce systemic increases in S1P in wild-type but not SK1<sup>-/-</sup> mice. Furthermore, a knockdown of SK1 in the cancer cells had only a modest effect on tumor growth and no effect on metastasis. Their results suggest that the extracellular S1P gradient alone determines lung metastases irrespective of cancer cell SK1 activity.

The monoclonal antibody against S1P, sphingomab, was shown to decrease tumor proliferation and angiogenesis in breast, ovarian and lung cancer xenografts in pre-clinical models (249). This has now progressed into Phase II trials. A specific

inhibitor of SK1 (SK1-I or BML-258) prevents tumor growth and angiogenesis in a xenograft model of glioblastoma (370) and leukemia (371). The same inhibitor decreased tumor growth, heme- and lymph-angiogenesis in a syngeneic model of breast cancer (369). However, another potent inhibitor of SK1, PF-543, decreased S1P levels without any effect on the survival of cancer cells *in vitro* (372). Another small molecule inhibitor SKi (SKi-II) was shown to induce proteosomal degradation of SK1 and apoptosis in cancer cells (373). These compounds show great promise for the future development of more potent and selective SK1 inhibitors. The role of S1P in cancer and chemo-resistance is discussed further in the following section.

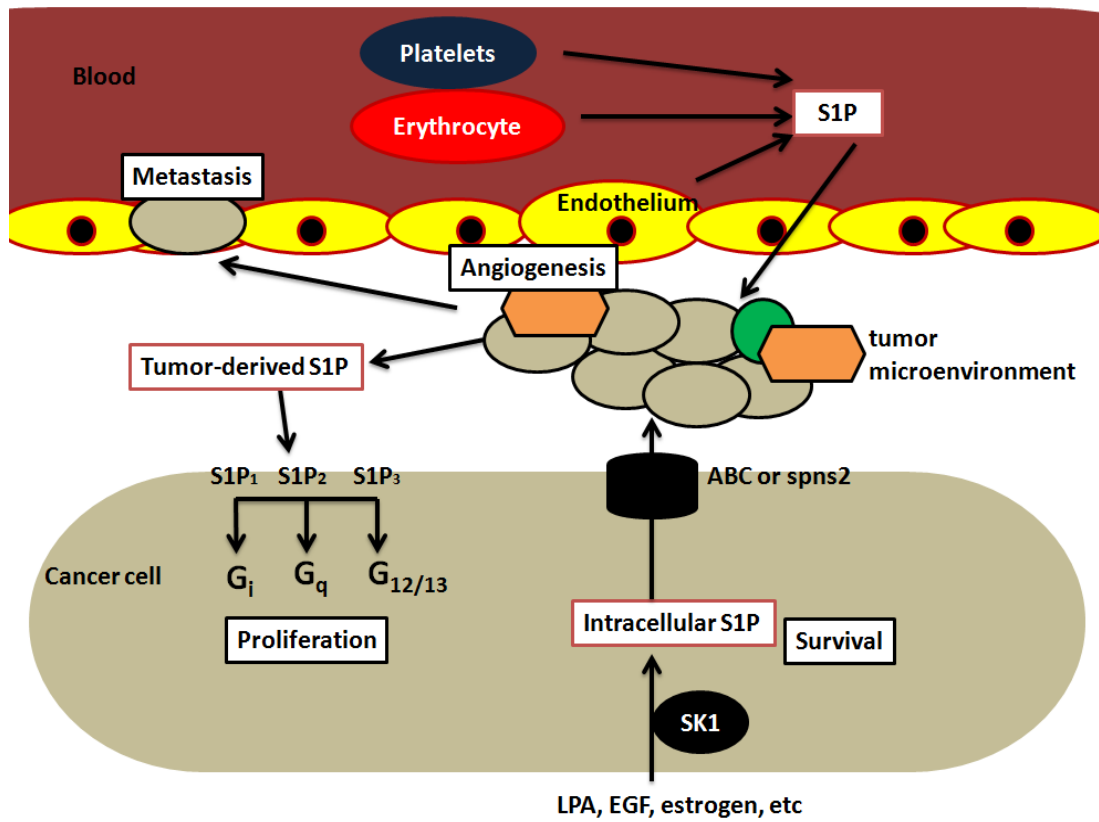


**Figure 1.8: Functions of SK1-derived S1P from various cell sources in the tumor microenvironment** – SK1 is activated by growth factors, hormones, GPCR ligands and other agonists in the cancer and stromal cells. Intracellular S1P has distinct signaling roles in the cancer cell resulting in increased survival. Intracellular S1P is also secreted outside the cell by the action of ABC- or Spns2- transporters. S1P in the circulation is derived from various sources such as erythrocytes, endothelium, and platelets and is bound to HDL, LDL or albumin. S1P gradients in the tumor microenvironment drive survival, proliferation, metastasis and angiogenesis by activation of the S1P receptors.

#### 1.4.8 S1P and ceramide rheostat

The rapid turnover of S1P from ceramide breakdown, terminal degradation of S1P by S1P-lyase and the opposing effects of ceramide/S1P on stress signaling and cell survival suggest that SK1 is a key regulator of sphingolipid metabolism. The ceramide rheostat model argues that the metabolic conversion of ceramide to S1P

determines cell survival. Apoptotic ceramides (and sphingosine) feature on one end while S1P is on the other end of the death-survival balance (Fig. 1.6). Any sphingolipid modifying enzyme activity that tips this balance, can affect cell survival and apoptotic pathways. This was supported by an initial study in Cuvillier *et al.*, (374) where SK1 activity counteracted ceramide-induced effects on apoptosis. Several studies have since come out in support of this model (See Section 1.4.9). The validity of the ceramide rheostat model has been questioned because of the differences in relative abundance of these lipids in cell. These are explained by differences in the localization, diversity of the ceramide species (>200) and existence of other ceramide regulatory pathways (Fig. 1.6).

#### **1.4.9 SK1 activation and resistance to therapy**

The role of SK1 activation in cancer progression and chemo-resistance has been well described in many cancers such as breast, prostate, colon cancers, glioblastoma and leukemia (267, 375). MCF-7 breast cancer cells showed increase sensitivity to doxorubicin when SK1 was silenced (376). Bonhoure *et al.*, (377) showed the S1P-ceramide rheostat contributed to resistance to doxorubicin and etoposide, which could be circumvented by addition of ceramides to these cells. The authors also reported sustained activation of SK1 and decreased accumulation of ceramides in drug-resistant cells. The SK1/S1P axis reduced C18-ceramide levels and blocked apoptosis in chronic myelogenous leukemia cells that are resistant to imatinib (378). SK1 overexpression increased resistance to docetaxel treatment and

reversed ceramide-induced apoptosis (379), whereas siRNA knockdown of SK1 lead to increased docetaxel sensitivity (380) in a mouse model of prostate cancer. SK1 overexpression caused resistance to platins, doxorubicin and vincristine and interfered with ceramide synthase-induced sensitivity to these drugs (381). SK1 overexpression increases the resistance of breast cancer cells to tamoxifen, whereas knocking down SK1 was enough to restore sensitivity of resistant cells (382). Expression of SK1 and S1P<sub>1,3</sub> receptors were inversely correlated with tamoxifen sensitivity in breast cancer patients (365). SK1 expression was also inversely correlated with survival in glioblastoma patients (366). Further, inhibition of SK1 activity in glioblastoma results in increased apoptosis (383) and restores sensitivity to temozolomide (384).

Dimethylsphingosine (DMS), a non-specific inhibitor of SK1, was shown to increase apoptosis in leukemia and colon cancer cells. DMS also decreased the growth of tumors independently or in combination with doxorubicin in epidermoid carcinoma cells injected subcutaneously into female BALB/c mice (385). Safingol, a competitive SK1 inhibitor, sensitizes multi-drug resistant cancer cells to doxorubicin (386). A role for oxidative stress mediated cell death has been proposed in these actions (387). A Phase I trial for Safingol with cisplatin in combination therapy is now complete (388) and could be the first of SK1 inhibitors to make it to the clinics. French *et al.*, (389) compared SK1 expression in several solid tumors to the normal tissue of patients and found it was increased. Furthermore, a library of small molecule inhibitors of SK1 was shown to induce apoptosis in several cancer cell

lines including drug-resistant cells and decrease tumor growth in a subcutaneous BALB/c cancer model.

Experiments on S1P degrading enzymes show most of the above mentioned effects of SK1 are mediated by S1P itself and not its metabolites. For instance, genetic ablation of S1P lyase can cause increased tumor formation in nude mice and resistance to doxorubicin and etoposide-treatments (390). S1P phosphatases are a target for miR-95, which promotes radiation resistance in a prostate cancer xenograft model (391).

#### **1.4.10 Alternate sphingolipid pathways in drug resistance**

Decreased ceramide generation by both *de novo* synthesis and the salvage pathway (Fig. 1.6) has been linked to drug resistance (375). Thus targeting the enzymes involved in modulation of ceramide levels has been suggested as a strategy for overcoming drug resistance (392). Several chemotherapeutic agents and radiation have been shown to induce ceramide formation. Doxorubicin, for example, produces ceramides both by *de novo* synthesis and activation of sphingomyelinases. Our group showed that LPA protects from paclitaxel-induced cell killing in breast cancer cells by decreased ceramide production (211). The role of extracellular LPA in regulation of ceramide generation pathways remains poorly understood. The existing literature on ceramide generation pathways and drug resistance are discussed in the following sections.

#### **1.4.10.1 Ceramide synthesis by *de novo* pathway**

Multiple chemotherapeutics can increase ceramide production by *de novo* pathway (Fig. 1.6). These include daunorubicin (393), doxorubicin (394), camptothecins (394), paclitaxel (395), cisplatin (381) and etoposide (396). Alterations in ceramide synthase activity have been commonly linked to resistance to apoptotic ligands, chemotherapies and radiotherapy (397, 398).

#### **1.4.10.2 Sphingomyelinases**

Increased sphingomyelin synthase activity has been linked to doxorubicin resistance in leukemia patients (399). Mutations in acid or neutral sphingomyelinases can cause a loss of ceramide production and lead to resistance to  $\gamma$ -radiation therapy (400, 401). Overexpression of acid sphingomyelinase reduced tumor burden together with  $\gamma$ -radiation in a subcutaneous melanoma model (402). Acid sphingomyelinase<sup>-/-</sup> knockout mice with fibrosarcomas develop radiation resistance (403). Generation of ceramides from sphingomyelin was found to be decreased in TNF- $\alpha$  resistant cells (404). However, other ceramide pathway enzymes such as glycosylceramide synthase, ceramidase may also be involved in ceramide generation and resistance to  $\gamma$ -radiation (405).

#### **1.4.10.3 Glycosylation of ceramides**

The formation of glycosylceramides has been shown to be a major pathway by which resistant cells avoid ceramide-induced apoptosis. Initial work showed an



increase in glycosylceramide levels in multi-drug-resistant cancers (406). A correlation was also made between the expression of MDRT, ABCB1 and ABCC1, and generation of glycosylceramides (407, 408). Overexpression of glycosylceramide synthase confers resistance to drugs like doxorubicin (399, 409). Galactosylceramides (410) and complex gangliosides have also been linked to increased tumorigenesis and resistance to chemotherapy. Targeting glycosylceramide synthase alone did not have any effect on altering the sensitivity of melanomas to doxorubicin and reversing multi-drug resistance because of the existence of other *de novo* and salvage pathways for ceramide generation (411). A multi-inhibitor approach was used to target ceramide conversion pathways and this resulted in enhanced ceramide levels and sensitization of radio-resistant carcinomas (405). The MDRT modulator, PSC833 (412), a cyclosporineA analog, was able to reverse glycosylceramide-mediated resistance to chemotherapy by increasing ceramide levels (406). Interestingly, MRP1 can flip glycosylceramides and sphingomyelin across the membrane (413).

### **1.5 Summary and thesis objectives**

ATX is a wound healing and tissue remodelling factor recruited by cancer cells to generate LPA in the tumor microenvironment. Strong evidence supports a role for ATX/LPA signaling in early stages of tumorigenesis, tumor progression and advanced metastatic disease in breast and other cancers. Additionally, LPA signaling promotes survival and confers resistance to various chemotherapies in cell culture

and animals models of cancer. The mechanism for LPA's role in the acquisition and maintenance of resistance to various chemotherapeutics is not clear. The first aim of my thesis was to determine the role of LPA signaling in initiating adaptive mechanisms that result in acquisition of multi-drug resistance to chemotherapeutics in cancers.

Cell lines have been used primarily to investigate multi-drug resistance mechanisms. However, recent studies suggest that cell culture models are limited in their usage to model clinical resistance since they lack the heterogeneity associated with tumors (414). Additionally, cell lines cannot entirely account for the role of tumor microenvironment in development of resistance to therapies. The second aim of my thesis was to investigate the role of ATX/LPA signaling in promoting resistance to doxorubicin in a syngeneic orthotopic model of breast cancer. LPA levels in these mice were decreased by inhibition of ATX activity with ONO-8430506. The experiments with doxorubicin were extended to investigate resistance to tamoxifen, another widely used first line therapy in breast cancer.

Alterations to sphingolipid metabolism have been reported as one of the mechanisms contributing towards chemo-resistance. S1P generated by SK1 activity plays an important role in cell survival both as intracellular second messengers and as an extracellular factor with mitogenic properties. The final aim of my thesis was to investigate the mechanism of activation of SK1 by LPA in doxorubicin-resistant breast cancer cells.

## **CHAPTER 2 – MATERIALS AND METHODS**

## **2 MATERIALS AND METHODS**

### **2.1 Reagents**

All chemicals and reagents were from Sigma-Aldrich (Oakville, ON) unless stated otherwise. DMEM, RMPI-1640, DMEM-F12, OPTI-MEM, penicillin/streptomycin and trypsin-ethylenediaminetetraacetic acid, G418 and blasticidin were from Life Technologies (Gaithersburg, MD, USA). LB powder, granulated agar was from Difco Laboratories (Detroit, MI, USA). Ampicillin, kanamycin, spectinomycin and chloroamphenicol were from Sigma. FBS was from Mediatech Inc (Westmount, QC). MEGM (Lonza, Mississauga, ON). Doxorubicin HCl (Cayman Chemicals, Ann Arbor, MI, USA), etoposide (Sigma); PA (mixed species) was from Sigma-Aldrich. Caspase 3/7 Glo assay kit, GSH-Glo and Luciferase assay kit were from Promega (Mississauga, ON).

The following LPA receptor agonists and antagonists were used: 18:1-LPA, VPC31143(R) and VPC32183 were from Avanti Polar lipids (Alabaster, AL, USA). Ki16425, 2S-OMPT, tetradecylphosphonate were from Cayman Chemicals (Ann Arbor, MI, USA). LP-105 was obtained from Enzo Lifesciences (Farmingdale, NY, USA). wls31 (415, 416) was synthesized by Mr. N. Patwardhan and kindly provided by Dr. W. Santos, Department of Chemistry, Virginia Tech (Blacksburg, VA, USA) (See Table 2).

**TABLE 3: Pharmacological activators/inhibitors used in the study**

| <b>Name</b>     | <b>Supplier</b>   | <b>Action</b>            | <b>Final concentration</b> |
|-----------------|-------------------|--------------------------|----------------------------|
| LY294002        | BIOMOL            | PI3K inhibitor           | 10 $\mu$ M                 |
| PD98059         | Calbiochem        | MEK inhibitor            | 20 $\mu$ M                 |
| Gö6983          | Calbiochem        | PKC inhibitor            | 10 $\mu$ M                 |
| AG1296          | Calbiochem        | PDGFR kinase inhibitor   | 10 $\mu$ M                 |
| AG1478          | Calbiochem        | EGFR kinase inhibitor    | 10 $\mu$ M                 |
| Wortmannin      | Sigma             | PI3K inhibitor           | 1 $\mu$ M                  |
| Pertussis toxin | Sigma             | G <sub>i</sub> inhibitor | 0.1 $\mu$ g/ml             |
| U73122          | Sigma             | PLC inhibitor            | 1 $\mu$ M                  |
| ActinomycinD    | Sigma             | Transcription inhibitor  | 10 $\mu$ g/ml              |
| MG132           | Sigma             | Proteosomal inhibitor    | 10-25 $\mu$ M              |
| t-BHQ           | Sigma             | Nrf2 activator           | 10-25 $\mu$ M              |
| Probenecid      | Sigma             | MRP inhibitor            | 1-5 mM                     |
| CyclosporineA   | Sigma             | MDR inhibitor            | 5 $\mu$ M                  |
| MK571           | Sigma             | ABCC1 inhibitor          | 20 $\mu$ M                 |
| FTC             | Sigma             | ABCG2 inhibitor          | 20 $\mu$ M                 |
| VU0155056       | Avanti            | Pan PLD inhibitor        | 1 $\mu$ M                  |
| VU0359595       | Avanti            | PLD1 inhibitor           | 0.5 $\mu$ M                |
| VU0285685-1     | Avanti            | PLD2 inhibitor           | 0.5 $\mu$ M                |
| FIPI            | Sigma             | Pan PLD inhibitor        | 1 $\mu$ M                  |
| ZVAD-FMK        | Enzo Lifesciences | Pan caspase inhibitor    | 50 $\mu$ M                 |

The following pharmacological activators and inhibitors were used: MG132, t-BHQ, probenecid, cyclosporineA, MK-571, FTC, DAPT and FIPI were from Sigma-Aldrich. VU0155056, VU0359595, VU0285685-1 were from Avanti. PD98059, Gö6983, AG1296, AG1478 were from Calbiochem (Millipore, Etobicoke, ON). Wortmannin, pertussis toxin, U73122, rapamycin, cucurbitacin 1 and actinomycin D were from Sigma. LY294002 was from BIOMOL (Enzo Lifesciences, Farmingdale, NY, USA). See full list and details in Table 3.

## 2.2 Cell culture

### 2.2.1 Cell lines

MCF-7 (HTB-22), MDA-MB-231 (HTB-26), MDA-MB-468 (HTB-132), MDA-MB-453 (HTB-131), Hs578T (HTB-126), Hs578Bst (HTB-125), MCF10A (CRL-10317), MCF12A (CRL-10782), 4T1 (CRL-2539), MDA-MB-435S (HTB-129), A549 (CCL-185), HEL299 (CCC-137), MRC-5 (CCL-171), WI-38 (CCL-75), HT1080 (CCL-121), GM-10 (Dr. Mirzayans), GM-0637 (Dr. Mirzayans), HepG2 (HB-8065), HEK293 (CRL-1573) and HEK 293T (CRL-11268), were all purchased from ATCC (Manassas, VA, USA). BCPAP (ACC-273), 8305C (ACC-133) were from DSMZ (Braunschweig, Germany). TPC-1 was obtained from Dr. Todd McMullen, University of Alberta. HUVECs were obtained from Dr. Denise Hemmings, University of Alberta. 4T1-12B cells were purchased from Dr. G. Sahagian (Department of Physiology, Tufts University School of Medicine, Boston, MA, USA). All cells were used at low passage number. Growth media and characteristics are described in the Table 4. All cells were maintained in an incubator at pH 7.4, humidity, 5% CO<sub>2</sub> atmosphere at 37<sup>0</sup>C. The inducible, minimal antioxidant response element (ARE) cell line, AREc32 (417), was a kind gift from Prof. Roland Wolf and Cancer Research UK. It was made by stably expressing a pGL3 luciferase vector inserted with 8 repeats of the short, functional cis element of rat Glutathione-S-Transferase  $\alpha$ 2 (GSTA2) in MCF-7 cells (Table 5).

**TABLE 4: LIST OF CELL LINES USED IN THE STUDY**

| <b>CELL LINE</b> | <b>CULTURE MEDIUM</b> | <b>SUPPLIER</b>    | <b>Type</b>                                |
|------------------|-----------------------|--------------------|--|
| MDA-MB-231       | DMEM + 10% FBS        | ATCC               | Breast adenocarcinoma                      |
| MCF-7            | DMEM + 10% FBS        | ATCC               | Invasive ductal carcinoma                  |
| MDA-MB-468       | DMEM + 10% FBS        | ATCC               | Breast Adenocarcinoma                      |
| MDA-MB-453       | DMEM + 10% FBS        | ATCC               | Breast adenocarcinoma                      |
| 4T1              | DMEM + 10% FBS        | ATCC               | Murine carcinoma                           |
| 4T1-12B          | DMEM + 10% FBS        | Dr. Sahagian       | 4T1 stably expressing firefly luciferase   |
| AREc32           | DMEM+ 10% FBS +G418   | Cancer research UK | Derived from MCF-7 cells                   |
| Hs578T           | DMEM+ 10% FBS         | ATCC               | Invasive ductal carcinoma                  |
| Hs578Bst         | DMEM + 10%FBS         | ATCC               | Peripheral tissue to Hst87T                |
| MCF10A           | ATCC medium           | ATCC               | Breast epithelial cells                    |
| MCF12A           | ATCC medium           | ATCC               | Breast epithelial cells                    |
| MCF-7 DOX        | DMEM + 10% FBS        | Dr. Parrissenti    | Derived from MCF-7 cells                   |
| MCF-7 TAX        | DMEM + 10% FBS        | Dr. Parrissenti    | Derived from MCF-7 cells                   |
| HepG2            | DMEM + 10% FBS        | ATCC               | Hepatacellular carcinoma                   |
| A549             | DMEM+10% FBS          | ATCC               | Lung adenocarcinoma                        |
| WI-38            | DMEM + 10% FBS        | ATCC               | Lung fibroblasts                           |
| HEL-299          | RPMI + 10%FBS         | ATCC               | Lung fibroblasts                           |
| MRC-5            | RPMI + 10%FBS         | ATCC               | Lung fibroblasts                           |
| HT-1080          | DMEM+ 10% FBS         | ATCC               | Fibrosarcoma                               |
| MDA-MB-435S      | DMEM + 10% FBS        | ATCC               | Melanoma                                   |
| GM-10            | HamF12/DMEM           |                    | Skin fibroblasts                           |
| GM-0637          | HamF12/DMEM           |                    | Skin fibroblasts                           |
| 8305C            | RPMI + 10% FBS        | DSMZ               | Thyroid carcinoma                          |
| BCPAP            | RPMI + 10% FBS        | DMSZ               | Thyroid carcinoma                          |
| TPC1             | RPMI + 10% FBS        | Dr. McMullen       | Thyroid carcinoma                          |
| HUVECs           |                       | Dr. Hemmings       | Human umbilical vascular endothelial cells |
| HEK293           | DMEM + 10% FBS        | ATCC               | Human embryonic kidney                     |
| HEK293T          | DMEM +10% FBS         | ATCC               | Human embryonic kidney                     |

**TABLE 5: Comparison of antioxidant response element (ARE) for Nrf2-regulated genes used in this study**

| <b>GENE</b>       | <b>Species</b> | <b>5'- ARE Sequence – 3'</b><br><b>nTGACnnnGCn</b>  | <b>Reference</b> |
|-------------------|----------------|---|------------------|
| <b>PGL-8x ARE</b> | -              | <b>GTGACAAAGCACCC</b><br><b>GTGACAAAGCACCC</b><br><b>GTGACAAAGCACCC</b><br><b>GTGACAAAGCACCC</b><br><b>GTGACAAAGCACCC</b><br><b>GTGACAAAGCACCC</b><br><b>GTGACAAAGCACCC</b><br><b>GTGACAAAGCACCC</b><br><b>GTGACAAAGCACCC</b> | (417)            |
| <b>Gsta2</b>      | Rat            | <b>GTGACAAAGCA</b>  | (417)            |
| <b>Nqo1</b>       | Rat            | <b>GTGACTTGGCA</b>  | (418)            |
| <b>nqo1</b>       | mouse          | <b>GTGAGTCGGCA</b>  | (418)            |
| <b>NQO1</b>       | Human          | <b>GTGACTCAGCA</b>  | (418)            |
| <b>HMOX1 – 1</b>  | Human          | <b>GTGACTCAGCG</b>  | (419)            |
| <b>HMOX1 - 2</b>  | Human          | <b>GTGACTCAGCG</b>  | (419)            |
| <b>HMOX1- 3</b>   | Human          | <b>GTGACTCAGCA</b>  | (419)            |
| <b>ABCC1 -1</b>   | Human          | <b>GTGACTCAGCT</b>  | (420, 421)       |
| <b>ABCC1 – 2</b>  | Human          | <b>GTGAGCGGGCG</b>  | (421)            |
| <b>abcc1 – 1</b>  | mouse          | <b>TTGAGTTAGCT</b>  | (422)            |
| <b>abcc1 – 2</b>  | mouse          | <b>TTGAGACAGCA</b>  | (422)            |
| <b>ABCC2 – 1</b>  | Human          | <b>AAGACTGTGCA</b>  | (422)            |
| <b>ABCC2 – 2</b>  | Human          | <b>GTGACAGTACA</b>  | (422)            |
| <b>ABCC2- 3</b>   | Human          | <b>CTGATGCTGCC</b>  | (422)            |
| <b>abcc2</b>      | mouse          | <b>ATGACATAGCA</b>  | (423)            |
| <b>abcc3</b>      | mouse          | <b>ATGACTCTGCT</b>  | (422)            |
| <b>abcc4</b>      | mouse          | <b>GTGACCTGGCA</b>  | (422)            |
| <b>ABCG2</b>      | Human          | <b>GTGACTGGGCA</b>  | (83)             |

**Abbreviations:**

**PGL-8x ARE** – 8x putative Nrf2 binding site (TGACnnnGCn) from rat GSTA2 ARE core sequence; **GSTA2** – Glutathione-S-Transferase  $\alpha$ 2; **NQO1**–NAD(P)H quinone oxidoreductase-1; **HMOX1** –heme oxygenase 1; **ABCC/G** – human or mouse ATP-binding cassette transporters, subfamily C or G members.



Doxorubicin-resistant MCF-7<sub>DOX2</sub> and isogenic control MCF-7<sub>cc</sub> cell lines were described earlier (424) and were a kind gift from Dr. Amadeo Parissenti (Laurentian University, Sudbury, ON). Dose 8, 10, 12 correspond to selection doxorubicin doses of 19.4, 43.6, 98.1 nM respectively. CTRL cells were MCF-7 cells cultured similar to MCF-7<sub>DOX2</sub> without any drug present to account for any changes associated with long-term handling and culture of these cells. The cell lines were maintained at their selection doses. MCF-7<sub>DOX1</sub> cells, which express high levels of ABCB1, were maintained at 300 nM doxorubicin (425).

### **2.2.2 Transient transfection of cultured cells with plasmids**

N-terminal hemagglutinin (3xHA) tagged LPA<sub>1,2,3</sub> receptor ORFs inserted into Kpn1 (5') and Xho1 (3') sites within the MCS of a pCDNA3.1 vector (Life Technologies) were purchased from University of Missouri cDNA Resource Center (Rolla, MO, USA). The insert sizes were 1179, 1140 and 1146 bp respectively. An empty pCDNA3.1 vector expressing 3xHA was used as control. EGFP (13031) or EGFP-Nrf2 plasmid (21549) on a pCDNA3 vector was from Addgene (Cambridge, MA, USA) (426). mCherry-SK1, SK-eCFP and 3xHA-SK1 plasmids were obtained from GeneCopoeia (Rockville, MD, USA). The plasmids were transformed in Subcloning Efficiency DH5 $\alpha$ <sup>TM</sup> (Life Technologies), plated in LB Agar (1.5% w/v agar in LB medium) plates containing 100  $\mu$ g/ml Ampicillin and incubated at 37<sup>o</sup>C for obtaining *Escherichia Coli* colonies. They were propagated further for obtaining plasmid DNA. The plasmid DNA was isolated using the QIAprep kits (Qiagen,

Toronto, ON) and quantified using a nanodrop spectrophotometer ND-1000 (Thermo Scientific, Rockford, IL, USA). Plasmid transfections were achieved with Polyjet (Signagen, Gaithersburg, MD, USA) according to the manufacturer's instructions. Protein expression was verified by immunoblotting. Gene expression was verified by qRT-PCR and by immunoblotting for protein expression and insert sequences were verified in the Applied Genomics Core, University of Alberta.

### **2.2.3 siRNA knockdown of LPA<sub>1/2/3</sub> and Nrf2**

siRNAs for human LPAR<sub>1</sub> (a-SI00376229, b-SI00376236), Allstars Negative Control siRNA<sup>TM</sup> with no homology to any mammalian gene (SI03650318) and a positive control siRNA targeting human or mouse MAPK1<sup>TM</sup> (SI03650367) were from QIAGEN (Qiagen, Toronto, ON). siRNA transfections were achieved with INTERFERin reagent (POLYPLUS Transfection, Illkirch, France) according to the manufacturer's instructions. The siRNA conditions were initially optimized by monitoring cell death induced by Allstars Celldeath Control<sup>TM</sup> siRNA (SI04939025). MDA-MB-231 cells were seeded in 6- or 12-well plates at 150,000 and 50,000 cells per well respectively. Transfections were done at 50% confluency with siRNA-INTERFERin complex prepared in OPTI-MEM. The final concentration of siRNA resulting in a knockdown was 50-100 nM after 36-48 h incubation after transfection. The target sequences were as follows:

siRNA A 5'-CAAGACTTGATATATATTGAA-3',

siRNA B 5'-CACTATAATATTGTTCCCATATA-3'.

For RNAi silencing of Nrf2, 5 dicer-substrate siRNA (DsiRNA) duplexes were designed using Predesigned DsiRNA selection tool from Integrated DNA Technologies Inc. (Coralville, IA, USA). A non-targeting siRNA duplex that does not target any sequence in human, mouse and rat transcriptomes was used as a control. The sequences are shown below:

**TABLE 6: Nrf2 DsiRNA sequences**

|    |   |
|----|---|
| 1) | <pre> 5'  rG_rC_rA_rG_rG_rA_rC_rA_rU_rG_rG_rA_rU_rU_rG_rA_rU_rU_rG_rA_rC_rA  T  C  rG_rU_rC_rG_rU_rC_rC_rU_rG_rU_rA_rC_rC_rU_rA_rA_rA_rC_rU_rA_rA_rC_rU_rG_rU_rA_rG  5' </pre>    |
| 2) | <pre> 5'  rG_rC_rA_rC_rC_rA_rU_rU_rG_rG_rA_rG_rA_rG_rU_rU_rC_rU_rG_rU  T  T  rU_rC_rC_rG_rU_rG_rG_rU_rA_rA_rA_rC_rC_rC_rU_rC_rU_rC_rA_rA_rA_rG_rA_rC_rA_rA_rA  5' </pre>          |
| 3) | <pre> 5'  rG_rC_rA_rG_rC_rA_rU_rA_rG_rA_rG_rC_rA_rG_rG_rA_rC_rA_rU_rG_rG_rA_rG  C  A  rU_rU_rC_rG_rU_rC_rG_rU_rA_rU_rC_rU_rC_rG_rU_rC_rC_rU_rG_rU_rA_rC_rC_rU_rC_rG_rU  5' </pre> |
| 4) | <pre> 5'  rG_rC_rA_rU_rG_rA_rU_rG_rG_rA_rC_rU_rU_rG_rG_rA_rG_rU_rU_rG_rC_rA  C  C  rG_rU_rC_rG_rU_rA_rC_rU_rA_rC_rC_rU_rG_rA_rA_rC_rC_rU_rC_rA_rA_rC_rG_rG_rU_rG_rG  5' </pre>    |
| 5) | <pre> 5'  rC_rC_rA_rG_rA_rG_rA_rU_rG_rG_rC_rA_rA_rU_rG_rU_rG_rU_rU_rC_rC_rU_rU  G  T  rU_rU_rG_rG_rU_rC_rU_rC_rU_rA_rC_rC_rG_rU_rU_rA_rC_rA_rC_rA_rA_rG_rG_rA_rA_rC_rA  5' </pre> |

200,000 4T1 cells were seeded in 6 well plates and allowed to grow for one day. After 24 h the DsiRNAs were added in a fresh antibiotic-free medium at a final concentration of 40 nM per well. The DsiRNA transfections were done using Lipofectamine RNAiMAX transfection reagent (Life technologies) and Opti-MEM reduced serum medium (life technologies) according to the manufacturer’s protocol.

#### **2.2.4 Preparation of charcoal-treated serum (FBS-C)**

Two grams of activated charcoal (Nortit Nederland BV, Amsterdam, Netherlands) was washed twice with PBS and then added to 50 ml FBS. The mixture was rotated overnight at 4°C, centrifuged in 2800 rpm for 20 min and the supernatant filtered through 0.22 µm filter (Millipore, Mississauga, ON). The amount of LPA in the supernatant was determined to be <98% of that in the original serum as determined by the recovery of [<sup>32</sup>P]LPA (211). Ten % delipidated serum was prepared and used similarly to 10 % FBS in DMEM containing antibiotics.

#### **2.2.5 Adenoviral inoculation of cells**

Adenoviral overexpression of wild type or catalytically inactive mutants of PLD1 and PLD2 in a human cell line was described earlier (128). They were originally a gift from Dr. Natarajan (University of Chicago, IL, USA) and were prepared by the Gene Transfer Vector Core, University of Iowa (Iowa City, IA, USA). The adenovirus was produced using the pAdEasy-1 system (Stratagene, La Jolla, CA, USA) (427) from cDNAs encoding wild-type human PLD1 and mouse PLD2 or catalytically inactive PLD1(K899R) and PLD2(K758R) mutants. Adenovirus made from β-galactosidase-expressing vector backbone was used as a control in experiments. To infect cancer cells we used 50 plaque forming units/ cell of the adenovirus, which was diluted in full growth medium. We observed no significant cell death at this concentration for up to 48 h. Briefly, MDA-MB-231 or Dose12 MCF-7 dox-resistant cells were plated in 6 well dishes with antibiotic-free

growth medium before inoculation with virus. The virus-containing medium was replaced after 12 h. The cells were allowed to grow for another 24 h before starvation and subsequent treatments.

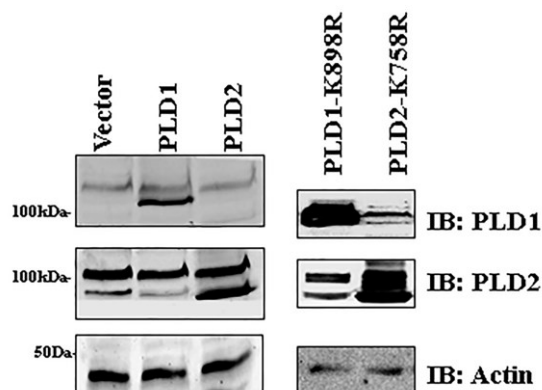


**Figure 2.1: Adenoviral overexpression of phospholipase D in cancer cells** – MCF-7 cells were infected with adenovirus as described in Section 2.2.5 before being analyzed by immunoblotting for PLD1 and PLD2. The catalytically inactive PLD1-K899R and PLD2-K758R are also shown.

## 2.2.6 shRNA knockdown of PLD1/2 in cancer cells

shRNA targeting PLD1 and 2 were a kind gift from Dr. Guangwei Du, University of Texas Health Sciences Center (Houston, TX, USA) (428). siRNAs were designed matching hPLD1 ORF 547-565 and two mPLD2 ORFs 723-741 and 1145-1164 under a H1 promoter in pCDNA6/SUPER or RFP-expressing pDsRed2 backbone. They were used for transient transfections in Dose12 MCF-7 dox-resistant cell lines using PolyJet (Signagen), according to the manufacturer's instructions. Transfection efficiency determined by RFP fluorescence was about 20%.

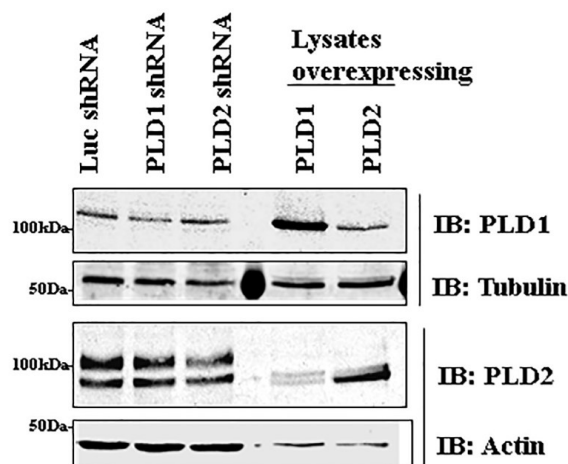


**Figure 2.2: shRNA knockdown of phospholipase D in cancer cells** – MCF-7 DOX cells transfected with PLD1 or PLD2 shRNAs as described in the protocol were analyzed by immunoblotting for their protein expression.

### 2.2.7 Plasmids, lentiviral production and stable expression in cancer cells

EGFP (Addgene: 25899), SPHK1 (Addgene: 23704), SPHK2 (Addgene: 23714) ORFs in entry vectors (429) were cloned into the destination vector PLX304 (Addgene: 25890) using the gateway LR reaction™ and transformed in chemically competent DH5 $\alpha$  cells. Lentiviral plasmids were propagated in cultures grown at 30°C for 24 h to avoid spontaneous recombination. The inserts were verified by sequencing and restriction digestion with BsrG1 (New England BioLabs, Beverly, MA, USA) in 1% agarose gel. HEK293T cells were seeded in flasks and pre-coated with 50  $\mu$ g/ml poly-L-lysine before transfection. Lentivirus particles were prepared by transiently transfecting 2  $\mu$ g of the destination vector with the third generation packaging vectors. The packaging vectors encode the gag/pol/rev genes required for producing replication-incompetent lentivirus from the tat-independent, CMV

promoter-driven PLX304 vector. The final concentrations for the vectors were 2  $\mu\text{g}$  of pMDLg (Addgene: 12251), 0.7  $\mu\text{g}$  of pRSV-Rev (Addgene: 12253) and 0.7  $\mu\text{g}$  of an envelope vector pMD2.G (Addgene: 12259), using GenJet (Signagen, Gaithersburg, MD, USA) transfection reagent according to the manufacturer's instructions. The virus containing medium was collected for up to 48 h and a high titer was prepared by ultracentrifugation (Beckman Coulter).

Cancer cells grown in 10-cm dishes were pre-treated with hexadimethrine bromide (8  $\mu\text{g}/\text{ml}$ ) containing medium before viral transduction. They were selected in 2  $\mu\text{g}/\text{ml}$  blasticidin containing medium (Life Technologies) for a week before using them in experiments. Gene expression in cells was verified by immunoblotting for the C-terminal V5 tag fused to the ORFs (Fig. 2.3). Constitutive or inducible cell lines expressing catalytically inactive R217K or WT LPP1 were made by Dr. Xiaoyun Tang, University of Alberta. 4T1 cells inducibly expressing catalytically inactive R217K or WT LPP1 were used previously in animal experiments (183).

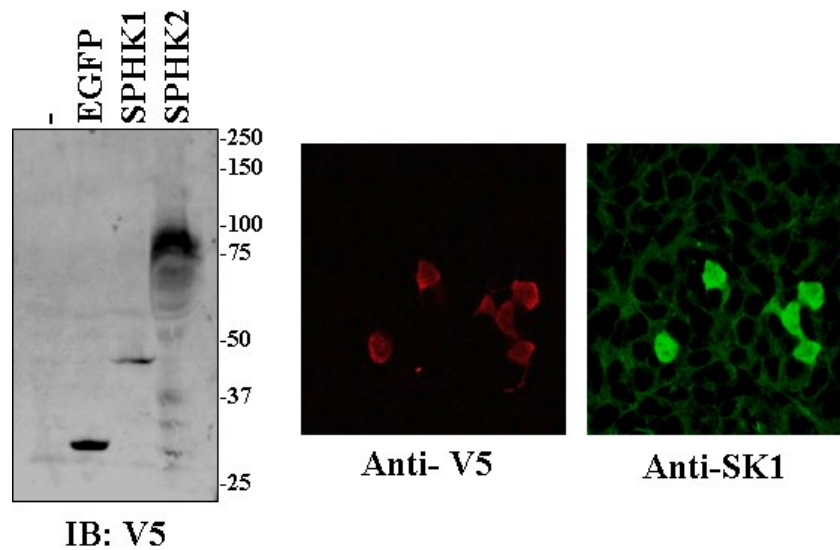


**Figure 2.3: Lentiviral expression and selection of SK1 and SK2 expressing cell lines:** MDA-MB-231 cells were infected with lentivirus and selected for a week with blasticidin (2  $\mu\text{g}/\text{ml}$ ) as described in the protocols. An immunoblot is shown on the left and confocal images are on the right for over-expression of V5-tagged sphingosine kinase-1. Scale bar – 25  $\mu\text{m}$ .

### 2.2.8 Transfection of PA probes

To study PA-formation and localization in different membranes we used a specific PA-biosensor prepared by Dr. Guangwei Du. This used the PA-binding domain of the yeast *spo20* in a pEGFP-C1 plasmid background (430) to generate a monomeric RFP-PASS, monomeric GFP-PASS or enhanced GFP-2XPASS plasmids as reported earlier (430). The plasmids were used at 1  $\mu\text{g}$  of each plasmid/well in a Polyjet complex as described in Section 2.2.2 above. At 18 h post-transfection, the cells were starved for 12 h before treating them with 1  $\mu\text{M}$  LPA for 5 min.



## **2.3 Measurement of doxorubicin sensitivity and accumulation**

### **2.3.1 Cell viability assays**

MTT (3-(4, 5-dimethylthiazolyl-2)-2, 5-diphenyltetrazolium bromide) was used to assess relative cell viability after treatment with doxorubicin or etoposide. The MTT viability assay was the first to be used in a 96-well format for high-throughput screening (431). The yellow tetrazolium salt is positively charged and enters the cell readily. It is reduced by metabolically active live cells to purple formazan in the presence of a reducing agent like NADH and NADPH. The cells were then subsequently solubilized in DMSO and the formazan was quantified by measuring the absorbance at 570 nm. Under conditions of apoptosis, the cells lose their ability to convert formazan and this can be used to differentiate viable cells from dead cells. The conditions were initially optimized to obtain linear cellular absorbance with low background and interference. Cells (50,000) were seeded into each well of a 96-well plate in full growth medium and allowed to grow overnight. The medium was replaced with starvation medium (DMEM + 0.1% BSA) for 12 h. LPA was added to this directly or in charcoal-treated medium (DMEM + 10% FBS-C) and the chemotherapeutic drug was added subsequently for up to 48 h. MTT dye (500 µg/ml) was then added for 1 h, the cells solubilized with DMSO for 10 min in a shaker and absorbance was measured at 570 nm in a spectrophotometer.

### **2.3.2 Caspase 3/7 activity assays**

Cells (2500) were plated in each well of white-walled 96-well plates and allowed to grow for 24 h. They were starved for 12 h and treated with 10  $\mu$ M LPA for 6 h. They were then treated with doxorubicin (0, 1, 2.5, 5  $\mu$ M) for another 12 h. A pan-caspase inhibitor, 50  $\mu$ M ZVAD-FMK (Enzo), was added 60 min before the treatment. A BCA protein assay was performed in the first plate while a caspase 3/7 assay was performed in the other plate. This assay is based on the conversion of a caspase 3/7 substrate (Z-DEVD-aminoluciferin) into amino-luciferin, which is used by luciferase to produce light. The Caspase-Glo reagent (100  $\mu$ l) was added to each well containing 100  $\mu$ l medium from the blank, no-treatment or drug-treated cells. The covered plates were incubated at room temperature for 2 h with gentle shaking. The resulting luminescence readings in the plates were then measured using a luminometer (Perkin-Elmer).

### **2.3.3 Doxorubicin fluorescence analysis**

Cancer cells (250,000) were grown on 6-well plates for 24 h, incubated with starvation medium containing 0.1% BSA with or without the addition of 10  $\mu$ M LPA for 12 h. The cells were then treated with 0.5  $\mu$ M doxorubicin in the presence or absence of inhibitors for up to 48 h. Cells were washed, trypsinized and resuspended in PBS + 1% BSA at 4<sup>o</sup>C. The cells were immediately subjected to FACS Canto II (BD Biosciences, Mississauga, ON) for fluorescence measurements. Mean doxorubicin fluorescence for at least 100,000 events was determined in the PE-channel.

For localization experiments, cancer cells were seeded on glass coverslips, loaded with 5  $\mu$ M doxorubicin for 4 h, washed and immediately fixed, permeabilized, counterstained with Hoescht 33342 and mounted on glass slides. Cell images were collected with an inverted fluorescence microscope (Axiovert 200, Carl Zeiss, Toronto, ON), which was equipped with a 63x/1.4 NA oil-immersion lens and a CCD camera coupled to the Northern Eclipse imaging program (Empix Imaging Inc., Mississauga, ON). Images were obtained from at least 3 fields of view and the experiment was repeated 3 times.

#### **2.3.4 [ $^{14}$ C]doxorubicin and Fluo3-AM efflux**

For Fluo3-AM efflux, MDA-MB-231 cells were grown in 6-well dishes. After 12 h starvation, the medium was changed 10% delipidated serum containing medium (211) with or without 10  $\mu$ M LPA for 24 h. Cells were trypsinized, labeled with 0.4  $\mu$ M Fluo3-AM (Life Technologies) for 1 h, centrifuged and washed twice. Fresh medium was then added with or without 5 mM probenecid. Cells were collected, washed and at least 100,000 cells were taken for analysis. Mean Fluo3 fluorescence was determined in the FITC-channel in FACS Canto II.

For measuring the uptake of doxorubicin, MDA-MB-231 cells were plated at 10000 cells/well in a 96-well plate. After 24 h they were treated with or without 10  $\mu$ M LPA overnight. The cells were then pretreated with 1 mM probenecid to inhibit efflux before labeling with starvation medium containing 5  $\mu$ M non-radioactive doxorubicin mixed with 5 nCi [ $^{14}$ C]doxorubicin (Perkin Elmer, Boston, MA, USA)

or approximately 10,000 dpm. The level of [<sup>14</sup>C]doxorubicin in the medium/cells at various times was determined by collecting 10 µl of the 200 µl/well total medium or 150 µl of 200 µl total cell lysate collected in 0.2 M NaOH. A blank of medium alone or 0.2 M NaOH was subtracted from the final counts. A few drops of glacial acetic acid were added to neutralize the solution and decrease background signal before adding two ml of scintillation fluid and counting.

## **2.4 Measurement of gene expression**

A two-step RT-PCR was carried out to measure expression of several genes at the level of mRNA. This involved mRNA isolation from protein and DNA, reverse transcription of the mRNA into cDNA and finally detection of the amplified transcripts by PCR as described below.

### **2.4.1 RNA isolation**

RNAqueous kit (Life Technologies) was used for isolation of mRNA from cell lysates. Cells grown in 3.5- or 6-cm dishes were collected using the Lysis/Binding buffer, which denatures cell proteins and inactivates RNAses. The viscosity was reduced by passing the samples through a 26-gauge needle and diluting in ethanol. Samples were extracted into a glass fiber pad-based filter cartridge, which can bind to RNA/DNA under chaotropic conditions. The bound nucleic acids were eluted into a low ionic strength buffer pre-heated to 80°C. Genomic DNA was removed using the DNA-free kit (Life Technologies). qScript

cDNA Supermix (Quanta Biosciences, Gaithersburg, MD, USA) or RT<sup>2</sup> first Strand kit (Qiagen) was used for reverse-transcription of 100-500 ng of isolated mRNA. The thermocycler conditions were as follows: Step 1 - 25<sup>0</sup>C for 10 min; Step 2 - 42<sup>0</sup>C for 60 min; Step 3 -95<sup>0</sup>C for 5 min; Step 4 - 4<sup>0</sup>C 10 min. The samples were stored in -20<sup>0</sup>C until needed.

#### **2.4.2 Quantitative real time PCR**

The cDNA samples were assayed with RT<sup>2</sup> SYBR green qPCR mastermix (Qiagen) in the Applied Biosystems 7500 real-time RT-PCR system (Life Technologies). A singleplex PCR with only one set of primers per well was used. A standard dilution curve from a mixture of the cDNA samples was used to calculate changes between the treatment and control. The thermocycler conditions were as follows: STEP 1 – 50<sup>0</sup>C for 2 min; STEP 2 - 95<sup>0</sup>C for 10 min, STEP 3 – 40 x 95<sup>0</sup>C for 15 s and 60<sup>0</sup>C for 1 min. The increase in fluorescence following denaturation of cDNA, primer annealing and amplification of PCR product was detected by the instrument. SYBR-Green dye in the mastermix binds non-specifically to all double-stranded DNA sequences and was used for detection of the amplified products in STEP 3. The change in SYBR-dye fluorescence was quantified by a specific-filter and the ROX-dye was used as a passive reference dye. Primer-dimers and non-specific products compete with the target gene for amplification, which can reduce the efficiency of the PCR. Dissociation curves were established for detection of non-specific product formation as follows: STEP 1 - 95<sup>0</sup>C for 15s; STEP 2 - 60<sup>0</sup>C

for 1 min; STEP 3 - 95°C for 15s. The melt curves plot the real-time changes in fluorescence as a function of the first derivative temperature *versus* temperature. This displays changes in fluorescence as distinct peaks. Melting temperature for the primer was verified from this step. Also primer-dimers, which appear as peaks at lower temperatures or non-specific products, which can appear elsewhere were monitored. When a primer-dimer or non-specific product was detected, the primers were discarded and new primers were designed. Amplified products were verified on a 2% agarose gel. Primers were designed with Primer-BLAST web software (NCBI) with default specificity and prepared by Integrated DNA Technologies Inc (Coralville, IA, USA). Results were expressed relative to cyclophilin A (PPIA). Similar results were obtained using hypoxanthine-guanine phosphoribosyltransferase (HPRT). The primer sequences used for the RT-PCR analysis are listed in Table 7.

### **2.4.3 Pathway gene expression array**

Tumors were collected in TRIzol reagent (Invitrogen) and kept at -80°C until needed. mRNA was isolated by chloroform extraction, purified by alcohol precipitation and by treatment with DNA free kit. RNA (1 µg) was reverse transcribed into cDNA. The samples were initially analyzed for PCR efficiency with HPRT as before. Samples with similar PCR efficiencies were analyzed using the mouse Oxidative Stress and Antioxidant Defence PCR array and cancer drug resistance PCR arrays (Qiagen). The arrays have built-in validated primers in each well, which allow analysis of 84 unique genes in a 96-well plate. The PCR analysis

was done as before with a melt curve to confirm the specificity of the PCR products.  $C_t$  numbers generated from plates corresponding to 6 control or 6 ONO-8430506 treated tumors were used to calculate fold change relative to the built in housekeeping gene. Housekeeping genes used for normalization were Actb, GAPDH and hsp90ab1. The analysis was performed online (<http://pcrdataanalysis.sabiosciences.com/pcr/arrayanalysis.php>) for fold change using the  $\Delta\Delta C_t$  method (432) and statistical significance between the two treatments for individual genes were calculated using the student's t-test ( $P < 0.01$ ). Significantly decreased genes in ONO-8430506-treated tumors were represented as fold changes (ONO-8430506 versus CTRL) and 95% confidence intervals.

#### **2.4.4 Tissue microarray data from breast cancer patients**

The protocol for tissue microarray of breast tumor biopsies was published previously (433, 434). All experiments were performed jointly with Raie Bekele and Matthew Benesch from arrays obtained from Dr. John Mackey. Briefly, tissue microarrays were generated from 176 treatment-naive breast cancer patients and 10 normal breast tissue samples (from breast reduction surgery) obtained from Canadian Breast Cancer Foundation tumor bank. Tissue microarray slides were immunostained for RALBP1 (1:50), developed and counterstained as described in detail in Section 2.7.3. Tissue staining intensity was quantified for 142 cancer samples and 5 normal tissue samples using ImageJ analysis.

**TABLE 7: PRIMER SEQUENCES USED IN PCR**

| <b>Gene</b>      | <b>5'- Forward primer- 3'</b> | <b>5'-Reverse primer-3'</b> |
|------------------|-------------------------------|-----------------------------|
| ABCC1            | GTGGAATTCCGGA ACTAC           | CGGAGGTCGTGCAGGCCG          |
| ABCG2            | AGATGGGTTTCCAAGCGTTCAT        | CCAGTCCCAGTACGACTGTGACA     |
| ABCB1            | GGCTGATTGGCTGGGCAGGAA         | TGGAACGGCCACCAAGACGTG       |
| ABCC2            | TCAGCGAGACCGTATCAGG           | TCACCAGCCAGTTCAGGG          |
| ABCC3            | GTCTCCTGTATGTGGGTCAAAGTG      | CTGTGGCGAGCGTATCTTGTG       |
| ABCC4            | ATGATTTGCTGCCGCTGAC           | CTGACACCTCTCTTCTGCTTTG      |
| ABCC5            | CAAGAGACCATCCGAGAAGC          | GAAACACACAAGCCAATCCG        |
| ABCC6            | GTCCCCACTCTTCAAAGCCA          | CGTGGTGAGCCACACAGTAG        |
| ABCC7            | GCAACAGTGGAGGAAAGCC           | TGGGTTTCATCAAGCAGCAAG       |
| ABCC8            | AAGATCCAGATCCAGAACCTGAGC      | TGTCCACCATGCGGAAGAAGG       |
| ABCC9            | TTGGTGTGCTTTTATTTTATCC        | CCGAATGGTGGTGAGTCC          |
| ABCC10           | CCTTCATCCTCAACATCCTCC         | GCAAACCTGGCACCTCTGG         |
| ABCC11           | CGTGGCTTTTGGCATTTC            | GGGTCTCTTGTCTCTGTATTTC      |
| ABCC12           | CATCACCTATCACCTCCTCTAC        | GGCTTGCGTCTCTGTTC           |
| ABCC13           | GACTCTGGCTGCTATGTGG           | CTCGCTTCCTCTCTCAACC         |
| LPA <sub>1</sub> | TTCACAGCCCCAGTTCACAG          | TTCCAAGTCCCATCACCAGC        |
| LPA <sub>2</sub> | TGCTCCTGGATGGTTTAGGC          | CTCAGCATCTCGGCAAGAGT        |
| LPA <sub>3</sub> | TGGGACGTTTTTCTGCCTGT          | TTCCAGCGAAGAAATCGGCA        |
| LPA <sub>4</sub> | TGCGCTTCCAAGCTATTACT          | GGCTTTGTGGTCSSSGGTGT        |
| LPA <sub>5</sub> | CTTGGCCCGTGTGGGGTTGG          | GGCTGGGGCCTAGAGGCTGT        |
| LPA <sub>6</sub> | AAATTGGACGTGCCTTTACG          | TAACCCAAGCACAAACACCA        |
| LPA <sub>7</sub> | GGCATA CGGCAGTCACCTAT         | GAATTGCCTGCTGGATTTGT        |
| LPA <sub>8</sub> | CCAGCTAAGCTCCAGGGAACCA        | AGCAGAGCAGGCAAAGGCT         |
| Nrf2             | TCCATTCTGAGTTACAGTGTC         | GCTGAAGGAATCCTCAAAGC        |
| HMOX1            | AACTTTCAGAAGGGCCAGGT          | CTGGGCTCTCCTTGTGTC          |
| NQO1             | TGAAGGACCCTGCGAACTTTC         | GAACACTCGCTCAAACCAGC        |
| mNrf2            | CAAGACTTGGGCCACTTAAAAGAC      | AGTAAGGCTTTCATCCTCATCAC     |
| mNQO1            | AGCTGGAAGCTGCAGACCTG          | CCTTTCAGAAATGGCTGGCA        |
| mHMOX1           | GCTAGCCTGGTGCAAGATACTG        | CACATTGGACAGAGTTCACAGC      |
| mSOD1            | CCAGTGCAGGACCTCATTTT          | CACCTTTGCCCAAGTCATCT        |
| mABCC1           | GCGCTGTCTATCGTAAGGCT          | AGAGGGGCTGACCAGATCAT        |
| mABCG2           | TGGACTCAAGCACAGCGAAT          | ATCCGCAGGGTTGTTGTAGG        |
| mABCC2           | ACTCAACACACGCCCCATCA          | TGATCGTCTTAAACTTGCTGGTGA    |
| mABCC3           | GGGCTCCAAGTTCTGGGAC           | CCGTCTTGAGCCTGGATAAC        |
| mRALBP1          | CTGGCCACTCTTGTGTTGTGC         | AAGAGGCCTTTGCTGATCCC        |
| CYPA             | CCACCGCCGAGGAAAACCGT          | AAAGGAGACGCGGCCCAAGG        |
| mCYPA            | CACCGTGTCTTCGACATCAC          | CCAGTGCTCAGAGCTCGA AAG      |



|                  |                        |                       |
|------------------|------------------------|-----------------------|
| HPRT             | CGACGAGCCCTCAGGCGAAC   | CGGGTCGCCATAACGGAGCC  |
| mHPRT            | GCTGGTGAAAAGGACCTCT    | CACAGGACTAGAACACCTGC  |
| SK1              | GCTCTGGTGGTCATGTCTGG   | GCAATAGCGTGCAGTTGGT   |
| SK2              | AGGAGCTGACCGGGAGCTGG   | AGGCCGCTGAGTCTGAGGGG  |
| S1P <sub>1</sub> | CCGGGCTCTCCGAACGCAAC   | CGGGGTGGCGCTACTCCAGA  |
| S1P <sub>2</sub> | CAGGAGACGACCTCCCGCCA   | GCTTGAGCGGACCACGCAGT  |
| S1P <sub>3</sub> | CCCATCTGGCATTGAGCGCA   | AAAAGGGCTCCTCCGTCGGCT |
| S1P <sub>4</sub> | GCACGCAGCCTCGCCTGTAT   | ACGGGGAGGTGGGGTGGTTG  |
| S1P <sub>5</sub> | GTGCCACGAAGACGCCTCC    | CCTACGCCGCAACATCCTAC  |
| SPNS2            | ACTTTGGGGTCAAGGACCGA   | AATCACCTTCTGTTGAAGCG  |
| mSPNS2           | AGAAGCCGCATCCTCAGTTAGC | CAGGCCAGAATCTCCCAAATC |
| PLX ORF          | CACCAAATCAACGGGACTT    | CAACACCACGGAATTGTCAG  |
| MAPK1            | CCAGCTGAACCACATTTTGGG  | TCAGCATTTGGGAACAGCCT  |
| ENPP2<br>m/h     | CATTTATTGGTGGAAACGCAGA | ACTTTGTCAAGCTCATTTCC  |
| IL-1 $\alpha$    | CTTCTGGGAAACTCACGGCA   | AGCACACCCAGTAGTCTTGC  |
| IL-1 $\beta$     | AACAGGCTGCTCTGGGATTC   | AGTCATCCTCATTGCCACTGT |
| IL-6             | AGTTCCTGCAGAAAAGGCAAAG | AAAGCTGCGCAGAATGAGATG |
| IL-8             | CCACCGGAAGGAACCATCTC   | CTCCTTGGCAAAACTGCACC  |
| TNF $\alpha$     | CCCATGTTGTAGCAAACCCTC  | CCCATGTTGTAGCAAACCCTC |
| IP10             | AGCAGAGGAACCTCCAGTCT   | ATGCAGGTACAGCGTACAGT  |
| MCP1             | AGCAGCAAGTGTCCCAAAGA   | TTTGCTTGTCCAGGTGGTCC  |
| GAPDH<br>m/h     | ACTTTGTCAAGCTCATTTCC   | TCTTACTCCTTGGAGGCCAT  |

**Abbreviations:**

**LPA<sub>1-8</sub>** - human LPA receptors 1-8; **S1P<sub>1-5</sub>** - human S1P receptor 1-5; **Nrf2, mNrf2** – human or mouse nuclear factor, erythroid 2-like 2; **NQO1, mNQO1** –human or mouse NAD(P)H quinone oxidoreductase-1; **HMOX1, mHMOX1** – human or mouse heme oxygenase 1; **mSOD1** – mouse superoxide dismutase 1; **ABC** – human or mouse ATP-binding cassette transporters; **SPNS2, mSPNS2** –human or mouse spinster homolog 2 (drosophila); **PLX ORF** – sequencing primers for ORF in PLX plasmid; **MAPK1**- human mitogen-activated protein kinase 1 or p42 MAPK; **CYPA, mCYPA** – human or mouse peptidylprolyl isomerase A/cyclophilin A; **HPRT, mHPRT** – human or mouse hypoxanthine phosphoribosyltransferase 1; **ENPP2 m/h** – human or mouse ATX; **IL-1 $\alpha$ , IL-1 $\beta$ , IL-6, IL-8** – human interleukins; **TNF $\alpha$**  – human tumor necrosis factor alpha; **IP10 or CXCL10** – human interferon gamma induced protein 10; **MCP1 or CCL2** – human monocyte chemotactic peptide 1; **GAPDH** – human or mouse glyceraldehyde 3-phosphate dehydrogenase.

**TABLE 8: ANTIBODIES USED IN THE STUDY**

| <b>Antibody, Clone</b>  | <b>Dilution</b> | <b>Detection</b> | <b>Supplier</b>              |
|-------------------------|-----------------|------------------|------------------------------|
| ABCC1, MRP1-m6          | 1:100           | HRP              | Enzo Lifesciences            |
| ABCG2, BXP-21           | 1:250           | HRP              | Novus Biologicals            |
| ABCB1, MDR1-D11         | 1:500           | IR680            | Santa Cruz                   |
| Nrf2, H-300             | 1:500           | IR800            | Santa Cruz                   |
| Nrf2, C-20              | 1:500           | IR800            | Santa Cruz                   |
| NQO1, A180              | 1:1000          | IR680            | Santa Cruz                   |
| HMOX1, H-105            | 1:1000          | IR800            | Cell Signaling               |
| Ki67, D3B5              | 1: 400          | HRP              | Cell Signaling               |
| Cleaved caspase 3, D175 | 1 :75           | HRP              | Cell Signaling               |
| PARP #9542              | 1:1000          | IR800            | Cell Signaling               |
| Calnexin                | 1:1000          | IR800            | Enzo Lifesciences            |
| $\beta$ -Actin, ab8227  | 1:2000          | IR800            | Abcam                        |
| GAPDH , 71.1            | 1:2000          | IR680            | Sigma                        |
| $\alpha$ -tubulin, B512 | 1:1000          | IR680            | Sigma                        |
| Lamin A/C , H-110       | 1:1000          | IR800            | Santa Cruz                   |
| HA-tag                  | 1:2000          | IR680            | Covance                      |
| V5-tag                  | 1:1000          | IR680            | Life Technologies            |
| Flag-tag                | 1;1000          | IR680            | Clontech                     |
| PLD1, 44-322            | 1:1000          | IR800            | Invitrogen                   |
| PLD2                    | 1:1000          | IR800            | Dr. Sylvain Bourgoin         |
| SK-1                    | 1:1000          | HRP              | Abcam /<br>Novus Biologicals |
| RALBP1                  | 1:1000          | IR800            | Cell Signaling               |

## 2.5 SDS-PAGE gel electrophoresis

Total cell extracts were sonicated in RIPA buffer containing 100 nM microcystin-LR and protease inhibitor cocktail to inhibit protein serine/threonine phosphatases and proteases, respectively. Tumor samples were homogenized using the TissueLyser II system (Qiagen), centrifuged and transferred to fresh tubes. Fifty to hundred µg total protein as determined by BCA assay (Pierce) was prepared in RIPA buffer containing 1X Sample loading buffer (6X- 375 mM Tris-HCl pH 6.8, 6% SDS, 48% glycerol, 0.003% bromophenol blue with 10% 2-mercaptoethanol added freshly before use). The samples were boiled for 5 min, spun down briefly and loaded into a 15- or 10-well SDS-PAGE gel. Precision Plus Protein All Blue Standards (Bio-Rad, Mississauga, ON) were loaded as a molecular weight ladder consisting of 250, 150, 100, 75, 50, 37, 25, 20, 15 and 10 kDa protein standards. For western blots of membrane proteins (eg: LPA receptor) the samples aggregated when they were boiled leading to poor resolution. These samples were treated with a urea-containing buffer with a loading dye (3x – 62 mM Tris-HCl pH 6.8, 6 M urea, 10% glycerol, 2% SDS, 0.003% bromophenol blue, 5% 2-mercaptoethanol) and loaded without boiling for improved recovery. Nitrocellulose membranes were blocked with 5% non-fat dry milk in TBST buffer (10 mM Tris-HCl pH 7.4, 150 mM NaCl, 0.1% Tween-20) and incubated with primary antibodies overnight at 4°C with gentle shaking. Blots were washed three times with TBST and incubated with horseradish peroxidase-conjugated secondary antibodies (1:10,000). Immuno-complexes were detected using Immunstar Western C kit (Biorad). PVDF

membranes were treated with blocking buffer (LI-COR Biosciences, Lincoln, NE, USA) in PBS containing 0.1% Tween-20 and incubated with primary antibodies overnight at 4°C with gentle shaking. Alexa Fluor® 680- and IRDye® 800CW- (LICOR) conjugated secondary antibodies (1:10,000) were used for staining and the fluorescent signals were visualized with the LICOR Odyssey® Imaging System. The antibodies used are as follows: Nrf2 (H-300), Nrf2 (C-20), MDR1 (D11), NQO1 (A180), Lamin A/C (H-110) were from Santa Cruz Biotechnology (Santa Cruz, CA, USA); PARP, HMOX1 (H105), Ki67 (D3B5), RALBP1 (I33) and cleaved caspase 3 (D175) were from Cell Signaling (Danvers, MA, USA); GAPDH and  $\alpha$ -tubulin were from Sigma-Aldrich; MRP1 (m6) and calnexin was from Enzo Lifesciences; ABCG2 (BXP-21), SK1 were from Novus Biologicals (Oakville, ON); PLD1 was from Biosource international (Invitrogen); Rabbit polyclonal antibody against PLD2 was a gift from Dr. Sylvain Bourgoin (Université Laval, QC); HA-tag antibody was from Covance (Princeton, NJ, USA); Flag-tag was from Clontech; V5-tag was from Life Technologies;  $\beta$ -Actin and SK1 were from Abcam (Toronto, ON).

### **2.5.1 Nuclear fractionation**

Cells were grown in 15-cm dishes, starved for 12 h and then treated with LPA or wls31 for 6 h. Cells were then trypsinized, pelleted and resuspended in 2 ml of hypotonic buffer (10 mM HEPES, pH 7.9, 1.5 mM MgCl<sub>2</sub>, 10 mM KCl, 0.5 mM DTT and protease/phosphatase inhibitors) maintained on an ice-bath. The hypotonic buffer was used to swell the cells prior to breaking them open. Cells were then

homogenized with a pre-chilled Dounce homogenizer by applying 10-15 tight strokes. The lysates were then centrifuged at 2000 rpm for 10 min at 4<sup>0</sup>C to obtain a supernatant and nuclear pellet. The supernatant was retained as the cytoplasmic fraction. The nuclear pellet was re-suspended in 1 ml of sucrose buffer I (0.25 M sucrose/10 mM MgCl<sub>2</sub>) layered over 1 ml of sucrose buffer II (0.88 M sucrose/0.5 mM MgCl<sub>2</sub>) and centrifuged at 13,000 rpm (DeSaga, Darmstadt, Germany) for 30 min at 4<sup>0</sup>C to obtain a cleaner nuclear pellet. The resulting 0.1 ml nuclear fraction was dissolved in 0.9 ml of RIPA buffer containing protease and phosphatases inhibitors. RIPA buffer (5X, 0.4 ml) was added to 1.6 ml of the resulting cytoplasmic fraction. Both fractions were sonicated on ice, centrifuged at 13,000 rpm (Desaga) and transferred to another tube (435). Protein concentrations were determined by BCA and equal amounts were loaded for immunoblotting.

## **2.6 Immunocytochemistry**

Cells were seeded on glass coverslips in a 12-well plate pre-coated with fibronectin (10 µg/ml) and grown for 24 h. Twenty four h after transfections, the cells were starved overnight followed by treatments as before. After treatments, cells were immediately fixed with 4% paraformaldehyde (freshly prepared) for 30 min, permeabilized with 10% Triton-X 100, blocked with 1% donkey serum in PBS for 1 h and washed. Samples were then treated with mouse anti-HA in blocking buffer at 4<sup>0</sup>C overnight and washed thrice. Coverslips were stained with donkey anti-mouse Alexa Fluor 555 (Life Technologies) for 1 h. They were then treated with Hoechst

33342 (Life Technologies) for 10 min to stain the DNA, washed, mounted with Prolong Gold Antifade (Invitrogen, Carlsbad, CA, USA) and sealed. Coverslips were then viewed in Leica TCS SP5 confocal microscope (Concord, ON) and at least 20 random cells from 3 different experiments were used for quantification.

## **2.7 Mouse model of breast cancer**

The syngeneic orthotopic mouse model of breast tumor growth and metastasis was described previously (137). All procedures were performed in accordance with the Canadian Council of Animal Care as approved by the University of Alberta Animal Welfare Committee. Female BALB/c mice were from Charles River (Kingston, ON). Mice were maintained in the animal facility at 21°C, 55% humidity and a standard 12 h light/dark cycle with free access to standard laboratory diet and water. For the orthotopic model, 4T1 or 4T1-12B cells (400,000 cells/ml) grown in cell culture were washed, trypsinized and resuspended in phenol red- and serum-free medium. An equal volume of Matrigel (BD Biosciences, Mississauga, ON) was added and a total of 100 µl of the mixture (20,000 cells + Matrigel) was injected using a 27-gauge needle into the fourth mammary fat pad of anesthetized mice. For the tail-vein metastatic model, 4T1 cells were injected directly into the tail-vein of the healthy mice in a total of 100 µl ( $1.5 \times 10^5$  cells in PBS).

### **2.7.1 Preparation and administration of drugs**

ONO-8430506 (Ono Pharmaceuticals Ltd., Osaka, Japan) was used as an ATX inhibitor *in vivo* as described previously (137, 262). ONO-8430506 stock solution was (10 mg/ml in 25 mM NaOH, heated to 60°C for 5 min) dissolved in water and administered at 10 mg/kg every day. Doxorubicin (0.32-0.64 mg/ml) was dissolved in PBS by briefly warming at 37°C and filtered through a 0.22 µm filter. Tamoxifen was prepared in 100% peanut oil at stock concentration of 50 mg/ml. For experiments with the ATX inhibitor and doxorubicin, >60 mice were randomly divided into 4 groups. Group 1 and 2 were gavaged daily with water and Groups 3 and 4 were gavaged daily with 10 mg/kg ONO-8430506 in water. Groups 1 and 3 received PBS by intraperitoneal (i.p.) injections while 2 and 4 received 4 mg/kg doxorubicin i.p. every third day starting from 3 days after tumor injection. Body weights were measured every day before the next gavage. Tumor volumes were estimated every day after Day 4 by taking caliper measurements of length and width using the formula  $0.52 \times \text{width}^2 \times \text{length}$ . On Day 12 or Day 21 the mice from all 4 groups were sacrificed, primary tumor and various organs were collected by dissection and flash frozen for various applications. For experiments with tamoxifen, the drug was given orally to mice with a loading dose of 400 mg/kg on Day 1 and 2, followed by a maintenance dose of 200 mg/kg for next four days and finally at 100 mg/kg for the remaining four days before tumor excision. All control mice received just the peanut oil. Mice with 4T1 tumors were euthanized on Day 11 and the primary tumors were excised and weighed. Collected tissue and tumors were either placed in 10% formalin for paraffin imbedding or flash frozen in liquid nitrogen.

### **2.7.2 Measurement of spontaneous and experimental metastasis**

To measure spontaneous metastasis, paraffin-embedded sections of the lungs and livers at Day 21 were prepared and stained with hematoxylin and eosin stain by the histology core at Alberta Diabetes Institute, University of Alberta. Images were acquired at 5X and 63X magnification using a Zeiss Axioskop 2 imaging system (Carl Zeiss Canada, Ltd, Toronto, ON). To measure experimental macro-metastasis, surface nodules were counted on the left lung after staining with Bouin's solution (picric acid, saturated aqueous solution – 75 ml; formalin, 37% aqueous solution – 25 ml; acetic acid, glacial – 5 ml).

### **2.7.3 Immunohistochemistry analysis**

The paraffin-embedded 5 µm tumor sections were coated on glass slides and immunostained using the Dako LSAB™+ Universal Kit (K0679) (137). The technique is based on antigen retrieval through a Labeled Streptavidin Biotin (LSAB) staining reagent. The primary antibody is bound to a biotinylated antibody, which is then linked to an alkaline phosphatase-labeled streptavidin. Staining was visualized using Dako Envision™+ Rabbit HRP (K4002) (Burlington, ON). Slides were initially dipped 3 times in xylene for 10 min. This was followed soaking in 100% ethanol for 3 x 20 dips, 80% ethanol for 1 x 20 dips, 50% ethanol in 1 x 20 dips and finally in running distilled water for 5 min. The slides were microwaved in a hydrated pressure cooker chamber for 20 min in 10 mM citric acid buffer pH 6.0. Cooled slides were again washed in running water. The slides were then blocked with 9:1 solution of methanol: 30% hydrogen peroxide to remove background from



endogenous peroxidase activity. They were soaked in PBS for 10 min, outlined in a wax pen and incubated with Dako blocking buffer for 30 min. Primary antibody incubation was done in the same buffer overnight at 4<sup>0</sup>C. Following PBS washes after every step, the slides were incubated with the secondary antibody for 30 min and developed using DAKO chromogen, which stains the sections brown. The reaction was quenched with a PBS wash followed by washing with running distilled water. One % copper sulfate was added to enhance the staining followed by another wash. Harris modified method hematoxylin (Fisher Scientific) was used to counterstain the slides for 3 min. The slides were then rinsed gently under warm tap water followed by washing in ethanol and xylene baths. Cover slips were mounted on the dry slides with xylene-based mounting medium (Fisher Scientific). Images were acquired at 5X and 63X using a Zeiss Axioskop 2 imaging system (Carl Zeiss Canada, Toronto, ON). 5X magnification images were used for counting and image analysis.

#### **2.7.4 Glutathione (GSH) measurements**

Reduced GSH was measured from freshly collected tumors using a specific GSH-Glo assay (Promega) according to the manufacturer's instructions. The assay is based on the conversion of the synthetic luciferase substrate into luciferin in the presence of reduced glutathione (GSH). The free luciferin thus reacts with luciferase buffer and the chemi-luminescent reaction is measured in a luminometer as relative light units. Total Glutathione (GSH + GSSG) levels were also measured

simultaneously by performing the assay in the presence of a reducing agent, Tris-(2-carboxyethyl) phosphine. A GSH standard curve was performed in the same plate. Samples were normalized to protein concentrations as measured using the BCA assay. Five mg of freshly extracted tumor sample was homogenized in 1 ml of PBS containing 2 mM EDTA. The samples were centrifuged and the supernatant was collected in a different tube. Fifty  $\mu$ l of the sample was added to wells of a white-wall 96 well plate and incubated with 50  $\mu$ l of the 2x GSH-Glo reagent for 30 min at room temperature with gentle shaking. Identical steps were performed to a well containing TCEP (500  $\mu$ M) to measure total glutathione. One hundred  $\mu$ l of the luciferin detection reagent was added and the samples were incubated for another 15 min at room temperature before measurement in a luminometer (Perkin Elmer).

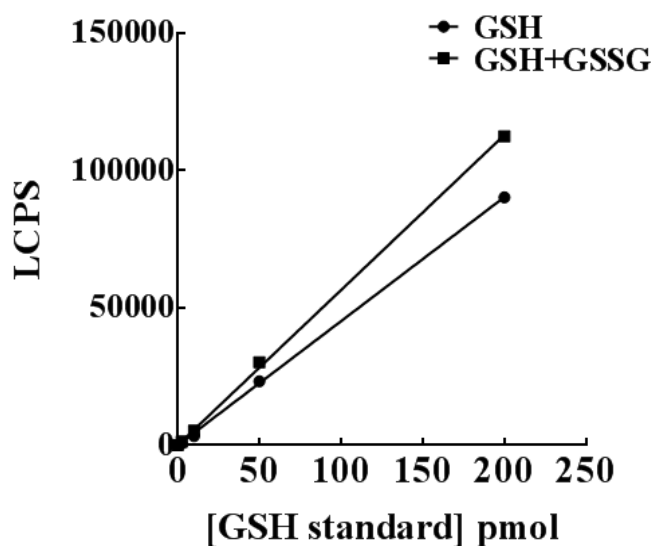


**Figure 2.4: Measurement of reduced and total glutathione from standards** – Luminescence readings from reduced and total glutathione standards were assessed as described in Section 2.7.4.

### **2.7.5 Leukocyte counts**

Blood was drawn from the mice using heparanized capillary tubes and immediately centrifuged in a bench top centrifuge at 13000 rpm for 5 min. The supernatant was transferred to a new tube for analysis of LPA by mass spectrometry. Ten  $\mu\text{l}$  of the pellet was added to 190  $\mu\text{l}$  red blood cell lysis buffer (388 mM  $\text{NH}_4\text{Cl}$ , 29.7 mM  $\text{NaHCO}_3$ , 25  $\mu\text{M}$   $\text{Na}_2\text{EDTA}$ ; pH 7.2). This buffer is a hypotonic solution that lyses red blood cells selectively by osmosis and leaves the white blood cells intact. The remaining white blood cells from each sample were counted using a hemocytometer.

### **2.7.6 Enzyme-linked immunosorbent assay (ELISA)**

#### **2.7.6.1 Multiplex cytokine/chemokine arrays**

Mouse cytokines, chemokines and growth factors were analyzed by Eve Technologies Corp. (Calgary, AB) using a MILLIPLEX mouse Cytokine/Chemokine 31-plex kit (Millipore, St. Charles, MO, USA), according to the manufacturer's protocol on a Luminex 100 system (Luminex, Austin, TX, USA). The following cytokine, chemokines and growth factors were analyzed from the multiplex array using individual standard curves: Eotaxin, G-CSF, GM-CSF,  $\text{IFN}\gamma$ ,  $\text{IL-1}\alpha$ ,  $\text{IL-1}\beta$ , IL-2, IL-3, IL-4, IL-5, IL-6, IL-7, IL-9, IL-10, IL-12 p40, IL-12 p70, IL-13, IL-15, IL-17, IP-10, KC/GRO, LIF, LIX, MCP-1, M-CSF, MIG, MIP-1a, MIP-1b, MIP2, RANTES,  $\text{TNF}\alpha$  and VEGF. Tumor or mammary adipose tissues specimens (20 mg) were homogenized in 400  $\mu\text{l}$  of 20 mM Tris HCl (pH 7.5) buffer

with 0.5% Tween 20, 150 mM NaCl and protease inhibitor, then centrifuged for 10 min at 4°C and the supernatant was transferred to a fresh tube. Protein content was measured using the BCA protein assay (Fisher Scientific) and adjusted to 0.5-2 µg/µl. One hundred µl of the normalized protein samples were shipped to Eve Technologies for analysis.

#### **2.7.6.2 ATX Sandwich ELISA**

ATX protein concentration was quantified from 2x 100 µl of tumor or fat pad tissue preparation (from 400 µl/20 mg supernatant prepared as before for the cytokine/chemokine arrays) using the ATX sandwich ELISA Kit (K-5600) from Echelon Biosciences Inc (Salt Lake City, UT, USA). A standard curve was run simultaneously with samples using recombinant ATX (0, 1.5625, 3.125, 6.25, 12.5, 25, 50 and 100 ng/ml). Samples and standards were incubated on the sandwich detection plate for 1 h at room temperature with gentle shaking. The plate was washed three times with 200 µl per well of PBST (PBS + 0.1% Tween 20). The plate was incubated with ATX antibody solution (100 µl per well) for 1 h at room temperature with gentle shaking and washed again with PBST three times. This was repeated with the secondary detection reagent. Blue color was allowed to develop in the dark using TMB solution (100 µl per well) added onto the plate for 30 min. The reaction was stopped with 50 µl of 1 N H<sub>2</sub>SO<sub>4</sub>. Absorbance was measured at 450 nm. ATX concentrations were determined by interpolating the standard curves and normalized to protein concentrations determined by the BCA assay (Thermo Scientific).

### **2.7.7 ATX activity assay**

The assay is based on release of choline by ATX under saturating LPC concentrations. The released choline is treated with choline oxidase to form hydrogen peroxide. The hydrogen peroxide formed is then detected in a HRP-based colorimetric detection kit that oxidizes TOOS (N-Ethyl-N-(2-hydroxy-3-sulfopropyl)-3-methylaniline, sodium salt, dehydrate) and 4-aminoantipyrine to form a purple product. One set of samples was separately treated with excess ONO-8430506 to block ATX activity completely and this provides the choline background for the total choline detected (154).

Ten  $\mu\text{l}$  of plasma from 10 vehicle or doxorubicin-treated mice was mixed with 10  $\mu\text{l}$  of Buffer A (100 mM Tris-HCl pH 9.0, 500 mM NaCl, 5 mM  $\text{MgCl}_2$ , 0.05% (v/v) Triton X-100). Five  $\mu\text{l}$  of Buffer A containing 10% DMSO or 10% DMSO containing 1 mM ONO-8430506 was added to the plasma samples and incubated at 37°C for 30 min. Twenty five  $\mu\text{l}$  of 6 mM C14:0 LPC in Buffer A was then added to the samples and incubated for 6 h at 37°C. Twenty  $\mu\text{l}$  of each sample in duplicates was pipetted into a 96-well plate and incubated with 90  $\mu\text{l}$  of Buffer C [9.65 ml Buffer B (100 mM Tris-HCl, pH 8.5, 5 mM  $\text{CaCl}_2$ ), 110  $\mu\text{l}$  of 30 mM TOOS (Dojindo Molecular Technologies, Rockville, MD, USA), 110  $\mu\text{l}$  of 50 mM 4-aminoantipyrine, 6.6  $\mu\text{l}$  of 1000 units/ml horseradish peroxidase, and 110  $\mu\text{l}$  of 300 units/ml choline oxidase]. Choline formation was measured after 20 min incubation using a spectrophotometer at 550 nm.

## **2.8 Measurement of SK1 activity**

The radioactive assay for determining sphingosine kinase activity was performed as described (436) with the following modifications : 0, 20, 40 µg protein lysates were incubated 100 µM sphingosine in 4 mg/ml BSA solution, 15 mM MgCl<sub>2</sub> and 3.5 mM ATP containing 2.5 µCi of [ $\gamma$ -<sup>32</sup>P]ATP (Perkin-Elmer, Mississauga, ON) in sphingosine kinase buffer (20 mM Tris-HCl pH 7.4, 1 mM EDTA, 0.5 µM deoxyripyridoxine, 15 mM NaF, 2 mM DTT, 1 mM sodium orthovanadate, 20% glycerol, 8.64 mg/ml  $\beta$ -glycerolphosphate, 30 nM microcystin-LR, 0.01 mg/ml trypsin inhibitor and protease inhibitor cocktail) for 60 min at 37°C. The activity of SK1 was measured in the presence of 0.5% Triton X-100. The activity of SK2 was determined in the presence of 0.5 M KCl (437). [<sup>32</sup>P]S1P was extracted into water-saturated butanol containing 10 nmoles of non-radioactive S1P as carrier (436), resolved on a silica TLC plate and visualized by spraying with 0.25% ninhydrin in acetone. The position of [<sup>32</sup>P]S1P was confirmed by autoradiography. Bands containing radioactive S1P were cut out. Two hundred µl of distilled H<sub>2</sub>O was added to hydrate the silica followed by 2 ml of scintillation fluid and the <sup>32</sup>P was quantified using a liquid scintillation counter.

### **2.8.1 Separation of cytosol from cell ghost by digitonin lysis**

Membrane and soluble fractions were prepared by digitonin lysis as described earlier (438). Briefly cells were treated with agonists for various times before adding the digitonin lysis buffer (10 mM HEPES, 0.5 mM DTT, 0.081 mM

digitonin, pH 7.4, protease and phosphatase inhibitors) on ice. The digitonin-soluble cytosolic fraction was collected after 5 min, the dishes were washed and the membrane fraction was collected in cell ghost buffer (10 mM HEPES, 0.5 mM DTT, 250 mM sucrose, pH 7.4, protease and phosphatase inhibitors). Alternatively, the membrane preparations were extracted in SK1 buffer described above for activity assays. The effectiveness of membrane/cytosolic separation was verified by LDH activity in the extracts and western blotting for calnexin and GAPDH (Fig. 5.5). To determine LDH activity, the conversion of NADH to NAD<sup>+</sup> was measured in a freshly made buffer (167 mM Tris pH 7.4, 1.33 mM sodium pyruvate and 0.33 mM NADH) containing cytosolic/membrane extracts in a multiwell plate and measuring absorbance at 340 nm (Spectramax 250; Molecular devices corporation, Sunnydale, CA, USA). Between 85-90% of total LDH activity was detected in the cytosolic fractions under these conditions indicating a successful lysis.

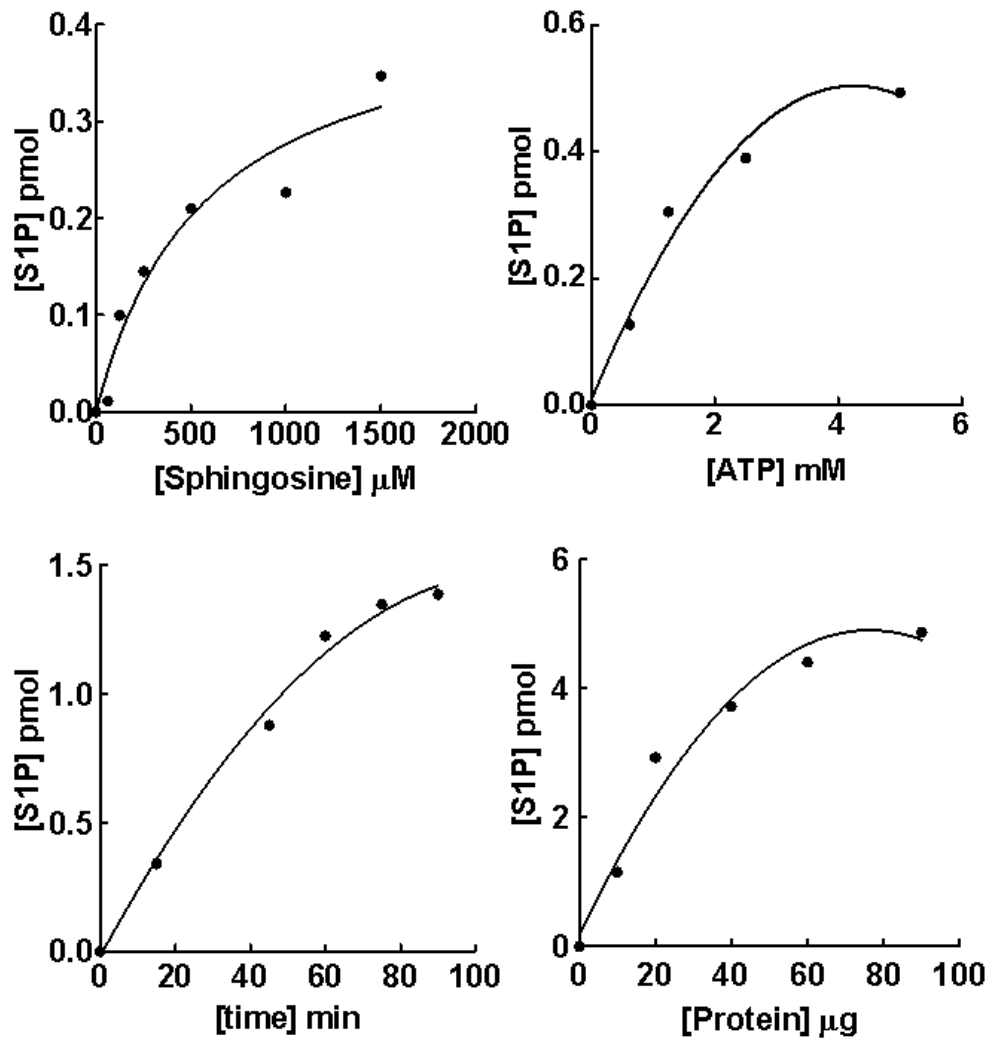


**Figure 2.5: Optimization of SK1 assay conditions** – Variable assay conditions were optimized for linearity of detection of sphingosine kinase activity from cell lysates as described in the protocol.



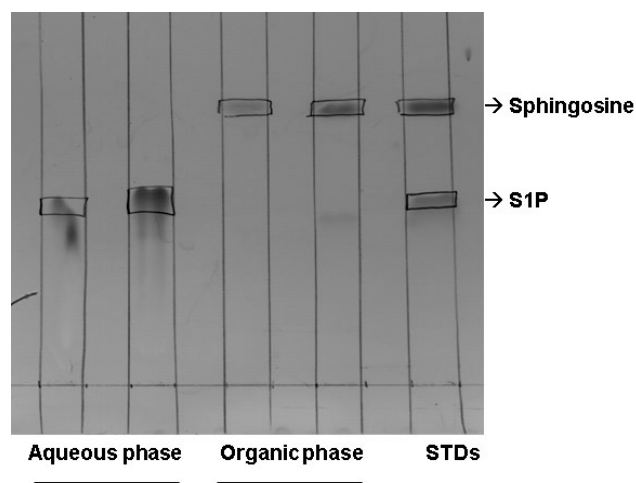


**Figure 2.6: TLC separation of [<sup>3</sup>H]S1P and [<sup>3</sup>H]sphingosine by differential extraction – S1P estimation by [<sup>3</sup>H]sphingosine labeling and differential extraction as described in the protocol.**

## 2.9 Sphingosine labeling and S1P secretion

S1P measurements were performed by labeling the cells with [<sup>3</sup>H]sphingosine (Perkin Elmer) and differential extraction of the sphingolipids as described previously (332, 439). Briefly, cells grown on 6-well plates were labeled with [<sup>3</sup>H]sphingosine (1.5 μM and 0.4 μCi) in starvation medium for 30 min. Treatment was done in fresh medium for 1 h before collecting the medium and cells. The lipids were extracted with methanol: chloroform: 1 M NaCl: 3 N NaOH (1:1:1:0.1). This resulted in selective partitioning of S1P into the aqueous phase at alkaline pH. Sphingosine, ceramides and other sphingolipids were still retained in the organic phase (332, 439). The differential separation of [<sup>3</sup>H]sphingosine from [<sup>3</sup>H]S1P is shown after TLC separation and ninhydrin staining of the aqueous and organic phase extracts (Fig. 2.6). Five hundred μl of each extract was used for scintillation counting. Alternatively, endogenous/agonist-induced long-term

secretion of S1P was measured by LC-MS (440). Briefly, cells were incubated in medium containing 1 mM semicarbazide (335) for 24 h. Cells were collected in 1 ml of PBS + 0.2% SDS. Five hundred  $\mu$ l of medium or cell lysate was mixed with 60  $\mu$ l of 200 mM citric acid + 270 mM phosphate buffer (pH 4). Twenty ng of  $^{13}\text{C}_2\text{D}_2$ -S1P (Toronto Research Chemicals, ON) was added as internal standard and the samples were sonicated. One ml of butan-1-ol and 500  $\mu$ l of water-saturated butanol were added to extract S1P. The butanol phase was dried down completely and re-dissolved in 200  $\mu$ l of ethanol. The results were expressed as pmol of S1P secreted/ml of medium or pmol of S1P/ $\mu$ g of protein.

#### **2.10 Measurement of PLD activity by formation of phosphatidylbutanol**

The PLD assay was performed as described earlier (185). Briefly, cells (200,000) were labeled with 1% BSA containing [ $^3\text{H}$ ]palmitate (5  $\mu$ Ci for 18 h). The medium was removed and the cells were then pre-treated with or without PLD inhibitors for 1 h before adding 30 mM butan-1-ol for 15 min. Phosphatidylbutanol (PB) formation were measured in the presence of 5  $\mu$ M LPA for 5 min to determine PLD activity. The reactions were stopped by ice-cold HEPES washes, cells were collected by scraping twice in 0.5 ml methanol. One molar KCl containing 0.2 M HCl (0.9 ml) was added to this to extract lipids. The bottom organic phase was dried under  $\text{N}_2$  before re-dissolving in chloroform/methanol (9:1) containing 50  $\mu$ g of 1,2 dioleoyl-*sn*-glycerol 3-phosphobutanol (Avanti). The lipids were resolved on a silica gel TLC plate (Merck, Germany) using ethylacetate/iso-octane/acetic acid/water

(130:20:30:100 v/v). Iodine staining was used to detect phosphatidylbutanol and the radioactivity of individual bands was measured by liquid scintillation. PLD activity was calculated as percentage of PB formed relative to the total labeling of phosphatidylcholine (PC) + phosphatidylethanolamine (PE).

### **2.11 Statistical Analysis**

Results were expressed as mean  $\pm$  SEM. A paired or unpaired two-tailed t-test was used to determine p values. For multiple comparisons, one-way or two-way ANOVA with a Bonferonni post-hoc test was used. \*, P<0.05 was considered significant. All analysis was performed in Graphpad Prism 6 (Graphpad, La Jolla, CA, USA).

### **2.12 Ethics approval**

Animal procedures were performed in accordance with the Canadian Council of Animal Care as approved by the University of Alberta Animal Welfare Committee. Human samples were obtained with approval of University of Alberta Health Research Ethics Board ID Pro00018758. De-identified patient data was obtained with approval from the Health Research Ethics Board of Alberta – Cancer Committee (“Lysophosphatidate Signaling as a Promoter of Breast Cancer Therapy Resistance and Metastasis”, ID 26195,01/16/2014).

**CHAPTER 3 – LYSOPHOSPHATIDATE SIGNALING REGULATES THE  
EXPRESSION OF MDRT AND ANTIOXIDANT GENES THROUGH  
INCREASED NRF2 EXPRESSION**

**A version of this chapter has been published in:**

**Venkatraman G**, Benesch MGK, Tang X, Dewald J, McMullen TPW and Brindley DN.  
(2015) Lysophosphatidate signaling stabilizes and increases the expression of genes  
involved in drug resistance and oxidative stress response: implications to cancer  
chemotherapy. *FASEB J* 29, 772-785.

### 3 CHAPTER 3

#### 3.1 INTRODUCTION

LPA is a bioactive lipid with ascribed roles in inflammation, wound healing and tissue remodeling in normal adults. In cancers, increased LPA signaling contributes to tumor progression and protects from the cytotoxic effects of chemotherapeutics (Discussed in Section 1.3). Our group previously showed that increased activation of PI3K signaling and decreased ceramide production contributes to taxol-resistance in breast cancer cells (211). However, it is still unclear how LPA coordinates these actions and contributes to the development of multi-drug resistance.

Modifications to drug uptake, efflux and metabolism are commonly observed as an adaptive response to the cytotoxic effects of chemotherapeutic drugs in cancer cells (Section 1.1). Nrf2, a transcription factor with short half-life, mediates the adaptive response to oxidative damage through increased stabilization, activation and binding to cis-acting antioxidant regulatory element (ARE) (422). Under normal conditions, Nrf2 is constantly targeted for ubiquitinylation and proteosomal degradation by an adaptor protein called Keap1 (426, 441). Pro-oxidants modify the critical cysteine thiols in Keap1 (and Nrf2) leading to Nrf2 stabilization and activation. Keap1-independent mechanisms for Nrf2 activation have been proposed as well. The chemical activator of Nrf2, *tert*-butylhydroquinone (*t*-BHQ), increases Nrf2 stabilization and activation of downstream target genes including drug metabolizing enzymes and drug transporters (422).

Nrf2 expression is high in several cancers including breast, lung, head and neck, ovarian and endometrial cancers (42). Frequent somatic mutations in Nrf2 or its adaptor proteins have been found in cancers such as lung cancer. Elevated Nrf2 increases tumor cell proliferation (442, 443), resistance to chemotherapies (45, 444) and suppression of reactive oxygen species (445). Nrf2 increases the expression of MDRT including ABCC1 (421, 446) and ABCG2 (83). Increased expression of ABC-transporters contributes to the acquisition and development of chemoresistance in breast cancer by decreased accumulation of cytotoxic chemotherapies and toxic oxidation products (424).

It has been suggested that blocking Nrf2 signaling could be an effective strategy in improving chemotherapy in several cancers (42). However, we know relatively little about how Nrf2 expression is regulated in cancers. We hypothesized that LPA increases the activity and expression of MDRT through increased Nrf2 stabilization in cancer cells. Increased Nrf2 turnover and ARE activation protects cancer cell from chemotherapy-induced apoptosis and contributes to chemoresistance. This chapter will provide evidence to support this hypothesis.

## **3.2 Results**

### **3.2.1 LPA protects cancer cells from doxorubicin-induced apoptosis**

Initially we tested the effects of LPA signaling on the sensitivity of cancer cells to different chemotherapeutics. Cancer cells grown in the presence or absence of LPA were treated with doxorubicin, an anthracycline, commonly used to treat

metastatic breast cancers. We also used a topoisomerase inhibitor, etoposide, and an antifolate, methotrexate, which have been used in the past to treat breast cancers. We found that LPA-treatment increased the relative cell viability of triple negative MDA-MB-231 cells treated with therapeutically effective dose of doxorubicin ( $\leq 0.5 \mu\text{M}$ ) (Fig. 3.1A). Similarly, LPA was effective against etoposide ( $\leq 12 \mu\text{M}$ ) (Fig. 3.1B). Unlike doxorubicin and etoposide, methotrexate only marginally affected cell viability in MDA-MB-231 cells even at relatively high concentrations in our experiments (Fig. 3.1C) and no significant differences among treatments were observed.

Poly-ADP ribose polymerase (PARP) undergoes caspase-induced proteolytic cleavage from an 116 kDa protein to 85 kDa and 25 kDa products during chemotherapy-induced apoptosis (447, 448). This is true for a variety of chemotherapeutics including doxorubicin (449).

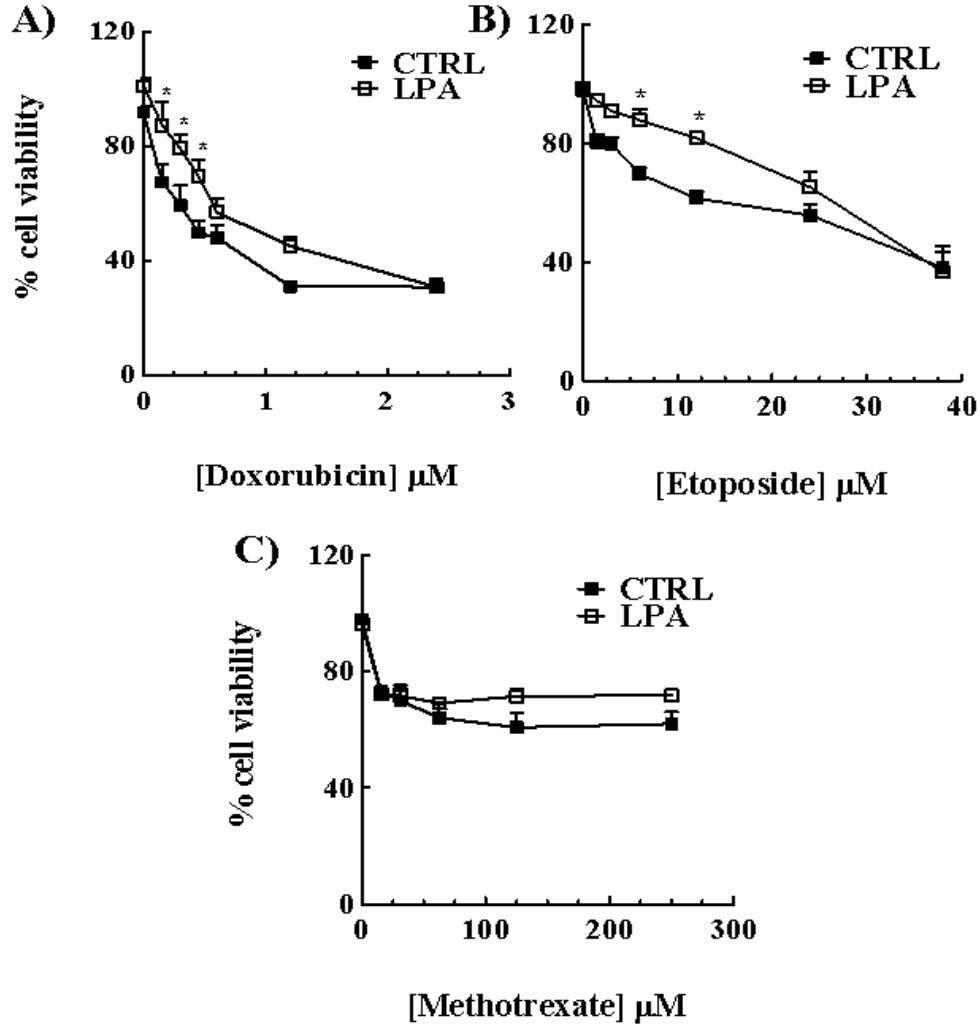


**Figure 3.1: Increased cell-viability to drugs in LPA-treated MDA-MB-231 breast cancer cells.** Cells were serum starved for 12 h and treated with vehicle (0.1% BSA) or LPA (10  $\mu\text{M}$  in 0.1% BSA) for 12 h followed by various concentrations of doxorubicin (A) or etoposide (B) or methotrexate (C) for 48 h. The relative cell viability was defined by MTT oxidation and was expressed relative to no drug treatment for 6 independent assays in A and 4 experiments in B and C. Results are expressed as means  $\pm$  SEM. Significance was calculated by two-way ANOVA with post-hoc test.\*  $p < 0.05$ .



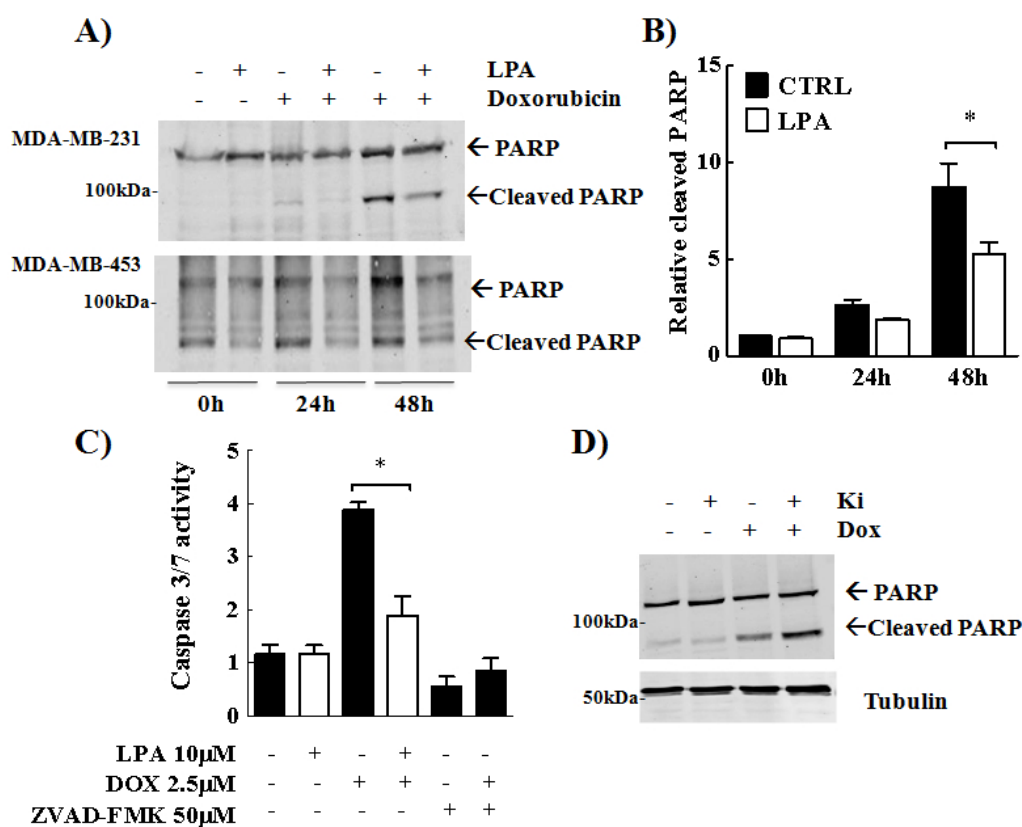


**Figure 3.2: Decreased PARP cleavage and apoptosis in breast cancer cells treated with LPA** - **A)** Cells were treated as before with vehicle or 0.5  $\mu\text{M}$  doxorubicin for 0, 24 or 48 h and immunoblotted for PARP. **B)** PARP cleavage was expressed relative to tubulin levels for 3 independent assays in MDA-MB-231 cells. **C)** Cells were treated as above with 2.5  $\mu\text{M}$  doxorubicin (Dox) for 12 h in the presence or absence of LPA. The pan-caspase inhibitor, ZVAD\_FMK was used to inhibit caspase activation. Caspase 3/7 activity was measured by luminescence measurements and expressed relative to no drug treatment for 6 independent assays. **D)** Cells grown in 10% FBS were pre-treated with LPA receptor antagonist Ki16425 (20  $\mu\text{M}$ ) for 12 h followed by 0.5  $\mu\text{M}$  doxorubicin for 48 h. Cell lysates were immunoblotted for PARP cleavage as before. Results are expressed as means  $\pm$  SEM. One-way ANOVA with post-hoc test was used for determining significance. \*  $p < 0.05$ .

We could detect doxorubicin-induced PARP cleavage as early as 24 h and also at 48 h in doxorubicin-treated cells. The protective effect of LPA as seen in cell viability after 48 h drug treatment was also reflected in decreased PARP cleavage. We found that LPA treatment significantly decreased doxorubicin-induced cleavage

of PARP (85 kDa) in MDA-MB-231 (Fig. 3.2A, top and 3.2B). Similar results were obtained in MDA-MB-453 cells (Fig. 3.2A, bottom).

We next measured the activation of caspase-3/7, an apoptotic event preceding PARP cleavage, by a luciferase-based assay. Doxorubicin-induced caspase-3/7 activity in MDA-MB-231 cells was detected as early as 12 h. The pan-caspase inhibitor ZVAD-FMK blocked this response completely, whereas LPA-treated cells showed significantly less caspase-3/7 activation (Fig. 3.2C). Finally, we pre-treated MDA-MB-231 cells grown in 10% serum medium with a LPA<sub>1/3</sub> receptor antagonist (Ki16425). These cells were sensitized to doxorubicin-induced PARP cleavage (Fig. 3.2D) even though the antagonist by itself had no effect. These results are consistent with previously described effects (134) demonstrating that extracellular LPA protects against apoptosis caused by several chemotherapeutic drugs.

### **3.2.2 Doxorubicin accumulation in cancer cells**

To study the mechanism of protection afforded by increased LPA signaling against doxorubicin-induced apoptosis, we initially looked at the localization of doxorubicin in MDA-MB-231 cells by fluorescence microscopy. We hypothesized that cancer cells grown in the presence of LPA exclude doxorubicin from the nucleus. Fixed cells loaded with doxorubicin show a predominantly nuclear localization pattern for doxorubicin, which was unaffected by LPA-treatment (Fig. 3.3A). Direct comparisons of cellular uptake were not made in these experiments

because of sensitivity and photo bleaching issues, which affected the interpretation of results. Instead, we measured doxorubicin fluorescence on live cells by fluorescent cell sorting (450) after 48 h of treatment (Fig. 3.3B). LPA-treated cells showed a 35% decrease in doxorubicin fluorescence, which demonstrates that LPA affects steady-state accumulation of doxorubicin in these cells. Pre-treatment of these cells with broad spectrum inhibitors of MDRT action, cyclosporineA (451) and probenecid (452), was able to prevent the decreases in doxorubicin accumulation, which indicates the LPA-dependent decrease was likely through increased efflux of the drug.

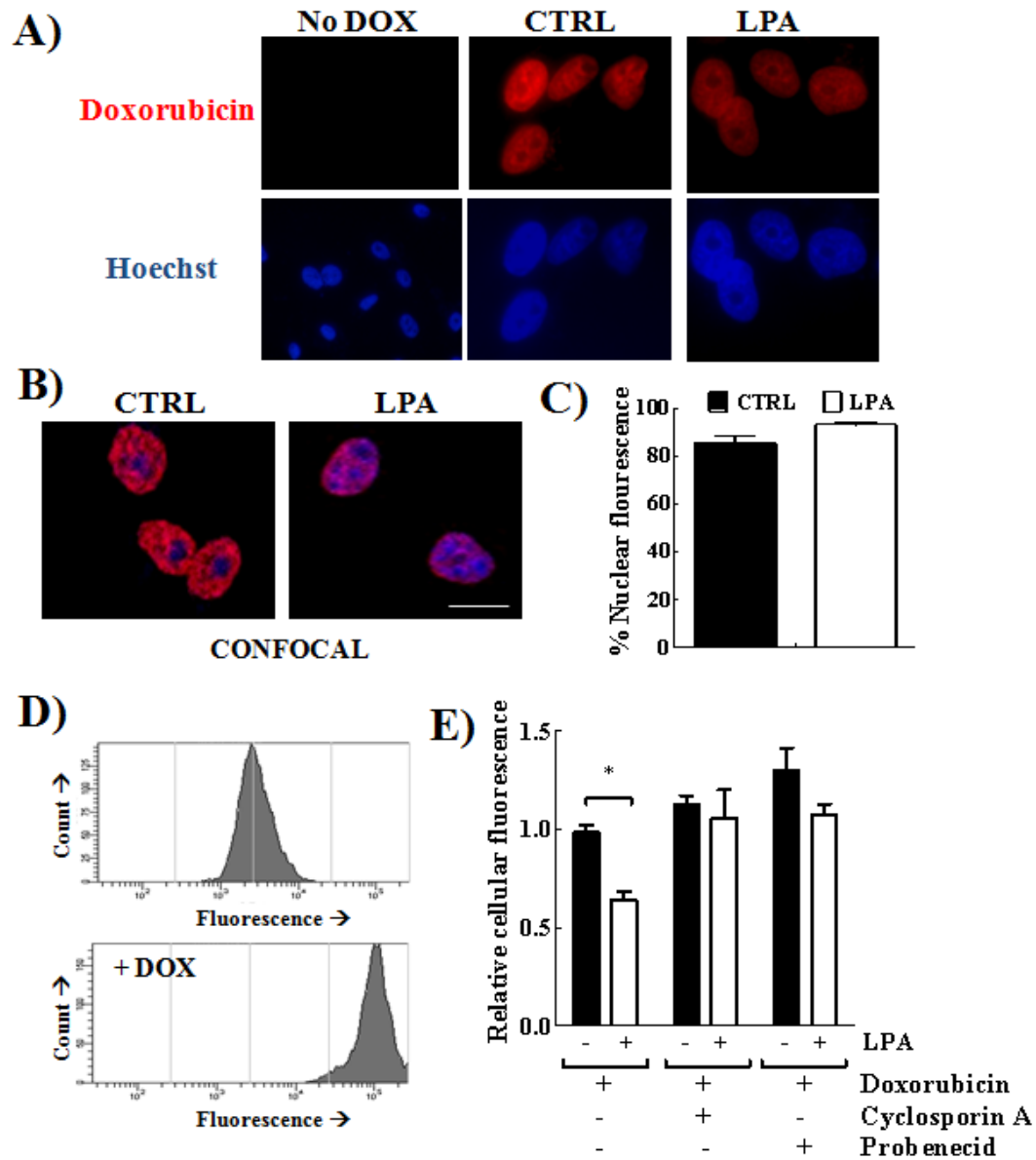


**Figure 3.3: LPA did not affect the predominant nuclear localization of doxorubicin but increased its expulsion in breast cancer cells.** Cells were fixed after doxorubicin treatment and visualized by fluorescence microscopy (A) or confocal microscopy (B) for doxorubicin localization. C) Nuclear doxorubicin fluorescence was calculated by co-localization with Hoechst stain from at least 20 cells/field of view from 3 different experiments by ImageJ analysis. D) Cells were treated with LPA as before for 12 h followed by pre-treatment with inhibitors for 1 h and 0.5  $\mu$ M doxorubicin treatment for 48 h. Cells were washed, trypsinized, resuspended in PBS + 1% BSA and analyzed for cellular fluorescence using FACS Canto II. A representative histogram obtained from FACS Canto II is shown. E) The mean fluorescence was recorded for 100,000 events for 4 independent assays. Results are expressed as means  $\pm$  SEM. \*  $p < 0.05$ . Scale bar – 10  $\mu$ M.

Cellular accumulation of doxorubicin can also be influenced by decreased uptake of the drug by the SLC transporters. To differentiate between uptake and efflux we used [<sup>14</sup>C]doxorubicin in probenecid-pretreated live cells and measured the uptake at various times. We did not see a significant effect on LPA-treated cells on the uptake of [<sup>14</sup>C]doxorubicin from the medium for up to 4.5 h (Fig. 3.4A). Over this time, cells continued to accumulate doxorubicin as seen by increased signal in the cell lysates and there was no effect of LPA-treatment (Fig. 3.4B).

Doxorubicin fluorescence was also monitored over a 4 h period in MCF-7 cells. This resulted in an increase in relative cellular fluorescence as expected from the labeling studies with [<sup>14</sup>C]doxorubicin (Fig. 3.5A). We also measured the accumulation of doxorubicin in cells selected for resistance to doxorubicin or docetaxel (424). These cells express high levels of the multi-drug transporters. Both cell lines selected for resistance to doxorubicin and taxanes were able to efflux doxorubicin rapidly within 4 h of treatment (Fig. 3.5B). These results suggest efflux and not uptake is associated with doxorubicin-resistance in cancer cells.

To study the effects of LPA on the efflux activity of the transporter we employed another flow cytometry based assay. Several fluorescent Ca<sup>2+</sup> and pH sensors are substrates for the MDRT (453). This property can be exploited as a functional assay to study the activity of transporters (454). These sensors have the advantage of rapid uptake/efflux kinetics unlike chemotherapeutics. We used Fluo3, a probenecid-sensitive substrate for MDRT (455). LPA-treated MDA-MB-231 cells

showed a significantly higher rate of export of Fluo3 as measured by decreased accumulation over time. This was blocked by pre-treatment with probenecid (Fig. 3.5C). Together, these results show that LPA-treatment increased efflux activity of the transporters in the short-term and decreased accumulation of the drug over long-term.

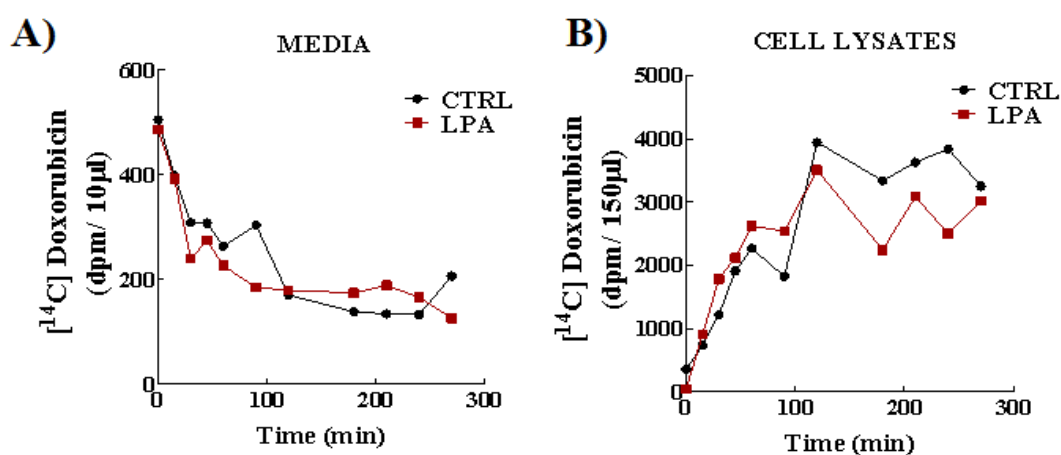


**Figure 3.4: LPA does not affect the uptake of  $[^{14}\text{C}]$ doxorubicin** - MDA-MB-231 cells were treated with LPA as before and then treated with  $[^{14}\text{C}]$ doxorubicin mixed with  $5\ \mu\text{M}$  doxorubicin in the presence of  $1\ \text{mM}$  probenecid. Radioactivity in the medium (**A**) and cell lysates (**B**) was determined at various time points.

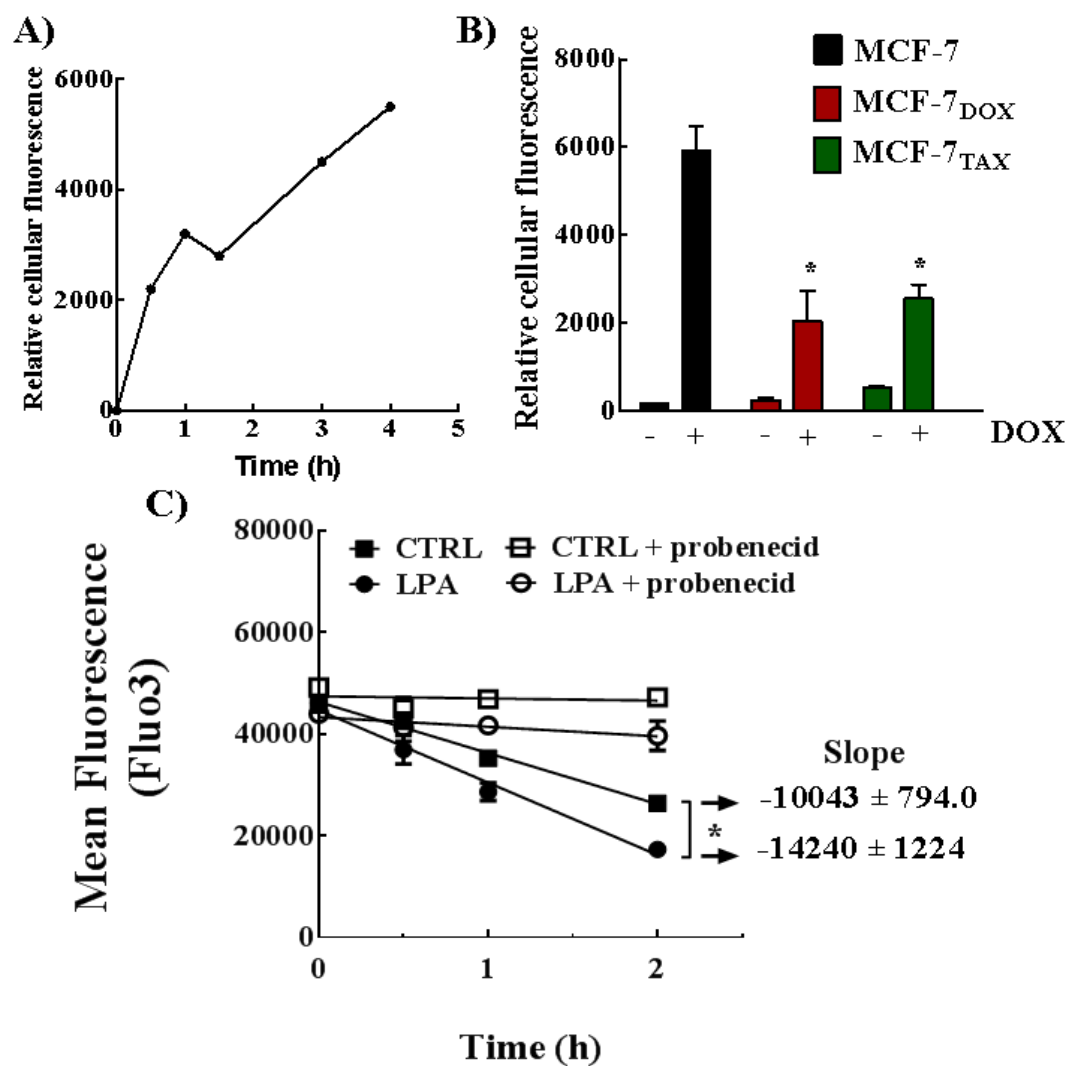


**Figure 3.5: LPA increases the efflux activity of the MDRT** **A)** MCF-7 cells were treated with 0.5  $\mu$ M doxorubicin for up to 4 h. Cells were analyzed for cellular fluorescence using FACS Canto II as described before **B)** Doxorubicin fluorescence was measured as before at 4 h for MCF-7, MCF-7<sub>DOX</sub> and MCF-7<sub>TAX</sub>. A two-tailed t-test was used to determine significance between the cell lines. **C)** MDA-MB-231 cells were starved as before followed by treatment with delipidated serum with/without 10  $\mu$ M LPA for 12 h. Trypsinized cells were loaded with Fluo3-AM (0.4  $\mu$ M) for 1 h. Cells were centrifuged, washed and treated with fresh medium with or without 5 mM probenecid. Cell fluorescence was determined using FACS Canto II. Results for 100,000 cells were expressed as mean fluorescence relative to no treatment for 3 independent assays. Two-way ANOVA with post-hoc test was used for determining significance between treatments.\*  $p < 0.05$ .

### 3.2.3 Expression of MDRT in breast cancer cells

Several studies have confirmed that the increased expression of the multi-drug resistant transporters, ABCB1, ABCC1 and ABCG2 in cancer cells can confer resistance to doxorubicin (16). We initially characterized the expression of these transporters using previously validated antibodies for ABCC1, ABCG2 and ABCB1 (333, 456, 457). *ABCC1* and *ABCG2* mRNA and proteins were detected in a panel of breast cancer cells, but *ABCB1* expression was not detected (Fig. 3.6A,B), as reported previously (458). Immunofluorescence of ABCC1, ABCG2 and ABCB1 in MCF-7 cells selected for resistance to doxorubicin (424) or docetaxel (425) showed staining pattern consistent with a plasma membrane localization for ABCC1 and ABCG2 (Fig. 3.6C). They were also expressed in intracellular compartments as shown previously (32, 34).



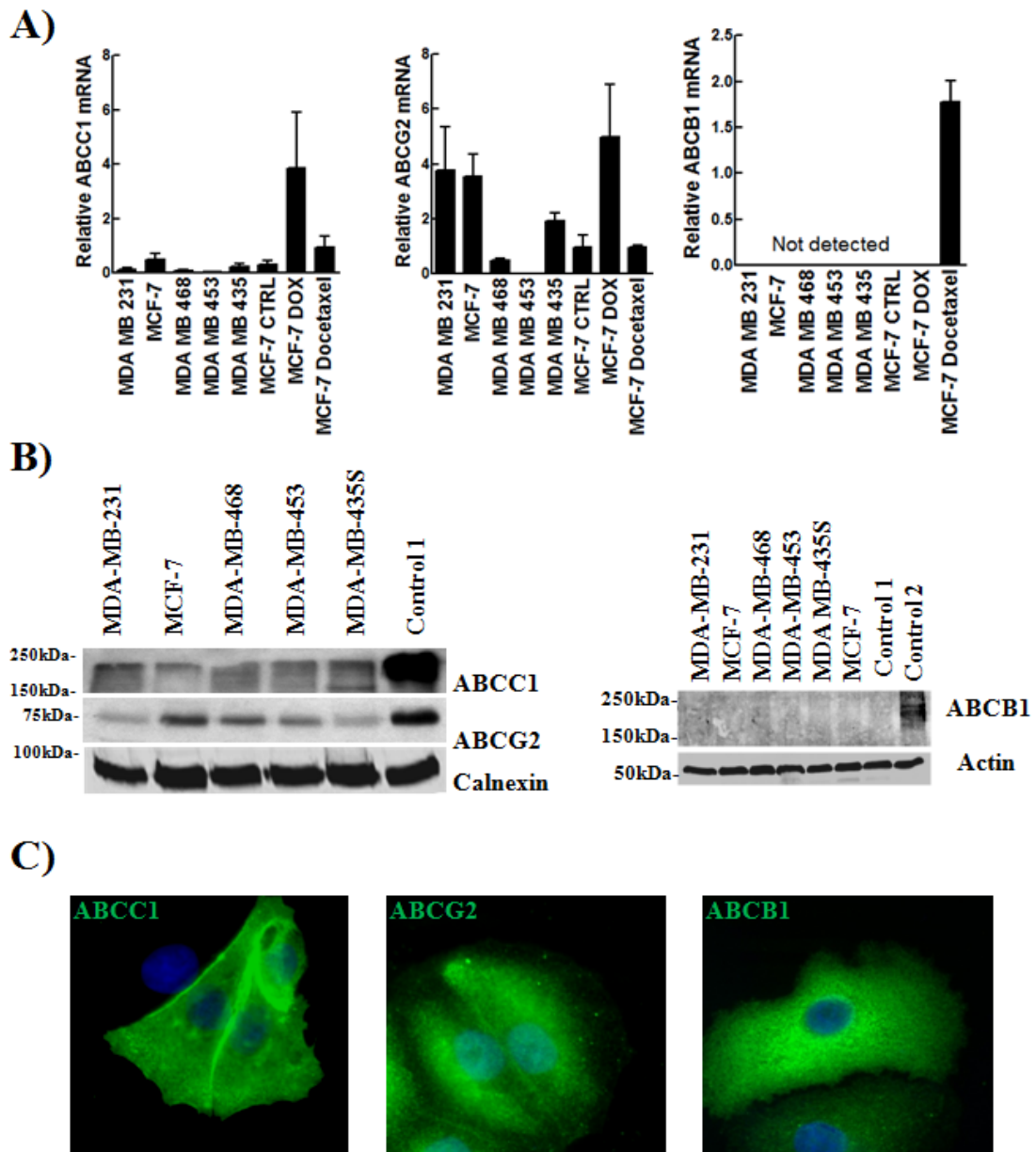


**Figure 3.6: Expression of MDRT in breast cancer cell lines: A) RT-PCR analysis and B) Immunoblots from various cancer cell lines grown in conditions described in Table 3 and C) Immunofluorescence of doxorubicin-resistant MCF-7 cells with increased expression of ABCB1 and ABCG2 or docetaxel-resistant MCF-7 cells expressing ABCB1.**

### **3.2.4 LPA increases the expression of MDRT through increased LPA<sub>1</sub>-dependent transcription**

Treatment with LPA increased *ABCC1* and *ABCG2* mRNA in MDA-MB-231 cells (Fig 3.7A left panel). The mRNA levels peaked after 4.5 h even though a small increase was maintained even at 9 h. These increases depended on the LPA concentration with peak increases seen at 5-10  $\mu$ M (Fig. 3.7A right panel). The mRNA increases corresponded to increases at the level of protein expression of ABCC1 and ABCG2 with 2-fold increase observed after 9 h in MDA-MB-231 cells (Fig. 3.7B, C). In addition to MDA-MB-231 cells, MCF-7 and MDA-MB-468 breast cancer cells also showed LPA-dependent increases in ABCC1 and ABCG2 (Fig. 3.7D).

Pre-treatment with 10  $\mu$ g/ml actinomycin D blocked this increase in transcription (Fig. 3.8A). Our laboratory previously used actinomycin D successfully at these concentrations to block transcription (459). LPA treatment also increased other members of the ABCC- family of transporters; *ABCC2* and *ABCC3* were increased by 2.1- and 1.6-fold respectively (Fig. 3.8B).

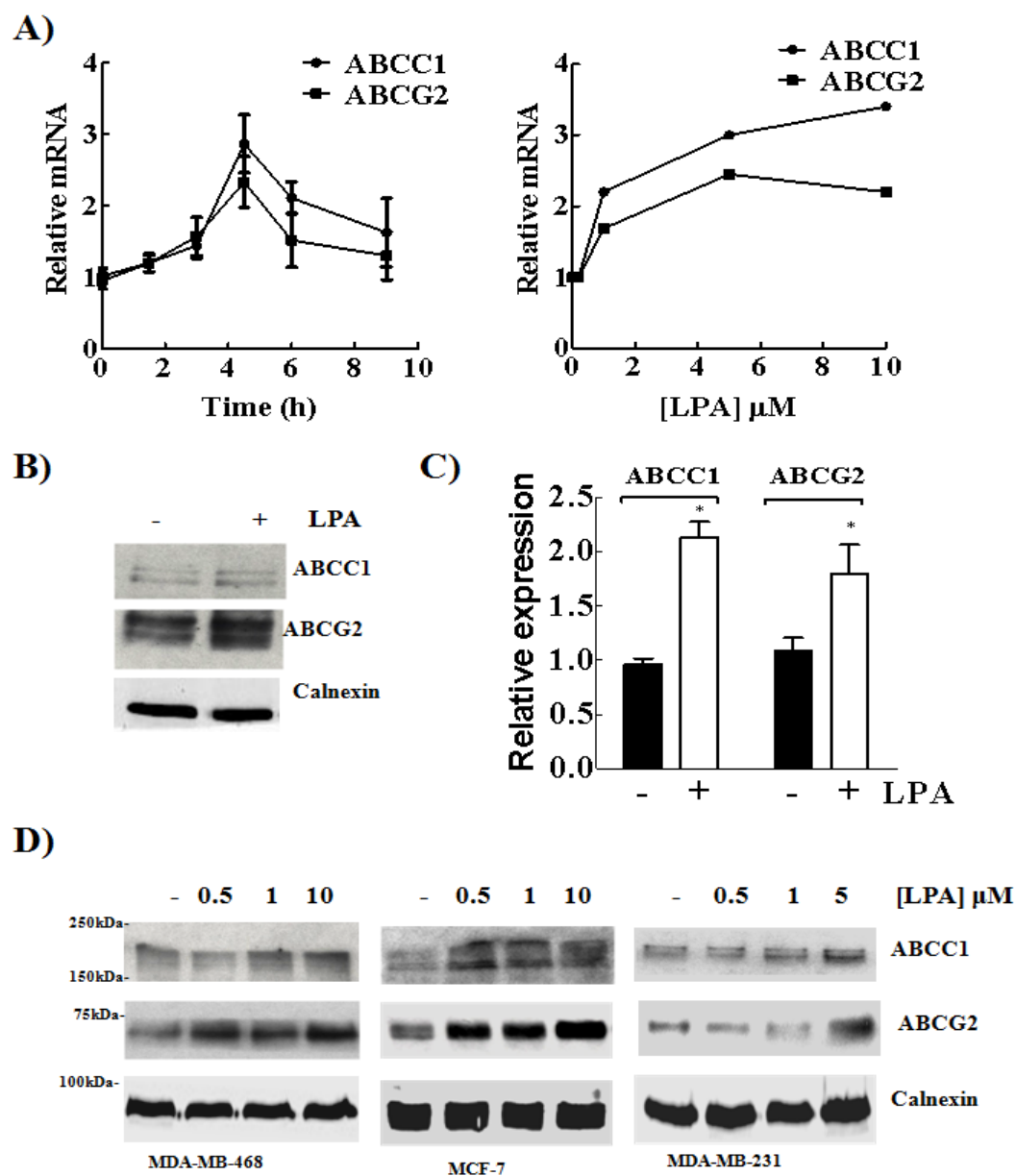


**Figure 3.7: LPA increases the MDRT- ABCC1 and ABCG2 levels in breast cancer cells**  
 – **A)** MDA-MB-231 cells were starved before treatment with LPA for various times (left panel) or at various LPA concentrations for 4.5 h (right panel). mRNA was analyzed by RT-PCR. **B)** MDA-MB-231 cells were treated with LPA for 12 h before collecting the lysates for immunoblotting. Results are representative of  $\geq 3$  different experiments **C)** Quantification of ABCC1 and ABCG2 protein levels. **C)** MDA-MB-231 cells, MDA-MB-468 and MCF-7 cells were starved for 12 h and treated with different LPA concentrations for another 12 h. Representative immunoblots are shown from 3 experiments. Results are expressed as means  $\pm$  SEM. \*  $p < 0.05$ .

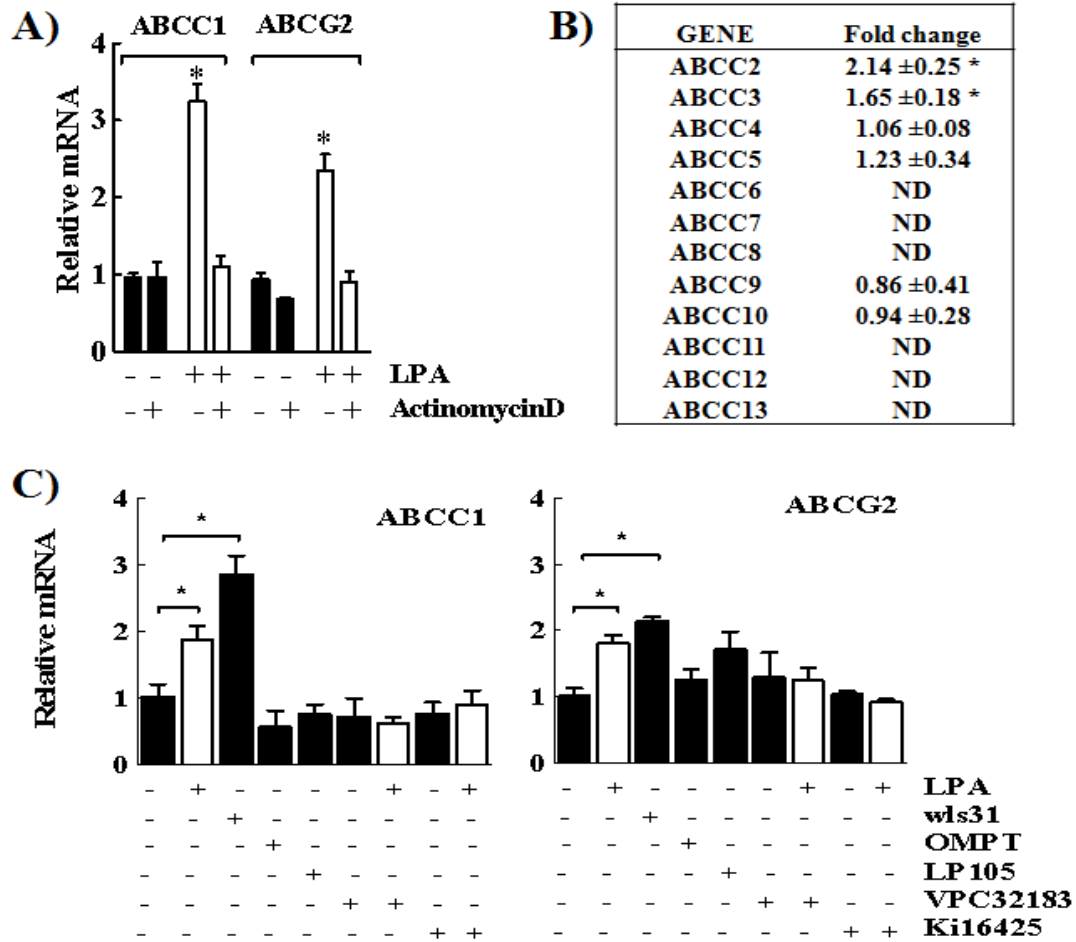


**Figure 3.8: LPA-LPA<sub>1</sub> signaling increases transcription of the ABC transporters** A) MDA-MB-231 cells were pre-treated with 10 µg/ml Actinomycin D for 30 min before addition of LPA and RT-PCR analysis B) mRNA levels of other transporters of the ABCC or MRP family were analyzed by RT-PCR as before. C) MDA-MB-231 cells were treated with LPA or other agonists or antagonists of the LPA receptor as described in Table 2 before RT-PCR analysis as before. A two-tailed t-test was used to determined significance. Results are expressed as means ± SEM. \* p<0.05.

The LPA<sub>1/2</sub> receptor agonist, wls31, which cannot be hydrolyzed by LPP activities, also increased ABCC1 and ABCG2 mRNA in MDA-MB-231 cells (Fig. 3.8C). The LPA<sub>2</sub>-selective agonist, LP105, and the LPA<sub>3</sub>-selective agonist, OMPT, did not have any effect on ABCC1 and ABCG2 even at high concentrations. Conversely, pre-treatment with the LPA<sub>1/3</sub> receptor antagonists Ki16425 and VPC32183 blocked the LPA-induced increases in ABCC1 and ABCG2 mRNA. To confirm the involvement of LPA<sub>1</sub> receptors we treated MDA-MB-231 cells with two different siRNA constructs, which decrease the expression of the LPA<sub>1</sub> receptor mRNA selectively (Fig. 3.9A). Knockdown of LPA<sub>1</sub> blocked LPA-induced increases in ABCC1 and ABCG2 (Fig. 3.9B). Unsurprisingly, LPA<sub>1</sub> is the major LPA receptor expressed in MDA-MB-231 cells (209).

Several signaling pathways are activated by the GPCR, LPA<sub>1</sub> receptor. To test the contribution of these pathways on transcription of ABCC1 we used various pharmacological inhibitors. LY294002 (10  $\mu$ M), a PI3K inhibitor, and pertussis toxin (0.1  $\mu$ g/ml), which blocks G $\alpha_i$  signaling, blocked wls31-induced increases in ABCC1. No significant effects on ABCC1 mRNA were found on pre-treatment with PD98059 (20  $\mu$ M), a MEK inhibitor; Gö6983 (10  $\mu$ M), a PKC inhibitor; and U73122 (1  $\mu$ M), an inhibitor of phospholipase C activated by Gq (Fig. 3.9C).

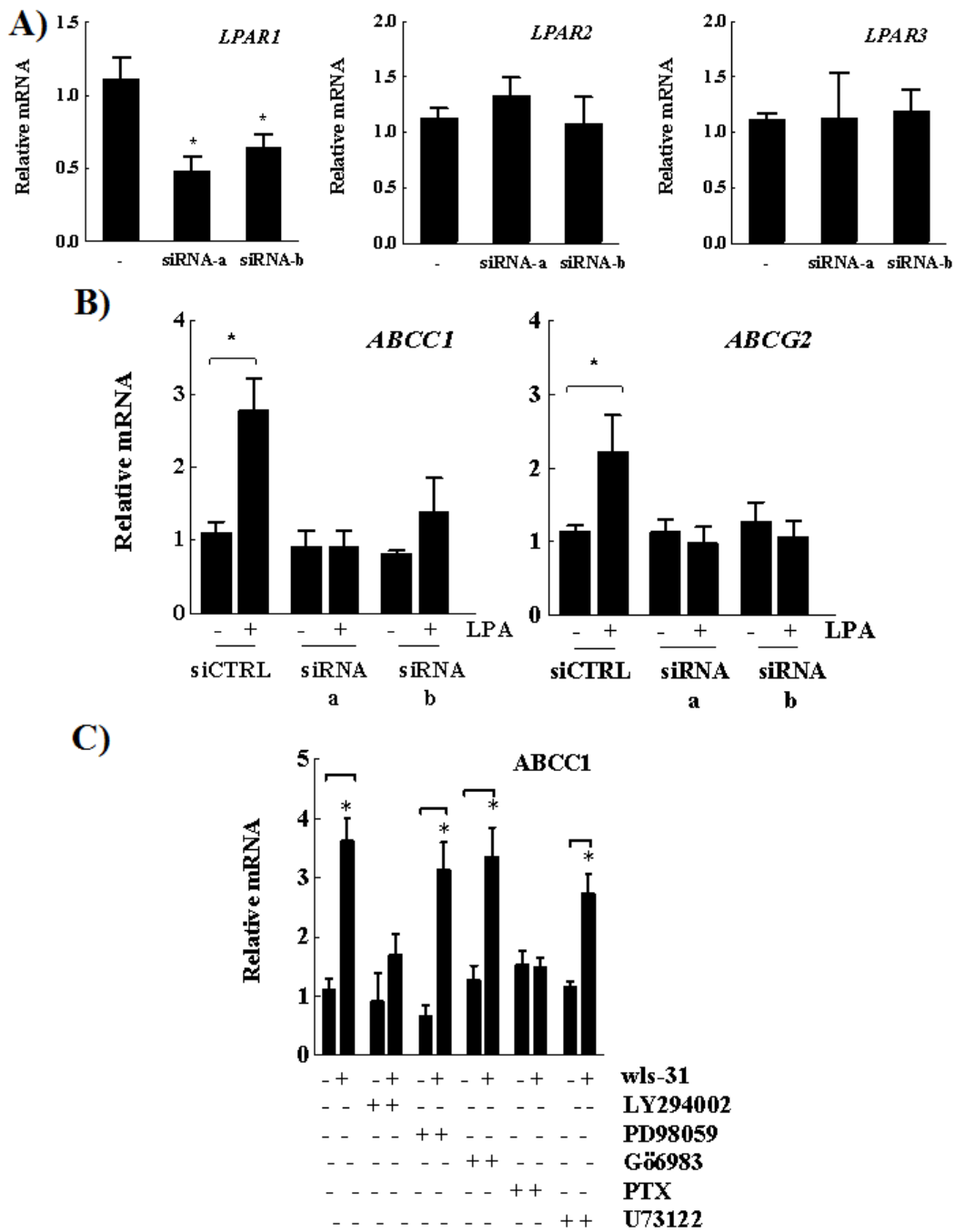


**Figure 3.9: LPA-LPA<sub>1</sub>-G<sub>i</sub>-PI3K signaling increases ABCC1 and ABCG2 mRNA levels -**  
**A)** MDA-MB-231 cells were treated with 50 nM siCTRL or different siRNA constructs targeting LPA<sub>1</sub>. After 48 h, mRNA was collected for RT-PCR analysis of receptor levels for LPA<sub>1,2,3</sub>. **B)** MDA-MB-231 cells were treated with 50 nM siCTRL or two different siRNA constructs targeting LPA<sub>1</sub> for 36 h and they were then starved for 12 h before treating them

with LPA 10  $\mu$ M for another 6 h. mRNA was analyzed for ABCC1 or ABCG2 levels. C) ABCC1 mRNA was assessed by RT-PCR as before. Results are expressed as means  $\pm$  SEM. A two-tailed t-test was used to determine significance. \*  $p < 0.05$

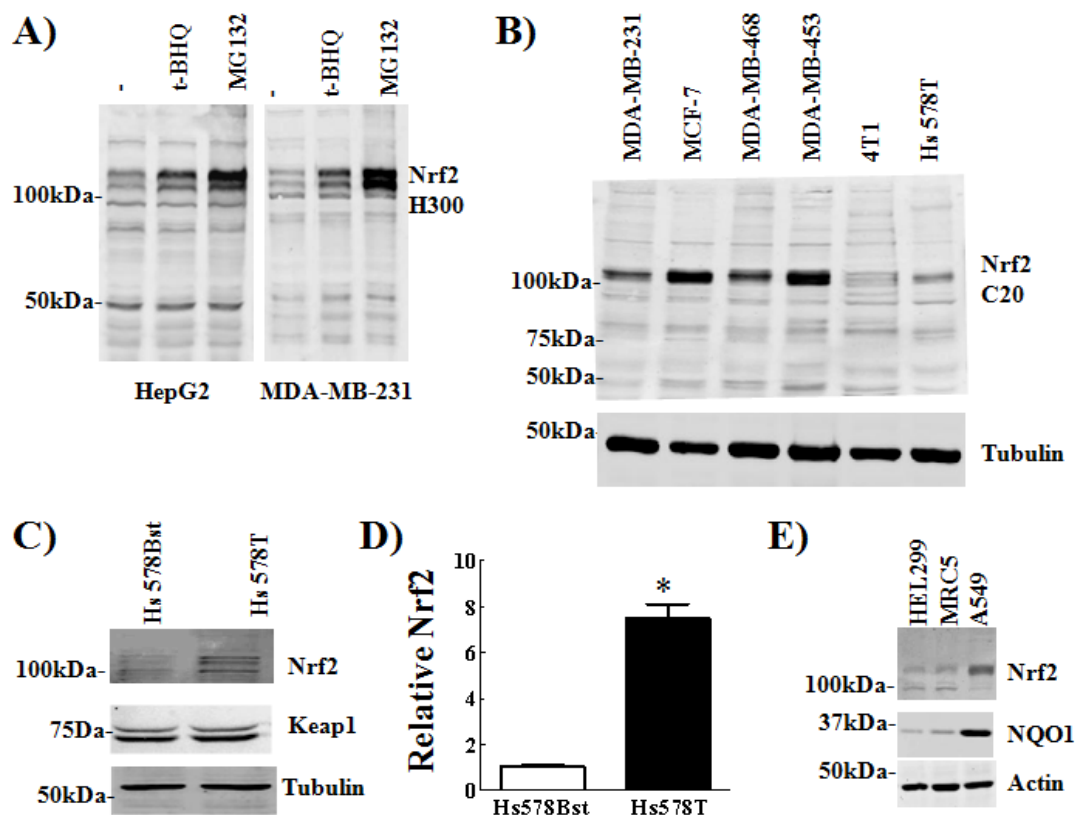


**Figure 3.10: Characterization of Nrf2 expression in breast, liver and lung carcinoma -**  
**A)** HepG2 and MDA-MB-231 cells were treated with t-BHQ or the proteosomal inhibitor, MG132 (25  $\mu$ M), for 4 h prior to collecting the cell lysates. They were immunoblotted for Nrf2 using an antibody, which detects N-terminus. **B)** A panel of sub-confluent breast cancer cell lines was grown in full growth medium and cell lysates were immunoblotted for Nrf2 using an antibody, which detects the C-terminus. **C)** Hs578T breast ductal carcinoma cells express higher Nrf2 compared to Hs578Bst cell line. The quantification of Nrf2 expression is shown in **(D)**.  $n=4$ . Results were expressed relative to tubulin expression. **E)** HEL299, MRC5 lung fibroblasts and A549 lung adenocarcinoma cells were immunoblotted for Nrf2 and NQO1 expression.

### 3.2.5 Nrf2 is stabilized by LPA-LPA<sub>1</sub> receptor signaling

Nrf2 protein migrates at 110 kDa in 8-10% separating gels (460) and it is rapidly stabilized by proteosomal inhibition. Nrf2 protein expression was detected in a variety of cancer cells with antibodies raised against its N-terminus (Fig. 3.10A) or C-terminus (Fig. 3.10B). Nrf2 expression was stabilized rapidly within 2-4 h of t-BHQ or MG132 treatment as expected. Nrf2 expression was significantly higher in Hs578T ductal carcinoma cells compared to the Hs578Bst cell line, which was derived from the tissue peripheral to the infiltrating carcinoma of the same patient (Fig. 3.10C, D). However, the expression of the negative regulator of Nrf2, Keap1, was unchanged in these experiments. Similarly, Nrf2 and its target NQO1 were increased in A549 lung carcinoma cells compared to lung fibroblasts cell lines HEL-299 and MRC5 (Fig. 3.10E).

Treatment of MDA-MB-231 cells with t-BHQ increased the transcription of *ABCC1*, *ABCG2*, *ABCC2*, *ABCC3*, and the antioxidant genes *HMOX1* and *NQO1* (Fig 3.11A). LPA on its own or in combination with t-BHQ also increased the expression of mRNA for these genes. LPA or t-BHQ alone increased Nrf2 protein expression by 2- to 3-fold. Together, they increased Nrf2-protein by about 5- to 6-fold. The additive effect was also seen in protein expression of the antioxidant genes and multi-drug resistant transporters, in MDA-MB-231 breast cancer (Fig. 3.11B). LPA had no effect on Keap1 protein levels by itself or in the presence of t-BHQ. However, Keap1 levels were decreased by about 40% after t-BHQ treatment (Fig. 3.11B). LPA or wls31 increased *NQO1* or *ABCC1* mRNA in 4T1 mouse breast



cancer cells (Fig. 3.12A). As before, LPA by itself or in the presence of t-BHQ increased Nrf2 expression and its transcriptional targets in 4T1 cells (Fig. 3.12B,C). A549 lung cancer and 8305C thyroid cancer cells also showed similar increases Nrf2 and NQO1, whereas Keap1 levels were not altered as shown previously (Fig. 3.12D).

*Nrf2* mRNA was unchanged by treatment with t-BHQ, LPA and wls31 in MDA-MB-231 and 4T1 cells (Fig. 3.13A,B). Nrf2 is rapidly degraded by proteosomal degradation in HEK-293T cells (426). Activation of the overexpressed LPA<sub>1</sub> receptor increased Nrf2 accumulation in HEK293T cells (Fig 3.14A). Similarly, GFP-tagged Nrf2 was increased by activation of the LPA<sub>1</sub> receptor. This was also observed in HepG2 carcinoma cells, which express detectable levels of endogenous Nrf2. Activation of LPA<sub>1</sub> receptor, but not LPA<sub>2/3</sub> receptors, significantly increased Nrf2 expression (Fig. 3.14B). MDA-MB-231 cells in which the LPA<sub>1</sub> receptor had been knocked down selectively showed no such increases in Nrf2 expression, although t-BHQ still increased Nrf2 expression (Fig. 3.14B).

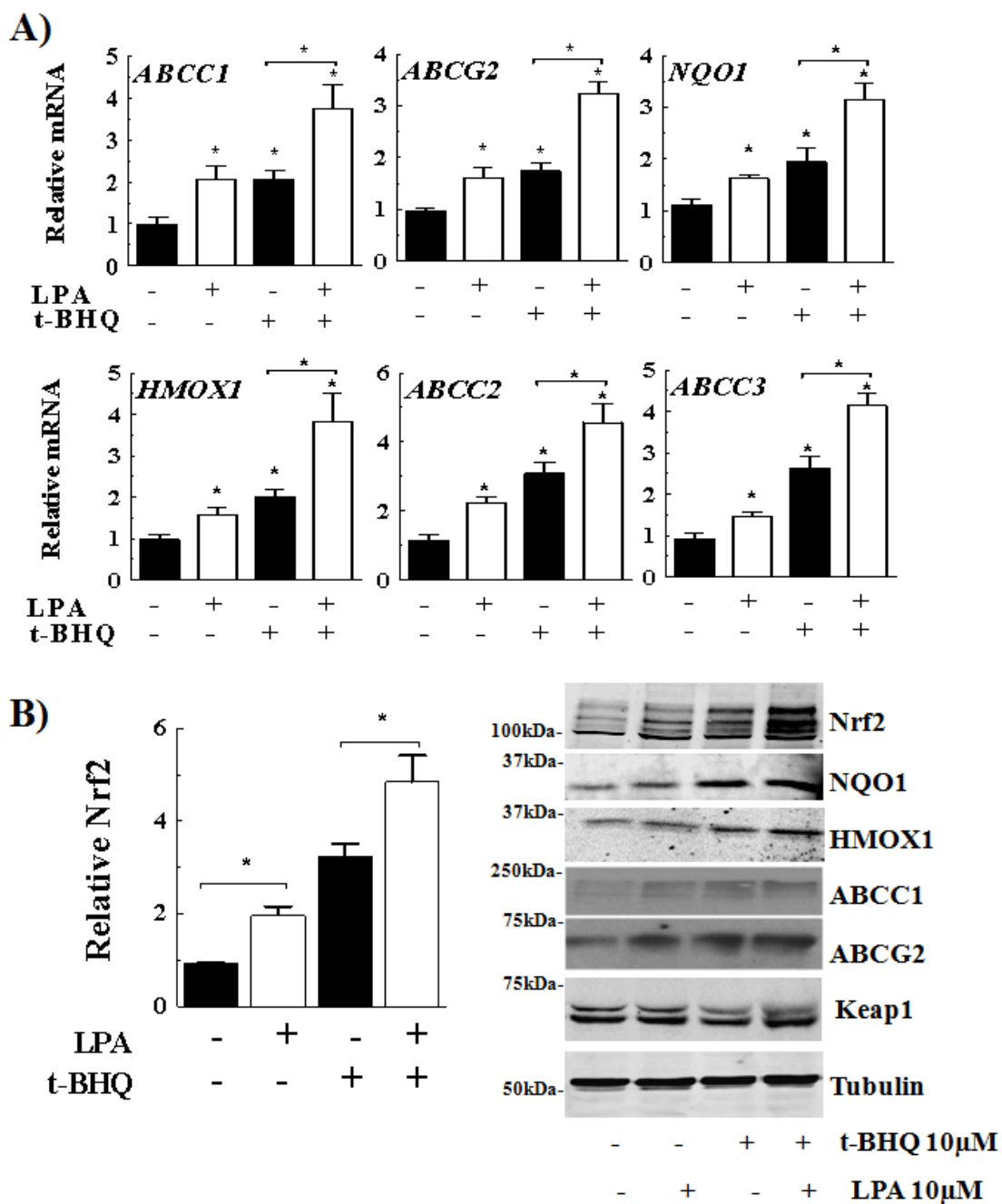


**Figure 3.11 : LPA increases Nrf2 expression and transcription of its targets** - MDA-MB-231 cells were starved for 12 h and treated with or without LPA (10 μM) for 6 h followed by the presence or absence of 10 μM t-BHQ for 6 h. (A) mRNA was collected and analyzed from 5 independent experiments by qRT-PCR. One-way ANOVA with post-hoc test was used for determining significance. \*,  $p \leq 0.01$  (B) Nrf2 protein expression (left panel) was analyzed by immunoblots (right panel) after 12 h. Results are expressed as means  $\pm$  SEM. \*  $p < 0.05$ .

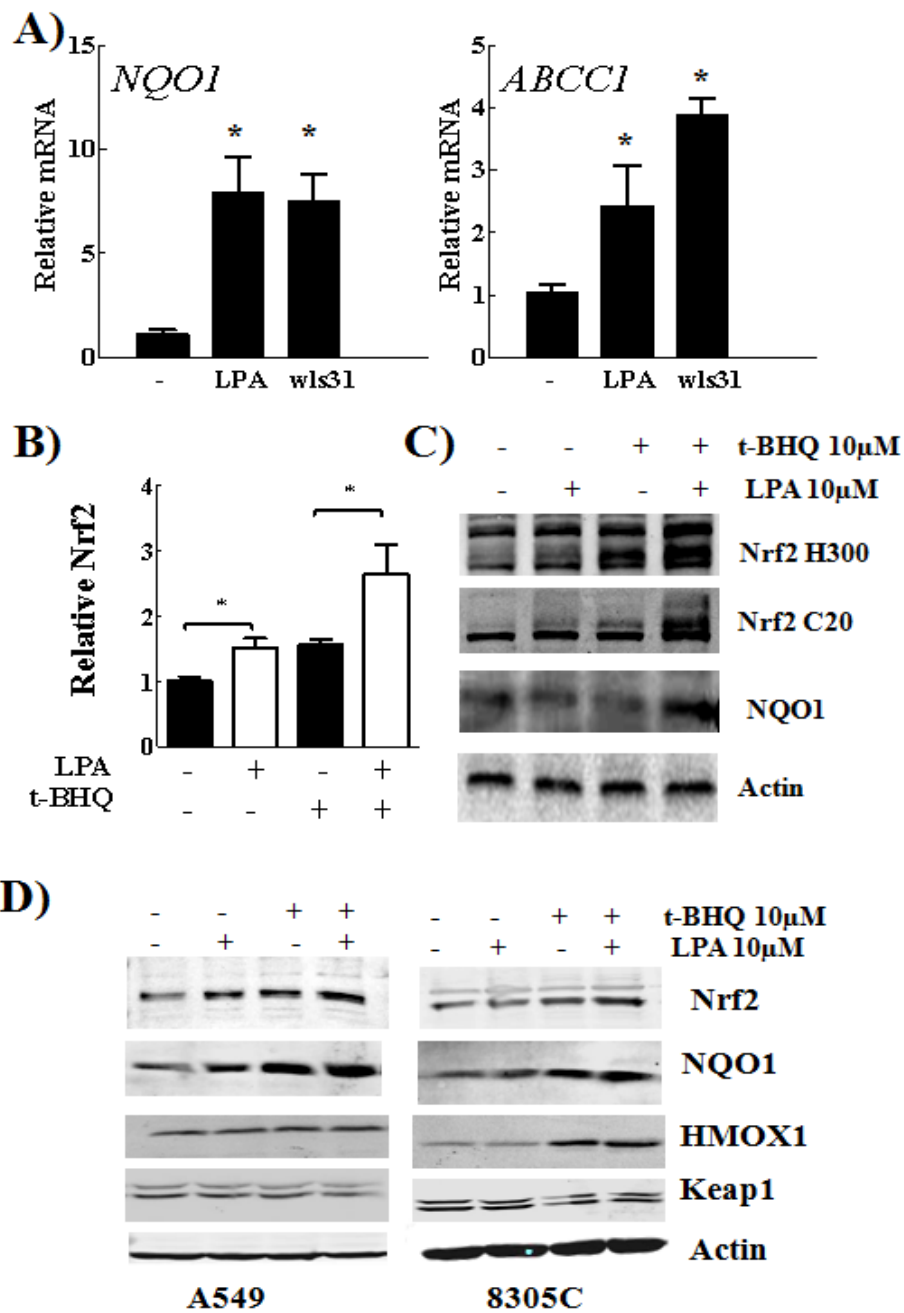


**Figure 3.12: LPA increases Nrf2 expression and transcription of its targets in different cancer cells** - 4T1 cells were starved for 12 h and treated with or without LPA (10 μM) or wls31 for 6 h. **B, C)** 4T1 cells were starved for 12 h and treated with or without LPA (10 μM) for 6 h followed by the presence or absence of 10 μM t-BHQ for 6 h. Nrf2 protein expression was analyzed by immunoblots after 12 h. Results are expressed as means ± SEM. \* p<0.05 **D)** A549 and 8305c cells were immunoblotted as before.

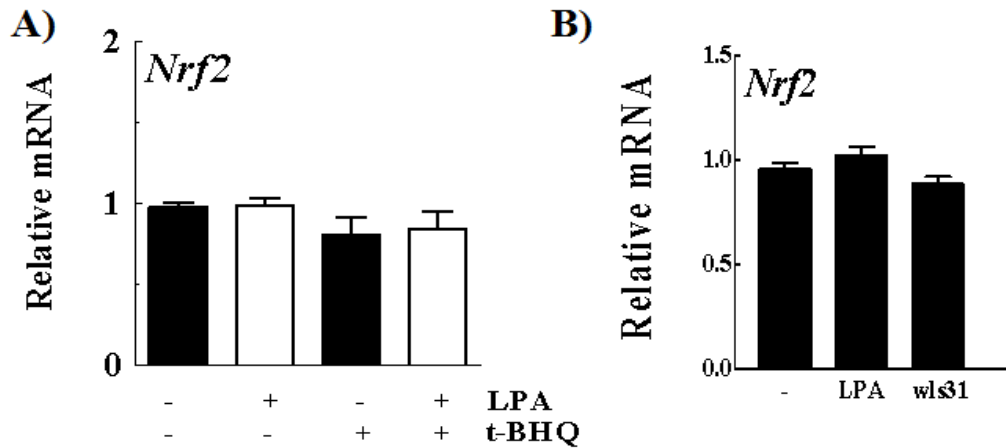


**Figure 3.13: LPA does not affect Nrf2 mRNA expression** – A) MDA-MB-231 cells or B) 4T1 cells were treated as described in previous experiments. Nrf2 mRNA expression was analyzed by RT-PCR. Results are expressed as means  $\pm$  SEM. \*  $p < 0.05$ .

### 3.2.6 Nrf2 is nuclear localized and increases antioxidant-response element (ARE) activity by PI3K signaling

Activation of the LPA<sub>1</sub> as before in HEK293T cells increased the nuclear localization of GFP-Nrf2 (Fig. 3.15A, B), in addition to increased protein levels. MDA-MB-231 cells, which were subjected to nuclear fractionation after LPA or wls31 treatment showed 4-6 fold increases in endogenous nuclear Nrf2 (Fig. 3.16A). Inhibition of PI3K by LY294002 or wortmannin blocked the LPA-dependent increases in Nrf2. Inhibition of the ERK pathway by the MEK inhibitor, PD98059, or PKC pathway by Gö6983 inhibitor had no effect on Nrf2 protein expression (Fig. 3.16B).

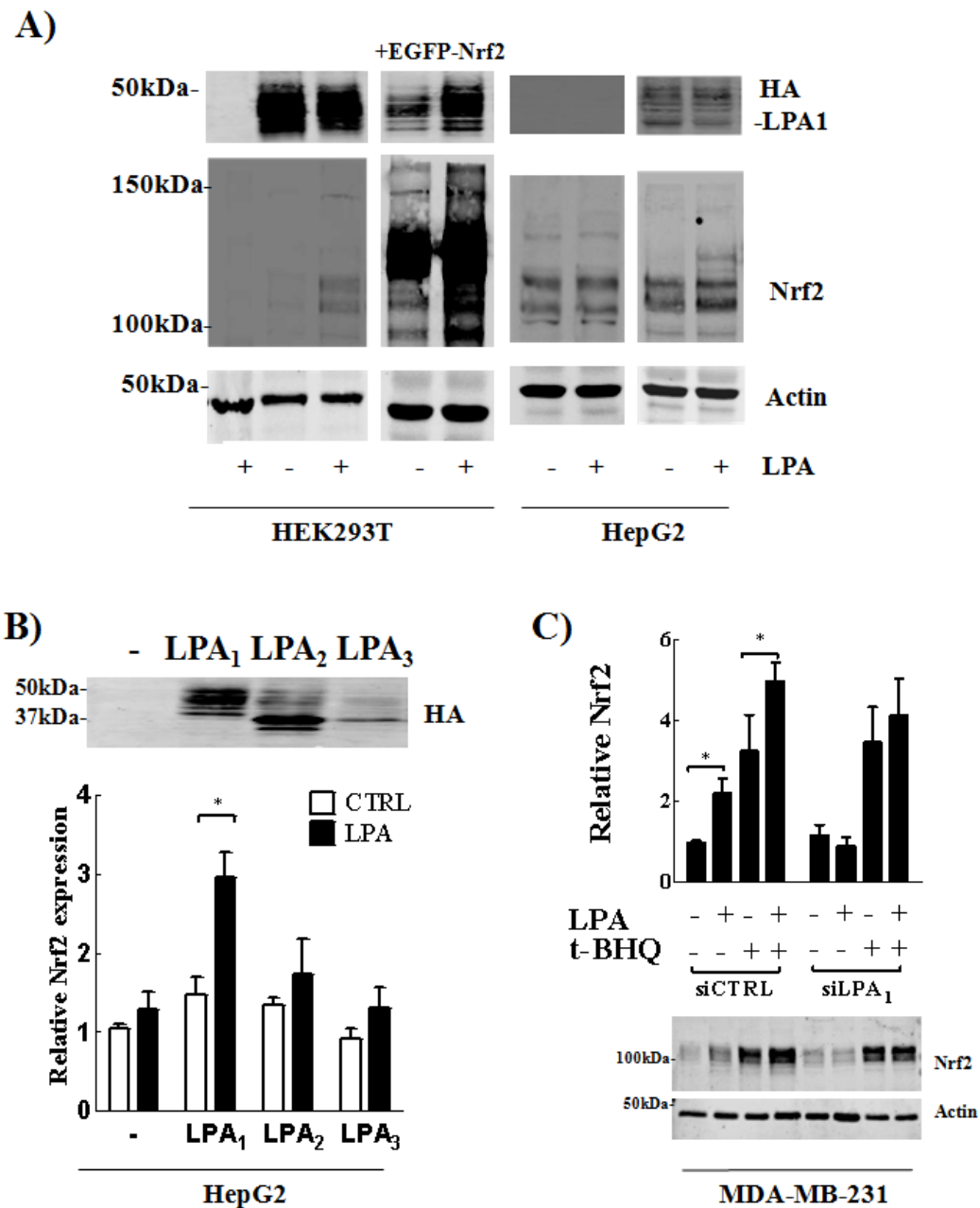


**Figure 3.14: LPA-LPA1 signaling increases basal and t-BHQ-induced Nrf2 expression**  
 - **A)** HEK293T or HepG2 cells were transfected with 0.5  $\mu$ g of each plasmid/well. After 16 h they were starved for 12 h, treated with 10  $\mu$ M LPA for 12 h and a representative immunoblot is shown from 3 independent experiments. **B)** Densitometry analysis of Nrf2 levels in HepG2 cells **C)** MDA-MB-231 cells were treated with 50 nM siCTRL or siLPA1 constructs as before. After 48 h, cells were starved for 12 h before treating them with 10  $\mu$ M LPA for 6 h. A representative Western blot for Nrf2 is shown. Results are expressed as means  $\pm$  SEM.\*  $p < 0.05$ .

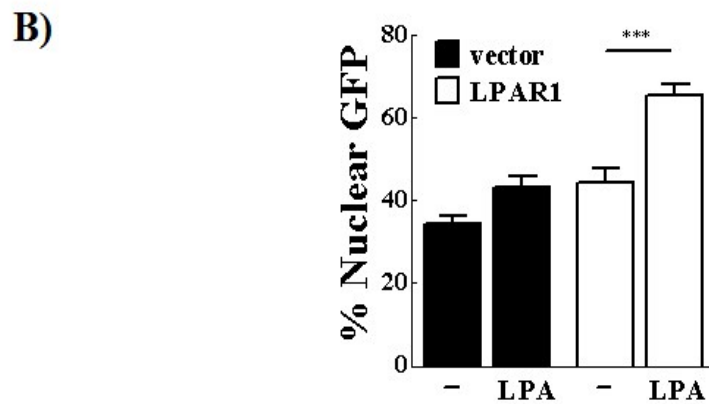
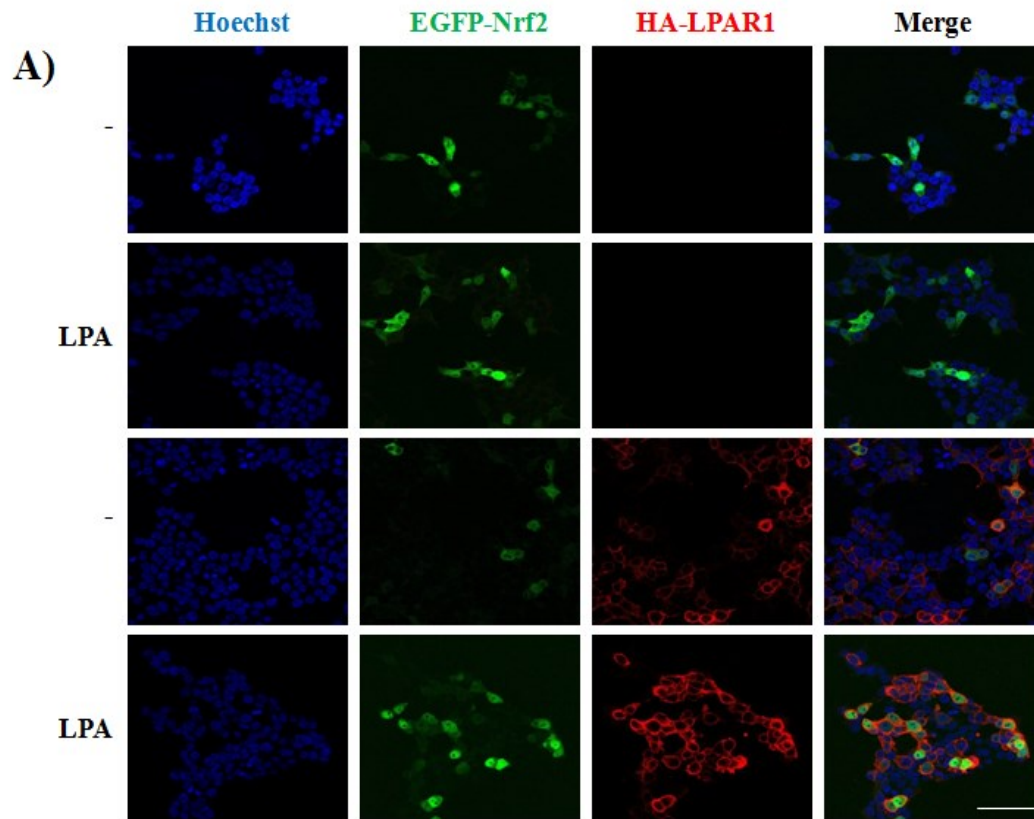


**Figure 3.15: LPA increases nuclear localization of EGFP-Nrf2** – **A)** HEK 293T cells were transfected with 0.5  $\mu\text{g}$  of EGFP-Nrf2 (all panels) and 0.5  $\mu\text{g}$  of HA-tagged empty vector (top two panels) or HA-tagged LPA<sub>1</sub> (bottom two panels) plasmids/well. They were incubated for another 16 h before starving them for 12 h. Treatments were performed as described for another 12 h. Samples were fixed and then immunostained as described in Materials and Methods. **B)** Nuclear GFP-Nrf2 fluorescence was determined based on co-localization with Hoechst by ImageJ analysis. Results are expressed as means  $\pm$  SEM. \*  $p < 0.05$ . Scale bar – 100  $\mu\text{M}$ .

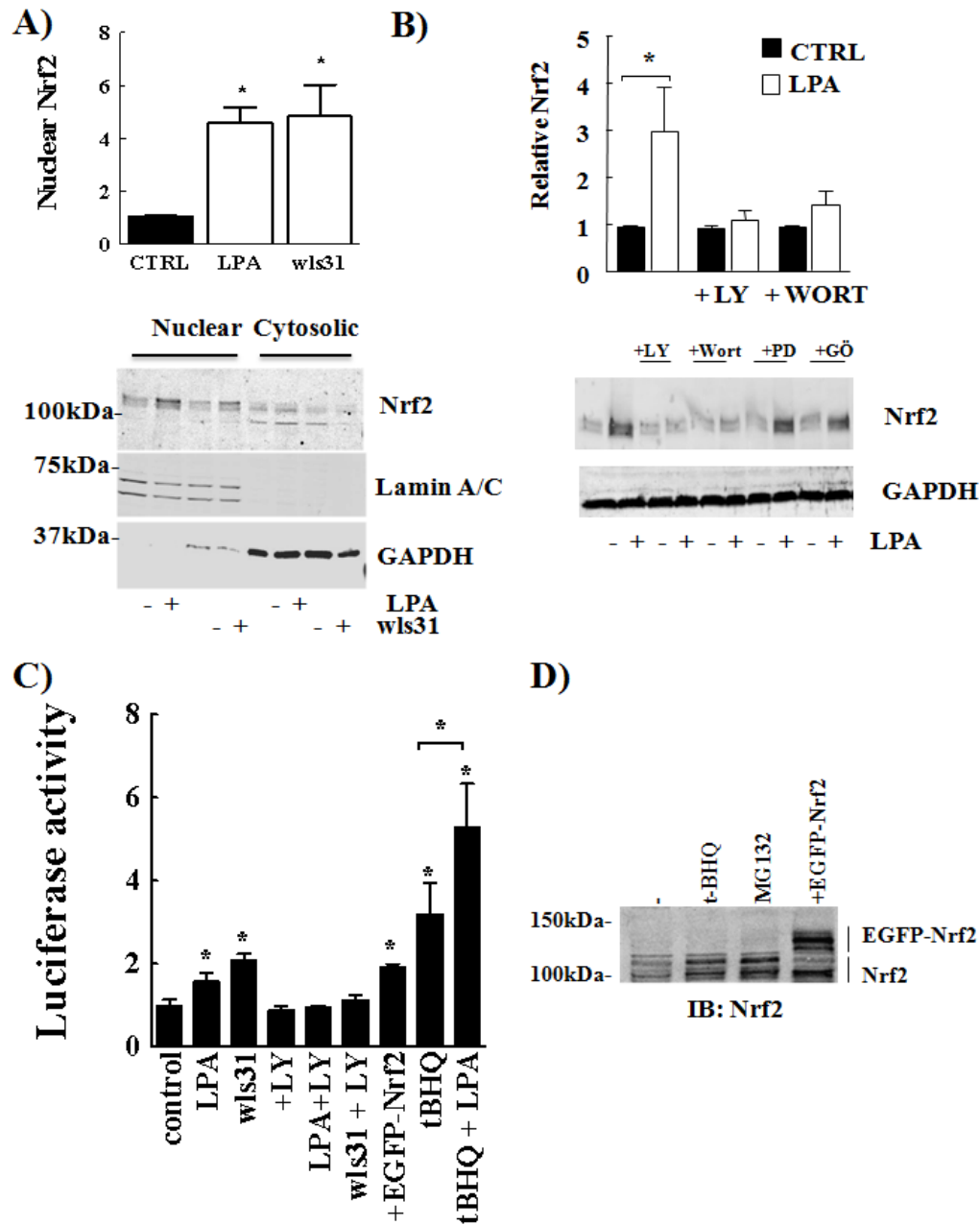


**Figure 3.16: LPA increases Nrf2 nuclear localization and ARE activity –**

**A)** MDA-MB-231 cells were starved for 12 h and then treated with vehicle (0.1% BSA), 10  $\mu$ M LPA or 1  $\mu$ M wls31 for 6 h in 3 independent experiments. Nuclear and cytoplasmic fractions were immunoblotted. Nuclear Nrf2 expression was expressed relative to Lamin A/C **B)** MDA-MB-231 cells were starved for 12 h before pre-treatment with 10  $\mu$ M LY294002 (LY) or 1  $\mu$ M wortmannin (Wort), 20  $\mu$ M PD98059 (PD) or 10  $\mu$ M Gö6983 (Gö) for 6 h. They were then treated with or without 10  $\mu$ M LPA for 12 h. Nrf2 protein expression was detected by immunoblotting and expressed relative to glyceraldehyde

phosphate dehydrogenase (GAPDH) in 3 independent experiments. **C)** MCF-7 AREc32 cells were transfected with 2  $\mu$ g of EGFP-Nrf2 or EGFP plasmid, grown for 18 h and then starved for 12 h with or without LY294002 (10 $\mu$ M) before treatments for 24 h. Luciferase assays were performed in triplicate using 25  $\mu$ g total protein. Results from 5 independent experiments are expressed relative to no treatment. Two-tailed t-test - was used for calculating p-values between treatments. **D)** AREc32 cells grown in 6-well plates were transfected with 2  $\mu$ g of EGFP plasmid (lanes 1-3) or EGFP-Nrf2 plasmid (lane 4) and incubated for 18 h. They were starved for 12 h followed by treatments with 10  $\mu$ M t-BHQ or 10  $\mu$ M MG132 for 4 h. Cell lysates were immunoblotted for Nrf2 expression. The band-shifted EGFP-Nrf2 is shown.

The core ARE sequence was initially identified as 5'-GTGACnnnGC-3' (461). However, later studies have shown that the flanking regions surrounding this core sequence may play a bigger role in robust induction of the antioxidant response by Nrf2 (422). MCF-7 breast cancer cells stably expressing the minimal ARE sequence coupled to luciferase expression has been used as a reporter cell line to identify novel Nrf2 regulators previously (417). Table 4 shows alignment of this ARE sequence against the consensus sequence of some of the other Nrf2-regulated genes used in the study. It is to be noted that some genes contain multiple ARE sequences in their promoter. LPA and wls31 increased the activity of this minimal promoter-element and these effects were enhanced by t-BHQ (Fig. 3.16C). Furthermore, PI3K inhibition completely blocked the LPA and wls31-induced increases in ARE-activity. Overexpression of the GFP-tagged Nrf2 (Fig. 3.16C, D) increased the luciferase activity, which confirmed the specificity of this assay.



### 3.3 DISCUSSION

LPA signaling contributes towards resistance to a variety of chemotherapeutic agents and radiotherapy (reviewed in (134)). The present work demonstrates a novel effect of LPA, which through activation of LPA<sub>1</sub> receptors increases Nrf2 protein expression and ARE activity. This protects breast cancer cells from doxorubicin-induced apoptosis since Nrf2-induced expression of anti-oxidant genes can diminish oxidative damage that occurs during chemotherapy. In addition, the MDRTs expel several chemotherapeutic agents and oxidation products from cancer cells including doxorubicin. Increased expressions of the MDRTs ABCB1 (9), ABCC1 (10), ABCG2 (11) and several anti-oxidant genes are implicated in resistance to cancer therapies (16).

Doxorubicin is thought to induce cell killing by DNA intercalation although additional mechanism like accumulation of ROS and redox-recycling have also been shown to contribute to its cytotoxicity (48, 462). Doxorubicin accumulation occurs slowly both by passive diffusion and solute-carried mediated events. The uptake assay described in our experiments rules out the possibility that LPA had any effect on the rapid uptake of doxorubicin. However, it does not address the role of LPA in long-term uptake of doxorubicin. The Fluo3 efflux assay shows only a modest increase in efflux in LPA-treated cancer cells. It is possible that only a small percentage of the cell population has a higher rate of efflux and survives chemotherapy initially. In fact, side population cells have been identified in cancer

cells, which express higher levels of ABCG2 (83). However, such experiments were not pursued further because of the technical challenges in isolating these cells and establishing their cancer stem cell-like phenotype. It remains possible that some doxorubicin is excluded from the nucleus. We will need to measure radioactive doxorubicin concentrations in nuclear and cytoplasmic preparations to test the nuclear exclusion of doxorubicin in LPA-treated cancer cells.

The cell-wide localization of the ABC transporters in drug-resistant cell is not surprising given their importance in export of a variety of other endogenous substrates such as glutathione, estrone 3-sulfate and leukotrienes. For example, ABCG2 localized to the mitochondria where it functions as an organic anion transporter (463). A trafficking mechanism to early endosomes may explain their localization in basolateral membranes (464). Similarly other ABC-transporters are also localized to internal membranes, where they contribute to increased compartmentalization and efflux of drugs. LPA increased other ABCC- family members, ABCC2 and ABCC3. Both ABCC2 and ABCC3 were previously shown to be regulated by Nrf2-mediated ARE activation (423, 465) and they are sensitive to the effects of inhibitory effects of probenecid used in our experiments.

Although we have focused on apoptosis, doxorubicin can also activate non-apoptotic killing such as p53-induced senescence and autophagy. The tumor suppressor, p53, is a mediator of cellular response to stress and DNA damage response. Cells respond to chemotherapeutic damage by p53-induced cell cycle arrest and apoptosis. It was previously demonstrated in lung cancer cells expressing

wild-type p53 that LPA-LPA<sub>1</sub> signaling could act directly on p53 stability by nuclear exclusion and proteosomal degradation (191). We showed that LPA-treated cancer cells are protected from doxorubicin-induced PARP cleavage in MDA-MB-231 and MDA-MB-453 cells. MDA-MB-231 cells harbor a p53 mutation, which may explain their increased resistance to starvation or drug-induced PARP cleavage. MDA-MB-453 cells, which are p53-null (466), were more sensitive to starvation/doxorubicin-induced PARP cleavage and were also protected by LPA.

We demonstrate that Nrf2 protein expression and activation is increased by LPA. Several signaling pathways including PI3K (442, 467), ERK (468, 469) and protein kinase C (470) are implicated in increasing Nrf2 expression and its transcriptional activity. Our results indicate that LPA activates LPA<sub>1</sub>-PI3K signaling pathway to increase Nrf2 stabilization and nuclear accumulation. This is likely through G<sub>i</sub> since LPA-induced increases in *ABCC1* and *ABCG2* mRNA were sensitive to pertussis toxin. Nrf2 is commonly stabilized by modification in another protein called Keap1, which binds to Nrf2 and targets it for ubiquitinylation (426, 471). Our results show that Keap1 protein expression was unchanged by LPA-treatment. Our results also demonstrate that PI3K activity is required for LPA-induced stabilization of Nrf2 expression and increased transcription of antioxidant and multi-drug resistant transporter genes. Although previous work also showed that PI3K is a major regulator of nuclear localization of Nrf2 and its transcriptional activity (442, 467, 472-474), it is less clear how this occurs.

We did not test the effects of LPA receptor activation on Keap1-Nrf2 or Keap1-independent stabilization mechanisms directly. We also did not measure cellular ROS levels directly in the presence of LPA and chemotherapy. Multiple phosphorylation sites have been identified on Nrf2 which are modulated by casein kinase1/2 (475), ERK (469), PKC (476) and GSK3 (477). One interesting possibility is that repression of GSK3 $\beta$  downstream of PI3K-Akt signaling is involved in increasing Nrf2 expression (477-479). High levels of oxidative stress could induce GSK3 $\beta$  activation to repress Nrf2 activity. Furthermore, inhibition of GSK3 $\beta$  blocks the effects of LY294002 on sensitizing lung cancer cells to chemotherapy (480). This would also explain why effects of t-BHQ and LPA are additive since t-BHQ operates by a Keap1-dependent mechanism, which can rapidly stabilize Nrf2 (471) independently of the effects of GSK3 $\beta$ .

In conclusion, increased expression of Nrf2 is involved in tumor proliferation, protection from oxidative damage and chemoresistance. However, little is known about factors that control Nrf2 expression in the tumors. We demonstrated that LPA increased stabilization of Nrf2, which results in increased transcription of antioxidant MDRT genes using cell culture models. The next Chapter will describe our work where we determined if some of these effects occur *in vivo* and if targeting ATX/LPA signaling selectively in cancers could improve the efficacy of chemotherapies.

**CHAPTER 4 – INHIBITION OF ATX/LPA SIGNALING DECREASES NRF2  
EXPRESSION AND SENSITIZES CANCER CELLS TO CHEMOTHERAPY-  
INDUCED KILLING IN A MOUSE MODEL OF BREAST CANCER.**

**A version of this chapter has been published in:**

**Venkatraman G**, Benesch MGK, Tang X, Dewald J, McMullen TPW and Brindley DN.  
(2015) Lysophosphatidate signaling stabilizes and increases the expression of genes  
involved in drug resistance and oxidative stress response: implications to cancer  
chemotherapy. *FASEB J* 29, 772-785.

[Some parts of this chapter are unpublished and currently under submission]

## 4 CHAPTER 4

### 4.1 INTRODUCTION

Cell culture models are limited by their inability to model the total tumor microenvironment thus limiting the study of drug resistance (69, 481). Mice models of breast cancer provide an excellent opportunity to study the role of ATX/LPA signaling in tumor growth, metastasis and drug resistance *in vivo*. Most breast cancer cell lines express little ATX and they depend on the tumor microenvironment for their ATX production (133, 137). We proposed two ways to target ATX/LPA signaling *in vivo* in the tumor microenvironment – 1) Blocking LPA production by inhibition of ATX and 2) Increasing the degradation of LPA and attenuating its ability to signal by overexpression of LPP1 or LPP3 (214).

The 4T1 syngeneic orthotopic breast cancer model is considered to be high-grade, triple-negative, stage IV breast cancer (482). Unlike the xenograft models, immune function is intact in these mice and plays an important role in regulating tumor growth and metastasis (483). Hence, syngeneic models are good candidates for testing the effect of chemotherapies and immunotherapies (484). The 4T1 breast cancer cell line was derived originally as a subpopulation from a spontaneous metastatic tumor in BALB/c mice (485, 486). The 4T1-12B and 4T1-luc cell lines were derived from a 4T1 cell line by stably overexpressing firefly luciferase, which allows for imaging of metastasis after injecting the live animals with D-luciferin (463,464). 4T1 tumors show inherently poor sensitivity to chemotherapies (485-488). Residual 4T1 cells continue to progress even after the removal of the primary

tumor by surgery (483, 489). 4T1 tumors are considered to be an inflammatory breast cancer model with increased inflammation in the tumor microenvironment and increased circulating cytokine/chemokine levels in the late stages of tumor progression (487, 490). The modified cell lines 4T1-12B and 4T1-luc2 cells regress following an initial phase of tumor growth unlike the parental 4T1 cell line (137). This is likely due to a robust immune response to the expression of luciferase resulting in necrosis of the tumors after 3-4 weeks (137, 487). The 4T1 model is used to model human metastatic breast cancers because of its ability to metastasize to multiple organs including lungs, liver, brain and bone when implanted orthotopically. This model is used to study early metastatic events from the event of transplantation into mammary fat pad to late stage metastasis. Metastasis to lungs and liver can occur as early as 8 days (491).

ONO-8430506 (ONO pharmaceuticals, Osaka, Japan; US patent application number 13807947 (261)) is a potent ( $IC_{90} \sim 100$  nM) and competitive ATX inhibitor, which was able to suppress plasma ATX activity and LPA levels in both regular and cancer-bearing BALB/c mice. Further, ONO-8430506 (10 mg/kg) was able to delay tumor growth by itself in a 4T1 orthotopic syngeneic model of breast cancer and decreased spontaneous lung metastasis (nodule formation) by 60% (137). A direct effect in decreasing the concentration of LPA species (-16:0, 16:1, 18:1, 18:2, 18:3, 20:4) was also observed. This suggests ONO-8430506 can block localized production of LPA in the tumor. A prior publication had suggested that ONO-8430506 effectively targeted plasma ATX activity in mouse, donkey, dog, rat and

humans. ONO-8430506 thus represents a highly bio-available ATX inhibitor and was reported to be highly specific for autotaxin (262).

LPP1 expression has been inversely correlated with increased cancer cell growth and proliferation in ovarian and breast cancers. Our group demonstrated that overexpression of LPP1 in syngeneic or xenograft tumor models resulted in decreased tumor progression and metastasis (183) by attenuating extracellular LPA signaling. LPP1 overexpression degraded extracellular LPA *in vitro*. However, we did not find any evidence for this in the tumor and the major effects of LPP1 are downstream of receptor activation (183).

Increased ATX/LPA signaling is observed in many chronic inflammatory conditions, such as cancer, where LPA promotes local wound healing and tissue remodeling. We used the previously developed 4T1 inflammatory breast cancer model to test some of our cell culture results described in the previous Chapter. Specifically, we tested if ATX inhibition increases the sensitivity of breast cancers to the commonly used chemotherapeutic doxorubicin by decreasing the adaptive response initiated by Nrf2 signaling. Finally we examined the effects of doxorubicin and tamoxifen on the inflamed tumor microenvironment, ATX production and activation of antioxidant response in the tumors.



## 4.2 RESULTS

### 4.2.1 Attenuation of LPA signaling decreases Nrf2 expression in a mice model of breast cancer

We hypothesized that Nrf2 expression is decreased in the two approaches of targeting LPA signaling described earlier. We initially tested the ATX inhibition model, where mice that had been treated with ONO-8430506 for up to 11 days showed a significant decrease in tumor progression (137). Immunoblots obtained from the 4T1-12B tumors of these mice on Day 11 show significantly decreased protein expression of Nrf2 and its gene target NQO1 in ONO-8430506-treated group (Fig. 4.1A and B).

We used RT-PCR to profile other previously identified Nrf2-targets in these tumors. Several genes including *GPXI*; glutathione peroxidase-1, *GCLM*: glutamate cysteine ligase modifier subunit, *SOD1*, 2: superoxide dismutase-1 and -2, *PRDX4*: peroxiredoxin-4, *TXNRD1*, 3: thioxyredoxin-1 and -3, *SCD1*: stearoyl CoA desaturase 1, *NQO1*, *IL19*: interleukin-19, *ABCC1*, *ABCBI*, and *BCL2L1* were decreased significantly in ONO-8430506-treated tumors (Fig. 4.1C). Additionally, we present preliminary evidence that LPP1 overexpression can regulate Nrf2 expression *in vivo*. Nrf2 expression was decreased in tumors obtained from xenograft models, where LPP1 was over-expressed in various cancer cell lines (Fig. 4.2). These include MDA-MB-231 orthotopic model; TPC1 and 8305c subcutaneous thyroid cancer models (183).

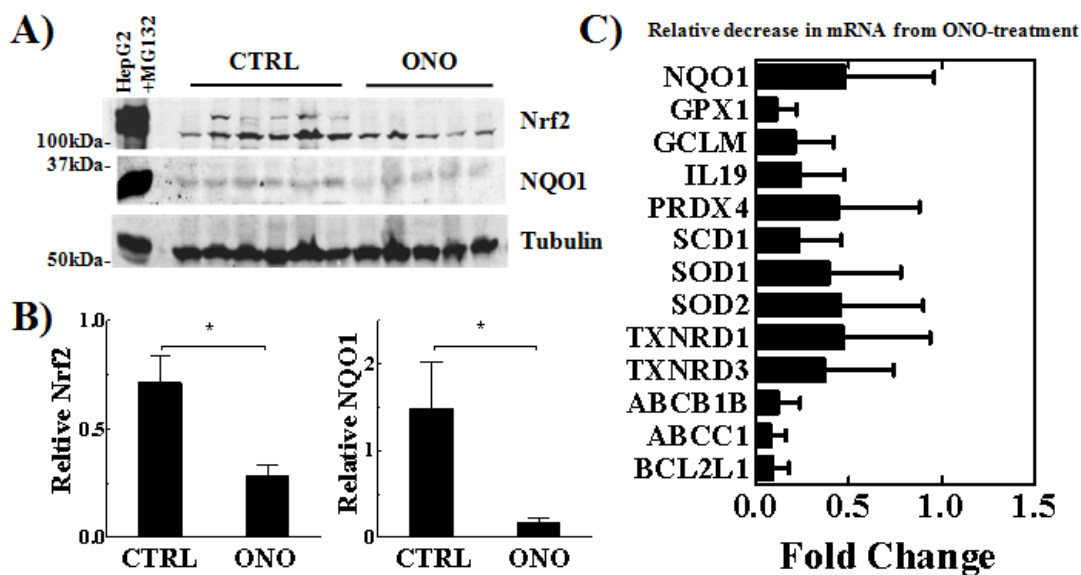


**Figure 4.1: The ATX inhibitor, ONO-8430506, decreased Nrf2 expression and the transcription of antioxidant genes and multi-drug resistant transporters in breast tumors.** Mouse 4T1-12B breast cancer cells were injected into mammary fat pad of female BALB/c mice, which were then gavaged daily with vehicle or 10 mg/kg ONO-8430506 (ONO) starting on the day after the injection until Day 11 (137). **A)** Western blots for Nrf2 and NQO1 relative to tubulin expression. **B)** Quantification of Nrf2 and NQO1 protein expression from (A). Significance was analyzed by two-tailed t-test. **C)** mRNA from 6 vehicle and 6 ONO-8430506-treated tumors were analyzed for 84-Nrf2 responsive genes using a limited oxidative stress and cancer drug resistance profiler array. P-value was calculated between treatments for individual genes. When p-value was <0.01, significant changes were reported as relative fold change  $\pm$  95% confidence intervals. NQO1, NAD(P)H dehydrogenase, quinone 1; GPX1, glutathione peroxidase 1; GCLM, glutamate-cysteine ligase, modifier subunit; IL19, interleukin 19; PRDX4, peroxiredoxin 4; SCD1, stearoyl-Coenzyme A desaturase 1; SOD1, Superoxide dismutase 1, soluble; SOD2, superoxide dismutase 2, mitochondrial; TXNRD1, thioredoxin reductase 1; TXNRD3, thioredoxin reductase 3; ABCB1B, ATP-binding cassette, sub-family B (MDR/TAP), member 1B; ABCC1, ATP-binding cassette, sub-family C (CFTR/MRP), member 1; BCL2L1. Bcl2-like 1.

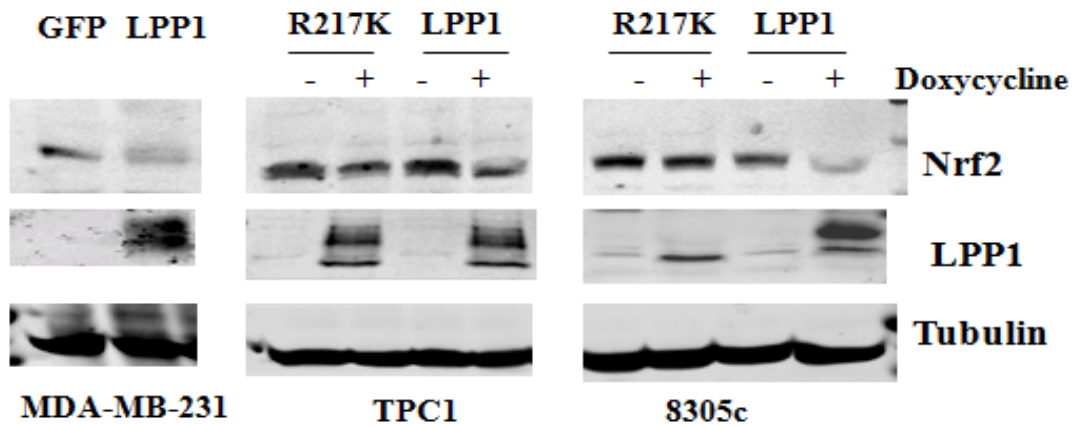


**Figure 4.2: Stable or doxycycline-induced LPP1 overexpression in xenograft tumors decreased Nrf2 expression:** LPP1 or the catalytically inactive R217K were stably overexpressed in a constitutive MDA-MB-231 orthotopic model or inducibly in TPC-1 and 8305C subcutaneous tumor xenografts by Tang *et al.*, (183). Tumors from these mice were immunoblotted for Nrf2, LPP1 and tubulin expression as described previously.

#### 4.2.2 ATX inhibition combined with doxorubicin decreased tumor formation and improved treatment outcome

To test if the decreased expression of Nrf2 expression, anti-oxidant genes and MDRTs could provide a novel mechanism for improving the sensitivity to chemotherapeutic agents, we used the previously described syngeneic orthotopic model of breast cancer. We tested if ONO-8430506 enhanced the effects of doxorubicin in decreasing breast tumor progression and metastasis. 4T1 breast cancer cells were used in these experiments since they produce more sustained tumor growth and metastasis compared to 4T1-12B cells (137).

Doxorubicin treatment on its own had very little effect on the breast tumor growth (Fig. 4.3A inset). However, the effectiveness of both doxorubicin and ONO-8430506 were enhanced when they were combined. ONO-8430506 on its own

decreased the growth of breast tumors, but only for about 11 days as expected (137). However, ONO-8430506 when combined with doxorubicin, further slowed tumor growth and extended the effectiveness of ONO-8430506 treatment until Day 17 (Fig. 4.3A). Tumor masses obtained on Day 12 reflected the decreases in tumor volume (Fig. 4.3B). Doxorubicin-treatments had no significant effect on the body weights of the mice until Day 14 and ONO-8430506 was well tolerated by the mice during the whole experiment (Fig. 4.3C). Blood leukocyte levels were unchanged between the treatments. However, the increase in blood leukocyte levels in DOX/DOX+ONO treatments on Day 21 were smaller compared to their controls with a corresponding decrease in body weights (Fig 4.4).

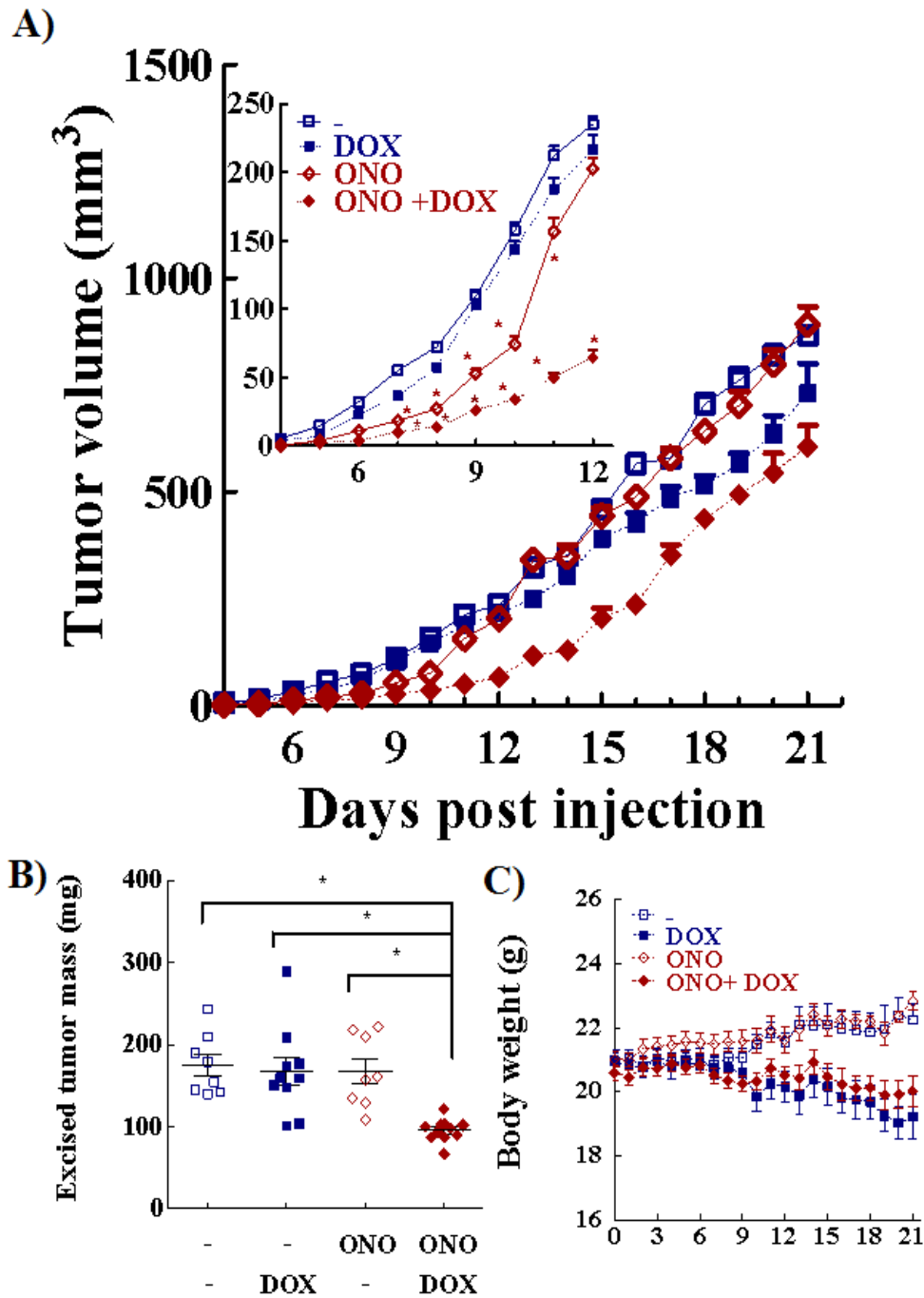


**Figure 4.3: Combination of ATX inhibition with doxorubicin treatment in decreasing breast tumor growth in mice.**

A) 4T1 cells were injected into the mammary fat pad of female BALB/c mice. Mice were gavaged daily with vehicle or 10 mg/kg ONO-8430506. They were injected i.p. with PBS or doxorubicin (4 mg/kg) every third day starting from Day 3 after the injection of 4T1 cells. Tumor volumes are shown from Day 4 until Day 21 and the inset shows an expanded view

up to Day 12. **B)** The weights of the excised tumor are shown at Day 12. **C)** Shows the body weights of the mice for 9 mice per group. Results are means  $\pm$  SEM (where large enough to be shown). Two-way or one-way ANOVA with post-hoc tests were used for calculating significance between treatments. \*  $p < 0.05$ .

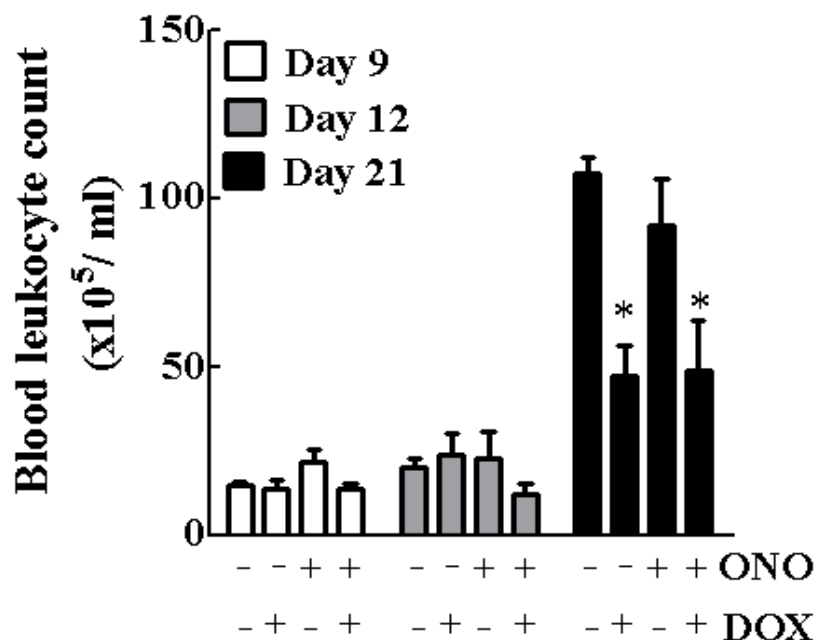


**Figure 4.4: Blood leukocyte count** – Blood leukocyte levels were determined from the 4 groups of mice as described in Materials and Methods from Days 9, 12 and 21. Results are means  $\pm$  SEM. n=5. One-way ANOVA with post-hoc test was used to calculate significance between treatments on each day. \*  $p < 0.05$ .

#### 4.2.3 Combination of doxorubicin and ATX inhibition decreased metastases in orthotopic and tail-vein 4T1 models

Inhibition of ATX/LPA signaling has been shown to decrease soft tissue and bone metastasis. We studied the effect of ONO-8430506 and doxorubicin treatments on distal sites of metastasis. Spontaneous 4T1 metastases in the lung and liver were decreased by the combination of ONO-8430506 with doxorubicin as measured by counting metastatic colonies in the H&E stained tissue sections (Fig. 4.5A). Next,

we injected 4T1 cells directly into the tail-vein of mice and this produced a large number of macroscopic lung nodules. Combination of doxorubicin and ONO-8430506 significantly decreased lung metastasis (Fig. 4.5B). This demonstrates that ATX inhibition enhances effectiveness of doxorubicin therapy in both the primary tumor and distal sites.

#### **4.2.4 Analysis of tumors treated with combination therapy show increase caspase3 activation, decreased proliferation and decreased GSH**

Glutathione (GSH) is a primary cellular antioxidant that is converted to glutathione disulfide (GSSG) upon oxidation. Cellular glutathione levels are commonly used to assess oxidative damage in cancers (492). We measured both reduced and total glutathione in the tumors using a luciferase-based assay. Reduced glutathione concentrations in the tumors were significantly decreased by the combination of doxorubicin with ONO-8430506 (Fig. 4.6). Total glutathione (GSH+GSSG) levels were not changed significantly in the samples analyzed (Fig. 4.6).

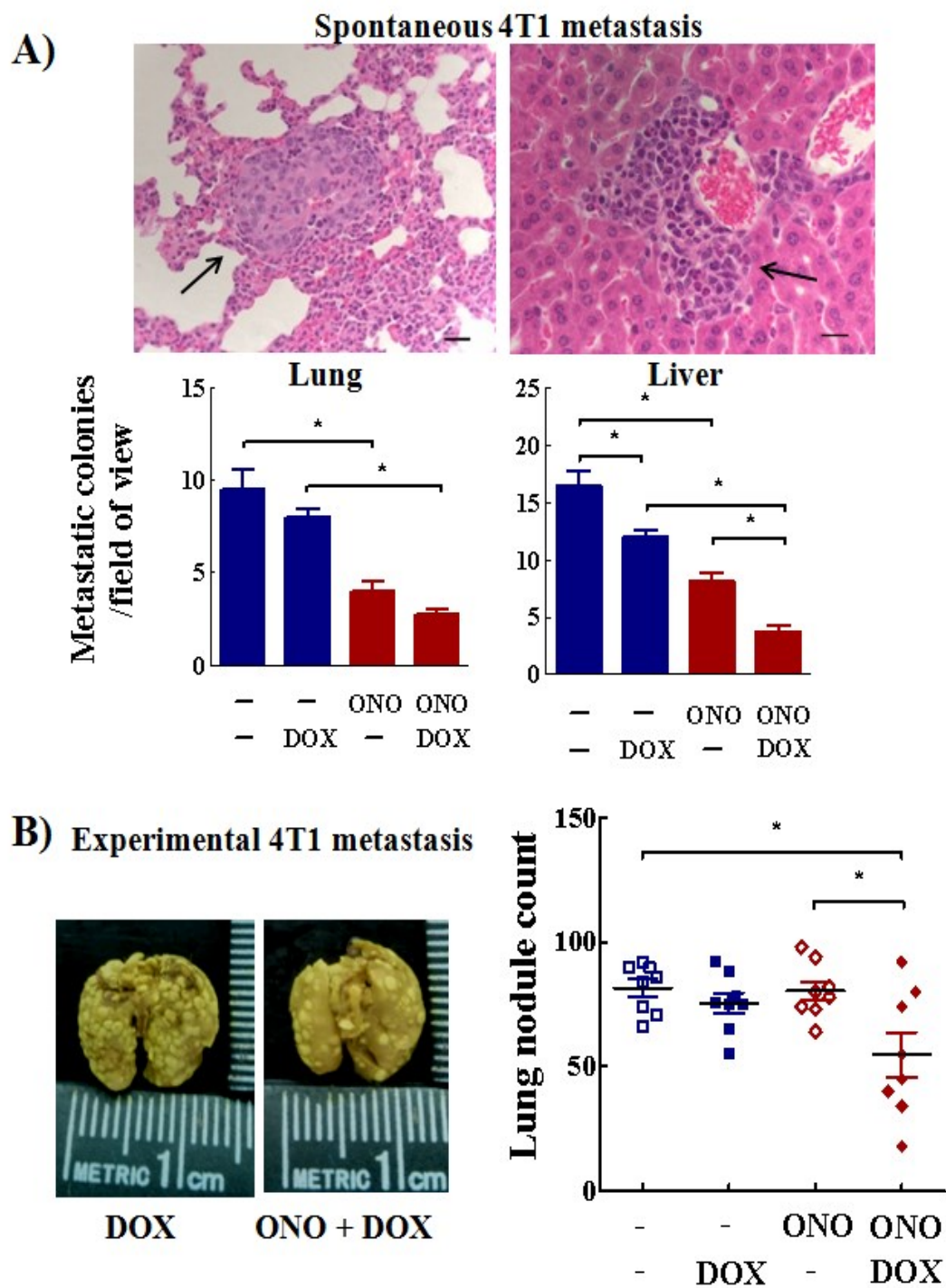


**Figure 4.5: ATX inhibition combined with doxorubicin decreased spontaneous and experimental metastasis in mice.** A) H&E stained sections of lung and liver were counted for metastatic colonies (top) at Day 21 from the experiments described in Figure 4.3. Quantification of lung and liver spontaneous metastases from these sections are shown



(bottom). Scale bar = 25  $\mu\text{m}$ . **B)** 4T1 cells were injected into the tail vein and mice were treated with ONO-8430506 and doxorubicin as in Figure 4.3. Lungs were excised on Day 14. A representative image of a lung from the groups is shown after staining in Bouin's solution (left). The left lobe of 8 mouse lungs from each group was counted for macroscopic nodules. Results are means  $\pm$  SEM. Significance was analyzed by one-way ANOVA with post-hoc test. \*  $p < 0.05$ .

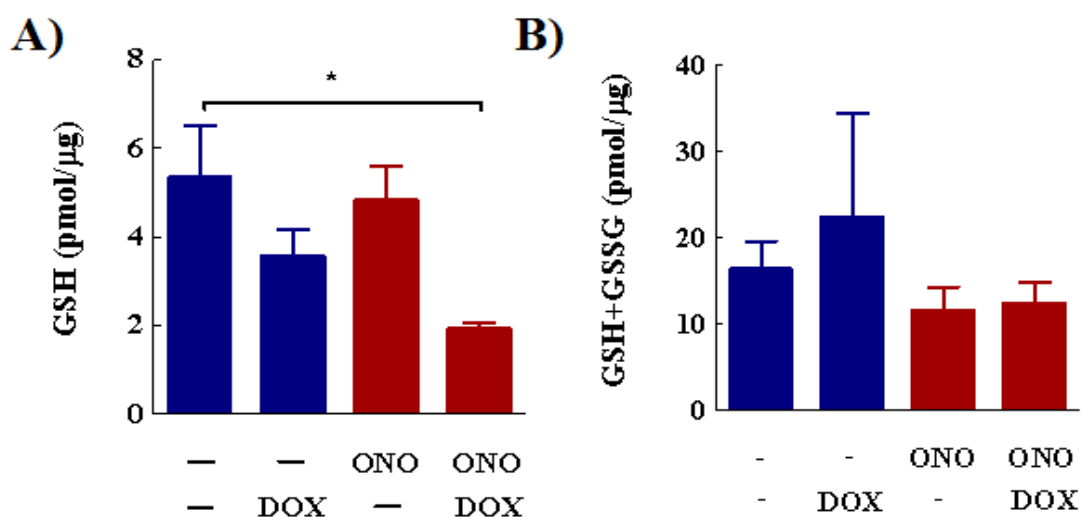


**Figure 4.6: Combination of ATX inhibition with doxorubicin decreases the concentration of glutathione (GSH) in the breast tumors.** Tumors obtained at Day 12 from the mice described in Figure 4.3 were analyzed for reduced glutathione (**A**) and total glutathione (**B**) concentration as described in materials and methods.  $n=4$ . Results are means  $\pm$  SEM. One-way ANOVA with post-hoc test was used for calculating significance. \*  $p < 0.05$ .

To assess the effect of these treatments on the survival and proliferation of the tumor cells we used immunohistochemical analysis. Cleaved caspase-3 staining showed significant increases in the tumors treated with ONO-8430506 and doxorubicin. This indicates higher levels of apoptosis. Ki67 levels were decreased in the tumors treated with ONO-8430506 and doxorubicin. Lower Ki67 levels indicates a decreased proliferation and mitotic index (Fig. 4.7).



way ANOVA with post-hoc test was used to assess the differences between the treatments. Scale bar = 25  $\mu$ m. \*  $p < 0.05$ .

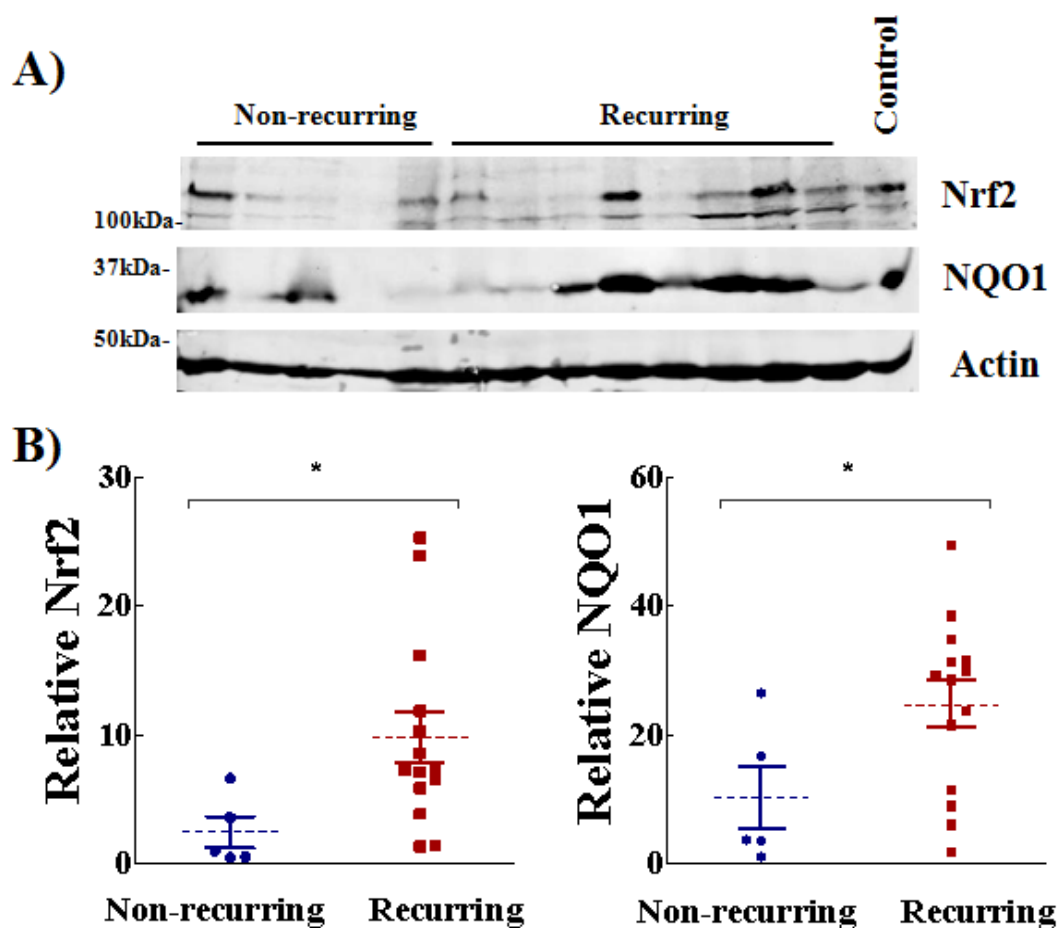


**Figure 4.8: Expression Nrf2 and NQO1 is increased in tumors from patients with recurrent breast cancer** – **A)** Banked primary breast tumors from patients were immunoblotted for Nrf2 and NQO1 expression. Patients were classified as recurring or non-recurring after one year based on their disease-free status following lumpectomy and subsequent therapy. **B)** Quantification of Nrf2 and NQO1 protein expression relative to actin. Results from 5 non-recurring and 14 recurring tumors were expressed as relative means  $\pm$  SEM. Significance was assessed by two-tailed t-test. \*  $p < 0.05$ .

#### 4.2.5 Analysis of banked patient samples

We determined Nrf2 expression in breast tumor samples from patients who had received prior doxorubicin therapy before surgery. Samples were retrospectively

classified as recurring or non-recurring tumors based on their disease-free recurrence up to one year after lumpectomy. Protein levels of Nrf2 and NQO1 in tumors were higher among patients with recurrent metastatic disease compared to non-recurring cancer (Fig. 4.8).

#### **4.2.6 Doxorubicin increases tumor-promoting inflammation and ATX production in the tumor adjacent fat pad**

Inflammation is inversely correlated to prognosis in patients and is associated with increased resistance to chemotherapy(172). Cancer cells and stromal cells in the tumor microenvironment produce cytokines, chemokines and growth factors that drive tumor growth, progression and resistance to therapies (69). Doxorubicin-treated tumors display increased inflammation in tumors and infiltration by tumor-promoting macrophages leading to chemo-resistance (493). However, we did not observe any differences in blood leukocyte levels by doxorubicin-treatment in the 4T1 model until late stages of tumor progression (Fig. 4.4).

Orthotopic tumor models are usually refractory to doxorubicin therapy. We tested if *in vivo* doxorubicin resistance is mediated by inflammation-driven production of ATX in the tumor microenvironment. LPA can in turn decrease the accumulation of doxorubicin in cancer cells and enhance repair from oxidative damage. Hence, we tested the effect of doxorubicin on the production of inflammatory mediators in the 4T1 orthotopic model. 4T1 tumors, adjacent mammary fat pad and contralateral mammary fat pad from control-/doxorubicin-

treated mice were analyzed by a cytokine/chemokine multiplex array ELISA. Several cytokines/chemokines such as MCP1, G-CSF, M-CSF, IL-6, IP10 and GRO were highly increased in the tumors when compared to either adjacent or contralateral fat pads (Fig. 4.9). These cytokines/chemokines were also higher in tumor-adjacent fat pad compared to contralateral fat pad indicative of inflammation in the tumor-adjacent fat pad. Doxorubicin-treatment further increased the cytokine/chemokine levels in the tumor-adjacent fat pad. The cytokine/chemokine levels were not changed in the inflamed tumors by doxorubicin treatment except for IL-6, which was increased by about 33% (Fig. 4.9).

Adipose tissue is a significant source of ATX and contributes to plasma LPA levels (145). We next measured ATX levels in the fat pads by ELISA to test if doxorubicin-induced inflammation in adjacent tissue leads to increased ATX production (154). Plasma ATX activity was unchanged in the doxorubicin-treated mice (Fig. 4.10A). ATX protein levels were significantly elevated in tumor adjacent fat pads (Fig. 4.10B), which is the main source of ATX activity in the tumors (137). Doxorubicin-treatment significantly increased ATX protein levels in the tumor-adjacent fat pad, similar to the results obtained for cytokine/chemokine production in the tumor-adjacent fat pad.

We previously showed that LPA-treated cells were protected from the cytotoxic effects of doxorubicin. Doxorubicin had no effect on cytokine/chemokine mRNA levels in MCF-7 cells grown in charcoal-depleted serum. However, the

combination of LPA and DOX was enough to increase cytokine/chemokine mRNA levels (Fig. 4.11). Similarly, we observed a correlation between endogenous

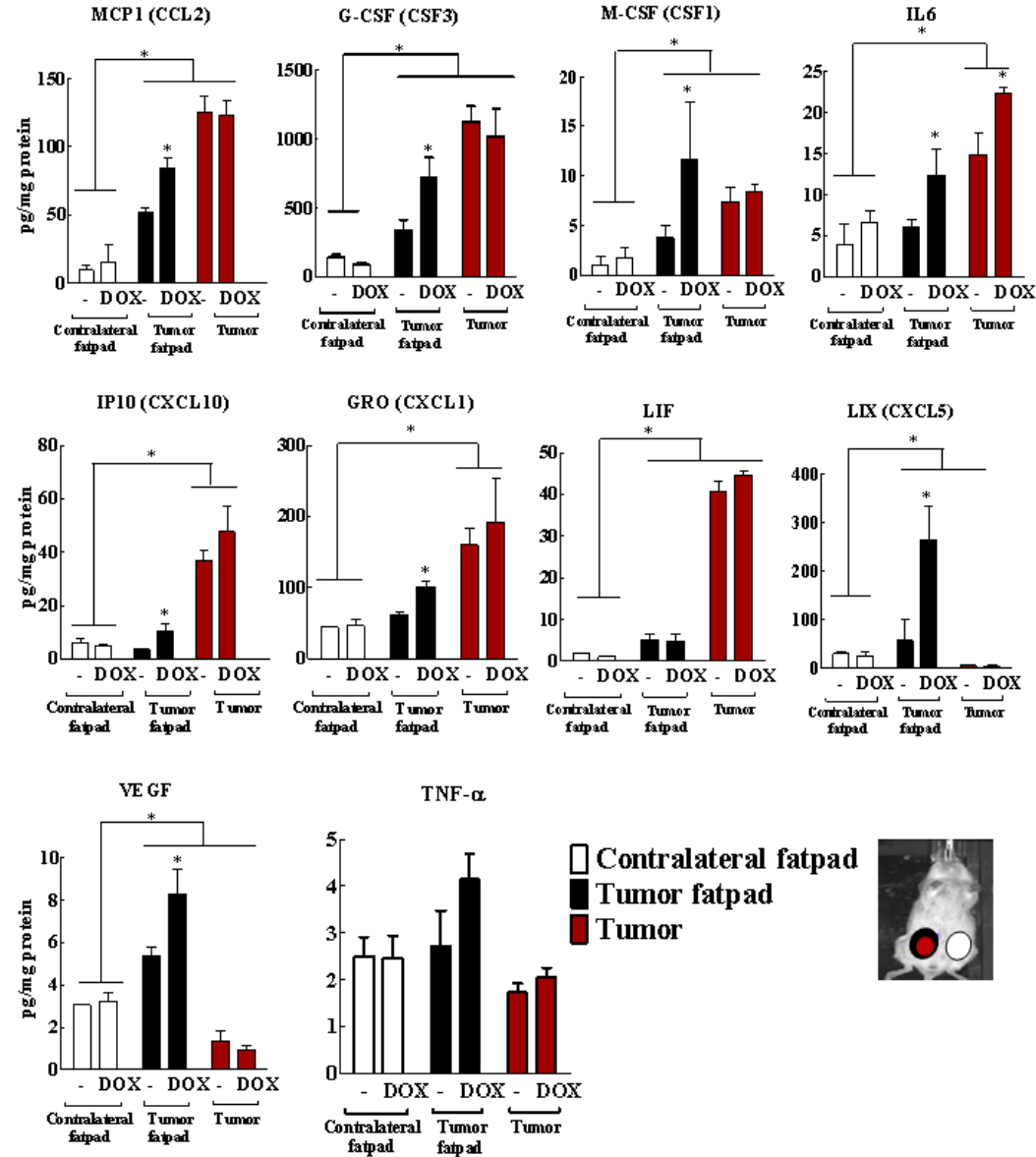


**Figure 4.9: Doxorubicin increases production of inflammatory cytokines in the tumor-adjacent fat pad in mice bearing 4T1 tumors** – Tumors, tumor adjacent fat pads (tumor fatpad) and contralateral fat pads were collected from 5 vehicle or doxorubicin-treated mice. Homogenized tissue lysates were adjusted for their protein concentration by BCA assay and

analyzed for 31 cytokine/chemokine levels by multiplex ELISA. Results are represented as mean  $\pm$  SEM. Significance was assessed by ANOVA with treatment-matching. \*  $p < 0.05$ .

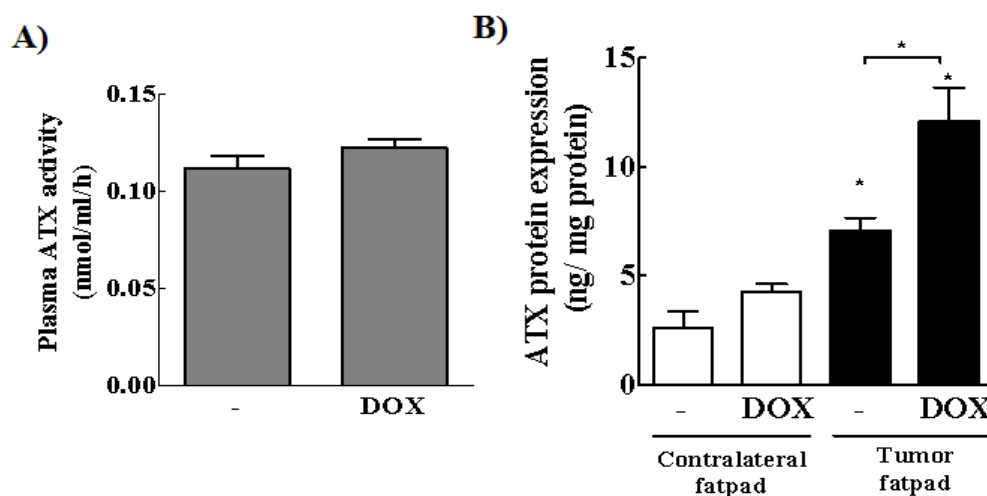


**Figure 4.10: Doxorubicin increases ATX protein expression in the tumor-adjacent fat pad in mice bearing 4T1 tumors** – A) Plasma ATX activity was determined in 10 vehicle or doxorubicin-treated mice. B) tumor adjacent fat pads and contralateral fat pads were collected from 8 mice treated with vehicle or doxorubicin. A standard curve was run alongside the samples to determine ATX protein expression quantitatively in a sandwich ELISA plate. Results are represented as mean  $\pm$  SEM. Significance was assessed by one-way ANOVA with a post-hoc test. \*  $p < 0.05$ .

cytokine/chemokine mRNA levels and resistance to doxorubicin in MCF-7 cells (Fig. 4.12). Together with our experiments *in vivo*, these results suggest that LPA signaling contributes to doxorubicin resistance through increased cytokine/chemokine production in the tumor microenvironment.

We next tested the effect of blocking LPA signaling on cytokine/chemokine production in the inflamed 4T1 tumors. ONO-8430506 had no effect on cytokine/chemokine levels either by itself or in the presence of doxorubicin in the

tumor (Fig. 4.13). Thus combination therapy did not affect cytokine/chemokine production in the tumors significantly despite the therapeutic benefit of the combination therapy.

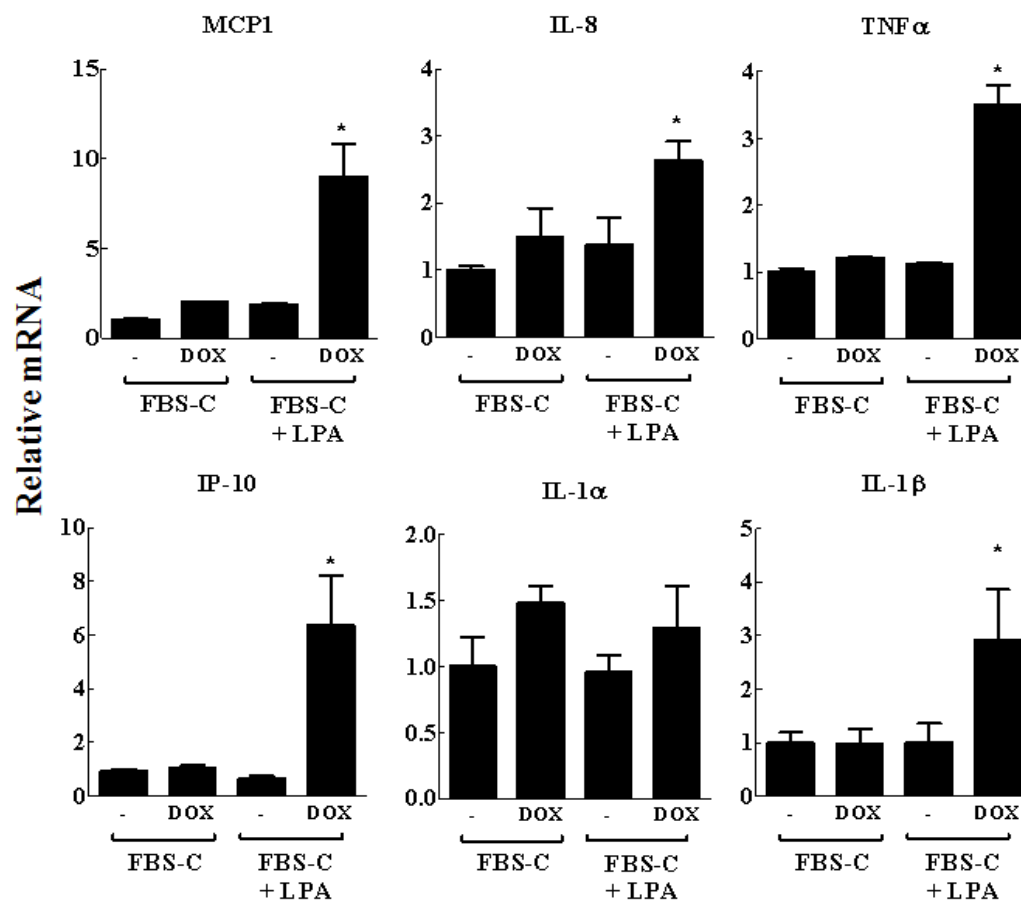


**Figure 4.11: Doxorubicin increases several cytokine/chemokine mRNA in LPA-treated MCF-7 breast cancer cells** – MCF-7 cells grown in regular growth media were changed to FBS-C media for 21 h before the addition of control or 1 μM LPA for another 3 h. One μM doxorubicin was then added to the cells and the mRNA was analyzed after 6 h. Results are represented as mean ± SEM. Significance was assessed by one-way ANOVA with a post-hoc test. \* p<0.05.



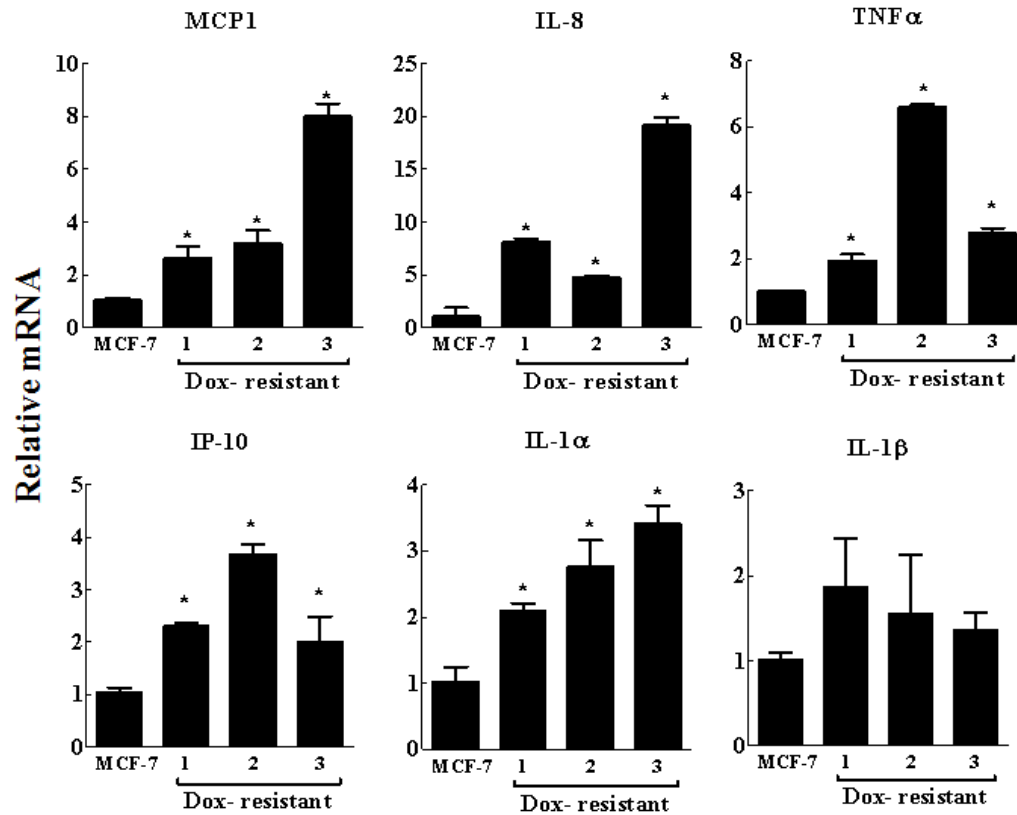


**Figure 4.12: MCF-7 selected for resistance to doxorubicin express higher levels of several cytokine/chemokine mRNA** – MCF-7 breast cancer cells or MCF-7 1, 2, 3 cells selected previously for resistance to doxorubicin at 43.6 nM, 98.1 nM and 300 nM respectively were analyzed for the mRNA levels of MCP1, IL-8, TNF $\alpha$ , IP-10, IL-1 $\alpha$  and IL-1 $\beta$ . Results are represented relative to GAPDH mRNA as mean  $\pm$  SEM. Significance was assessed by one-way ANOVA with a post-hoc test. \* p<0.05.

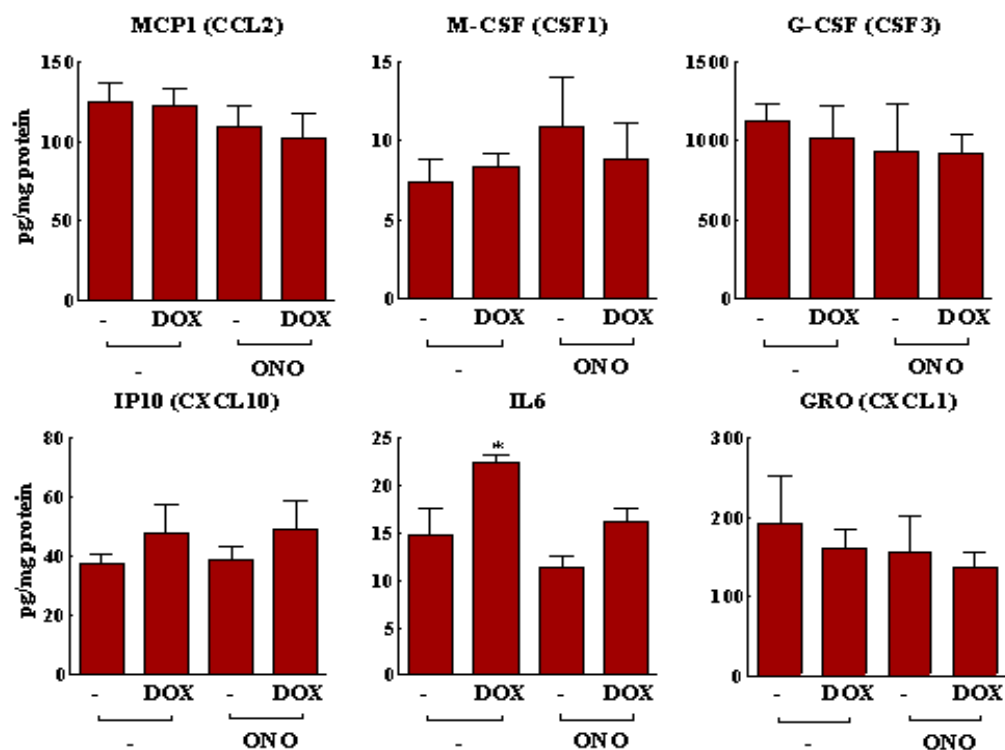


**Figure 4.13: Doxorubicin and ONO-8430506 treatment had no effect on the protein-normalized cytokine/chemokine production in 4T1 breast tumors** – Tumors were collected from 5 vehicle-, doxorubicin-, ONO-8430506- and combination-treated mice. Homogenized tissue lysates were adjusted for their protein concentration by BCA assay and analyzed for cytokine/chemokine levels by multiplex ELISA. Results are represented as mean  $\pm$  SEM. Significance was assessed by ANOVA with treatment-matching. \*  $p < 0.05$ .

#### 4.2.7 Nrf2 and RALBP1 in tamoxifen-resistance

Tamoxifen is a widely prescribed targeted therapy in breast cancers, where it prevents estrogen-dependent growth signaling (Section. 1.1.7). Tamoxifen and its active metabolites build up to  $\mu\text{M}$  concentrations in cancer tissue resulting in generation of ROS and activation of antioxidant response, independent of the ER-dependent growth inhibitory effects of tamoxifen (96-100). Increased activity of drug-metabolizing enzymes and drug transporters have been linked to poor

tamoxifen-response in breast cancer patients (104). MCF-7 cells selected for tamoxifen-resistance show increased expression of Nrf2 and its target antioxidant proteins and drug transporters (106). We therefore hypothesized that ATX/LPA signaling contributes to tamoxifen-resistance through increased stabilization of Nrf2. To test this, MCF-7 cells grown in full growth media were treated with 0, 1, 5, 10, 20, 30  $\mu$ M of the active, short-lived metabolite 4-HT. Here, 4-HT increased Nrf2, NQO1 and RALBP1 expression (Fig. 4.14A). As described in Section 1.1.1, RALBP1 is involved in the oxidative stress response by increasing the export of glutathione-conjugates and 4-HNE. GFP-Nrf2 overexpressing HEK-293 cells, when treated with 4-HT, showed increasing nuclear localization of Nrf2, as seen previously with LPA<sub>1</sub> activation (Fig. 4.14B). ARE-luciferase activity was increased by 4-HT treatment in cells grown in starvation medium. This was additive to the effect of LPA-treatment due to increased Nrf2 stabilization (Fig. 4.14C, left and right panels).

Since RALBP1 expression also increased with increasing levels of Nrf2 stabilization, we tested if Nrf2 is a novel regulator of RALBP1. Knockdown of Nrf2 mRNA and protein expression in 4T1 breast cancer cells was achieved using specific dicer-substrate siRNAs 1-5 against Nrf2 (Fig. 4.15A left and right panels). This resulted in significant decreases in antioxidant genes such as NQO1, SOD1 and the MDRT, ABCC1. However, RALBP1 levels were unchanged by Nrf2 knockdown (Fig. 4.15B). Thus, Nrf2 regulates antioxidant proteins and MDRT in 4T1 breast cancer cells as expected. However, Nrf2 knockdown did not change RALBP1 levels.

We next tested the effects of tamoxifen on Nrf2 expression in 4T1 breast tumors using the syngeneic mouse model described earlier. The tumor weights at Day 10 were significantly decreased in tamoxifen-treated animals, after which tamoxifen-monotherapy had no significant benefit in decreasing tumor growth (Fig. 4.16A). The protein expression of Nrf2 was elevated in Day 10 tumors indicating higher levels of oxidative stress response (Fig. 4.16B). mRNA expression of antioxidant proteins NQO1, HMOX1 and SOD1 and the drug transporters ABCC1, ABCC3 and ABCG2 were also elevated, indicating higher levels of Nrf2 and ARE activation (Fig. 4.16C). Taken together, these results show that Nrf2 is elevated in tamoxifen-treated cancers cells and in tumor models, which could be a contributing component to tamoxifen resistance. Furthermore combination of ONO-8430506 with tamoxifen-treatment might provide a good strategy for preventing increased Nrf2 stabilization and development of tamoxifen-resistance.

RALBP1 was also elevated in tamoxifen-treated MCF-7 cancer cells. We tested the expression of RALBP1 in tissue microarrays built from tissue obtained from 176 breast cancer patients and 10 normal patients with breast reduction therapy. 142/176 samples and 5/10 samples could be processed and analyzed for RALBP1 staining intensity using immunohistochemistry. In these samples, RALBP1 was significantly elevated in the cancer patients (Fig. 4.17A left and right panels). ONO-8430506-treated 4T1 tumors show reduced RALBP1 protein as determined by both immunoblotting and immunohistochemistry (Fig. 4.17B and C). Our preliminary

results indicate that ATX/LPA signaling is a novel regulator of RALBP1 in breast cancer.

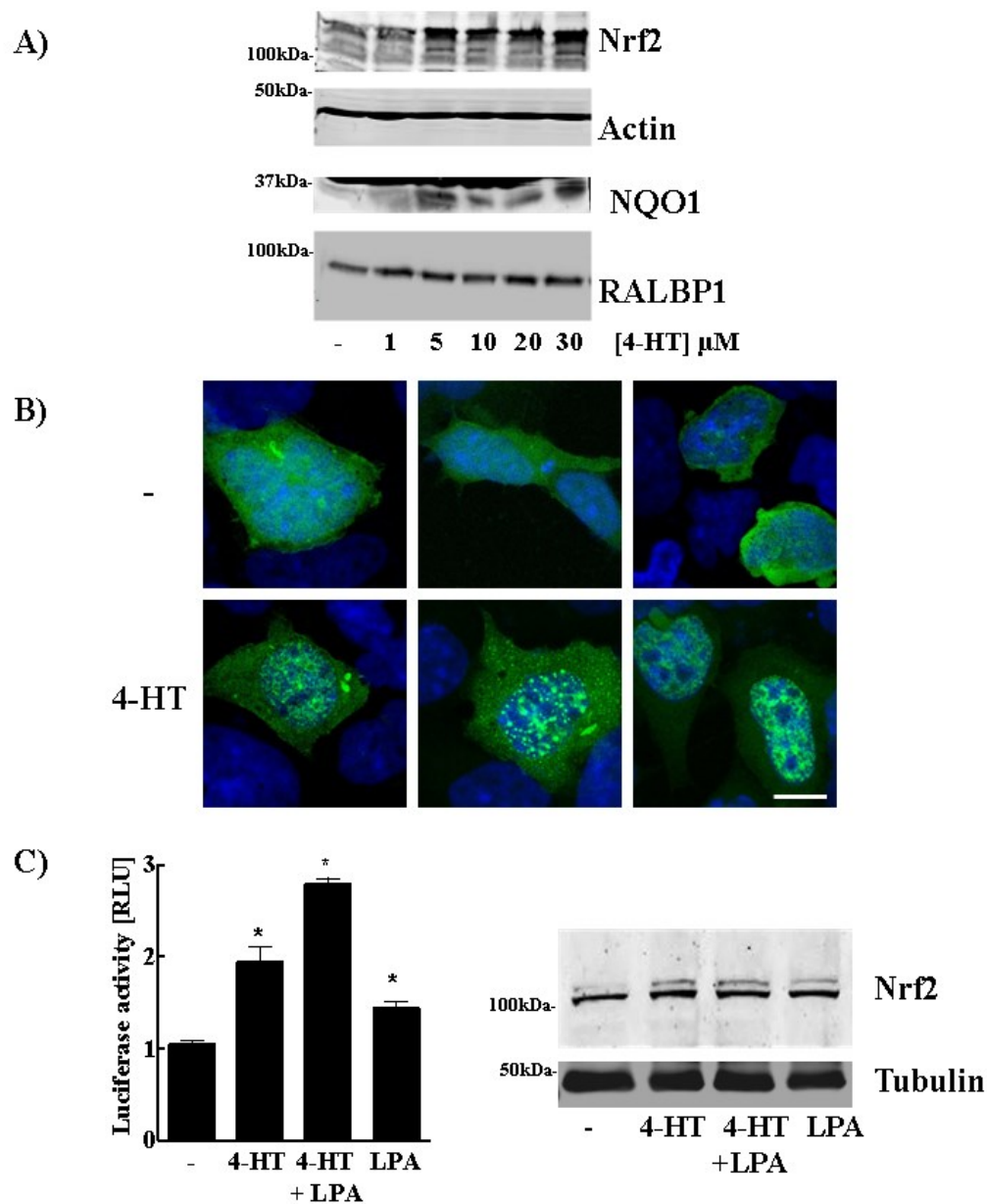


**Figure 4.14: 4-HT increases Nrf2 expression, nuclear localization and ARE activation** – **A)** MCF-7 were treated with 0, 1, 5, 10, 20, 30  $\mu$ M 4-HT in full growth media. Cell lysates were immunoblotting for Nrf2, NQO1 and RALBP1 expression **B)** HEK-293 cells grown in coverslips were transfected with 1  $\mu$ g GFP-Nrf2 per well for 24 h. Six h control or 20  $\mu$ M 4-HT treated cells were fixed and visualized by confocal microscopy. Scale bar is 10  $\mu$ m. **C)** AREc32 cells were grown in 4-HT with or without LPA in starvation media. The luciferase activity was measured as described before (left panel). Representative immunoblots of Nrf2

are shown for the treatments in the right panel. Results are represented as mean  $\pm$  SEM for 3 independent experiments. Significance was assessed by two-tailed t-test. \*  $p < 0.05$ .

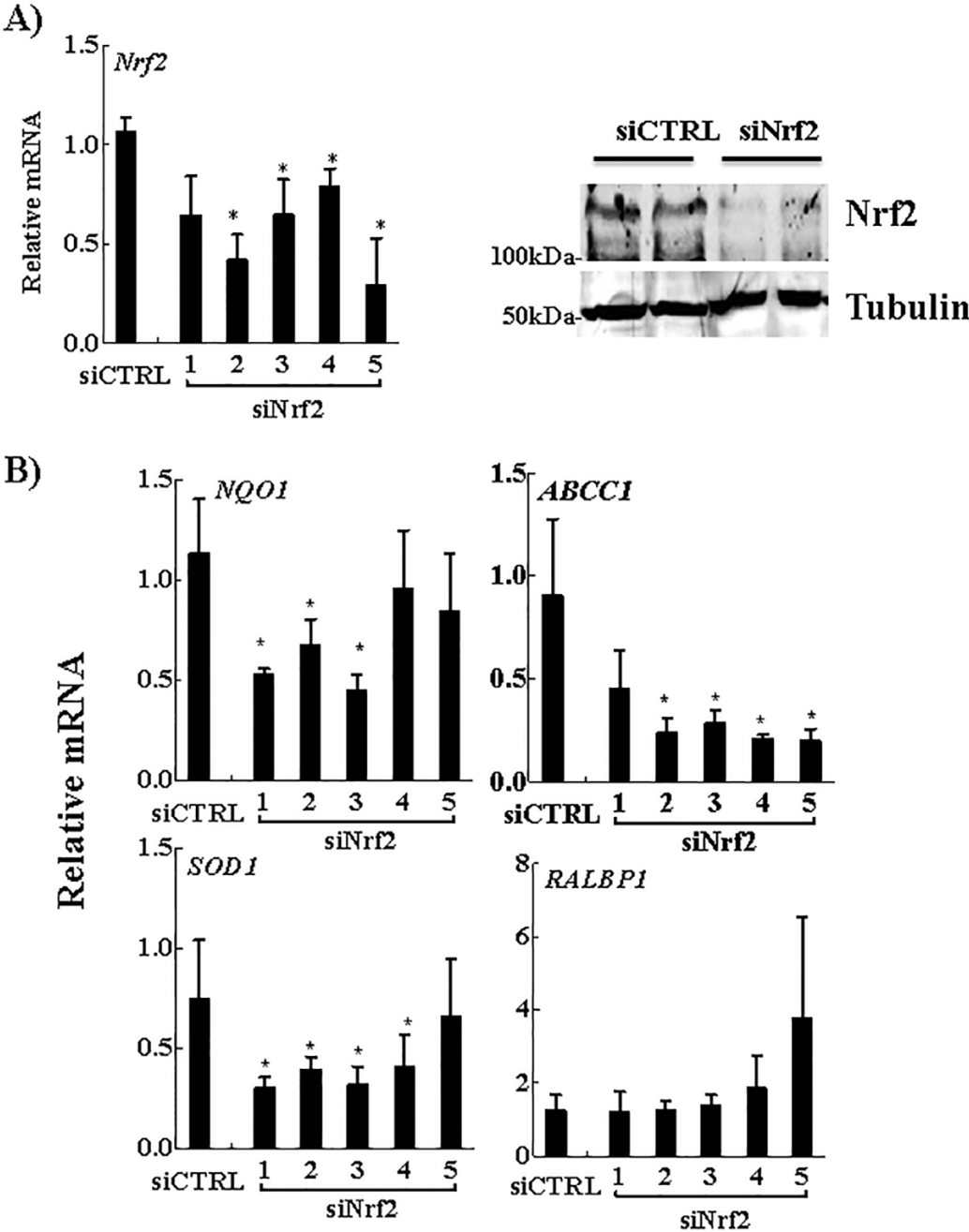


**Figure 4.15: Nrf2 knockdown in 4T1 cells decreases the expression of antioxidant and MDRT genes but not RALBP1 – A)** 4T1 cells were treated with 40nM of control or DsiRNAs 1-5 against Nrf2. The mRNA (left panel) and protein expression (right panel) of Nrf2 was determined after 48 h. **B)** NQO1, SOD1, ABCC1 and RALBP1 mRNA expression

was determined in 4T1 cells after treatment with Nrf2 DsiRNAs as described before. Results are represented as mean  $\pm$  SEM for 3 independent experiments. Significance was assessed by two-tailed t-test. \*  $p < 0.05$ .

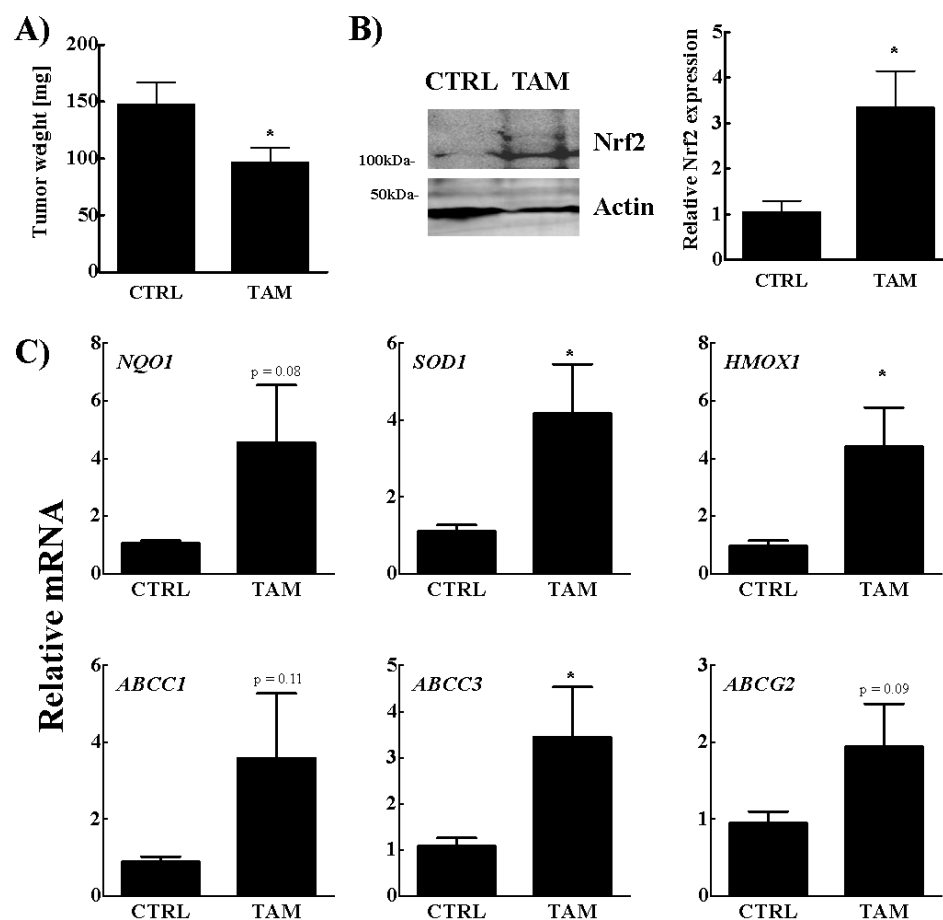


**Figure 4.16: Nrf2 expression is higher in tamoxifen-treated 4T1 breast tumors – A)** 4T1 breast tumors were excised and weighed as described before on Day 10 for 6 control or tamoxifen-treated mice. **B)** Nrf2 protein expression was determined in control or tamoxifen-treated tumors. Representative western blot and quantification are shown in the left and right panels **C)** NQO1, SOD1, HMOX1, ABCC1, ABCC3, ABCG2 mRNA expression was determined in the control or tamoxifen-treated tumors as described before. Results are represented as mean  $\pm$  SEM for 6 independent experiments. Significance was assessed by two-tailed t-test. \*  $p < 0.05$ .

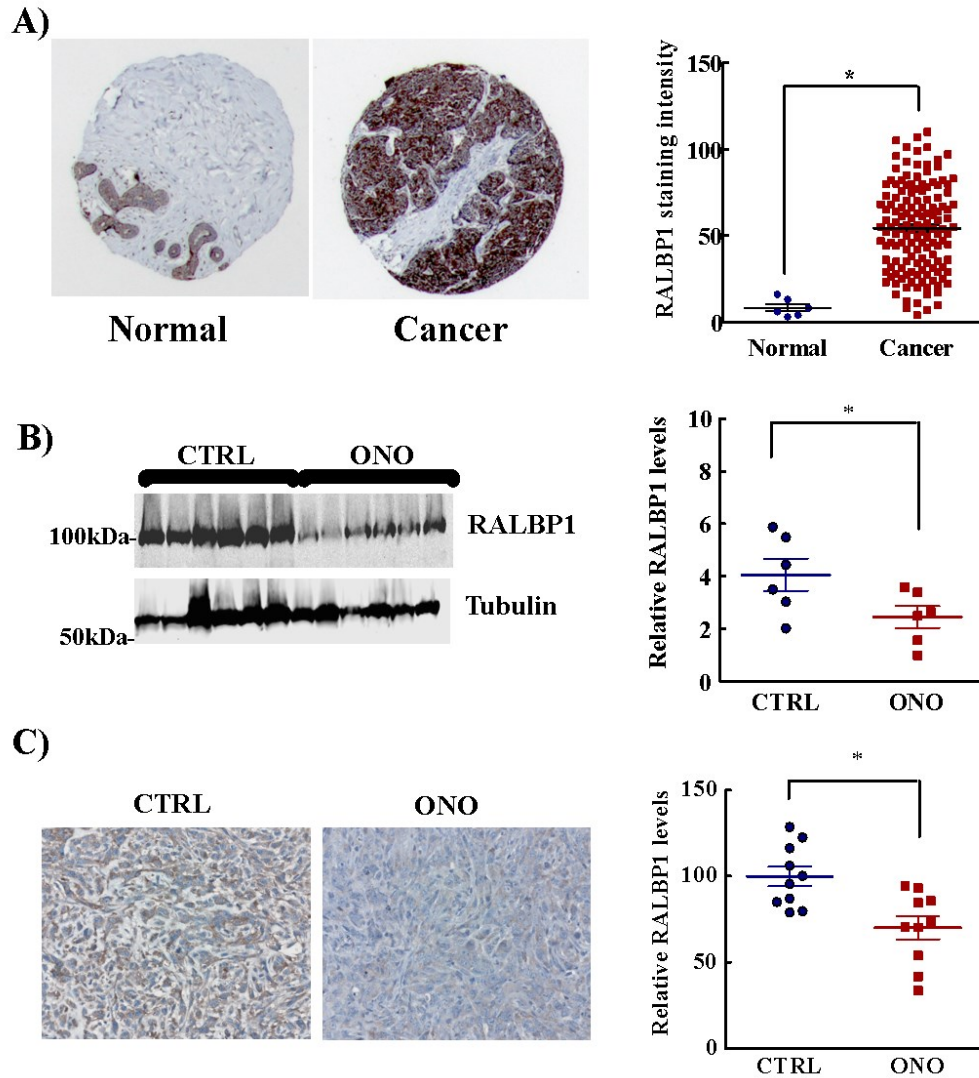


**Figure 4.17: RALBP1 is upregulated in breast cancer patients and is decreased in 4T1 breast tumors by ONO-8430506 treatment** – A) Tissue arrays from breast cancer patients or normal patients (breast reduction surgery) were stained for RALBP1 by immunohistochemistry. Representative images are shown in left panel. Quantification of RALBP1 staining intensity in 142 cancerous and 5 normal tissues is shown in the right panel. B) RALBP1 protein expression was determined in 4T1 breast tumors from 6 control or ONO-8430506-treated mice. Immunoblots are shown in left panel and quantification is shown in the right panel. C) 4T1 breast tumors from 10 control or ONO-8430506-treated mice were stained for RALBP1 by Immunohistochemistry. Representative images are shown in left panel and quantification is shown in the right panel. Results are represented as mean  $\pm$  SEM. Significance was assessed by two-tailed t-test. \*  $p < 0.05$ .



### 4.3 DISCUSSION

The role of ATX-LPA-LPA<sub>1</sub> signaling in tumor growth, migration and metastasis has been described and reviewed in Section 1.3. Our cell culture models predicted a role for LPA<sub>1</sub> in drug resistance. There is considerable redundancy in LPA receptor expression in tissues (494). LPA<sub>1</sub> is the predominant LPA receptor observed in many tissues (495) including breast cancer cells (209) such as MDA-MB-231 cells. Tissue expression of multiple LPA receptors represents a significant challenge in targeting it specifically and successfully *in vivo*. Despite these issues, several LPA receptor antagonists have shown promise in early clinical trials (248).

The ATX inhibitor, ONO-8430506, decreases LPA production *in vivo* in plasma and breast tumors of mice, especially of unsaturated LPA species. The drug is active over 24 h (137) and can persistently decrease LPA-signaling irrespective of tissue expression of LPA receptors. Blocking LPA signaling by this strategy decreased the expressions of Nrf2, antioxidant genes and MDRT in tumors. These changes increased the efficacy of doxorubicin in decreasing tumor growth and metastasis. Several Nrf2-regulated genes were downregulated in the ONO-8430506-treated tumors at the level of mRNA expression. The Nrf2 targets that were downregulated in ONO-8430506-treated tumors included the drug transporters ABCC1 and ABCB1 and the antioxidant proteins NQO1 and HMOX1 as predicted to be decreased from our cell culture studies. These proteins enhance the resistance of cancers to therapy (45). Additional candidates include several antioxidants. For example, GPX1, which was identified decades ago to mediate resistance to

doxorubicin (496), can also decrease sensitivity to chemotherapeutics. Only intrinsic differences in the gene expression between the primary tumors were evaluated in our studies. Another level of complexity can be added to these animal experiments by evaluating the neo-adjuvant and adjuvant response to combination therapy by surgical removal of the tumors. Mice that receive early neo-adjuvant combination therapy are expected to survive longer following surgery. Similarly, mice receiving adjuvant combination therapy to kill the remnant cancer cells following surgery are expected to remain disease-free longer.

We chose a low and relatively well-tolerated dose of doxorubicin, which on its own produced no significant effect on tumor growth. It would be unethical to prolong the experiments beyond the third week because of the aggressive nature of these tumors. Doxorubicin treatment was effective in inhibiting tumor growth and metastasis by about 70% at Day 12 when combined with ATX inhibition. The effects of ONO-8430506 on soft tissue metastasis can be explained partly by decreased growth of the primary tumor in the presence of ONO-8430506 (137). However, we demonstrate in an independent tail-vein model of metastasis that the combination of ATX inhibition and doxorubicin was effective in reducing lung nodule formation. ATX/LPA/LPA<sub>1</sub> signaling was previously shown to be an important component of the remodeling events in the distal site and increased bone metastasis (194, 226). One possibility is that ONO-8430506 blocks the colonization in the lung or liver by making them more susceptible to chemotherapeutic-damage. This can explain why

the combination alone was effective in decreasing the rapid lung colonization by circulating 4T1 cells.

ATX secretion can be increased by several factors amongst which inflammation is a key player (133). Chronic inflammation in the tumor environment promotes the survival of cancer cells and resistance to therapies (172). Inflammatory mediators such as TNF $\alpha$  increased the autocrine production of ATX while extracellular LPA increases cytokine production in thyroid cancers (176). ONO-8430506 was able to decrease tumor growth by overcoming this vicious cycle of tumor-promoting inflammation and cytokine production. Similarly in breast cancer, ONO-8430506 decreased inflammation in the tumor-adjacent mammary fat pads but not the tumor themselves or the in contralateral fat pad (154).

We predicted that chemotherapy, and the tissue damage that it produces, also fuels an inflammatory response, which promotes ATX secretion and increased LPA signaling (133). We now demonstrate that doxorubicin increases the production of cytokines, chemokines and growth factors in the tumor-adjacent mammary fat pad. Cytokine production in breast tumors was unaffected by ONO-8430506 and doxorubicin either by themselves or together. However, mice receiving the combination therapy have decreased tumor burden and hence decreased cytokine load in the mammary tissue. We demonstrate that doxorubicin-treatment increased the ATX production in the tumor-adjacent mammary fat pad, which is the major source of ATX in these tumors. ATX is secreted in the tumor microenvironment in a patho/physiological response designed to repair the injured area. Our results suggest

that tumor-promoting inflammation can contribute to doxorubicin resistance through increased LPA signaling. Blocking the protective mechanisms associated with LPA signaling improves the efficacy of doxorubicin by increasing oxidative damage-induced cell killing and decreasing the growth of breast tumors (Fig. 4.18). Thus, ATX/LPA signaling plays a key role in the interplay between chronic inflammation and oxidative stress leading to increased tumor survival, proliferation and chemo-resistance (497).

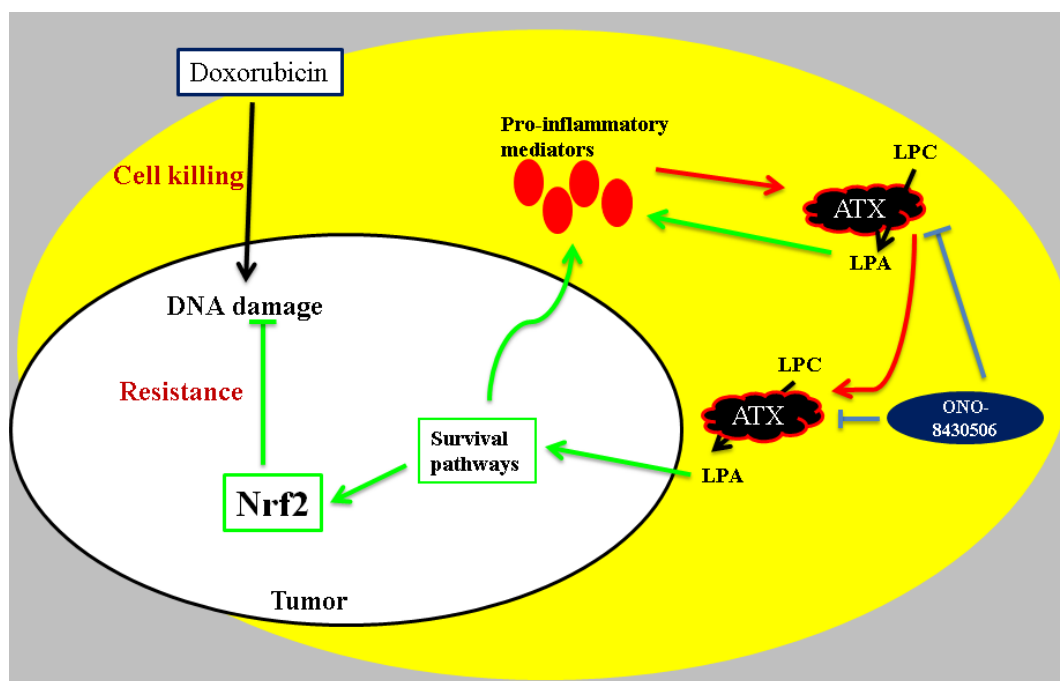


**Figure 4.18: Proposed mechanism for the role of ATX/LPA signaling in resistance to chemotherapy through Nrf2 activation** – Doxorubicin-treatment increases the production of pro-inflammatory mediators and ATX in the surrounding mammary fat pad (yellow). LPA further increases the production of pro-inflammatory mediators and ATX production in a paracrine loop. Further, LPA activates LPA receptor-mediated survival pathways, stabilizes Nrf2 and increase the transcription of antioxidant and MDRT genes (green arrow). This vicious cycle of ATX/LPA production makes the 4T1 tumors refractory to doxorubicin therapy (red arrow). Autotaxin inhibition by ONO-8430506 (blue) decreases inflammation in the mammary fat pad, decreases Nrf2 expression in the tumors and increases the oxidative damage-induced cell killing by doxorubicin.

LPA produces chemo-resistance by activating several survival pathways. Equally, it is well recognized that increased expressions of Nrf2, antioxidant and MDRT genes are related to chemo-resistance. Our results show that the protein levels of Nrf2 and NQO1 was higher in tumors of patients retrospectively classified with a recurrent metastatic disease following lumpectomy and doxorubicin therapy. Oncogenes such as K-Ras, B-Raf and myc have been reported to increase basal Nrf2 levels (445), which may explain their high expression in certain cancers. In many cancers, somatic mutations in Nrf2 or Keap1 allow for increased stabilization and activation of Nrf2 whereas it is normally post-translationally degraded (42). Our results show that decreasing LPA signaling by inhibition of ATX *in vivo* can decrease Nrf2 expression in the tumors. We did not see a correlation between ATX mRNA and tumor recurrence in a patient gene microarray dataset (433). This was expected since breast cancer cells express little ATX mRNA and ATX expression in the tumors reflects mainly the associated stroma and mammary adipose tissue (133, 137).

It is not clear from our experiments if Nrf2 is increased by cancer cells or cancer-associated stroma. IHC staining for Nrf2 with the N-terminal and C-terminal antibodies described earlier produced a non-specific staining pattern as seen by multiple non-specific bands in immunoblots. As shown in Chapter 3, LPA increases Nrf2 expression in 4T1 cells grown in a monolayer culture. Additionally, cancer cells express higher levels of Nrf2 compared to fibroblast cell lines. Finally, the relative abundance of Nrf2 seen in cultures of MDA-MB-231 and 4T1 cells is

maintained *in vivo*. It is therefore, most likely that the Nrf2 expression in the breast tumors originates from the cancer cells.

Tamoxifen is a widely prescribed adjuvant therapy in breast cancer. We examined if resistance to this effective therapy was due to increased Nrf2-stabilization. MCF-7 cells selected for resistance to tamoxifen have increased Nrf2 activation and the knockdown of Nrf2 in these cells restored partial sensitivity to tamoxifen (106). Xenografts derived from ER $\alpha$  positive MCF-7 cells that are resistant to the effects of tamoxifen have higher expression of antioxidant genes (100). We demonstrate that several antioxidants and drug transporters are downregulated by Nrf2 knockdown in ER $\alpha$  negative 4T1 cells. Our results show that the tamoxifen metabolite 4-HT increased the expression of Nrf2 in cancer cells. Further, LPA was additive with tamoxifen in increasing ARE activity. These effects are likely due to increased oxidative stress. Interestingly, estrogen-treatment was recently shown to increase Nrf2 stabilization in estrogen responsive mammary epithelial cells and cancers (498). Rapid signaling effects of estrogen are mediated through a GPCR called GPR30 (499). However, the contribution of GPR30 on Nrf2 stabilization was not examined by the authors.

Several drug transporters including ABCC1 and ABCG2 were increased in tamoxifen-treated 4T1 tumors. However, it is not clear if these drug transporters are directly involved in tamoxifen transport. Further, both ABCG2 and ABCC-family export a variety of endogenous substances such as estradiol that are locally synthesized in the mammary fat pad. It would be interesting to examine if

tamoxifen-treatment increased ATX production in the mammary fat pad of these mice similar to doxorubicin-treated tumors. We examined the effects of tamoxifen-treatment on the expression of the GTPase activating protein, RALBP1. Although RALBP1 is not an ABC-transporter, it was shown to have ATPase activity, increase the efflux of chemotherapeutics and GSH-conjugates, and play a role in tumor progression (25). We demonstrate that RALBP1 is increased in the tumors of breast cancer patients. We also show that RALBP1 is not an Nrf2-dependent gene unlike the MDRT. RALBP1 expression was elevated in tamoxifen-treated MCF-7 cells and downregulated by ONO-8430506-treatment in 4T1 tumors. We will now test the effects of LPA directly on RALBP1 regulation in breast cancer cells. We propose that RALBP1 is an oxidative stress response protein that is increased in breast cancers and mediates initial resistance to tamoxifen and other chemotherapeutics.

The importance of our present work is that it links LPA signaling to this increased Nrf2 expression and the transcription of antioxidant genes and multi-drug resistance transporters (Figure 4.9). Our present study also provides a novel and practical solution for decreasing the ability of cancer cells to protect themselves against the cytotoxic effects of chemotherapeutic agents. The ATX inhibitor was well tolerated by mice in our initial studies. We propose that inhibiting the ATX-LPA-Nrf2 axis can be a viable strategy for improving the efficacy of existing chemotherapies.

**CHAPTER 5 - LPA INCREASES SK1 ACTIVATION IN DOXORUBICIN  
RESISTANT CELLS THROUGH INCREASED PHOSPHOLIPASE D2  
ACTIVITY**

[The contents of this Chapter are unpublished]



## 5 CHAPTER 5

### 5.1 INTRODUCTION

Sphingolipids are structural and bioactive lipids enriched in membrane rafts and attributed with diverse cellular and signaling functions. One of the ways by which the sphingolipid pathway is commonly altered in cancers is by persistent activation of SK1 leading to drug resistance (500). SK1 is overexpressed in a variety of cancers including breast cancers. The product of SK1, S1P, is secreted by the active ABC transporters or Spns2 (spinster homolog 2). Extracellular S1P activates S1P receptors (S1P<sub>1-5</sub>) resulting in increased cell migration, survival, proliferation and angiogenesis (See Fig. 1.8). Both protein-protein interactions and protein-lipid interactions have been identified in the translocation and activation of SK1.

We tested the hypothesis that increased activation of SK1 and S1P receptors will contribute to chemo-resistance by protecting breast cancer cells from the apoptotic effects of chemotherapeutics. Specifically, we tested the effects of extracellular LPA on SK1 activation and S1P secretion in cells selected for resistance to doxorubicin. Our results show that SK1 activation and S1P formation is higher in cells that have acquired resistance to doxorubicin. We also demonstrate a role for increased PLD2 activity and PA formation in this signaling pathway.

## 5.2 RESULTS

### 5.2.1 Characterization of isogenic doxorubicin-resistant cancer cells

We initially characterized the ABC-transporter expression in MCF-7 cells selected for resistance to doxorubicin at 3 different concentrations. We found that the ABC drug transporters ABCC1 and ABCG2 are both increased in the resistant cell lines compared to their isogenic control cells (Fig. 5.1A). Cells selected at different concentrations of doxorubicin also show increased expression of ABCC1 and ABCG2 mRNA (Fig. 5.1B). This confirms previous work, which also showed increased ABCC1 protein expression in the resistant cells (424).

We next determined if these cell lines have increased resistance to doxorubicin as reported previously (424). Both the control MCF-7 cells and doxorubicin-resistant MCF-7 cells show decreased cell viability in the absence of serum factors to varying degrees (Fig. 5.2A and B). However, the resistant MCF-7 cells did not show a decrease in cell viability for  $\leq 48$  h in growth media (10% FBS) containing clinically relevant concentrations of doxorubicin. Under the same conditions, MCF-7 CTRL cells show decreased cell viability. Charcoal-treatment resulted in depletion of  $\sim 99\%$  of total LPA from serum (211). Addition of LPA to the delipidated serum protected doxorubicin-resistant MCF-7 cells from the cell killing induced by low dose doxorubicin. Addition of S1P similarly protected these cells from doxorubicin-induced killing in charcoal-treated medium (Fig. 5.2C). S1P is formed in the cells and is secreted outside by the ABC-transporters ABCC1 and

ABCG2.(332, 333). We next measured the secretion of S1P in these cells by labeling with [<sup>3</sup>H]sphingosine (439). S1P secretion was higher in cells selected for doxorubicin-resistance even under normal conditions when compared to control cells (Fig. 5.2D).

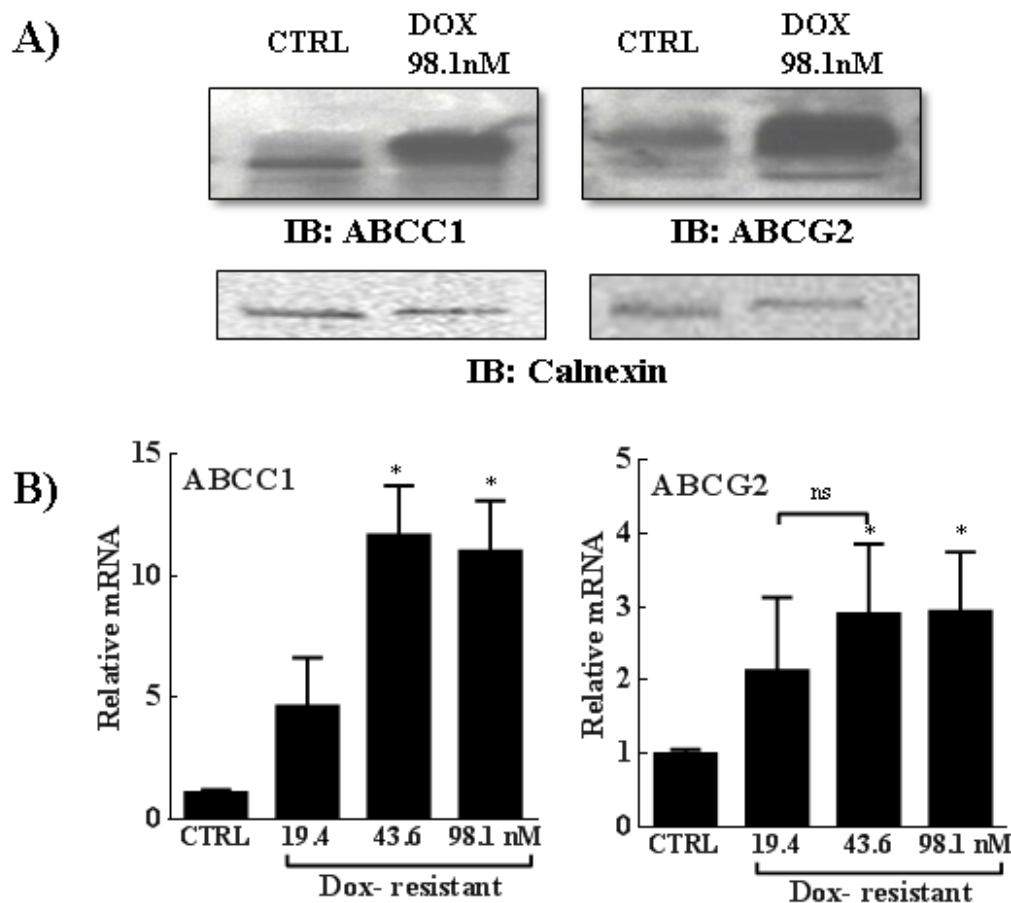


**Figure 5.1: Increased expression of ABCC1 and ABCG2 in doxorubicin-resistant MCF-7 cells** - A) protein and B) mRNA in MCF-7 cells previously selected for doxorubicin resistance at the indicated concentrations or MCF-7 control cells (424) were determined by immunoblotting and RT-PCR analysis as described in Chapter 2. Results were expressed as mean± SEM. Significance was analyzed by one-way ANOVA with post-hoc test. \* p<0.05.

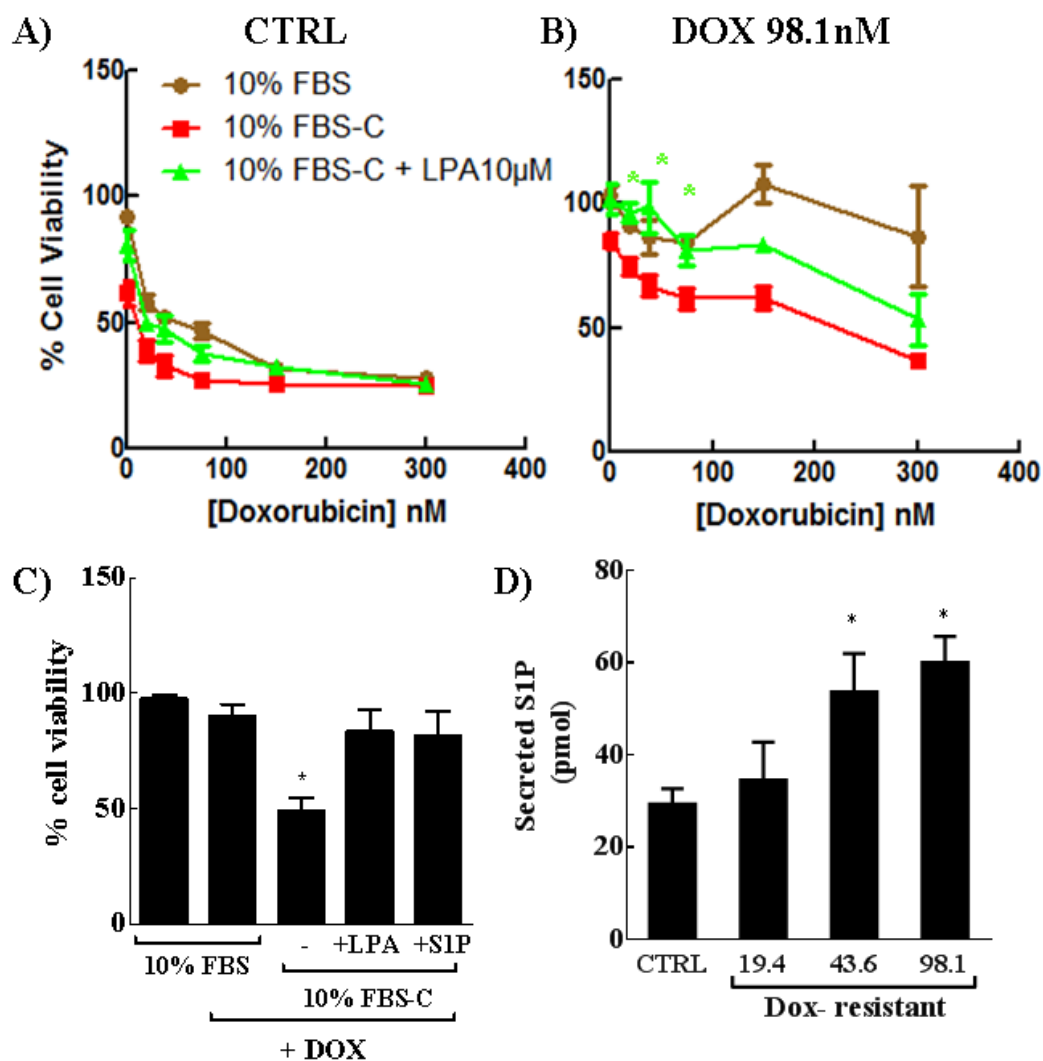


**Figure 5.2: The presence of LPA or S1P in the medium was enough to maintain the resistance phenotype of doxorubicin-resistant MCF-7 cells – A) MCF-7 CTRL or B) MCF-7 DOX cells were starved for 12 h before being replaced with 10% FBS, FBS-C or 10% FBS-C + LPA with various concentrations of doxorubicin for 48 h. The cell viability was assessed by MTT assay. Results were expressed as mean  $\pm$  SEM. n=6. Significance was analyzed by two-way ANOVA with post-hoc test. C) MCF-7 DOX cells were treated as above with 75 nM doxorubicin for 48 h with or without 10  $\mu$ M LPA and 100 nM S1P in FBS-C. D) [ $^3$ H]S1P secretion was measured after 2 h incubation in growth media for CTRL or resistant cells following 1 h labeling with [ $^3$ H]sphingosine. n=3. Results are expressed as mean  $\pm$  SEM. \* p<0.05.**

We characterized LPA receptor expression between the control and resistant cell lines since increased LPA receptor expression could explain the differences in protection from doxorubicin-induced cell killing seen in the resistant cells. DOX-resistant cells show no differences in LPA receptor expression (LPA<sub>1-6</sub>) when compared to isogenic control MCF-7 cells (Fig. 5.3A). We also characterized the expression of the related family of S1P receptors (S1P<sub>1-5</sub>). S1P<sub>2,3</sub> were significantly increased in the resistant cells when compared to the control MCF-7 cells (Fig. 5.3B). The higher levels of secreted S1P and S1P receptor expression suggest increased SK1-dependent signaling in the resistant cells.

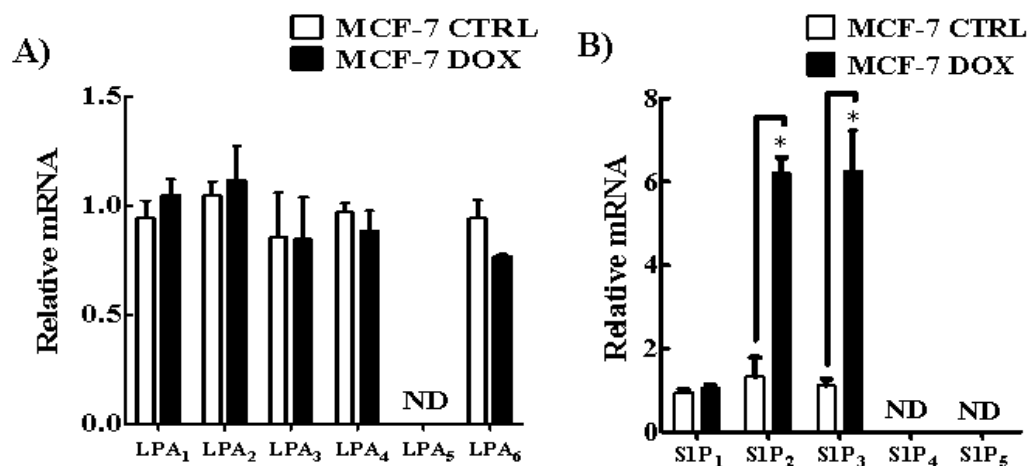


**Figure 5.3: Expression of LPA and S1P receptors in doxorubicin-resistant and control MCF-7 cells** – LPA<sub>1-6</sub> and S1P<sub>1-5</sub> expression was determined by RT-PCR in MCF-7 control or MCF-7 DOX 98.1 nM. Results were expressed as mean± SEM. Significance between MCF-7 CTRL and MCF-7 DOX was analyzed by two-tailed t-test. \* p<0.05.

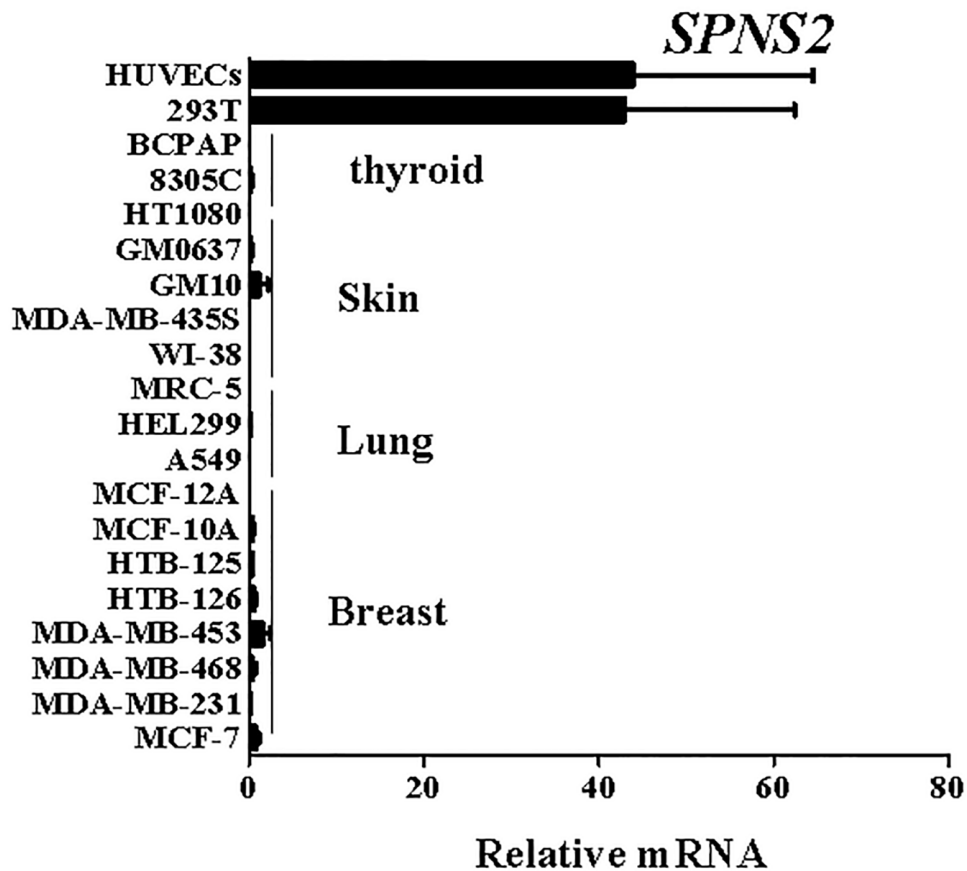


Figure 5.4: Expression of the S1P transporter, Spns2, in various cancer and normal cell lines - as determined by RT-PCR.

### 5.2.2 Expression of the specific S1P transporter, Spns2, in cancer cells

The Spns2 transporter was recently identified as the physiological S1P transporter. We determined the expression of Spns2 in a variety of cancer cell lines including those of breast, lung, skin and thyroid origin. In most of these cell lines, we could not detect the transcripts using a previously validated primer set (Fig. 5.4). Non-cancerous, non-immortalized, epithelial or fibroblast cell lines established from these tissues, like the Hs578Bst (HTB-125) cancer-associated fibroblast cell line, did

not express any Spns2 either. By comparison, Spns2 was easily detected in the human umbilical vein endothelial cells (HUVECs) and human embryonic kidney cells (HEK-293T) as reported previously (335).

### **5.2.3 LPA increases SK1 translocation to the membranes**

We next tested if LPA increases the activation of SK1, S1P secretion and autocrine/paracrine signaling through the S1P receptors. We initially optimized the assay conditions to measure SK1 activity accurately. All our assays for SK1 were performed in the presence of TritonX-100, which inhibits SK2 activity. These are shown in Fig. 2.4. A variety of growth signals can activate SK1 as discussed in Section 1.4. SK1 is recruited to the membranes, where it can access its substrate sphingosine. Some of the activators of SK1 include bioactive lipids such as LPA and S1P, and hormones such as estrogen. Depletion of these factors in culture medium, by charcoal-stripping the serum, can be used to assess their individual contribution. We found that addition of LPA to delipidated serum increases SK1 activity in the membranes of MDA-MB-231 cells by about 2-fold after 30 min (Fig. 5.5A). Digitonin-treatment resulted in separation of membrane and cytosolic fractions (Fig. 5.5A inset). SK1 activity was largely associated with the cytosolic fraction and this was also confirmed by confocal microscopy in HEK293 cells (Fig. 5.5B). Digitonin-lysed cells showed residual mCherry-SK1 staining and LPA-treatment resulted in an increase in the membrane-associated SK1. This staining pattern is consistent with a ~10% membrane-associated SK1 obtained from activity measurements. A time

course of the SK1 activity was performed for these LPA-induced increases in the control MCF-7 and doxorubicin resistant MCF-7 cells (Fig. 5.5C). The increase in membrane SK1 activity peaked after 20 min. Doxorubicin-resistant MCF-7 cells showed a 4-fold increase in membrane SK1 activity in response to LPA as compared to a 1.5-fold increase seen in control MCF-7 cells. Similar to the activity measurements, LPA-induced increases in membrane recruitment of SK1 protein was also seen in the doxorubicin-resistant cells (Fig. 5.5D).



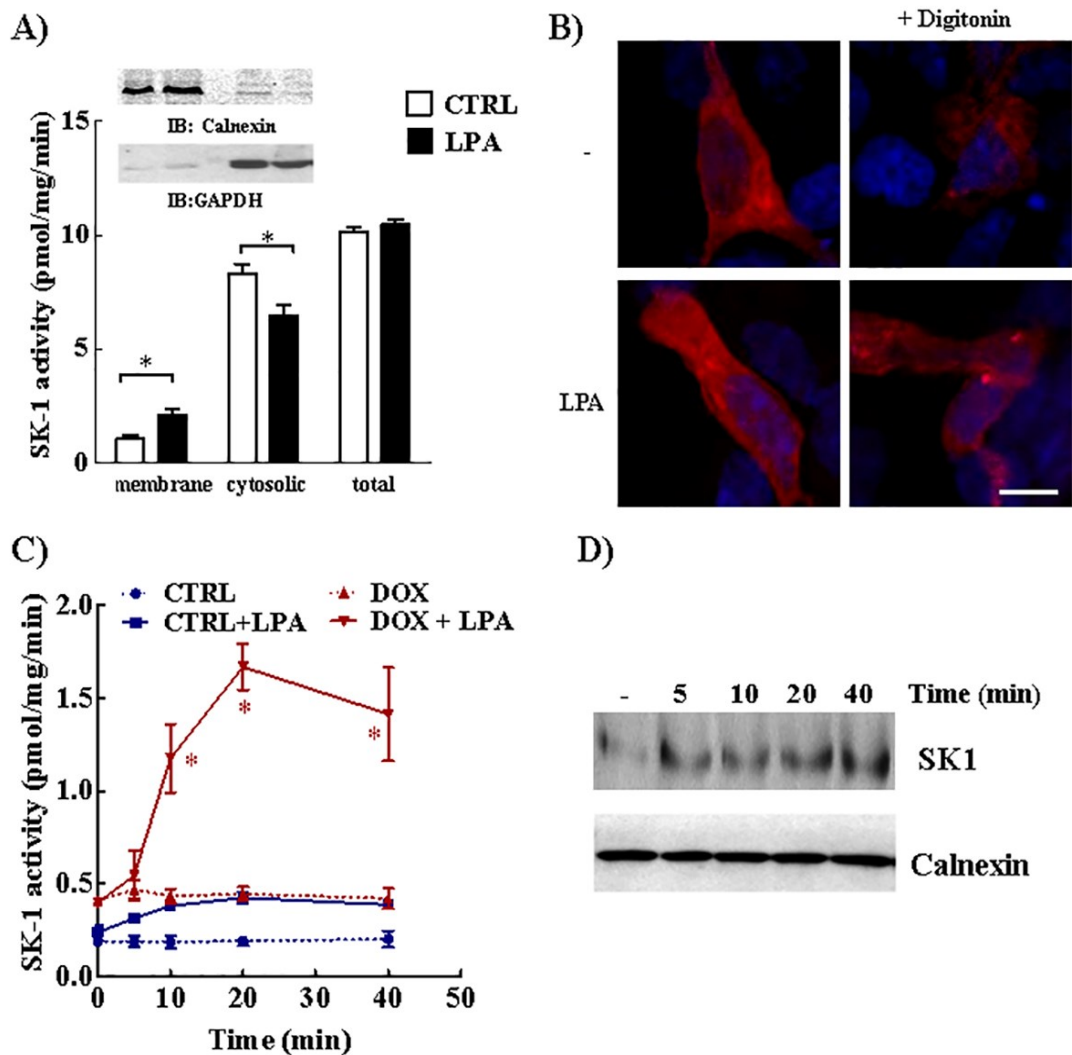


**Figure 5.5: LPA increases the membrane translocation of SK1 in cancer cells – A)** Membrane or cytosolic preparations from MDA-MB-231 cells were treated with or without LPA (10  $\mu$ M) for 40 min. SK1 activity was determined as described in Materials and Methods. Membrane and cytosolic preparations were immunoblotted for the cytosolic marker GAPDH and membrane marker calnexin (inset) **B)** HEK-293 cells grown on coverslips were transfected with mCherry-SK1, treated with control or LPA and digitonin lysed as before. The cells were visualized by confocal microscopy. **C)** SK1 activity was determined in the membrane fractions of digitonin-lysed CTRL or DOX MCF-7 cells at 0, 5, 10, 20 and 40 min after LPA-treatment. n = 6. Results are expressed as mean  $\pm$  SEM. Significance was analyzed by two-way ANOVA with post-hoc test. **D)** SK1 protein localization was determined by immunoblotting in the membrane preparations of DOX cells described previously. \* p<0.05.

#### **5.2.4 Phospholipase D2 activity is required for increased SK1 translocation**

Addition of PA to the SK1 assay buffer resulted in an increase in S1P formation in a concentration-dependent manner (Fig. 5.6A) as reported previously for several acidic phospholipids (315). PLD activity was previously shown to increase SK1 activity in the membrane. Further, mutations to the PA-binding region in SK1 results in its disperse cytosolic localization (285, 317). Since LPA is one of the previously characterized activators of PLD activity, we tested the role of PLD 1/2 on SK1 translocation to the membranes.

We found that pre-treatment with the PLD2-selective inhibitor and not PLD1-selective inhibitor attenuated the LPA-induced translocation of SK1 to the membranes in doxorubicin-resistant MCF-7 cells (Fig. 5.6B). LPA increased the PLD activity, which was blocked by pre-treatment with pharmacological inhibitors of PLD-1 or PLD-2 (Fig. 5.6C). This shows that both inhibitors were effective in decreasing the combined PLD activity.

We used a previously described method (439) to separate [<sup>3</sup>H]S1P selectively from cells labeled with [<sup>3</sup>H]sphingosine (Fig. 2.6). Doxorubicin-resistant MCF-7 cells show increased accumulation of intracellular [<sup>3</sup>H]S1P when treated with LPA, which was blocked by the PLD2 inhibitor (Fig. 5.6D). Similarly, 10% FBS-induced formation of intracellular S1P was also blocked by pre-treatment with the PLD2 inhibitor. S1P secretion into the medium was not significantly increased in these experiments.

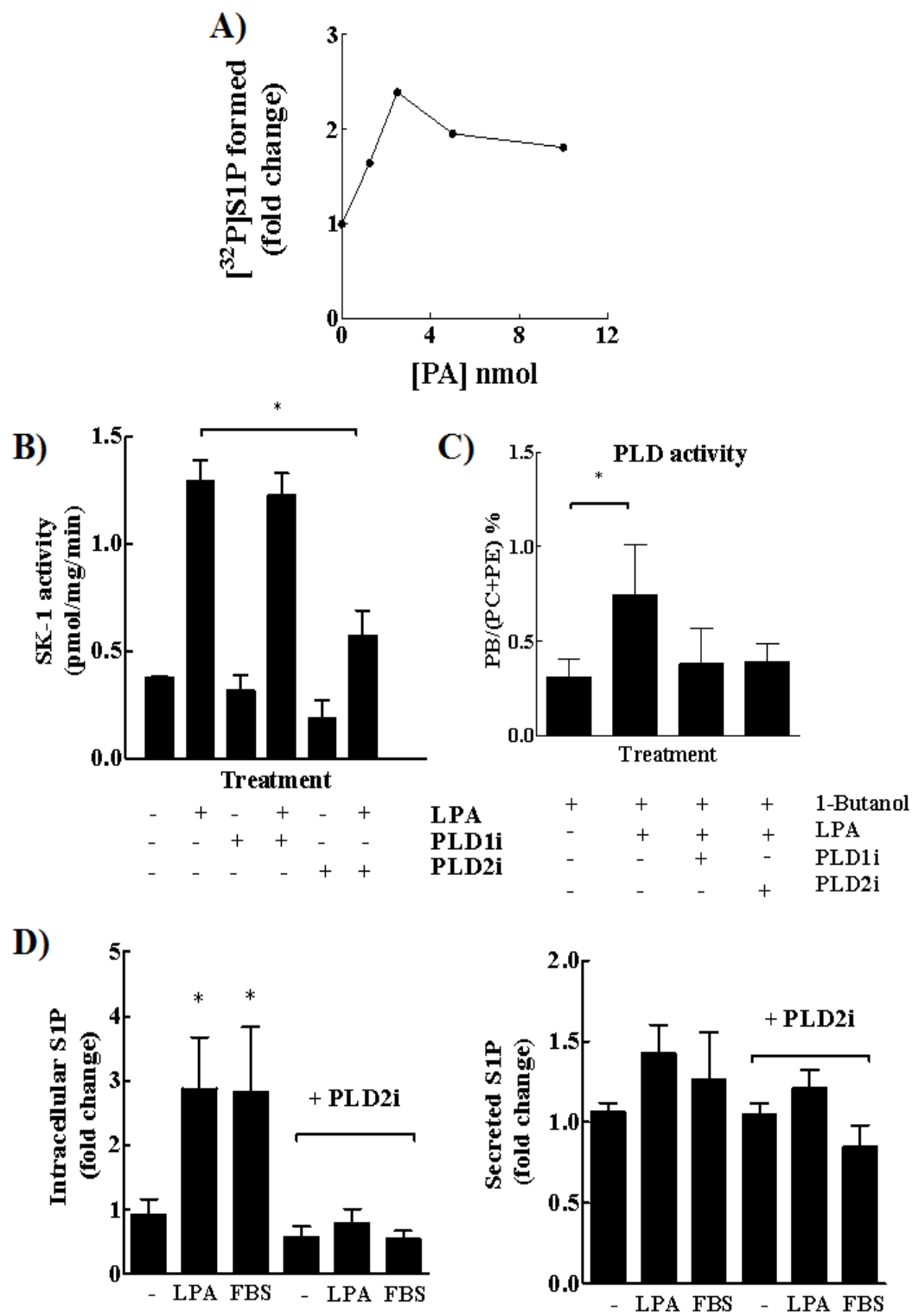


**Figure 5.6: LPA increases PLD2-dependent SK1 activity and intracellular S1P formation – A)** Addition of exogenous PA to Triton-X100 containing SK1 buffer increased

[<sup>32</sup>P]S1P formation. **B)** SK1 activity in the membrane extracts of MCF-7 DOX cells pre-treated with PLD1 or PLD2 inhibitor **C)** LPA-induced PLD activity was decreased in MCF-7 DOX cells in the presence of PLD1 or PLD2 inhibitor **D)** Intracellular [<sup>3</sup>H]S1P formation in MCF-7 DOX cells (left) and extracellular [<sup>3</sup>H]S1P secretion into the medium (right) was determined by labeling cells with [<sup>3</sup>H]sphingosine followed by stimulation with LPA (10 μM) in 10% FBS-C or 10% FBS with or without the PLD2 inhibitor (0.5 μM) for 1 h.

To determine if PA is formed by activation of the LPA receptor, we used a PA-biosensor, which binds to PA-rich regions of the cell. The PA-biosensor was used previously to visualize EGF-induced PLD activation in cancer cells (430). We used this in HEK293 cells, which express LPA<sub>1</sub> receptors, to directly visualize PA formation after LPA-treatment. After a 5 min treatment we could observe a distinct staining pattern from a normally cytoplasmic-localized PA-biosensor to an increasingly plasma membrane-localized pattern (Fig. 5.7A). This transient increase was observed in 3 independent constructs of the PA-biosensor. We also stably transfected the GFP-tagged PA-biosensor in doxorubicin-resistant MCF-7 cells. Here, LPA treatment resulted in rapid and persistent plasma membrane localization of the PA-biosensor (Fig. 5.7B). This is consistent with a higher SK1 activation seen in the resistant cells.

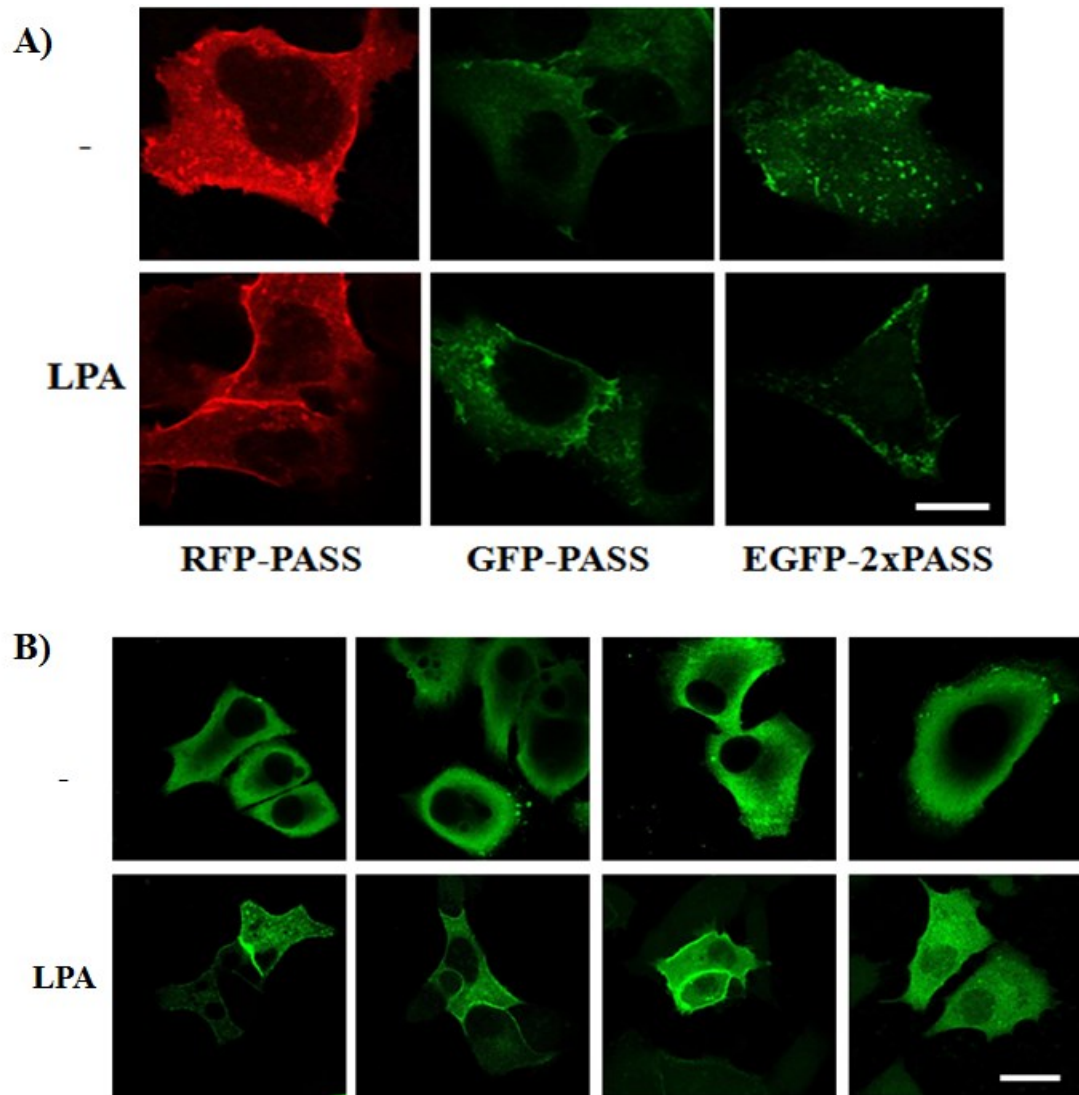


**Figure 5.7: Visualization of LPA-induced PLD activation in the cell by PA biosensors –**  
**A)** HEK293 cells were transfected with a plasmid expressing GFP- or RFP- fused to PASS (PA-binding motif) or EGFP-2XPASS (430). Cells were starved overnight before treatment with LPA for 5 min. Fixed cells were visualized by confocal microscopy as described in the materials and methods. **B)** Doxorubicin-resistant MCF-7 cells were stably transfected with GFP-PASS using a Lentiviral vector. Cells grown in delipidated-serum were treated with LPA for 5 min. z-projections of the confocal images obtained from ImageJ analysis are shown. Scale bar – 10  $\mu$ m.

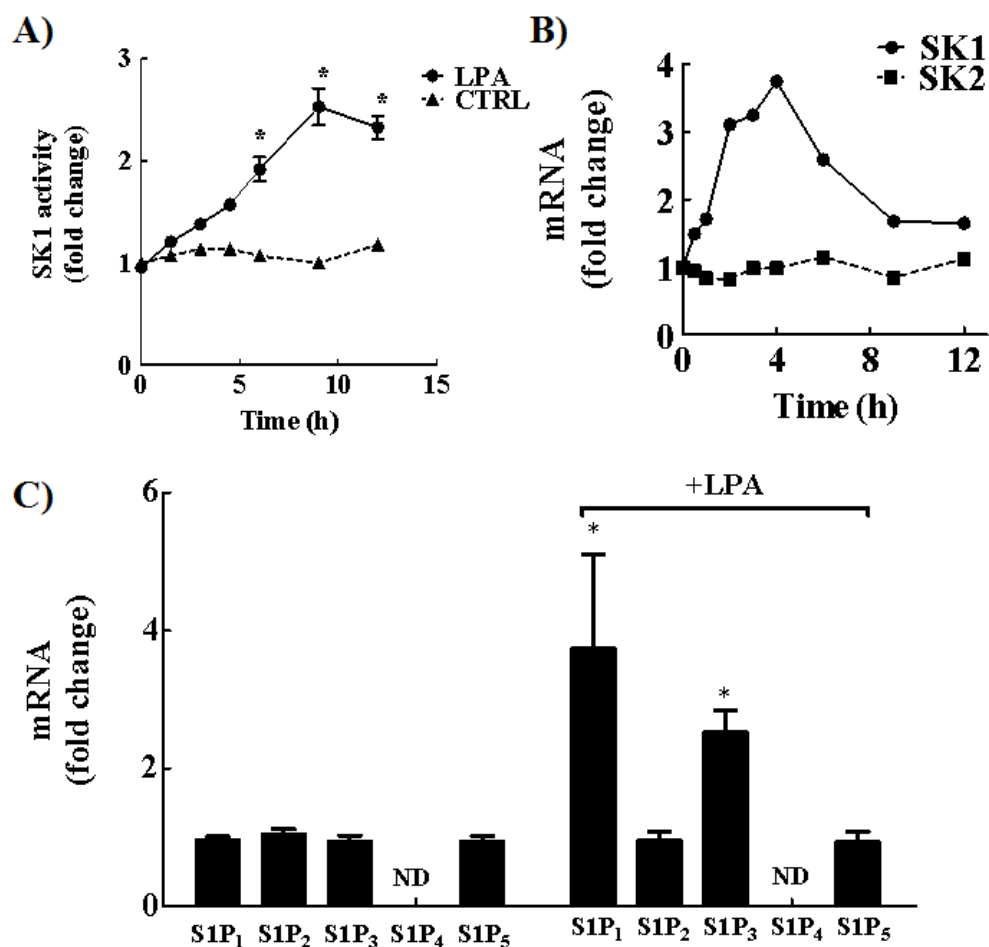


**Figure 5.8: LPA increases the transcription of SK1 and S1P<sub>1,3</sub> mRNA** A) SK1 activity was determined at 0, 1.5, 3, 6, 9 and 12 h after 10  $\mu$ M LPA treatment in MDA-MB-231 cells as described previously B) SK1 mRNA expression was determined at 0.5, 1, 2, 3, 4, 6, 9, 12 h after LPA treatment in MDA-MB-231 cells C) S1P<sub>1-5</sub> was determined at 4 h after LPA treatment. Results were expressed as mean $\pm$  SEM. Significance between treatments was determined by two-tailed t-test. \*  $p < 0.05$ .

### 5.2.5 LPA increases SK1 activity and S1P<sub>1/3</sub> mRNA expression

A biphasic response has been identified for many SK1 activators like phorbol esters, 17 $\beta$ -estradiol and LPA. In addition to increasing membrane translocation of SK1, we found LPA increases total SK1 activity (Fig. 5.8A) after 9 h in MDA-MB-

231 breast cancer cells. This is likely caused by the increase in SK1 mRNA (Fig. 5.8B). Furthermore, increases in S1P<sub>1</sub> and S1P<sub>3</sub> mRNA (Fig. 5.8C) were also detected in MDA-MB-231 cells. We will follow this up by immunoblotting for SK1 and S1P receptor protein levels. These results suggest a transcriptional role for increased SK1/S1P receptor signaling in the presence of LPA.

### **5.3 DISCUSSION AND FUTURE DIRECTIONS**

Doxorubicin-resistant MCF-7 cells discussed in this Chapter were selected in the presence of increasing concentrations of doxorubicin. Despite this, they were reported to be isogenic suggesting that acquired resistance was an adaptive response to the drug rather than clonal selection from an initial population (424). Additionally, several drug transporters were expressed in the cells during the initial stages of selection. These results show that, at least during the initial acquisition of drug resistance, multiple mechanisms may be responsible for promoting resistance to doxorubicin (424). We demonstrate increased expression of ABCC1 in doxorubicin-resistant cells, as reported previously (424). Additionally, we show ABCG2 was overexpressed in these cell lines.

Doxorubicin-resistant cells grown on delipidated serum showed increased sensitivity to doxorubicin compared to cells grown in normal growth medium or control MCF-7 cells grown on delipidated serum. A variety of lipid growth factors and hormones could potentially be removed by charcoal. Our group previously reported that 99% of LPA is removed by this treatment (211). Addition of external

LPA rescued the effects of charcoal-stripping on cell survival, which shows that LPA was enough to maintain the resistance of the selected doxorubicin-resistant cells. However, no differences in expression of LPA receptors were observed between the resistant and control MCF-7 cells. Since S1P secretion and S1P<sub>2/3</sub> receptors were increased in the doxorubicin-resistant MCF-7 cells, we proposed that LPA increases S1P signaling through SK1 activation and S1P secretion by the MDRT, ABCC1 and ABCG2 (Fig. 5.9).

We found that Spns2 mRNA was not expressed in various cell lines including breast, lung, and thyroid, skin cancer cells. Despite the lack of Spns2 mRNA, several cancers have been proposed to have high SK1 activity and increase S1P secretion. We will now test if Spns2 protein levels were similarly decreased in these cells. It was difficult to determine if LPA increased S1P secretion from our sphingosine labeling experiments because of the high background associated with [<sup>3</sup>H]S1P collected from the medium. Even 10% FBS, which is typically used in secretion experiments, did not increase extracellular S1P. In the future, we propose to use a collection medium, which contains inhibitor of S1P lyase activity. Semicarbazide, an inhibitor of S1P-lyase (501), has been used successfully in experiments to detect S1P secretion measurements (335). This would increase the available pool of [<sup>3</sup>H]S1P by preventing terminal degradation by the intracellular S1P lyases. Additionally, sodium orthovanadate or XY-14 (502) can be used to inhibit lipid phosphatase activity. Labeling with [<sup>3</sup>H]sphingosine in the presence of inhibitors represents artificial measurements so we propose to validate these results



with LC-MS measurements for endogenous S1P. The LC-MS measurements are accurate and easy to measure S1P in cancer cell lines stably overexpressing SK1/2 (Fig. 2.3) (333).

One of the other implications of increased SK1 activation is its effect on suppressing ceramide-effects of apoptosis (374). Our group showed the LPA can decrease paclitaxel-induced ceramide formation (211). We will now determine if LPA activation of SK1 suppressed ceramide formation in doxorubicin-resistant cells with varying sensitivities to doxorubicin (424). To do this we will simultaneously measure S1P and long-chain apoptotic ceramide species using LC-MS developed in collaboration with Dr. Jonathan Curtis (Department of Chemistry, University of Alberta) (440). We will compare intracellular/extracellular S1P formation and apoptotic ceramide formation in doxorubicin-resistant cell lines with varying sensitivities to doxorubicin. This will allow us to determine if there is any correlation between differences in SK1 activation and ceramide formation in drug resistant cells (Fig. 5.9).

We show that LPA increases the activation of SK1 based on TritonX-100 mixed micelle assays. However, we did not test if SK2 activity is completely inhibited under these conditions as reported previously. It is possible that SK2 activities also contributes to S1P formation when LPA receptor was activated. We show SK2 mRNA was not changed whereas SK1 mRNA and activity was increased by LPA. Further, SK1 and not SK2 responds to stimulation by hormones and lipid growth factors including LPA, estrogen and S1P. The stimulation by agonists results

in increased translocation of SK1 to the plasma membrane (308) or early endocytic vesicles (309). This early activation event is often followed by a transcriptional increase in SK1, as seen for LPA (Fig. 5.9). We will now examine the role of LPA in phosphorylation of SK1 by using antibodies raised against Ser-225-SK1. Interestingly, a splice isoform of SK1, SK1b, was shown to be constitutively membrane-associated (503). Normally, SK1b has short half-life, low expression levels and different migration pattern in SDS-PAGE making its detection difficult. We will also test if LPA increased SK1b stability in doxorubicin-resistant cells resulting in increases to membrane-associated SK1 activity.

SK1 activation and increased SK1 expression has been linked to increased drug resistance (See Section 1.5.9). We demonstrate that this depends on PLD2 activity in the doxorubicin-resistant cells using pharmacological inhibitors of PLD1/2. We will need to test if MCF-7 DOX cells have increased PLD2 activity, which leads to increased SK1 activation and S1P production. We will attempt to answer this question in different ways. First, we will manipulate PLD1/2 expression in cells using adenoviral overexpression of wild-type or catalytically inactive PLD1/2. We will also knockdown PLD1/2. These techniques have already been optimized for use in cancer cells and they produce the expected effects on PLD1/2 expression (Fig. 2.1 and 2.2) (185). Next, we will directly visualize LPA-induced PA formation in the plasma membrane for doxorubicin-resistant and control MCF-7 cells by using Lentiviral-plasmid constructs for the PA-biosensor. We will also attempt co-localization experiments to determine if the PA-biosensor and SK1 are

recruited to PA-rich regions. PLD2 is localized predominantly in the plasma membrane, whereas PLD1 is localized to perinuclear regions and the Golgi apparatus (428). Consistent with this, we observed increased plasma membrane localization of the PA-biosensor in the presence of LPA in our preliminary experiments. Since LPA can activate both PLD isoforms, it is likely that the staining pattern observed represents PA-localized to different organelles as well. Finally, we will determine if PLD2 activity regulates the “S1P-ceramide rheostat”. These experiments will help us understand the role PLD2 activation, PA formation, SK1 recruitment to the membranes and potentially a link between extracellular LPA signaling to S1P signaling (Fig. 5.9).

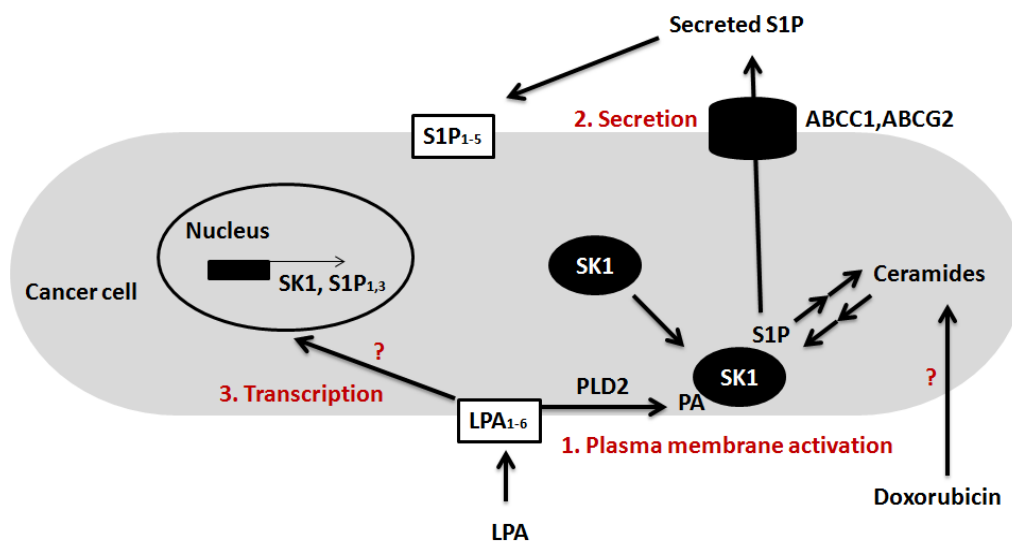


**Figure 5.9: Proposed model for modulation of SK1 signaling in cancer cells by LPA –**  
**1.** Extracellular LPA signaling activates PLD2-dependent PA formation in the plasma membrane. PA-mediated recruitment of SK1 to the plasma membrane, where SK1 can access sphingosine, results in increased S1P formation. This activates intracellular S1P signaling events. **2.** LPA-dependent increases in ABCG1 and ABCG2 efflux activities result in increased S1P secretion. This results in autocrine-paracrine signaling events through the activation of S1P receptors. **3.** LPA increases the transcription of SK1 and S1P<sub>1,3</sub> receptors through unknown mechanisms. Consequently, we propose that doxorubicin-induced

activation of apoptotic ceramides may be counter-balanced by increased SK1-dependent S1P formation and signaling.

It was previously demonstrated that LPA-LPA<sub>1</sub> signaling can increase SK1 transcription through the transactivation of EGFR (127). We demonstrate a biphasic response of LPA on SK1 activity in cancer cells. We will now test if the increase in long-term expression of SK1 and S1P<sub>1/3</sub> receptors is regulated by Nrf2. We previously showed that LPA signaling can stabilize Nrf2 expression, which results in transcription of oxidative stress response genes by increasing the expression of antioxidants and drug transporters. We will also test if PI3K activity is required for increased transcription of SK1, S1P<sub>1,3</sub> as seen for Nrf2-regulated genes. There is no direct evidence to suggest that SK1, S1P<sub>1,3</sub> are Nrf2-regulated genes. Sphingolipid metabolism in the ER and SK1 activation have been linked previously to increased stress signaling (267). Evidence from Nrf2<sup>-/-</sup> mice suggests that sulforaphane, a well known Nrf2-activator, could increase SK1 and SK2 gene expression modestly (504, 505). A SK1 inhibitor was recently shown to be a Nrf2 activator (506). Could this increase in Nrf2 be part of a feedback loop leading to increased expression of SK1 and S1P receptors? We will test these ideas using LPA, t-BHQ and other SK1 inhibitors (Fig. 5.9).

In conclusion, we demonstrate that LPA regulates SK1-dependent S1P signaling in cancers. Increased S1P formation occurs through PLD2-dependent recruitment of SK1 to the PA-rich regions of the membrane. Increased secretion of S1P is likely mediated by the ABC-transporters, which are increased by LPA.

Increased transcription of SK1 and S1P<sub>1,3</sub> further amplifies LPA signaling through increasing S1P signaling. We have proposed future experiments needed to take this work further. Recent studies have identified a novel role for PLD in increased breast tumor progression and metastasis (507). Our studies will determine the contribution of PLD2-induced SK1 activation-loop in cancer cell survival and drug resistance.

## **CHAPTER 6 – GENERAL DISCUSSION AND FUTURE DIRECTIONS**

## 6.1 General discussion and future directions

Lysophosphatidate (LPA) is a relatively simple lipid with a variety of signaling functions attributed to it. ATX/LPA signaling functions in cancer are mainly through its growth-factor like effects in promoting cancer cell survival, migration, proliferation, angiogenesis and cytokine secretion. ATX/LPA signaling had been shown to increase resistance to chemotherapeutic drugs but the mechanisms activated by LPA signaling to promote multi-drug resistance were not clear. We demonstrate now that LPA protects from doxorubicin-induced cell killing by directly regulating the cellular accumulation of doxorubicin through the MDRT. Although doxorubicin and other chemotherapeutics are mainly metabolized in the liver, it is possible that cancer cell metabolism of doxorubicin into derivatives like doxorubinol can also contribute to their decreased cytotoxicity (508). Additionally, drug metabolites and conjugates are easily transported outside the cell by the MDRT (509). Chemotherapeutics like doxorubicin are also sequestered in other compartments by drug transporters (510). The sequestration in cellular compartments decreases drug toxicity and increases efflux (33, 69). A future direction would be to study the accumulation of doxorubicin metabolites in the tumor, fat pads and plasma of our breast cancer model. This would require the development of sensitive methods of detection such as HPLC or LC-MS (511). Next, the effect of doxorubicin-metabolites on cell toxicity and drug transporter activity needs to be determined.

Cancer-initiating cells or cancer stem cells express high-levels of MDRT. One interesting possibility is that ATX/LPA signaling in the tumor microenvironment is required to maintain the cancer stem cell phenotype. We could test this model in cell-culture by studying the ABCG2-expressing side-population cells (81, 82, 84). The side-population cells are used as markers of stem-cell phenotype based on their increased expression and activity of ABCG2. We will initially compare side-population phenotype in high ATX expressing cancer cell lines against low ATX expressing cancer cells. This will be followed up with testing patients treated with chemotherapy for their cancer stem cell signatures (88).

We proposed that LPA levels in the tumor microenvironment depend on both high ATX activity and low LPP activity (214). This should allow for relatively high LPA levels in the tumor microenvironment as seen in ovarian cancer patients. We observed local increases in ATX expression and LPA levels in the tumor microenvironment (137). Plasma LPA levels obtained from mice bearing mammary tumors were normal. However, systemic increases in ATX occurred in the very late stages of tumor progression (137). Most of our results were obtained with 5-10  $\mu$ M LPA, whereas plasma LPA levels are typically  $\leq 1$   $\mu$ M. In experiments where LPA was replaced with 1  $\mu$ M wls31, a stable LPA analog, we observed similar effects. Our group found that the half-life for extracellular LPA in cell culture was about 8-10 h (211). All of our cell culture experiments were done with 18:1-LPA, which has been used in LPA research predominantly. Since several species of polyunsaturated LPA including the abundant 20:4-LPA (39%), 18:2-LPA (38%) are present in the



serum (512), the individual relevance of these on receptor activation and signaling effects needs to be determined.

Our study links LPA signaling to increased oxidative stress response and drug resistance through Nrf2 stabilization. We demonstrate LPA-LPA<sub>1</sub>-PI3K signaling prevents the post-translational degradation of Nrf2. Additionally, LPA cooperates with t-BHQ resulting in additive increases in the expression of drug transporters and other Nrf2 targets. There are still some missing gaps in our understanding of this signaling pathway. A direct increase in Nrf2 activation in cells treated with doxorubicin was not demonstrated in our studies. However, other studies have confirmed the activation of Nrf2 in the presence of doxorubicin (444) or etoposide (513). The physiological activators of Nrf2 are poorly understood despite the important role for Nrf2 in cancers. It will be useful to determine if LPA is a physiological activator of Nrf2 by comparing the antioxidant response in wild-type or ATX transgenic mice treated with ARE-activators.

We found that PI3K activity is necessary for increased accumulation and ARE activity of Nrf2. Constitutive activation of PI3K was sufficient to drive Nrf2-signaling (442, 473). Several post-translational modifications have been found on Nrf2 protein. These include phosphorylation by several kinases and ubiquitinylation. Nrf2 is additionally sumoylated (514). These post-translational modifications regulate Nrf2 expression, nuclear localization and transcriptional activity. However, the contribution of these modifications to LPA-induced increases in Nrf2 is not clear.

LPA can transactivate growth factor receptor kinase mediated signaling pathways (127, 128). Some of the growth factor receptors have been linked previously to chemotherapeutic resistance. Pharmacological inhibitors of growth factor receptor kinases are readily available and can be used for a preliminary screen to assess their *in vitro* effects on LPA signaling. Interestingly, PLD2 activity has been linked to the transactivation of growth factor receptors by LPA (128). PA formation has been proposed to act as a signaling hub by increasing the plasma membrane recruitment of proteins such as SK1 (321). A future direction could to assess the role of PLD in nuclear/cytoplasmic localization and stabilization of Nrf2.

Cancer-specific mutations in ATX and LPA receptor genes are rare events. Instead, ATX/LPA in the microenvironment has been suggested to contribute to tumorigenesis by cooperating with secondary mutations and increasing the survival and aggressiveness of cancers (515). For example, PI3K/PTEN and Ras oncogenic pathways are activated by LPA receptor signaling. In contrast, somatic mutations in Nrf2 are frequently found in certain cancers like lung cancers. The constitutive high expression of Nrf2 seen in many cancers, even in the absence of pro-oxidants, give them a survival advantage. Newly identified targets for Nrf2 in cancers include genes involved in glycolytic pathways resulting in metabolic reprogramming (442). This results in increased proliferation, which is consistent with the role of ATX/LPA signaling in tumor progression. Furthermore, proliferating cancer cells generate high levels of ROS due to their rapid metabolism, which is balanced by higher activation levels of Nrf2 (443, 445). It will be useful to determine if Nrf2 expression correlates

with increased tumor progression in our cancer model. Nrf2 expression is expected to be higher in later stages of tumor proliferation and in metastatic cancers. ONO-8430506 delayed tumor growth by itself for up to 11 days in our breast cancer model and these tumors also exhibit decreased Nrf2 expression. It would be interesting to determine if ONO-8430506 had similar effects on genes involved in the glycolytic pathway as seen for Nrf2 (443, 445).

We did not test the effects of ATX in our cell culture studies directly. This will require the use of LPC and ONO-8430506 instead of LPA and LPA antagonists. A serious limitation in doing such studies was that ONO-8430506 had no effect in breast cancer cells such as 4T1, MCF-7 and MDA-MB-231, which express little ATX and most of the ATX is secreted from the mammary fat pad into the breast tumors (137). ATX-expressing cell lines, such as the MDA-MB-435 melanoma cell line, could be used instead to test these effects of ONO-8430506 (211, 516). Alternatively, co-cultures of cancer cells and ATX-expressing fibroblasts could be employed. A future direction could be use ATX inhibitors or LPA receptor antagonists in ATX-expressing cells to study their effects on Nrf2-induced chemoresistance. Modification of Nrf2 expression in breast cancer cells by overexpression or knockdown can affect their sensitivity to chemotherapies (45). Additionally a knockdown of Nrf2 in lung cancers made them more sensitive to platin-therapy in a xenograft model (517). We will use an autocrine model of ATX production and secretion (Fig. 1.4) to test the link between ATX and Nrf2 directly. Although several transcriptional targets of Nrf2 were found to be downregulated in ONO-8430506-

treated tumors, we did not pursue these further. For example, the antioxidant GPX1 or glutathione peroxidase 1 was one of the downregulated gene targets. GPX1 has been linked to doxorubicin resistance in multiple studies done in cell lines, animals and patients (518-521). We will need to validate the protein expression for these results.

We used the 4T1 syngeneic model primarily as a proof of concept. The fast progression of the disease makes it primarily a good model to study metastatic disease. Future studies with different models such as syngeneic allografts or gene knockout model are needed to establish the role of ATX inhibitors in sensitizing tumors to chemotherapies. The allograft model is particularly useful for studying the long-term acquisition of drug resistance by serial implantation of tumors from drug-treated cell lines. However, this would require significant time and investment.

A comparison of gene signatures in primary tumors and metastatic sites could be attempted to help understand why the combination of ONO-8430506 and doxorubicin was effective in attenuating both spontaneous and experimental metastasis. This can be done by collecting metastatic colonies and primary tumors and processing them for gene arrays. LPA production in metastatic sites, where ATX is locally recruited, may be required to establish tissue remodeling events (194, 226). Both the spread and colonization of the cancer cells in the lung could be affected by the combination therapy.

While we present preliminary evidence that tumors derived from cancers overexpressing LPP1 also show decreased Nrf2 expression, this was not pursued any

further. We will now test if LPP1-overexpressing cancer cells show increased sensitivity to chemotherapeutics such as doxorubicin or cisplatin. The LPP1 xenograft and syngeneic models provides us with two different tumor models for testing of the effects of LPP1 on chemo-sensitivity *in vivo* (183). Unlike the ATX inhibition model, LPP1 overexpression in the cancer cells did not result in decreases in plasma LPA levels. The lack of effects on plasma LPA suggest that LPP1 effects are largely localized and possibly downstream of LPA receptor activation. LPP1 can degrade not just LPA but also S1P, PA, C1P, etc. *in vitro* (177). In addition, LPP1 has been shown to act downstream of growth factor signaling (183, 185) and this effect is dependent on LPP1 catalytic activity. The identity of these intracellular targets, which can be phospholipids or sphingolipids, needs to be identified.

A variety of roles have been attributed to Nrf2 in normal and pathophysiological conditions. Nrf2<sup>-/-</sup> mice have increased susceptibility to chemically-induced carcinogenesis and several studies have validated the protective role of Nrf2 in normal cells (42). The protective role of Nrf2 is best explained by increased doxorubicin-induced cardiotoxicity in Nrf2<sup>-/-</sup> mice (522). In contrast, high Nrf2 expression is seen in cancers and decreases sensitivity to chemotherapeutics. Despite the opposing evidence, several Nrf2 inhibitors are under development for use as radio-/chemo-sensitizer (523). Similarly, ATX/LPA signaling is involved in a variety of normal processes like wound healing, cell migration, platelet aggregation and smooth cell contraction (See Section 1.3).

We did not find any obvious differences in toxicity of combination-therapy over doxorubicin monotherapy. However, we will need to assess the effects of ATX inhibition by itself or together with chemotherapy more carefully. A future direction could be to go back to our IHC specimens to look for signs of doxorubicin-induced cardiotoxicity, a side-effect seen in patients. Systemic chemotherapy and radiation-therapy affect the normal wound-healing response in patients. Some patients have additional risk factors, which affects their normal wound-healing response, such as diabetes (524). Approved therapies like those targeting VEGF-signaling have been used in combination with chemotherapies to treat cancer patients, despite complications associated with wound-healing (525). LPA signaling has been shown to be involved in multiple steps of the wound-healing response (See Section 1.3). We will need to assess the effects of ATX inhibition on wound-healing carefully as this could have potentially adverse-effects in patients. Our results suggest ATX levels in the tumor microenvironment are increased with doxorubicin therapy. Thus, ATX inhibitors may be selectively beneficial. A pre-clinical mouse model of wound-healing can be used to assess the effects of ATX inhibitors on the normal wound-healing response. It should be noted that modulation of ATX activity does not affect all LPA species in circulation and other routes of LPA biosynthesis are present. Additionally, several drugs targeting LPA signaling have been shown to have good safety profiles and efficacy in both pre-clinical and early clinical studies (248).

The immediate future directions are divided into four Sections – 6.1.1 Cancer-associated inflammation and ATX production drive resistance to doxorubicin

therapy in tumors, 6.1.2 Nrf2 activation and tamoxifen-resistance, 6.1.3 Regulation of RALBP1 expression by ATX/LPA signaling and 6.1.4 LPA activates SK1 autocrine/paracrine signaling in doxorubicin-resistant cells.

### **6.1.1 Cancer-associated inflammation and ATX production drive resistance to doxorubicin therapy in tumors**

The link between inflammation, ATX/LPA production and Nrf2 activation needs to be examined in our tumor models. The inflamed tumor microenvironment can make the tumors inherently less sensitive to chemotherapy and contribute towards selection for acquired resistance (526). It is likely that different types of cells within the tumor microenvironment signal to each other and further tumor growth and chemoresistance. For example, cancer-associated fibroblasts in patients secrete cytokines in response to chemotherapy, which helps in survival of cancer cells (88). We have demonstrated that the tumor adjacent mammary fat pad is inflamed by doxorubicin treatment and also increases ATX secretion, LPA production and Nrf2 activation in the tumors. Activation of Nrf2 leads to metabolic adaptations in the tumors and protection from oxidative damage (442). ATX/LPA signaling can thus contribute to a vicious cycle of tumor growth, genetic instability, proliferation and metastasis by recruitment of leukocytes and fibroblasts to the tumors (133, 176). This can affect chemotherapy penetration and response by efficient wound repair, metabolism and efflux of the drug.

Inhibition of ATX with ONO-8430506 decreased both plasma and tumor-specific LPA levels and decreased tumor progression and metastasis (137).

Furthermore, ATX was higher in the tumor-adjacent mammary fat pads compared to contralateral fat pads and this was increased further by the chemotherapeutic-insult with doxorubicin. Hence, the production of LPA in the tumor microenvironment is a likely mediator of tumor growth, metastasis and resistance. A direct validation of increased LPA levels in the interstitial fluid of patient breast cancers is not available until now. However, increased LPA levels have been demonstrated in ascites, synovial fluid, blisters, bronchoalveolar lavage fluid, where ATX/LPA signaling has been proposed to play important roles (133). A limitation of our study is the lack of a genetic model of ATX/LPA signaling in our animal studies. We tried to develop a 4T1-breast cancer model in a ATX transgenic BALB/c mice from a previously described transgenic model of ATX with a liver-specific promoter (144). However, we were not successful in increasing plasma ATX levels in BALB/c mice by this transgenic model, probably because adipose is the major source of circulating ATX activity (145). The MMTV-driven transgenic model of ATX and LPA receptors is another model we have considered (193). However, this model produces late-onset and inconsistent tumors making therapeutic studies challenging. Conditional knockout of ATX in adipose tissue (145) may be a useful model in future studies, given the importance of the inflamed adjacent mammary fat pad on ATX production in our breast cancer model (137). If we can acquire ATX<sup>-/-</sup> adipose-specific conditional knockout mice, we will attempt to grow tumors in these mice using our BALB/c or C57BL/6 syngeneic orthotopic models. Both plasma and tumor-specific LPA concentrations are expected to be decreased in these mice. We will also test if



doxorubicin has a significant therapeutic benefit under these conditions as expected from our results. We also expect decreased inflammation, slower growing tumors and reduced metastasis in the knockout mice.

We will initially determine ATX levels in the 4T1 tumors treated with doxorubicin. We expect ATX levels to be higher in doxorubicin-treated mice similar to tumor-adjacent mammary fat pads. We will also examine the effects of ATX inhibition and doxorubicin therapy on infiltration of leukocytes within the tumor. We will measure cytokine production both during early and late stages of tumor progression. We expect leukocyte infiltration to be decreased in the mammary adipose treated with combination therapy as seen in ONO-8430506-monotherapy treated adipose tissue (133, 176). Similarly, we expect the production of inflammatory mediators in the tumor-adjacent adipose to be decreased by combination therapy. In the future, we will try different doses of chemotherapeutics or radiation therapy to see if there were changes to inflammation and ATX production within the tumor. An inflammatory cancer model such as the chemically-induced colitis (223), where there is evidence of increased oxidative damage (527), might be a useful model to test the link between ATX/LPA signaling and Nrf2. Alternatively, we could study the effects of chemotherapy on expression of cytokines and antioxidants in various cell populations using specific cell markers in multi-color flow cytometry (528). The effects of the tumor microenvironment are not easy to study outside the tumor model although co-cultures or *ex vivo* preparations of cancer cells will be attempted with macrophages and adipocytes. We expect the co-

cultures, but not the cancer cells alone, to produce higher cytokine and ATX levels in response to chemotherapy.

ATX/LPA signaling has been shown previously to activate NFκB-mediated cytokine production in different cell types (160). In addition to this, a wide variety of chemotherapeutics including doxorubicin, cisplatin, paclitaxel, vincristine, 5-fluorouracil can further fuel inflammation in the tumors by activating factors such as NFκB (497). We demonstrate that doxorubicin in the presence of LPA increases cytokine production in MCF-7 breast cancer cells. We will now test if this is mediated by activation of NFκB using pharmacological inhibitors. We will also test the effects of Nrf2 on cytokine production using the previously established knockdown using Nrf2 DsiRNAs.

Although LPA has been shown to promote resistance to radiotherapy (238-241, 257) we have not yet examined these effects in our studies. The link between Nrf2 and radio-resistance is not well understood compared to its role in chemoresistance. Increased Nrf2 has been linked to resistance to radiotherapy in lung cancer cell lines (529). Similarly inflammation has been linked to radioresistance (497). We will need to establish the role of LPA in promoting radio-resistance through cell culture models initially. One particular experiment might be to use LPA with low and high dose radiation. Under low dose radiation, p53 activated Nrf2-mediated survival pathways whereas high-dose radiation resulted in p53-mediated death (530). It would be useful to determine if ROS production is altered under these conditions. At low doses, an efficient antioxidant repair in the

presence of LPA likely promotes cell survival since LPA has been shown to attenuate the p53 response (191, 192). Similarly, cytokine/chemokine production under low dose radiation is likely higher in LPA-treated cells. The C57BL/6 syngeneic model can be used alternatively as 4T1 breast cancer cells are p53-deficient. This needs to be followed up in tumor models where the tumor microenvironment affects radiation sensitivity (531). Finally, radio-sensitivity of LPP1 expressing xenograft or syngeneic tumors can be determined easily (183).

### **6.1.2 Nrf2 activation and tamoxifen-resistance**

Our group recently showed that tamoxifen and its metabolites activate oxidative-stress mediated apoptosis in breast cancer cells independent of their ER-status (Bekele R *et al.*, unpublished). We have now demonstrated that Nrf2 is activated by tamoxifen and its metabolites in cancer cells and tumor models. Increased Nrf2 expression has been linked previously to tamoxifen-resistance in isolated cancer cells (106). To determine if this has any clinical significance, we will now examine a previously published gene microarray data of breast cancer patients (433) and assess if Nrf2 and its targets like NQO1 are predictive for therapeutic response. We will also attempt immunohistochemical staining of a tissue microarray to determine prognostic value of Nrf2 protein in chemotherapy-treated patients compared to Nrf2 mRNA (434). Finally, we will attempt to create a gene signature from multiple Nrf2 targets obtained from our cell culture and animal experiments using 4-HT to determine if a group of genes had better prognostic value for the

effectiveness of tamoxifen treatment in breast cancer patients. We have already completed bulk of this work and we expect the future experiments to progress rapidly based on previously established protocols (434).

### **6.1.3 Regulation of RALBP1 expression by ATX/LPA signaling**

RALBP1 was initially identified as a GTPase activating protein (532). It was subsequently demonstrated that RALBP1 has ATPase activity, effluxes GSH-conjugates and plays a role in chemoresistance (25). We demonstrate that unlike the MDRT, regulation of RALBP1 does not depend on Nrf2 activation. Thus Nrf2 and RALBP1 represent two different pathways that increase resistance to apoptosis from oxidative-damage. We also present evidence showing that RALBP1 is upregulated in patient tumors and that ATX inhibition decreased RALBP1 expression in 4T1 tumors. We will now test the effects of LPA on modulating RALBP1 mRNA and protein expression in cancer cells. We will also test the effects of pro-inflammatory mediators, such as TNF $\alpha$  and IL-1 $\beta$ , on RALBP1 expression. We predict that high levels of inflammatory mediators and LPA in the tumors are associated with higher RALBP1 expression and oxidative stress response in the tumors. We will also determine if RALBP1 is regulated at the level of protein expression like Nrf2 using pharmacological inhibitors of protein degradation and synthesis. We will test the effects of RALBP1 expression on cancer cell sensitivity to tamoxifen and 4-HNE by performing siRNA knockdown of RALBP1. We will also decrease RALBP1 expression in tamoxifen-resistant MCF-7 cells to determine if this improves their

sensitivity to tamoxifen and 4-HNE. Since RALBP1 accounts for the bulk of 4-HNE export, we expect cancer cells with low RALBP1 expression to be sensitized to oxidative stress-mediated apoptosis. This will be followed up with analysis in a breast cancer patient database for RALBP1's prognostic value for the effectiveness of therapy with tamoxifen and cytotoxic chemotherapies as described before.

#### **6.1.4 LPA activates SK1 autocrine/paracrine signaling in doxorubicin-resistant cells**

LPA and S1P are both extracellular bioactive lipids, which activate G-protein coupled receptors. While they both activate similar bioactive pathways their differences lie mainly in their cell-specific expression and regulation. Extracellular LPA and S1P levels were decreased in iPLA<sub>2</sub> $\beta^{-/-}$  knockout mice injected with ovarian cancers when compared to wild-type mice (533). Since PLA<sub>2</sub> activity increases only LPA, the authors suggested that S1P levels were likely altered indirectly. We tested if LPA increased S1P concentrations in tumors by directly by activating SK1. We demonstrate that LPA increased the activation and expression of SK1, intracellular S1P concentrations and S1P<sub>1,3</sub> receptor expression. However, *in vivo* S1P concentrations in the plasma and tumors are not altered by inhibition of ATX with ONO-8430506 (137). Other extracellular signals besides LPA possibly regulate S1P levels and secretion in tumors. Since a variety of growth factors increase S1P it would be interesting to test if a PLD inhibitor like FIPI or VUO155056 can produce sustained decreases in the secreted S1P levels.

SK1 overexpressing 4T1 cells that were injected orthotopically in mice increased plasma S1P levels (369). However, a recent paper showed the increase in plasma S1P in cancer-bearing mice was not from cancer cell-associated SK1 activity (252). Cancer-specific S1P contributes to the tumor growth (252). However, it is not clear if SK1 effects on tumor growth are through increased secretion of S1P by cancer cells. Several intracellular effects have been attributed to S1P. Most of these involve either activation of the intracellular S1P receptor, alterations to sphingolipid metabolism and through lipid-protein binding interactions (345, 534). We have proposed several experiments in Chapter 5 mainly involving measurement of the concentrations of S1P and different species of ceramides using a previously established LC-MS technique (440, 535). Monitoring the changes to intracellular S1P and ceramides in cell culture models of drug resistance would help us understand the link between generation of intracellular sphingolipids and drug resistance. Targeting the ceramide-escape pathways such as SK1 could potentially be used to chemo/radio-sensitize tumors (405). Several sphingolipid modulators including the clinically approved FTY-720 show promising effects in pre-clinical cancer models (249, 369-371, 373, 385, 386, 388, 389). Our experiments suggest PLD2 could potentially regulate this pathway by increasing SK1 membrane activation and contribute to doxorubicin-resistance.

## **6.2 SUMMARY**

Overall, our studies have demonstrated a potentially important role for ATX/LPA signaling in increasing resistance to chemotherapies and development of multi-drug resistance through increased expression of Nrf2. The consequent transcription of antioxidant genes and MDRT add a new level of understanding to the role of ATX/LPA in chemoresistance. There are no current ATX inhibitors in the clinic. We demonstrate the utility of an ATX inhibitor in decreasing tumor growth, metastasis and resistance to therapies. Our work provides a practical solution for potentially overcoming chemoresistance through blocking LPA formation by ATX inhibition. Several LPA receptor antagonists are in clinical trials for inflammatory conditions, such as pulmonary fibrosis (536) or systemic sclerosis (537). The Monoclonal antibodies against LPA and S1P have also entered Phase I and II clinical trials respectively (253, 538, 539). The emergence of bio-available ATX inhibitors will present another opportunity to target ATX/LPA signaling in the clinics and thereby improve the treatments of cancer and other inflammatory conditions.

## BIBLIOGRAPHY

1. Gonzalez-Angulo, A. M., Morales-Vasquez, F., and Hortobagyi, G. N. (2007) Overview of resistance to systemic therapy in patients with breast cancer. *Advances in experimental medicine and biology* **608**, 1-22
2. Lage, H. (2008) An overview of cancer multidrug resistance: a still unsolved problem. *Cellular and molecular life sciences : CMLS* **65**, 3145-3167
3. Mimeault, M., Hauke, R., and Batra, S. K. (2008) Recent advances on the molecular mechanisms involved in the drug resistance of cancer cells and novel targeting therapies. *Clin Pharmacol Ther* **83**, 673-691
4. Gillet, J. P., and Gottesman, M. M. (2012) Overcoming multidrug resistance in cancer: 35 years after the discovery of ABCB1. *Drug Resist Updat* **15**, 2-4
5. Gillet, J. P., and Gottesman, M. M. (2010) Mechanisms of multidrug resistance in cancer. *Methods Mol Biol* **596**, 47-76
6. Ponnusamy, S., Meyers-Needham, M., Senkal, C. E., Saddoughi, S. A., Sentelle, D., Selvam, S. P., Salas, A., and Ogretmen, B. (2010) Sphingolipids and cancer: ceramide and sphingosine-1-phosphate in the regulation of cell death and drug resistance. *Future Oncol* **6**, 1603-1624
7. Morad, S. A., and Cabot, M. C. (2013) Ceramide-orchestrated signalling in cancer cells. *Nat Rev Cancer* **13**, 51-65
8. Szakacs, G., Paterson, J. K., Ludwig, J. A., Booth-Genthe, C., and Gottesman, M. M. (2006) Targeting multidrug resistance in cancer. *Nat Rev Drug Discov* **5**, 219-234
9. Juliano, R. L., and Ling, V. (1976) A surface glycoprotein modulating drug permeability in Chinese hamster ovary cell mutants. *Biochimica et biophysica acta* **455**, 152-162
10. Cole, S. P., Bhardwaj, G., Gerlach, J. H., Mackie, J. E., Grant, C. E., Almquist, K. C., Stewart, A. J., Kurz, E. U., Duncan, A. M., and Deeley, R. G. (1992) Overexpression of a transporter gene in a multidrug-resistant human lung cancer cell line. *Science* **258**, 1650-1654



11. Doyle, L. A., Yang, W., Abruzzo, L. V., Krogmann, T., Gao, Y., Rishi, A. K., and Ross, D. D. (1998) A multidrug resistance transporter from human MCF-7 breast cancer cells. *Proc Natl Acad Sci U S A* **95**, 15665-15670
12. Shaffer, B. C., Gillet, J. P., Patel, C., Baer, M. R., Bates, S. E., and Gottesman, M. M. (2012) Drug resistance: still a daunting challenge to the successful treatment of AML. *Drug Resist Updat* **15**, 62-69
13. Sharom, F. J. (2008) ABC multidrug transporters: structure, function and role in chemoresistance. *Pharmacogenomics* **9**, 105-127
14. Gillet, J. P., Calcagno, A. M., Varma, S., Davidson, B., Bunkholt Elstrand, M., Ganapathi, R., Kamat, A. A., Sood, A. K., Ambudkar, S. V., Seiden, M. V., Rueda, B. R., and Gottesman, M. M. (2012) Multidrug resistance-linked gene signature predicts overall survival of patients with primary ovarian serous carcinoma. *Clin Cancer Res* **18**, 3197-3206
15. Leslie, E. M., Deeley, R. G., and Cole, S. P. (2005) Multidrug resistance proteins: role of P-glycoprotein, MRP1, MRP2, and BCRP (ABCG2) in tissue defense. *Toxicol Appl Pharmacol* **204**, 216-237
16. Gottesman, M. M., Fojo, T., and Bates, S. E. (2002) Multidrug resistance in cancer: role of ATP-dependent transporters. *Nat Rev Cancer* **2**, 48-58
17. Huisman, M. T., Chhatta, A. A., van Tellingen, O., Beijnen, J. H., and Schinkel, A. H. (2005) MRP2 (ABCC2) transports taxanes and confers paclitaxel resistance and both processes are stimulated by probenecid. *Int J Cancer* **116**, 824-829
18. Liedert, B., Materna, V., Schadendorf, D., Thomale, J., and Lage, H. (2003) Overexpression of cMOAT (MRP2/ABCC2) is associated with decreased formation of platinum-DNA adducts and decreased G2-arrest in melanoma cells resistant to cisplatin. *J Invest Dermatol* **121**, 172-176
19. Szakacs, G., Annereau, J. P., Lababidi, S., Shankavaram, U., Arciello, A., Bussey, K. J., Reinhold, W., Guo, Y., Kruh, G. D., Reimers, M., Weinstein, J. N., and Gottesman, M. M. (2004) Predicting drug sensitivity and resistance: profiling ABC transporter genes in cancer cells. *Cancer Cell* **6**, 129-137

20. Inoue, Y., Matsumoto, H., Yamada, S., Kawai, K., Suemizu, H., Gika, M., Takanami, I., Iwazaki, M., and Nakamura, M. (2010) Association of ATP7A expression and in vitro sensitivity to cisplatin in non-small cell lung cancer. *Oncol Lett* **1**, 837-840
21. Surowiak, P., Materna, V., Kaplenko, I., Spaczynski, M., Dolinska-Krajewska, B., Gebarowska, E., Dietel, M., Zabel, M., and Lage, H. (2006) ABCC2 (MRP2, cMOAT) can be localized in the nuclear membrane of ovarian carcinomas and correlates with resistance to cisplatin and clinical outcome. *Clin Cancer Res* **12**, 7149-7158
22. Awasthi, S., Cheng, J., Singhal, S. S., Saini, M. K., Pandya, U., Pikula, S., Bandorowicz-Pikula, J., Singh, S. V., Zimniak, P., and Awasthi, Y. C. (2000) Novel function of human RLIP76: ATP-dependent transport of glutathione conjugates and doxorubicin. *Biochemistry* **39**, 9327-9334
23. Awasthi, S., Singhal, S. S., Awasthi, Y. C., Martin, B., Woo, J. H., Cunningham, C. C., and Frankel, A. E. (2008) RLIP76 and Cancer. *Clin Cancer Res* **14**, 4372-4377
24. Cheng, J. Z., Sharma, R., Yang, Y., Singhal, S. S., Sharma, A., Saini, M. K., Singh, S. V., Zimniak, P., Awasthi, S., and Awasthi, Y. C. (2001) Accelerated metabolism and exclusion of 4-hydroxynonenal through induction of RLIP76 and hGST5.8 is an early adaptive response of cells to heat and oxidative stress. *J Biol Chem* **276**, 41213-41223
25. Awasthi, Y. C., Sharma, R., Yadav, S., Dwivedi, S., Sharma, A., and Awasthi, S. (2007) The non-ABC drug transporter RLIP76 (RALBP-1) plays a major role in the mechanisms of drug resistance. *Curr Drug Metab* **8**, 315-323
26. Hediger, M. A., Romero, M. F., Peng, J. B., Rolfs, A., Takanaga, H., and Bruford, E. A. (2004) The ABCs of solute carriers: physiological, pathological and therapeutic implications of human membrane transport proteins. *Physiol Rev* **84**, 481-514
27. Smith, N. F., Marsh, S., Scott-Horton, T. J., Hamada, A., Mielke, S., Mross, K., Figg, W. D., Verweij, J., McLeod, H. L., and Sparreboom, A. (2007) Variants in the SLCO1B3 gene: interethnic distribution and association with paclitaxel pharmacokinetics. *Clin Pharmacol Ther* **81**, 76-82

28. Okabe, M., Szakacs, G., Reimers, M. A., Suzuki, T., Hall, M. D., Abe, T., Weinstein, J. N., and Gottesman, M. M. (2008) Profiling SLCO and SLC22 genes in the NCI-60 cancer cell lines to identify drug uptake transporters. *Mol Cancer Ther* **7**, 3081-3091
29. Sprowl, J. A., Mikkelsen, T. S., Giovanazzo, H., and Sparreboom, A. (2012) Contribution of tumoral and host solute carriers to clinical drug response. *Drug Resist Updat* **15**, 5-20
30. Liang, X. J., Shen, D. W., Chen, K. G., Wincovitch, S. M., Garfield, S. H., and Gottesman, M. M. (2005) Trafficking and localization of platinum complexes in cisplatin-resistant cell lines monitored by fluorescence-labeled platinum. *J Cell Physiol* **202**, 635-641
31. Safaei, R., Katano, K., Larson, B. J., Samimi, G., Holzer, A. K., Naerdemann, W., Tomioka, M., Goodman, M., and Howell, S. B. (2005) Intracellular localization and trafficking of fluorescein-labeled cisplatin in human ovarian carcinoma cells. *Clin Cancer Res* **11**, 756-767
32. Hurwitz, S. J., Terashima, M., Mizunuma, N., and Slapak, C. A. (1997) Vesicular anthracycline accumulation in doxorubicin-selected U-937 cells: participation of lysosomes. *Blood* **89**, 3745-3754
33. Chen, K. G., Valencia, J. C., Lai, B., Zhang, G., Paterson, J. K., Rouzaud, F., Berens, W., Wincovitch, S. M., Garfield, S. H., Leapman, R. D., Hearing, V. J., and Gottesman, M. M. (2006) Melanosomal sequestration of cytotoxic drugs contributes to the intractability of malignant melanomas. *Proc Natl Acad Sci U S A* **103**, 9903-9907
34. Bao, L., Haque, A., Jackson, K., Hazari, S., Moroz, K., Jetly, R., and Dash, S. (2011) Increased expression of P-glycoprotein is associated with doxorubicin chemoresistance in the metastatic 4T1 breast cancer model. *Am J Pathol* **178**, 838-852
35. Nakata, K., Tanaka, Y., Nakano, T., Adachi, T., Tanaka, H., Kaminuma, T., and Ishikawa, T. (2006) Nuclear receptor-mediated transcriptional regulation in Phase I, II, and III xenobiotic metabolizing systems. *Drug Metab Pharmacokinet* **21**, 437-457
36. Miners, J. O., Knights, K. M., Houston, J. B., and Mackenzie, P. I. (2006) In vitro-in vivo correlation for drugs and other compounds eliminated by glucuronidation in humans: pitfalls and promises. *Biochem Pharmacol* **71**, 1531-1539

37. Gamage, N., Barnett, A., Hempel, N., Duggleby, R. G., Windmill, K. F., Martin, J. L., and McManus, M. E. (2006) Human sulfotransferases and their role in chemical metabolism. *Toxicol Sci* **90**, 5-22
38. Ghezzi, P., and Di Simplicio, P. (2007) Glutathionylation pathways in drug response. *Curr Opin Pharmacol* **7**, 398-403
39. Ishikawa, T., Bao, J. J., Yamane, Y., Akimaru, K., Frindrich, K., Wright, C. D., and Kuo, M. T. (1996) Coordinated induction of MRP/GS-X pump and gamma-glutamylcysteine synthetase by heavy metals in human leukemia cells. *J Biol Chem* **271**, 14981-14988
40. Ishikawa, T., Wright, C. D., and Ishizuka, H. (1994) GS-X pump is functionally overexpressed in cis-diamminedichloroplatinum (II)-resistant human leukemia HL-60 cells and down-regulated by cell differentiation. *J Biol Chem* **269**, 29085-29093
41. Yamane, Y., Furuichi, M., Song, R., Van, N. T., Mulcahy, R. T., Ishikawa, T., and Kuo, M. T. (1998) Expression of multidrug resistance protein/GS-X pump and gamma-glutamylcysteine synthetase genes is regulated by oxidative stress. *J Biol Chem* **273**, 31075-31085
42. Jaramillo, M. C., and Zhang, D. D. (2013) The emerging role of the Nrf2-Keap1 signaling pathway in cancer. *Genes Dev* **27**, 2179-2191
43. Trachootham, D., Alexandre, J., and Huang, P. (2009) Targeting cancer cells by ROS-mediated mechanisms: a radical therapeutic approach? *Nat Rev Drug Discov* **8**, 579-591
44. Thorn, C. F., Oshiro, C., Marsh, S., Hernandez-Boussard, T., McLeod, H., Klein, T. E., and Altman, R. B. (2011) Doxorubicin pathways: pharmacodynamics and adverse effects. *Pharmacogenet Genomics* **21**, 440-446
45. Wang, X. J., Sun, Z., Villeneuve, N. F., Zhang, S., Zhao, F., Li, Y., Chen, W., Yi, X., Zheng, W., Wondrak, G. T., Wong, P. K., and Zhang, D. D. (2008) Nrf2 enhances resistance of cancer cells to chemotherapeutic drugs, the dark side of Nrf2. *Carcinogenesis* **29**, 1235-1243
46. Gorrini, C., Baniasadi, P. S., Harris, I. S., Silvester, J., Inoue, S., Snow, B., Joshi, P. A., Wakeham, A., Molyneux, S. D., Martin, B., Bouwman, P., Cescon, D. W., Elia, A. J., Winterton-Perks, Z., Cruickshank, J., Brenner, D., Tseng, A., Musgrave, M., Berman, H. K.,

- Khokha, R., Jonkers, J., Mak, T. W., and Gauthier, M. L. (2013) BRCA1 interacts with Nrf2 to regulate antioxidant signaling and cell survival. *J Exp Med* **210**, 1529-1544
47. Goldstein, M., and Kastan, M. B. (2015) The DNA damage response: implications for tumor responses to radiation and chemotherapy. *Annu Rev Med* **66**, 129-143
48. Kurz, E. U., Douglas, P., and Lees-Miller, S. P. (2004) Doxorubicin activates ATM-dependent phosphorylation of multiple downstream targets in part through the generation of reactive oxygen species. *J Biol Chem* **279**, 53272-53281
49. Lage, H., and Dietel, M. (1999) Involvement of the DNA mismatch repair system in antineoplastic drug resistance. *J Cancer Res Clin Oncol* **125**, 156-165
50. Ashwell, S., and Zabludoff, S. (2008) DNA damage detection and repair pathways--recent advances with inhibitors of checkpoint kinases in cancer therapy. *Clin Cancer Res* **14**, 4032-4037
51. Bao, S., Wu, Q., McLendon, R. E., Hao, Y., Shi, Q., Hjelmeland, A. B., Dewhirst, M. W., Bigner, D. D., and Rich, J. N. (2006) Glioma stem cells promote radioresistance by preferential activation of the DNA damage response. *Nature* **444**, 756-760
52. Martin, L. P., Hamilton, T. C., and Schilder, R. J. (2008) Platinum resistance: the role of DNA repair pathways. *Clin Cancer Res* **14**, 1291-1295
53. Swann, P. F., Waters, T. R., Moulton, D. C., Xu, Y. Z., Zheng, Q., Edwards, M., and Mace, R. (1996) Role of postreplicative DNA mismatch repair in the cytotoxic action of thioguanine. *Science* **273**, 1109-1111
54. Sarkaria, J. N., Kitange, G. J., James, C. D., Plummer, R., Calvert, H., Weller, M., and Wick, W. (2008) Mechanisms of chemoresistance to alkylating agents in malignant glioma. *Clin Cancer Res* **14**, 2900-2908
55. Wang, J. C. (2002) Cellular roles of DNA topoisomerases: a molecular perspective. *Nat Rev Mol Cell Biol* **3**, 430-440
56. Hanahan, D., and Weinberg, R. A. (2011) Hallmarks of cancer: the next generation. *Cell* **144**, 646-674

57. Okada, H., and Mak, T. W. (2004) Pathways of apoptotic and non-apoptotic death in tumour cells. *Nat Rev Cancer* **4**, 592-603
58. Brown, J. M., and Attardi, L. D. (2005) The role of apoptosis in cancer development and treatment response. *Nat Rev Cancer* **5**, 231-237
59. Rodriguez-Nieto, S., and Zhivotovsky, B. (2006) Role of alterations in the apoptotic machinery in sensitivity of cancer cells to treatment. *Curr Pharm Des* **12**, 4411-4425
60. Sjostrom, J., Blomqvist, C., von Boguslawski, K., Bengtsson, N. O., Mjaaland, I., Malmstrom, P., Ostenstadt, B., Wist, E., Valvere, V., Takayama, S., Reed, J. C., and Saksela, E. (2002) The predictive value of bcl-2, bax, bcl-xL, bag-1, fas, and fasL for chemotherapy response in advanced breast cancer. *Clin Cancer Res* **8**, 811-816
61. Krug, L. M., Miller, V. A., Filippa, D. A., Venkatraman, E., Ng, K. K., and Kris, M. G. (2003) Bcl-2 and bax expression in advanced non-small cell lung cancer: lack of correlation with chemotherapy response or survival in patients treated with docetaxel plus vinorelbine. *Lung Cancer* **39**, 139-143
62. Malamou-Mitsi, V., Gogas, H., Dafni, U., Bourli, A., Fillipidis, T., Sotiropoulou, M., Vlachodimitropoulos, D., Papadopoulos, S., Tzaida, O., Kafiri, G., Kyriakou, V., Markaki, S., Papaspyrou, I., Karagianni, E., Pavlakis, K., Toliou, T., Scopa, C., Papakostas, P., Bafaloukos, D., Christodoulou, C., and Fountzilias, G. (2006) Evaluation of the prognostic and predictive value of p53 and Bcl-2 in breast cancer patients participating in a randomized study with dose-dense sequential adjuvant chemotherapy. *Ann Oncol* **17**, 1504-1511
63. de Groot, D. J., van der Deen, M., Le, T. K., Regeling, A., de Jong, S., and de Vries, E. G. (2007) Indomethacin induces apoptosis via a MRP1-dependent mechanism in doxorubicin-resistant small-cell lung cancer cells overexpressing MRP1. *Br J Cancer* **97**, 1077-1083
64. Johnstone, R. W., Cretney, E., and Smyth, M. J. (1999) P-glycoprotein protects leukemia cells against caspase-dependent, but not caspase-independent, cell death. *Blood* **93**, 1075-1085
65. Kojima, H., Endo, K., Moriyama, H., Tanaka, Y., Alnemri, E. S., Slapak, C. A., Teicher, B., Kufe, D., and Datta, R. (1998) Abrogation of mitochondrial cytochrome c release and caspase-3 activation in acquired multidrug resistance. *J Biol Chem* **273**, 16647-16650

66. Shah, M. A., and Schwartz, G. K. (2001) Cell cycle-mediated drug resistance: an emerging concept in cancer therapy. *Clin Cancer Res* **7**, 2168-2181
67. Gottesman, M. M. (2002) Mechanisms of cancer drug resistance. *Annu Rev Med* **53**, 615-627
68. Isoyama, S., Dan, S., Nishimura, Y., Nakamura, N., Kajiwara, G., Seki, M., Irimura, T., and Yamori, T. (2012) Establishment of phosphatidylinositol 3-kinase inhibitor-resistant cancer cell lines and therapeutic strategies for overcoming the resistance. *Cancer Sci* **103**, 1955-1960
69. Tredan, O., Galmarini, C. M., Patel, K., and Tannock, I. F. (2007) Drug resistance and the solid tumor microenvironment. *J Natl Cancer Inst* **99**, 1441-1454
70. Finak, G., Bertos, N., Pepin, F., Sadekova, S., Souleimanova, M., Zhao, H., Chen, H., Omeroglu, G., Meterissian, S., Omeroglu, A., Hallett, M., and Park, M. (2008) Stromal gene expression predicts clinical outcome in breast cancer. *Nature medicine* **14**, 518-527
71. Wyckoff, J. B., Wang, Y., Lin, E. Y., Li, J. F., Goswami, S., Stanley, E. R., Segall, J. E., Pollard, J. W., and Condeelis, J. (2007) Direct visualization of macrophage-assisted tumor cell intravasation in mammary tumors. *Cancer Res* **67**, 2649-2656
72. Meads, M. B., Gatenby, R. A., and Dalton, W. S. (2009) Environment-mediated drug resistance: a major contributor to minimal residual disease. *Nat Rev Cancer* **9**, 665-674
73. Rottenberg, S., Vollebergh, M. A., de Hoon, B., de Ronde, J., Schouten, P. C., Kersbergen, A., Zander, S. A., Pajic, M., Jaspers, J. E., Jonkers, M., Loden, M., Sol, W., van der Burg, E., Wesseling, J., Gillet, J. P., Gottesman, M. M., Gribnau, J., Wessels, L., Linn, S. C., Jonkers, J., and Borst, P. (2012) Impact of intertumoral heterogeneity on predicting chemotherapy response of BRCA1-deficient mammary tumors. *Cancer Res* **72**, 2350-2361
74. Sethi, T., Rintoul, R. C., Moore, S. M., MacKinnon, A. C., Salter, D., Choo, C., Chilvers, E. R., Dransfield, I., Donnelly, S. C., Strieter, R., and Haslett, C. (1999) Extracellular matrix proteins protect small cell lung cancer cells against apoptosis: a mechanism for small cell lung cancer growth and drug resistance in vivo. *Nature medicine* **5**, 662-668

75. Stupp, R., and Rugg, C. (2007) Integrin inhibitors reaching the clinic. *J Clin Oncol* **25**, 1637-1638
76. Braun, S., Kantenich, C., Janni, W., Hepp, F., de Waal, J., Willgeroth, F., Sommer, H., and Pantel, K. (2000) Lack of effect of adjuvant chemotherapy on the elimination of single dormant tumor cells in bone marrow of high-risk breast cancer patients. *J Clin Oncol* **18**, 80-86
77. Bidard, F. C., Vincent-Salomon, A., Gomme, S., Nos, C., de Rycke, Y., Thiery, J. P., Sigal-Zafrani, B., Mignot, L., Sastre-Garau, X., and Pierga, J. Y. (2008) Disseminated tumor cells of breast cancer patients: a strong prognostic factor for distant and local relapse. *Clin Cancer Res* **14**, 3306-3311
78. Peinado, H., Lavotshkin, S., and Lyden, D. (2011) The secreted factors responsible for pre-metastatic niche formation: old sayings and new thoughts. *Semin Cancer Biol* **21**, 139-146
79. Clarke, M. F., Dick, J. E., Dirks, P. B., Eaves, C. J., Jamieson, C. H., Jones, D. L., Visvader, J., Weissman, I. L., and Wahl, G. M. (2006) Cancer stem cells--perspectives on current status and future directions: AACR Workshop on cancer stem cells. *Cancer Res* **66**, 9339-9344
80. Bunting, K. D. (2002) ABC transporters as phenotypic markers and functional regulators of stem cells. *Stem Cells* **20**, 11-20
81. Kim, M., Turnquist, H., Jackson, J., Sgagias, M., Yan, Y., Gong, M., Dean, M., Sharp, J. G., and Cowan, K. (2002) The multidrug resistance transporter ABCG2 (breast cancer resistance protein 1) effluxes Hoechst 33342 and is overexpressed in hematopoietic stem cells. *Clin Cancer Res* **8**, 22-28
82. Hirschmann-Jax, C., Foster, A. E., Wulf, G. G., Nuchtern, J. G., Jax, T. W., Gobel, U., Goodell, M. A., and Brenner, M. K. (2004) A distinct "side population" of cells with high drug efflux capacity in human tumor cells. *Proc Natl Acad Sci U S A* **101**, 14228-14233
83. Singh, A., Wu, H., Zhang, P., Happel, C., Ma, J., and Biswal, S. (2010) Expression of ABCG2 (BCRP) is regulated by Nrf2 in cancer cells that confers side population and chemoresistance phenotype. *Mol Cancer Ther* **9**, 2365-2376
84. Zhou, S., Schuetz, J. D., Bunting, K. D., Colapietro, A. M., Sampath, J., Morris, J. J., Lagutina, I., Grosveld, G. C., Osawa, M., Nakauchi,



- H., and Sorrentino, B. P. (2001) The ABC transporter Bcrp1/ABCG2 is expressed in a wide variety of stem cells and is a molecular determinant of the side-population phenotype. *Nature medicine* **7**, 1028-1034
85. Singh, A., and Settleman, J. (2010) EMT, cancer stem cells and drug resistance: an emerging axis of evil in the war on cancer. *Oncogene* **29**, 4741-4751
86. Creighton, C. J., Li, X., Landis, M., Dixon, J. M., Neumeister, V. M., Sjolund, A., Rimm, D. L., Wong, H., Rodriguez, A., Herschkowitz, J. I., Fan, C., Zhang, X., He, X., Pavlick, A., Gutierrez, M. C., Renshaw, L., Larionov, A. A., Faratian, D., Hilsenbeck, S. G., Perou, C. M., Lewis, M. T., Rosen, J. M., and Chang, J. C. (2009) Residual breast cancers after conventional therapy display mesenchymal as well as tumor-initiating features. *Proc Natl Acad Sci U S A* **106**, 13820-13825
87. Li, X., Lewis, M. T., Huang, J., Gutierrez, C., Osborne, C. K., Wu, M. F., Hilsenbeck, S. G., Pavlick, A., Zhang, X., Chamness, G. C., Wong, H., Rosen, J., and Chang, J. C. (2008) Intrinsic resistance of tumorigenic breast cancer cells to chemotherapy. *J Natl Cancer Inst* **100**, 672-679
88. Lotti, F., Jarrar, A. M., Pai, R. K., Hitomi, M., Lathia, J., Mace, A., Gantt, G. A., Jr., Sukhdeo, K., DeVecchio, J., Vasanji, A., Leahy, P., Hjelmeland, A. B., Kalady, M. F., and Rich, J. N. (2013) Chemotherapy activates cancer-associated fibroblasts to maintain colorectal cancer-initiating cells by IL-17A. *J Exp Med* **210**, 2851-2872
89. (1998) Tamoxifen for early breast cancer: an overview of the randomised trials. Early Breast Cancer Trialists' Collaborative Group. *Lancet* **351**, 1451-1467
90. Ring, A., and Dowsett, M. (2004) Mechanisms of tamoxifen resistance. *Endocr Relat Cancer* **11**, 643-658
91. Harrell, J. C., Dye, W. W., Harvell, D. M., Pinto, M., Jedlicka, P., Sartorius, C. A., and Horwitz, K. B. (2007) Estrogen insensitivity in a model of estrogen receptor positive breast cancer lymph node metastasis. *Cancer Res* **67**, 10582-10591
92. Jordan, V. C. (2003) Tamoxifen: a most unlikely pioneering medicine. *Nat Rev Drug Discov* **2**, 205-213

93. Jordan, V. C., Collins, M. M., Rowsby, L., and Prestwich, G. (1977) A monohydroxylated metabolite of tamoxifen with potent antioestrogenic activity. *The Journal of endocrinology* **75**, 305-316
94. Allen, K. E., Clark, E. R., and Jordan, V. C. (1980) Evidence for the metabolic activation of non-steroidal antioestrogens: a study of structure-activity relationships. *British journal of pharmacology* **71**, 83-91
95. Jones, A. (2003) Combining trastuzumab (Herceptin) with hormonal therapy in breast cancer: what can be expected and why? *Ann Oncol* **14**, 1697-1704
96. Robinson, S. P., Langan-Fahey, S. M., Johnson, D. A., and Jordan, V. C. (1991) Metabolites, pharmacodynamics, and pharmacokinetics of tamoxifen in rats and mice compared to the breast cancer patient. *Drug metabolism and disposition: the biological fate of chemicals* **19**, 36-43
97. Kisanga, E. R., Gjerde, J., Guerrieri-Gonzaga, A., Pigatto, F., Pesci-Feltri, A., Robertson, C., Serrano, D., Pelosi, G., Decensi, A., and Lien, E. A. (2004) Tamoxifen and metabolite concentrations in serum and breast cancer tissue during three dose regimens in a randomized preoperative trial. *Clin Cancer Res* **10**, 2336-2343
98. Ferlini, C., Scambia, G., Marone, M., Distefano, M., Gaggini, C., Ferrandina, G., Fattorossi, A., Isola, G., Benedetti Panici, P., and Mancuso, S. (1999) Tamoxifen induces oxidative stress and apoptosis in oestrogen receptor-negative human cancer cell lines. *Br J Cancer* **79**, 257-263
99. Gundimeda, U., Chen, Z. H., and Gopalakrishna, R. (1996) Tamoxifen modulates protein kinase C via oxidative stress in estrogen receptor-negative breast cancer cells. *J Biol Chem* **271**, 13504-13514
100. Schiff, R., Reddy, P., Ahotupa, M., Coronado-Heinsohn, E., Grim, M., Hilsenbeck, S. G., Lawrence, R., Deneke, S., Herrera, R., Chamness, G. C., Fuqua, S. A., Brown, P. H., and Osborne, C. K. (2000) Oxidative stress and AP-1 activity in tamoxifen-resistant breast tumors in vivo. *J Natl Cancer Inst* **92**, 1926-1934
101. Iusuf, D., Teunissen, S. F., Wagenaar, E., Rosing, H., Beijnen, J. H., and Schinkel, A. H. (2011) P-glycoprotein (ABCB1) transports the primary active tamoxifen metabolites endoxifen and 4-

hydroxytamoxifen and restricts their brain penetration. *J Pharmacol Exp Ther* **337**, 710-717

102. Teft, W. A., Mansell, S. E., and Kim, R. B. (2011) Endoxifen, the active metabolite of tamoxifen, is a substrate of the efflux transporter P-glycoprotein (multidrug resistance 1). *Drug metabolism and disposition: the biological fate of chemicals* **39**, 558-562
103. Dubrovskaja, A., Hartung, A., Bouchez, L. C., Walker, J. R., Reddy, V. A., Cho, C. Y., and Schultz, P. G. (2012) CXCR4 activation maintains a stem cell population in tamoxifen-resistant breast cancer cells through AhR signalling. *Br J Cancer* **107**, 43-52
104. Kiyotani, K., Mushiroda, T., Nakamura, Y., and Zembutsu, H. (2012) Pharmacogenomics of tamoxifen: roles of drug metabolizing enzymes and transporters. *Drug Metab Pharmacokinet* **27**, 122-131
105. Nowell, S., Sweeney, C., Winters, M., Stone, A., Lang, N. P., Hutchins, L. F., Kadlubar, F. F., and Ambrosone, C. B. (2002) Association between sulfotransferase 1A1 genotype and survival of breast cancer patients receiving tamoxifen therapy. *J Natl Cancer Inst* **94**, 1635-1640
106. Kim, S. K., Yang, J. W., Kim, M. R., Roh, S. H., Kim, H. G., Lee, K. Y., Jeong, H. G., and Kang, K. W. (2008) Increased expression of Nrf2/ARE-dependent anti-oxidant proteins in tamoxifen-resistant breast cancer cells. *Free Radic Biol Med* **45**, 537-546
107. Choi, H. K., Yang, J. W., Roh, S. H., Han, C. Y., and Kang, K. W. (2007) Induction of multidrug resistance associated protein 2 in tamoxifen-resistant breast cancer cells. *Endocr Relat Cancer* **14**, 293-303
108. Mahon, F. X., Belloc, F., Lagarde, V., Chollet, C., Moreau-Gaudry, F., Reiffers, J., Goldman, J. M., and Melo, J. V. (2003) MDR1 gene overexpression confers resistance to imatinib mesylate in leukemia cell line models. *Blood* **101**, 2368-2373
109. Burger, H., van Tol, H., Boersma, A. W., Brok, M., Wiemer, E. A., Stoter, G., and Nooter, K. (2004) Imatinib mesylate (STI571) is a substrate for the breast cancer resistance protein (BCRP)/ABCG2 drug pump. *Blood* **104**, 2940-2942

110. Cascorbi, I. (2006) Role of pharmacogenetics of ATP-binding cassette transporters in the pharmacokinetics of drugs. *Pharmacol Ther* **112**, 457-473
111. Yung, Y. C., Stoddard, N. C., and Chun, J. (2014) LPA receptor signaling: pharmacology, physiology, and pathophysiology. *J Lipid Res* **55**, 1192-1214
112. Tokumura, A., Fukuzawa, K., Akamatsu, Y., Yamada, S., Suzuki, T., and Tsukatani, H. (1978) Identification of vasopressor phospholipid in crude soybean lecithin. *Lipids* **13**, 468-472
113. Tokumura, A., Fukuzawa, K., and Tsukatani, H. (1978) Effects of synthetic and natural lysophosphatidic acids on the arterial blood pressure of different animal species. *Lipids* **13**, 572-574
114. Tokumura, A., Harada, K., Fukuzawa, K., and Tsukatani, H. (1986) Involvement of lysophospholipase D in the production of lysophosphatidic acid in rat plasma. *Biochimica et biophysica acta* **875**, 31-38
115. Tokumura, A., Majima, E., Kariya, Y., Tominaga, K., Kogure, K., Yasuda, K., and Fukuzawa, K. (2002) Identification of human plasma lysophospholipase D, a lysophosphatidic acid-producing enzyme, as autotaxin, a multifunctional phosphodiesterase. *J Biol Chem* **277**, 39436-39442
116. Umezu-Goto, M., Kishi, Y., Taira, A., Hama, K., Dohmae, N., Takio, K., Yamori, T., Mills, G. B., Inoue, K., Aoki, J., and Arai, H. (2002) Autotaxin has lysophospholipase D activity leading to tumor cell growth and motility by lysophosphatidic acid production. *J Cell Biol* **158**, 227-233
117. Stracke, M. L., Krutzsch, H. C., Unsworth, E. J., Arestad, A., Cioce, V., Schiffmann, E., and Liotta, L. A. (1992) Identification, purification, and partial sequence analysis of autotaxin, a novel motility-stimulating protein. *J Biol Chem* **267**, 2524-2529
118. Hecht, J. H., Weiner, J. A., Post, S. R., and Chun, J. (1996) Ventricular zone gene-1 (vzg-1) encodes a lysophosphatidic acid receptor expressed in neurogenic regions of the developing cerebral cortex. *J Cell Biol* **135**, 1071-1083
119. Chun, J., Hla, T., Lynch, K. R., Spiegel, S., and Moolenaar, W. H. (2010) International Union of Basic and Clinical Pharmacology.

LXXVIII. Lysophospholipid receptor nomenclature. *Pharmacol Rev* **62**, 579-587

120. Howe, L. R., and Marshall, C. J. (1993) Lysophosphatidic acid stimulates mitogen-activated protein kinase activation via a G-protein-coupled pathway requiring p21ras and p74raf-1. *J Biol Chem* **268**, 20717-20720
121. Stoyanov, B., Volinia, S., Hanck, T., Rubio, I., Loubtchenkov, M., Malek, D., Stoyanova, S., Vanhaesebroeck, B., Dhand, R., Nurnberg, B., and et al. (1995) Cloning and characterization of a G protein-activated human phosphoinositide-3 kinase. *Science* **269**, 690-693
122. van Corven, E. J., Groenink, A., Jalink, K., Eichholtz, T., and Moolenaar, W. H. (1989) Lysophosphatidate-induced cell proliferation: identification and dissection of signaling pathways mediated by G proteins. *Cell* **59**, 45-54
123. Kumagai, N., Morii, N., Fujisawa, K., Nemoto, Y., and Narumiya, S. (1993) ADP-ribosylation of rho p21 inhibits lysophosphatidic acid-induced protein tyrosine phosphorylation and phosphatidylinositol 3-kinase activation in cultured Swiss 3T3 cells. *J Biol Chem* **268**, 24535-24538
124. Brindley, D. N. (2004) Lipid phosphate phosphatases and related proteins: signaling functions in development, cell division, and cancer. *J Cell Biochem* **92**, 900-912
125. Fourcade, O., Simon, M. F., Viode, C., Rugani, N., Leballe, F., Ragab, A., Fournie, B., Sarda, L., and Chap, H. (1995) Secretory phospholipase A2 generates the novel lipid mediator lysophosphatidic acid in membrane microvesicles shed from activated cells. *Cell* **80**, 919-927
126. Sano, T., Baker, D., Virag, T., Wada, A., Yatomi, Y., Kobayashi, T., Igarashi, Y., and Tigyi, G. (2002) Multiple mechanisms linked to platelet activation result in lysophosphatidic acid and sphingosine 1-phosphate generation in blood. *J Biol Chem* **277**, 21197-21206
127. Shida, D., Fang, X., Kordula, T., Takabe, K., Lepine, S., Alvarez, S. E., Milstien, S., and Spiegel, S. (2008) Cross-talk between LPA1 and epidermal growth factor receptors mediates up-regulation of sphingosine kinase 1 to promote gastric cancer cell motility and invasion. *Cancer Res* **68**, 6569-6577

128. Wang, L., Cummings, R., Zhao, Y., Kazlauskas, A., Sham, J. K., Morris, A., Georas, S., Brindley, D. N., and Natarajan, V. (2003) Involvement of phospholipase D2 in lysophosphatidate-induced transactivation of platelet-derived growth factor receptor-beta in human bronchial epithelial cells. *J Biol Chem* **278**, 39931-39940
129. Tager, A. M., LaCamera, P., Shea, B. S., Campanella, G. S., Selman, M., Zhao, Z., Polosukhin, V., Wain, J., Karimi-Shah, B. A., Kim, N. D., Hart, W. K., Pardo, A., Blackwell, T. S., Xu, Y., Chun, J., and Luster, A. D. (2008) The lysophosphatidic acid receptor LPA1 links pulmonary fibrosis to lung injury by mediating fibroblast recruitment and vascular leak. *Nature medicine* **14**, 45-54
130. Inoue, M., Yamaguchi, A., Kawakami, M., Chun, J., and Ueda, H. (2006) Loss of spinal substance P pain transmission under the condition of LPA1 receptor-mediated neuropathic pain. *Mol Pain* **2**, 25
131. Ye, X., Hama, K., Contos, J. J., Anliker, B., Inoue, A., Skinner, M. K., Suzuki, H., Amano, T., Kennedy, G., Arai, H., Aoki, J., and Chun, J. (2005) LPA3-mediated lysophosphatidic acid signalling in embryo implantation and spacing. *Nature* **435**, 104-108
132. Pasternack, S. M., von Kugelgen, I., Al Aboud, K., Lee, Y. A., Ruschendorf, F., Voss, K., Hillmer, A. M., Molderings, G. J., Franz, T., Ramirez, A., Nurnberg, P., Nothen, M. M., and Betz, R. C. (2008) G protein-coupled receptor P2Y5 and its ligand LPA are involved in maintenance of human hair growth. *Nat Genet* **40**, 329-334
133. Benesch, M. G., Ko, Y. M., McMullen, T. P., and Brindley, D. N. (2014) Autotaxin in the crosshairs: taking aim at cancer and other inflammatory conditions. *FEBS Lett* **588**, 2712-2727
134. Brindley, D. N., Lin, F. T., and Tigyi, G. J. (2013) Role of the autotaxin-lysophosphatidate axis in cancer resistance to chemotherapy and radiotherapy. *Biochimica et biophysica acta* **1831**, 74-85
135. Croset, M., Brossard, N., Polette, A., and Lagarde, M. (2000) Characterization of plasma unsaturated lysophosphatidylcholines in human and rat. *Biochem J* **345 Pt 1**, 61-67
136. Aoki, J., Taira, A., Takanezawa, Y., Kishi, Y., Hama, K., Kishimoto, T., Mizuno, K., Saku, K., Taguchi, R., and Arai, H. (2002) Serum lysophosphatidic acid is produced through diverse phospholipase pathways. *J Biol Chem* **277**, 48737-48744

137. Benesch, M. G., Tang, X., Maeda, T., Ohhata, A., Zhao, Y. Y., Kok, B. P., Dewald, J., Hitt, M., Curtis, J. M., McMullen, T. P., and Brindley, D. N. (2014) Inhibition of autotaxin delays breast tumor growth and lung metastasis in mice. *FASEB J* **28**, 2655-2666
138. Salous, A. K., Panchatcharam, M., Sunkara, M., Mueller, P., Dong, A., Wang, Y., Graf, G. A., Smyth, S. S., and Morris, A. J. (2013) Mechanism of rapid elimination of lysophosphatidic acid and related lipids from the circulation of mice. *J Lipid Res* **54**, 2775-2784
139. Tomsig, J. L., Snyder, A. H., Berdyshev, E. V., Skobeleva, A., Mataya, C., Natarajan, V., Brindley, D. N., and Lynch, K. R. (2009) Lipid phosphate phosphohydrolase type 1 (LPP1) degrades extracellular lysophosphatidic acid in vivo. *Biochem J* **419**, 611-618
140. Albers, H. M., Dong, A., van Meeteren, L. A., Egan, D. A., Sunkara, M., van Tilburg, E. W., Schuurman, K., van Tellingen, O., Morris, A. J., Smyth, S. S., Moolenaar, W. H., and Ovaa, H. (2010) Boronic acid-based inhibitor of autotaxin reveals rapid turnover of LPA in the circulation. *Proc Natl Acad Sci U S A* **107**, 7257-7262
141. Gierse, J., Thorarensen, A., Beltey, K., Bradshaw-Pierce, E., Cortes-Burgos, L., Hall, T., Johnston, A., Murphy, M., Nemirovskiy, O., Ogawa, S., Pegg, L., Pelc, M., Prinsen, M., Schnute, M., Wendling, J., Wene, S., Weinberg, R., Wittwer, A., Zweifel, B., and Masferrer, J. (2010) A novel autotaxin inhibitor reduces lysophosphatidic acid levels in plasma and the site of inflammation. *J Pharmacol Exp Ther* **334**, 310-317
142. van Meeteren, L. A., Ruurs, P., Stortelers, C., Bouwman, P., van Rooijen, M. A., Pradere, J. P., Pettit, T. R., Wakelam, M. J., Saulnier-Blache, J. S., Mummery, C. L., Moolenaar, W. H., and Jonkers, J. (2006) Autotaxin, a secreted lysophospholipase D, is essential for blood vessel formation during development. *Mol Cell Biol* **26**, 5015-5022
143. Tanaka, M., Okudaira, S., Kishi, Y., Ohkawa, R., Iseki, S., Ota, M., Noji, S., Yatomi, Y., Aoki, J., and Arai, H. (2006) Autotaxin stabilizes blood vessels and is required for embryonic vasculature by producing lysophosphatidic acid. *J Biol Chem* **281**, 25822-25830
144. Pamuklar, Z., Federico, L., Liu, S., Umezu-Goto, M., Dong, A., Panchatcharam, M., Fulkerson, Z., Berdyshev, E., Natarajan, V., Fang, X., van Meeteren, L. A., Moolenaar, W. H., Mills, G. B., Morris, A. J., and Smyth, S. S. (2009) Autotaxin/lysopholipase D and

lysophosphatidic acid regulate murine hemostasis and thrombosis. *J Biol Chem* **284**, 7385-7394

145. Dusaulcy, R., Rancoule, C., Gres, S., Wanecq, E., Colom, A., Guigne, C., van Meeteren, L. A., Moolenaar, W. H., Valet, P., and Saulnier-Blache, J. S. (2011) Adipose-specific disruption of autotaxin enhances nutritional fattening and reduces plasma lysophosphatidic acid. *J Lipid Res* **52**, 1247-1255
146. Masuda, A., Nakamura, K., Izutsu, K., Igarashi, K., Ohkawa, R., Jona, M., Higashi, K., Yokota, H., Okudaira, S., Kishimoto, T., Watanabe, T., Koike, Y., Ikeda, H., Kozai, Y., Kurokawa, M., Aoki, J., and Yatomi, Y. (2008) Serum autotaxin measurement in haematological malignancies: a promising marker for follicular lymphoma. *Br J Haematol* **143**, 60-70
147. Aoki, J., Inoue, A., and Okudaira, S. (2008) Two pathways for lysophosphatidic acid production. *Biochimica et biophysica acta* **1781**, 513-518
148. Jansen, S., Stefan, C., Creemers, J. W., Waelkens, E., Van Eynde, A., Stalmans, W., and Bollen, M. (2005) Proteolytic maturation and activation of autotaxin (NPP2), a secreted metastasis-enhancing lysophospholipase D. *J Cell Sci* **118**, 3081-3089
149. Houben, A. J., van Wijk, X. M., van Meeteren, L. A., van Zeijl, L., van de Westerlo, E. M., Hausmann, J., Fish, A., Perrakis, A., van Kuppevelt, T. H., and Moolenaar, W. H. (2013) The polybasic insertion in autotaxin alpha confers specific binding to heparin and cell surface heparan sulfate proteoglycans. *J Biol Chem* **288**, 510-519
150. Fulkerson, Z., Wu, T., Sunkara, M., Kooi, C. V., Morris, A. J., and Smyth, S. S. (2011) Binding of autotaxin to integrins localizes lysophosphatidic acid production to platelets and mammalian cells. *J Biol Chem* **286**, 34654-34663
151. Wu, T., Kooi, C. V., Shah, P., Charnigo, R., Huang, C., Smyth, S. S., and Morris, A. J. (2014) Integrin-mediated cell surface recruitment of autotaxin promotes persistent directional cell migration. *FASEB J* **28**, 861-870
152. Hausmann, J., Kamtekar, S., Christodoulou, E., Day, J. E., Wu, T., Fulkerson, Z., Albers, H. M., van Meeteren, L. A., Houben, A. J., van Zeijl, L., Jansen, S., Andries, M., Hall, T., Pegg, L. E., Benson, T. E., Kasiem, M., Harlos, K., Kooi, C. W., Smyth, S. S., Ovaa, H., Bollen,



- M., Morris, A. J., Moolenaar, W. H., and Perrakis, A. (2011) Structural basis of substrate discrimination and integrin binding by autotaxin. *Nat Struct Mol Biol* **18**, 198-204
153. Nishimasu, H., Okudaira, S., Hama, K., Mihara, E., Dohmae, N., Inoue, A., Ishitani, R., Takagi, J., Aoki, J., and Nureki, O. (2011) Crystal structure of autotaxin and insight into GPCR activation by lipid mediators. *Nat Struct Mol Biol* **18**, 205-212
154. Benesch, M. G., Zhao, Y. Y., Curtis, J. M., McMullen, T. P., and Brindley, D. N. (2015) Regulation of autotaxin expression and secretion by lysophosphatidate and sphingosine 1-phosphate. *J Lipid Res* **56**, 1134-1144
155. Olorundare, O. E., Peyruchaud, O., Albrecht, R. M., and Mosher, D. F. (2001) Assembly of a fibronectin matrix by adherent platelets stimulated by lysophosphatidic acid and other agonists. *Blood* **98**, 117-124
156. Kai, M., Sakane, F., Jia, Y. J., Imai, S., Yasuda, S., and Kanoh, H. (2006) Lipid phosphate phosphatases 1 and 3 are localized in distinct lipid rafts. *J Biochem* **140**, 677-686
157. Mazereeuw-Hautier, J., Gres, S., Fanguin, M., Cariven, C., Fauvel, J., Perret, B., Chap, H., Salles, J. P., and Saulnier-Blache, J. S. (2005) Production of lysophosphatidic acid in blister fluid: involvement of a lysophospholipase D activity. *J Invest Dermatol* **125**, 421-427
158. Tokumura, A., Taira, S., Kikuchi, M., Tsutsumi, T., Shimizu, Y., and Watsky, M. A. (2012) Lysophospholipids and lysophospholipase D in rabbit aqueous humor following corneal injury. *Prostaglandins Other Lipid Mediat* **97**, 83-89
159. Knowlden, S., and Georas, S. N. (2014) The autotaxin-LPA axis emerges as a novel regulator of lymphocyte homing and inflammation. *J Immunol* **192**, 851-857
160. Cummings, R., Zhao, Y., Jacoby, D., Spannhake, E. W., Ohba, M., Garcia, J. G., Watkins, T., He, D., Saatian, B., and Natarajan, V. (2004) Protein kinase Cdelta mediates lysophosphatidic acid-induced NF-kappaB activation and interleukin-8 secretion in human bronchial epithelial cells. *J Biol Chem* **279**, 41085-41094
161. Fang, X., Yu, S., Bast, R. C., Liu, S., Xu, H. J., Hu, S. X., LaPushin, R., Claret, F. X., Aggarwal, B. B., Lu, Y., and Mills, G. B. (2004)

Mechanisms for lysophosphatidic acid-induced cytokine production in ovarian cancer cells. *J Biol Chem* **279**, 9653-9661

162. Seo, J. H., Jeong, K. J., Oh, W. J., Sul, H. J., Sohn, J. S., Kim, Y. K., Cho do, Y., Kang, J. K., Park, C. G., and Lee, H. Y. (2010) Lysophosphatidic acid induces STAT3 phosphorylation and ovarian cancer cell motility: their inhibition by curcumin. *Cancer Lett* **288**, 50-56
163. Saatian, B., Zhao, Y., He, D., Georas, S. N., Watkins, T., Spannhake, E. W., and Natarajan, V. (2006) Transcriptional regulation of lysophosphatidic acid-induced interleukin-8 expression and secretion by p38 MAPK and JNK in human bronchial epithelial cells. *Biochem J* **393**, 657-668
164. Lee, J., Park, S. Y., Lee, E. K., Park, C. G., Chung, H. C., Rha, S. Y., Kim, Y. K., Bae, G. U., Kim, B. K., Han, J. W., and Lee, H. Y. (2006) Activation of hypoxia-inducible factor-1alpha is necessary for lysophosphatidic acid-induced vascular endothelial growth factor expression. *Clin Cancer Res* **12**, 6351-6358
165. Liu, S., Murph, M., Panupinthu, N., and Mills, G. B. (2009) ATX-LPA receptor axis in inflammation and cancer. *Cell Cycle* **8**, 3695-3701
166. Bourgoin, S. G., and Zhao, C. (2010) Autotaxin and lysophospholipids in rheumatoid arthritis. *Curr Opin Investig Drugs* **11**, 515-526
167. Georas, S. N., Berdyshev, E., Hubbard, W., Gorshkova, I. A., Usatyuk, P. V., Saatian, B., Myers, A. C., Williams, M. A., Xiao, H. Q., Liu, M., and Natarajan, V. (2007) Lysophosphatidic acid is detectable in human bronchoalveolar lavage fluids at baseline and increased after segmental allergen challenge. *Clin Exp Allergy* **37**, 311-322
168. Park, G. Y., Lee, Y. G., Berdyshev, E., Nyenhuis, S., Du, J., Fu, P., Gorshkova, I. A., Li, Y., Chung, S., Karpurapu, M., Deng, J., Ranjan, R., Xiao, L., Jaffe, H. A., Corbridge, S. J., Kelly, E. A., Jarjour, N. N., Chun, J., Prestwich, G. D., Kaffe, E., Ninou, I., Aidinis, V., Morris, A. J., Smyth, S. S., Ackerman, S. J., Natarajan, V., and Christman, J. W. (2013) Autotaxin production of lysophosphatidic acid mediates allergic asthmatic inflammation. *Am J Respir Crit Care Med* **188**, 928-940
169. Nochi, H., Tomura, H., Tobo, M., Tanaka, N., Sato, K., Shinozaki, T., Kobayashi, T., Takagishi, K., Ohta, H., Okajima, F., and Tamoto, K. (2008) Stimulatory role of lysophosphatidic acid in cyclooxygenase-2

induction by synovial fluid of patients with rheumatoid arthritis in fibroblast-like synovial cells. *J Immunol* **181**, 5111-5119

170. Siess, W., Zangl, K. J., Essler, M., Bauer, M., Brandl, R., Corrinth, C., Bittman, R., Tigyi, G., and Aepfelbacher, M. (1999) Lysophosphatidic acid mediates the rapid activation of platelets and endothelial cells by mildly oxidized low density lipoprotein and accumulates in human atherosclerotic lesions. *Proc Natl Acad Sci U S A* **96**, 6931-6936
171. Rother, E., Brandl, R., Baker, D. L., Goyal, P., Gebhard, H., Tigyi, G., and Siess, W. (2003) Subtype-selective antagonists of lysophosphatidic Acid receptors inhibit platelet activation triggered by the lipid core of atherosclerotic plaques. *Circulation* **108**, 741-747
172. Mantovani, A., Allavena, P., Sica, A., and Balkwill, F. (2008) Cancer-related inflammation. *Nature* **454**, 436-444
173. Cooper, A. B., Wu, J. M., Lu, D. B., and Maluccio, M. A. (2007) Is autotaxin (ENPP2) the link between Hepatitis C and hepatocellular cancer? *J Gastrointest Surg* **11**, 1628-1634
174. Wu, J. M., Xu, Y., Skill, N. J., Sheng, H., Zhao, Z., Yu, M., Saxena, R., and Maluccio, M. A. (2010) Autotaxin expression and its connection with the TNF-alpha-NF-kappaB axis in human hepatocellular carcinoma. *Mol Cancer* **9**, 71
175. Hozumi, H., Hokari, R., Kurihara, C., Narimatsu, K., Sato, H., Sato, S., Ueda, T., Higashiyama, M., Okada, Y., Watanabe, C., Komoto, S., Tomita, K., Kawaguchi, A., Nagao, S., and Miura, S. (2013) Involvement of autotaxin/lysophospholipase D expression in intestinal vessels in aggravation of intestinal damage through lymphocyte migration. *Laboratory investigation; a journal of technical methods and pathology*
176. Benesch, M. G., Ko, Y. M., Tang, X., Dewald, J., Lopez-Campistrous, A., Zhao, Y. Y., Lai, R., Curtis, J. M., Brindley, D., and McMullen, T. P. (2015) Autotaxin is an inflammatory mediator and therapeutic target in thyroid cancer. *Endocr Relat Cancer*
177. Jasinska, R., Zhang, Q. X., Pilquill, C., Singh, I., Xu, J., Dewald, J., Dillon, D. A., Berthiaume, L. G., Carman, G. M., Waggoner, D. W., and Brindley, D. N. (1999) Lipid phosphate phosphohydrolase-1 degrades exogenous glycerolipid and sphingolipid phosphate esters. *Biochem J* **340**, 677-686

178. Dillon, D. A., Chen, X., Zeimet, G. M., Wu, W. I., Waggoner, D. W., Dewald, J., Brindley, D. N., and Carman, G. M. (1997) Mammalian Mg<sup>2+</sup>-independent phosphatidate phosphatase (PAP2) displays diacylglycerol pyrophosphate phosphatase activity. *J Biol Chem* **272**, 10361-10366
179. Hooks, S. B., Ragan, S. P., and Lynch, K. R. (1998) Identification of a novel human phosphatidic acid phosphatase type 2 isoform. *FEBS Lett* **427**, 188-192
180. Jamal, Z., Martin, A., Gómez-Muñoz, A., and Brindley, D. N. (1991) Plasma membrane fractions from rat liver contain a phosphatidate phosphohydrolase distinct from that in the endoplasmic reticulum and cytosol. *J Biol Chem* **266**, 2988-2996
181. Tanyi, J. L., Hasegawa, Y., Lapushin, R., Morris, A. J., Wolf, J. K., Berchuck, A., Lu, K., Smith, D. I., Kalli, K., Hartmann, L. C., McCune, K., Fishman, D., Broaddus, R., Cheng, K. W., Atkinson, E. N., Yamal, J. M., Bast, R. C., Felix, E. A., Newman, R. A., and Mills, G. B. (2003) Role of decreased levels of lipid phosphate phosphatase-1 in accumulation of lysophosphatidic acid in ovarian cancer. *Clin Cancer Res* **9**, 3534-3545
182. Tang, X., Benesch, M. G., and Brindley, D. N. (2015) Lipid phosphate phosphatases and their roles in mammalian physiology and pathology. *J Lipid Res*
183. Tang, X., Benesch, M. G., Dewald, J., Zhao, Y. Y., Patwardhan, N., Santos, W. L., Curtis, J. M., McMullen, T. P., and Brindley, D. N. (2014) Lipid phosphate phosphatase-1 expression in cancer cells attenuates tumor growth and metastasis in mice. *J Lipid Res* **55**, 2389-2400
184. Tanyi, J. L., Morris, A. J., Wolf, J. K., Fang, X., Hasegawa, Y., Lapushin, R., Auersperg, N., Sigal, Y. J., Newman, R. A., Felix, E. A., Atkinson, E. N., and Mills, G. B. (2003) The human lipid phosphate phosphatase-3 decreases the growth, survival, and tumorigenesis of ovarian cancer cells: validation of the lysophosphatidic acid signaling cascade as a target for therapy in ovarian cancer. *Cancer Res* **63**, 1073-1082
185. Pilquill, C., Dewald, J., Cherney, A., Gorshkova, I., Tigyi, G., English, D., Natarajan, V., and Brindley, D. N. (2006) Lipid phosphate phosphatase-1 regulates lysophosphatidate-induced fibroblast

migration by controlling phospholipase D2-dependent phosphatidate generation. *J Biol Chem* **281**, 38418-38429

186. Alderton, F., Darroch, P., Sambhi, B., McKie, A., Ahmed, I. S., Pyne, N., and Pyne, S. (2001) G-protein-coupled receptor stimulation of the p42/p44 mitogen-activated protein kinase pathway is attenuated by lipid phosphate phosphatases 1, 1a, and 2 in human embryonic kidney 293 cells. *J Biol Chem* **276**, 13452-13460
187. Long, J., Darroch, P., Wan, K. F., Kong, K. C., Ktistakis, N., Pyne, N. J., and Pyne, S. (2005) Regulation of cell survival by lipid phosphate phosphatases involves the modulation of intracellular phosphatidic acid and sphingosine 1-phosphate pools. *Biochem J* **391**, 25-32
188. Zhao, Y., Kalari, S. K., Usatyuk, P. V., Gorshkova, I., He, D., Watkins, T., Brindley, D. N., Sun, C., Bittman, R., Garcia, J. G., Berdyshev, E. V., and Natarajan, V. (2007) Intracellular generation of sphingosine 1-phosphate in human lung endothelial cells: role of lipid phosphate phosphatase-1 and sphingosine kinase 1. *J Biol Chem* **282**, 14165-14177
189. Kok, B. P., Venkatraman, G., Capatos, D., and Brindley, D. N. (2012) Unlike two peas in a pod: lipid phosphate phosphatases and phosphatidate phosphatases. *Chem Rev* **112**, 5121-5146
190. Taghavi, P., Verhoeven, E., Jacobs, J. J., Lambooj, J. P., Stortelers, C., Tanger, E., Moolenaar, W. H., and van Lohuizen, M. (2008) In vitro genetic screen identifies a cooperative role for LPA signaling and c-Myc in cell transformation. *Oncogene* **27**, 6806-6816
191. Murph, M. M., Hurst-Kennedy, J., Newton, V., Brindley, D. N., and Radhakrishna, H. (2007) Lysophosphatidic acid decreases the nuclear localization and cellular abundance of the p53 tumor suppressor in A549 lung carcinoma cells. *Mol Cancer Res* **5**, 1201-1211
192. Kortlever, R. M., Brummelkamp, T. R., van Meeteren, L. A., Moolenaar, W. H., and Bernards, R. (2008) Suppression of the p53-dependent replicative senescence response by lysophosphatidic acid signaling. *Mol Cancer Res* **6**, 1452-1460
193. Liu, S., Umezu-Goto, M., Murph, M., Lu, Y., Liu, W., Zhang, F., Yu, S., Stephens, L. C., Cui, X., Murrow, G., Coombes, K., Muller, W., Hung, M. C., Perou, C. M., Lee, A. V., Fang, X., and Mills, G. B. (2009) Expression of autotaxin and lysophosphatidic acid receptors

increases mammary tumorigenesis, invasion, and metastases. *Cancer Cell* **15**, 539-550

194. Boucharaba, A., Serre, C. M., Guglielmi, J., Bordet, J. C., Clezardin, P., and Peyruchaud, O. (2006) The type 1 lysophosphatidic acid receptor is a target for therapy in bone metastases. *Proc Natl Acad Sci U S A* **103**, 9643-9648
195. Euer, N., Schwirzke, M., Evtimova, V., Burtscher, H., Jarsch, M., Tarin, D., and Weidle, U. H. (2002) Identification of genes associated with metastasis of mammary carcinoma in metastatic versus non-metastatic cell lines. *Anticancer Res* **22**, 733-740
196. Fishman, D. A., Liu, Y., Ellerbroek, S. M., and Stack, M. S. (2001) Lysophosphatidic acid promotes matrix metalloproteinase (MMP) activation and MMP-dependent invasion in ovarian cancer cells. *Cancer Res* **61**, 3194-3199
197. Xu, X., and Prestwich, G. D. (2010) Inhibition of tumor growth and angiogenesis by a lysophosphatidic acid antagonist in an engineered three-dimensional lung cancer xenograft model. *Cancer* **116**, 1739-1750
198. Rivera-Lopez, C. M., Tucker, A. L., and Lynch, K. R. (2008) Lysophosphatidic acid (LPA) and angiogenesis. *Angiogenesis* **11**, 301-310
199. Chen, R. J., Chen, S. U., Chou, C. H., and Lin, M. C. (2012) Lysophosphatidic acid receptor 2/3-mediated IL-8-dependent angiogenesis in cervical cancer cells. *Int J Cancer* **131**, 789-802
200. Huang, M. C., Lee, H. Y., Yeh, C. C., Kong, Y., Zaloudek, C. J., and Goetzl, E. J. (2004) Induction of protein growth factor systems in the ovaries of transgenic mice overexpressing human type 2 lysophosphatidic acid G protein-coupled receptor (LPA2). *Oncogene* **23**, 122-129
201. Sedlakova, I., Vavrova, J., Tosner, J., and Hanousek, L. (2011) Lysophosphatidic acid (LPA)-a perspective marker in ovarian cancer. *Tumour Biol* **32**, 311-316
202. Xu, Y., Gaudette, D. C., Boynton, J. D., Frankel, A., Fang, X. J., Sharma, A., Hurteau, J., Casey, G., Goodbody, A., Mellors, A., and et al. (1995) Characterization of an ovarian cancer activating factor in ascites from ovarian cancer patients. *Clin Cancer Res* **1**, 1223-1232

203. Xu, Y., Fang, X. J., Casey, G., and Mills, G. B. (1995) Lysophospholipids activate ovarian and breast cancer cells. *Biochem J* **309** ( Pt 3), 933-940
204. Wang, P., Wu, X., Chen, W., Liu, J., and Wang, X. (2007) The lysophosphatidic acid (LPA) receptors their expression and significance in epithelial ovarian neoplasms. *Gynecol Oncol* **104**, 714-720
205. Nakamoto, T., Yasuda, K., Yasuhara, M., Yoshimura, T., Kinoshita, T., Nakajima, T., Okada, H., Ikuta, A., and Kanzaki, H. (2005) Expression of the endothelial cell differentiation gene 7 (EDG-7), a lysophosphatidic acid receptor, in ovarian tumor. *J Obstet Gynaecol Res* **31**, 344-351
206. Westermann, A. M., Havik, E., Postma, F. R., Beijnen, J. H., Dalesio, O., Moolenaar, W. H., and Rodenhuis, S. (1998) Malignant effusions contain lysophosphatidic acid (LPA)-like activity. *Ann Oncol* **9**, 437-442
207. Sutphen, R., Xu, Y., Wilbanks, G. D., Fiorica, J., Grendys, E. C., Jr., LaPolla, J. P., Arango, H., Hoffman, M. S., Martino, M., Wakeley, K., Griffin, D., Blanco, R. W., Cantor, A. B., Xiao, Y. J., and Krischer, J. P. (2004) Lysophospholipids are potential biomarkers of ovarian cancer. *Cancer Epidemiol Biomarkers Prev* **13**, 1185-1191
208. Nakamura, K., Igarashi, K., Ohkawa, R., Yokota, H., Masuda, A., Nakagawa, S., Yano, T., Ikeda, H., Aoki, J., and Yatomi, Y. (2012) Serum autotaxin is not a useful biomarker for ovarian cancer. *Lipids* **47**, 927-930
209. Chen, M., Towers, L. N., and O'Connor, K. L. (2007) LPA2 (EDG4) mediates Rho-dependent chemotaxis with lower efficacy than LPA1 (EDG2) in breast carcinoma cells. *Am J Physiol Cell Physiol* **292**, C1927-1933
210. Kitayama, J., Shida, D., Sako, A., Ishikawa, M., Hama, K., Aoki, J., Arai, H., and Nagawa, H. (2004) Over-expression of lysophosphatidic acid receptor-2 in human invasive ductal carcinoma. *Breast Cancer Res* **6**, R640-646
211. Samadi, N., Gaetano, C., Goping, I. S., and Brindley, D. N. (2009) Autotaxin protects MCF-7 breast cancer and MDA-MB-435 melanoma cells against Taxol-induced apoptosis. *Oncogene* **28**, 1028-1039

212. Gaetano, C. G., Samadi, N., Tomsig, J. L., Macdonald, T. L., Lynch, K. R., and Brindley, D. N. (2009) Inhibition of autotaxin production or activity blocks lysophosphatidylcholine-induced migration of human breast cancer and melanoma cells. *Mol Carcinog* **48**, 801-809
213. Popnikolov, N. K., Dalwadi, B. H., Thomas, J. D., Johannes, G. J., and Imagawa, W. T. (2012) Association of autotaxin and lysophosphatidic acid receptor 3 with aggressiveness of human breast carcinoma. *Tumour Biol* **33**, 2237-2243
214. Samadi, N., Bekele, R., Capatos, D., Venkatraman, G., Sariahmetoglu, M., and Brindley, D. N. (2011) Regulation of lysophosphatidate signaling by autotaxin and lipid phosphate phosphatases with respect to tumor progression, angiogenesis, metastasis and chemo-resistance. *Biochimie* **93**, 61-70
215. Guo, R., Kasbohm, E. A., Arora, P., Sample, C. J., Baban, B., Sud, N., Sivashanmugam, P., Moniri, N. H., and Daaka, Y. (2006) Expression and function of lysophosphatidic acid LPA1 receptor in prostate cancer cells. *Endocrinology* **147**, 4883-4892
216. Ward, Y., Lake, R., Yin, J. J., Heger, C. D., Raffeld, M., Goldsmith, P. K., Merino, M., and Kelly, K. (2011) LPA receptor heterodimerizes with CD97 to amplify LPA-initiated RHO-dependent signaling and invasion in prostate cancer cells. *Cancer Res* **71**, 7301-7311
217. Hwang, Y. S., Hodge, J. C., Sivapurapu, N., and Lindholm, P. F. (2006) Lysophosphatidic acid stimulates PC-3 prostate cancer cell Matrigel invasion through activation of RhoA and NF-kappaB activity. *Mol Carcinog* **45**, 518-529
218. Kishi, Y., Okudaira, S., Tanaka, M., Hama, K., Shida, D., Kitayama, J., Yamori, T., Aoki, J., Fujimaki, T., and Arai, H. (2006) Autotaxin is overexpressed in glioblastoma multiforme and contributes to cell motility of glioblastoma by converting lysophosphatidylcholine to lysophosphatidic acid. *J Biol Chem* **281**, 17492-17500
219. Chen, S. U., Lee, H., Chang, D. Y., Chou, C. H., Chang, C. Y., Chao, K. H., Lin, C. W., and Yang, Y. S. (2008) Lysophosphatidic acid mediates interleukin-8 expression in human endometrial stromal cells through its receptor and nuclear factor-kappaB-dependent pathway: a possible role in angiogenesis of endometrium and placenta. *Endocrinology* **149**, 5888-5896



220. Hope, J. M., Wang, F. Q., Whyte, J. S., Ariztia, E. V., Abdalla, W., Long, K., and Fishman, D. A. (2009) LPA receptor 2 mediates LPA-induced endometrial cancer invasion. *Gynecol Oncol* **112**, 215-223
221. Wang, F. Q., Ariztia, E. V., Boyd, L. R., Horton, F. R., Smicun, Y., Hetherington, J. A., Smith, P. J., and Fishman, D. A. (2010) Lysophosphatidic acid (LPA) effects on endometrial carcinoma in vitro proliferation, invasion, and matrix metalloproteinase activity. *Gynecol Oncol* **117**, 88-95
222. Nam, S. W., Clair, T., Campo, C. K., Lee, H. Y., Liotta, L. A., and Stracke, M. L. (2000) Autotaxin (ATX), a potent tumor motogen, augments invasive and metastatic potential of ras-transformed cells. *Oncogene* **19**, 241-247
223. Lin, S., Wang, D., Iyer, S., Ghaleb, A. M., Shim, H., Yang, V. W., Chun, J., and Yun, C. C. (2009) The absence of LPA2 attenuates tumor formation in an experimental model of colitis-associated cancer. *Gastroenterology* **136**, 1711-1720
224. Lin, S., Lee, S. J., Shim, H., Chun, J., and Yun, C. C. (2010) The absence of LPA receptor 2 reduces the tumorigenesis by ApcMin mutation in the intestine. *Am J Physiol Gastrointest Liver Physiol* **299**, G1128-1138
225. Peyruchaud, O., Winding, B., Pecheur, I., Serre, C. M., Delmas, P., and Clezardin, P. (2001) Early detection of bone metastases in a murine model using fluorescent human breast cancer cells: application to the use of the bisphosphonate zoledronic acid in the treatment of osteolytic lesions. *J Bone Miner Res* **16**, 2027-2034
226. Boucharaba, A., Serre, C. M., Gres, S., Saulnier-Blache, J. S., Bordet, J. C., Guglielmi, J., Clezardin, P., and Peyruchaud, O. (2004) Platelet-derived lysophosphatidic acid supports the progression of osteolytic bone metastases in breast cancer. *J Clin Invest* **114**, 1714-1725
227. David, M., Wannecq, E., Descotes, F., Jansen, S., Deux, B., Ribeiro, J., Serre, C. M., Gres, S., Bendriss-Vermare, N., Bollen, M., Saez, S., Aoki, J., Saulnier-Blache, J. S., Clezardin, P., and Peyruchaud, O. (2010) Cancer cell expression of autotaxin controls bone metastasis formation in mouse through lysophosphatidic acid-dependent activation of osteoclasts. *PLoS One* **5**, e9741
228. Leblanc, R., Lee, S. C., David, M., Bordet, J. C., Norman, D. D., Patil, R., Miller, D., Sahay, D., Ribeiro, J., Clezardin, P., Tigyi, G. J., and

- Peyruchaud, O. (2014) Interaction of platelet-derived autotaxin with tumor integrin  $\alpha V\beta 3$  controls metastasis of breast cancer cells to bone. *Blood* **124**, 3141-3150
229. Marshall, J. C., Collins, J. W., Nakayama, J., Horak, C. E., Liewehr, D. J., Steinberg, S. M., Albaugh, M., Vidal-Vanaclocha, F., Palmieri, D., Barbier, M., Murone, M., and Steeg, P. S. (2012) Effect of inhibition of the lysophosphatidic acid receptor 1 on metastasis and metastatic dormancy in breast cancer. *J Natl Cancer Inst* **104**, 1306-1319
230. Lee, S. C., Fujiwara, Y., Liu, J., Yue, J., Shimizu, Y., Norman, D. D., Wang, Y., Tsukahara, R., Szabo, E., Patil, R., Banerjee, S., Miller, D. D., Balazs, L., Ghosh, M. C., Waters, C. M., Oravec, T., and Tigyi, G. J. (2015) Autotaxin and LPA1 and LPA5 Receptors Exert Disparate Functions in Tumor Cells versus the Host Tissue Microenvironment in Melanoma Invasion and Metastasis. *Mol Cancer Res* **13**, 174-185
231. Eder, A. M., Sasagawa, T., Mao, M., Aoki, J., and Mills, G. B. (2000) Constitutive and lysophosphatidic acid (LPA)-induced LPA production: role of phospholipase D and phospholipase A2. *Clin Cancer Res* **6**, 2482-2491
232. Frankel, A., and Mills, G. B. (1996) Peptide and lipid growth factors decrease cis-diamminedichloroplatinum-induced cell death in human ovarian cancer cells. *Clin Cancer Res* **2**, 1307-1313
233. Furui, T., LaPushin, R., Mao, M., Khan, H., Watt, S. R., Watt, M. A., Lu, Y., Fang, X., Tsutsui, S., Siddik, Z. H., Bast, R. C., and Mills, G. B. (1999) Overexpression of *edg-2/vzg-1* induces apoptosis and anoikis in ovarian cancer cells in a lysophosphatidic acid-independent manner. *Clin Cancer Res* **5**, 4308-4318
234. Sun, H., Ren, J., Zhu, Q., Kong, F. Z., Wu, L., and Pan, B. R. (2009) Effects of lysophosphatidic acid on human colon cancer cells and its mechanisms of action. *World J Gastroenterol* **15**, 4547-4555
235. Jazaeri, A. A., Awtrey, C. S., Chandramouli, G. V., Chuang, Y. E., Khan, J., Sotiriou, C., Aprelikova, O., Yee, C. J., Zorn, K. K., Birrer, M. J., Barrett, J. C., and Boyd, J. (2005) Gene expression profiles associated with response to chemotherapy in epithelial ovarian cancers. *Clin Cancer Res* **11**, 6300-6310
236. Vidot, S., Witham, J., Agarwal, R., Greenhough, S., Bamrah, H. S., Tigyi, G. J., Kaye, S. B., and Richardson, A. (2010) Autotaxin delays

apoptosis induced by carboplatin in ovarian cancer cells. *Cell Signal* **22**, 926-935

237. Samadi, N., Bekele, R. T., Goping, I. S., Schang, L. M., and Brindley, D. N. (2011) Lysophosphatidate induces chemo-resistance by releasing breast cancer cells from taxol-induced mitotic arrest. *PLoS One* **6**, e20608
238. Lin, F. T., Lai, Y. J., Makarova, N., Tigyi, G., and Lin, W. C. (2007) The lysophosphatidic acid 2 receptor mediates down-regulation of Siva-1 to promote cell survival. *J Biol Chem* **282**, 37759-37769
239. Xue, L., Chu, F., Cheng, Y., Sun, X., Borthakur, A., Ramarao, M., Pandey, P., Wu, M., Schlossman, S. F., and Prasad, K. V. (2002) Siva-1 binds to and inhibits BCL-X(L)-mediated protection against UV radiation-induced apoptosis. *Proc Natl Acad Sci U S A* **99**, 6925-6930
240. E, S., Lai, Y. J., Tsukahara, R., Chen, C. S., Fujiwara, Y., Yue, J., Yu, J. H., Guo, H., Kihara, A., Tigyi, G., and Lin, F. T. (2009) Lysophosphatidic acid 2 receptor-mediated supramolecular complex formation regulates its antiapoptotic effect. *J Biol Chem* **284**, 14558-14571
241. Kiss, G. N., Lee, S. C., Fells, J. I., Liu, J., Valentine, W. J., Fujiwara, Y., Thompson, K. E., Yates, C. R., Sumegi, B., and Tigyi, G. (2013) Mitigation of radiation injury by selective stimulation of the LPA(2) receptor. *Biochimica et biophysica acta* **1831**, 117-125
242. Fukui, R., Kato, K., Okabe, K., Kitayoshi, M., Tanabe, E., Fukushima, N., and Tsujiuchi, T. (2012) Enhancement of Drug Resistance by Lysophosphatidic Acid Receptor-3 in Mouse Mammary Tumor FM3A Cells. *J Toxicol Pathol* **25**, 225-228
243. Okabe, K., Hayashi, M., Yamawaki, Y., Teranishi, M., Honoki, K., Mori, T., Fukushima, N., and Tsujiuchi, T. (2011) Possible involvement of lysophosphatidic acid receptor-5 gene in the acquisition of growth advantage of rat tumor cells. *Mol Carcinog* **50**, 635-642
244. Su, S. C., Hu, X., Kenney, P. A., Merrill, M. M., Babaian, K. N., Zhang, X. Y., Maity, T., Yang, S. F., Lin, X., and Wood, C. G. (2013) Autotaxin-lysophosphatidic acid signaling axis mediates tumorigenesis and development of acquired resistance to sunitinib in renal cell carcinoma. *Clin Cancer Res* **19**, 6461-6472

245. Okabe, K., Hayashi, M., Kato, K., Okumura, M., Fukui, R., Honoki, K., Fukushima, N., and Tsujiuchi, T. (2013) Lysophosphatidic acid receptor-3 increases tumorigenicity and aggressiveness of rat hepatoma RH7777 cells. *Mol Carcinog* **52**, 247-254
246. Barbayianni, E., Magrioti, V., Moutevelis-Minakakis, P., and Kokotos, G. (2013) Autotaxin inhibitors: a patent review. *Expert Opin Ther Pat* **23**, 1123-1132
247. David, M., Ribeiro, J., Descotes, F., Serre, C. M., Barbier, M., Murone, M., Clezardin, P., and Peyruchaud, O. (2012) Targeting lysophosphatidic acid receptor type 1 with Debio 0719 inhibits spontaneous metastasis dissemination of breast cancer cells independently of cell proliferation and angiogenesis. *Int J Oncol* **40**, 1133-1141
248. Stoddard, N. C., and Chun, J. (2015) Promising pharmacological directions in the world of lysophosphatidic Acid signaling. *Biomol Ther (Seoul)* **23**, 1-11
249. Visentin, B., Vekich, J. A., Sibbald, B. J., Cavalli, A. L., Moreno, K. M., Matteo, R. G., Garland, W. A., Lu, Y., Yu, S., Hall, H. S., Kundra, V., Mills, G. B., and Sabbadini, R. A. (2006) Validation of an anti-sphingosine-1-phosphate antibody as a potential therapeutic in reducing growth, invasion, and angiogenesis in multiple tumor lineages. *Cancer Cell* **9**, 225-238
250. O'Brien, N., Jones, S. T., Williams, D. G., Cunningham, H. B., Moreno, K., Visentin, B., Gentile, A., Vekich, J., Shestowsky, W., Hiraiwa, M., Matteo, R., Cavalli, A., Grotjahn, D., Grant, M., Hansen, G., Campbell, M. A., and Sabbadini, R. (2009) Production and characterization of monoclonal anti-sphingosine-1-phosphate antibodies. *J Lipid Res* **50**, 2245-2257
251. Crack, P. J., Zhang, M., Morganti-Kossmann, M. C., Morris, A. J., Wojciak, J. M., Fleming, J. K., Karve, I., Wright, D., Sashindranath, M., Goldshmit, Y., Conquest, A., Daglas, M., Johnston, L. A., Medcalf, R. L., Sabbadini, R. A., and Pebay, A. (2014) Anti-lysophosphatidic acid antibodies improve traumatic brain injury outcomes. *J Neuroinflammation* **11**, 37
252. Ponnusamy, S., Selvam, S. P., Mehrotra, S., Kawamori, T., Snider, A. J., Obeid, L. M., Shao, Y., Sabbadini, R., and Ogretmen, B. (2012) Communication between host organism and cancer cells is transduced by systemic sphingosine kinase 1/sphingosine 1-

phosphate signalling to regulate tumour metastasis. *EMBO Mol Med* **4**, 761-775

253. <http://ClinicalTrials.gov/show/NCT02341508> A Phase 1a, Double-Blind, Placebo-Controlled, Single Ascending Dose Study to Evaluate the Safety, Tolerability, Pharmacokinetics, and Pharmacodynamics of Lpathomab in Subjects With Neuropathic Pain.
254. Goldshmit, Y., Matteo, R., Sztal, T., Ellett, F., Frisca, F., Moreno, K., Crombie, D., Lieschke, G. J., Currie, P. D., Sabbadini, R. A., and Pebay, A. (2012) Blockage of lysophosphatidic acid signaling improves spinal cord injury outcomes. *Am J Pathol* **181**, 978-992
255. Zhang, H., Xu, X., Gajewiak, J., Tsukahara, R., Fujiwara, Y., Liu, J., Fells, J. I., Perygin, D., Parrill, A. L., Tigyi, G., and Prestwich, G. D. (2009) Dual activity lysophosphatidic acid receptor pan-antagonist/autotaxin inhibitor reduces breast cancer cell migration in vitro and causes tumor regression in vivo. *Cancer Res* **69**, 5441-5449
256. Xu, X., Yang, G., Zhang, H., and Prestwich, G. D. (2009) Evaluating dual activity LPA receptor pan-antagonist/autotaxin inhibitors as anti-cancer agents in vivo using engineered human tumors. *Prostaglandins Other Lipid Mediat* **89**, 140-146
257. Schleicher, S. M., Thotala, D. K., Linkous, A. G., Hu, R., Leahy, K. M., Yazlovitskaya, E. M., and Hallahan, D. E. (2011) Autotaxin and LPA receptors represent potential molecular targets for the radiosensitization of murine glioma through effects on tumor vasculature. *PLoS One* **6**, e22182
258. Mazzocca, A., Dituri, F., Lupo, L., Quaranta, M., Antonaci, S., and Giannelli, G. (2011) Tumor-secreted lysophosphatidic acid accelerates hepatocellular carcinoma progression by promoting differentiation of peritumoral fibroblasts in myofibroblasts. *Hepatology* **54**, 920-930
259. Baker, D. L., Fujiwara, Y., Pigg, K. R., Tsukahara, R., Kobayashi, S., Murofushi, H., Uchiyama, A., Murakami-Murofushi, K., Koh, E., Bandle, R. W., Byun, H. S., Bittman, R., Fan, D., Murph, M., Mills, G. B., and Tigyi, G. (2006) Carba analogs of cyclic phosphatidic acid are selective inhibitors of autotaxin and cancer cell invasion and metastasis. *J Biol Chem* **281**, 22786-22793
260. Bhave, S. R., Dadey, D. Y., Karvas, R. M., Ferraro, D. J., Kotipatruni, R. P., Jaboin, J. J., Hallahan, A. N., Dewees, T. A., Linkous, A. G., Hallahan, D. E., and Thotala, D. (2013) Autotaxin Inhibition with PF-

8380 Enhances the Radiosensitivity of Human and Murine Glioblastoma Cell Lines. *Frontiers in oncology* **3**, 236

261. (2012) TETRAHYDROCARBOLINE DERIVATIVE. In WO/2012/005227, ONO PHARMACEUTICAL CO., LTD., JAPAN
262. Saga, H., Ohhata, A., Hayashi, A., Katoh, M., Maeda, T., Mizuno, H., Takada, Y., Komichi, Y., Ota, H., Matsumura, N., Shibaya, M., Sugiyama, T., Nakade, S., and Kishikawa, K. (2014) A novel highly potent autotaxin/ENPP2 inhibitor produces prolonged decreases in plasma lysophosphatidic acid formation in vivo and regulates urethral tension. *PLoS One* **9**, e93230
263. Clair, T., Aoki, J., Koh, E., Bandle, R. W., Nam, S. W., Ptaszynska, M. M., Mills, G. B., Schiffmann, E., Liotta, L. A., and Stracke, M. L. (2003) Autotaxin hydrolyzes sphingosylphosphorylcholine to produce the regulator of migration, sphingosine-1-phosphate. *Cancer Res* **63**, 5446-5453
264. Mizugishi, K., Yamashita, T., Olivera, A., Miller, G. F., Spiegel, S., and Proia, R. L. (2005) Essential role for sphingosine kinases in neural and vascular development. *Mol Cell Biol* **25**, 11113-11121
265. Brown, D. A., and London, E. (1998) Functions of lipid rafts in biological membranes. *Annu Rev Cell Dev Biol* **14**, 111-136
266. Wattenberg, B. W., Pitson, S. M., and Raben, D. M. (2006) The sphingosine and diacylglycerol kinase superfamily of signaling kinases: localization as a key to signaling function. *J Lipid Res* **47**, 1128-1139
267. Pyne, N. J., and Pyne, S. (2010) Sphingosine 1-phosphate and cancer. *Nat Rev Cancer* **10**, 489-503
268. Merrill, A. H., Jr. (2002) De novo sphingolipid biosynthesis: a necessary, but dangerous, pathway. *J Biol Chem* **277**, 25843-25846
269. Hannun, Y. A., and Obeid, L. M. (2002) The Ceramide-centric universe of lipid-mediated cell regulation: stress encounters of the lipid kind. *J Biol Chem* **277**, 25847-25850
270. Perry, D. K., and Hannun, Y. A. (1998) The role of ceramide in cell signaling. *Biochimica et biophysica acta* **1436**, 233-243

271. van Meer, G., and Lisman, Q. (2002) Sphingolipid transport: rafts and translocators. *J Biol Chem* **277**, 25855-25858
272. Kitatani, K., Idkowiak-Baldys, J., and Hannun, Y. A. (2008) The sphingolipid salvage pathway in ceramide metabolism and signaling. *Cell Signal* **20**, 1010-1018
273. Schulze, H., and Sandhoff, K. (2011) Lysosomal lipid storage diseases. *Cold Spring Harb Perspect Biol* **3**
274. Hannun, Y. A., and Obeid, L. M. (2011) Many ceramides. *J Biol Chem* **286**, 27855-27862
275. Bornancin, F. (2011) Ceramide kinase: the first decade. *Cell Signal* **23**, 999-1008
276. Mandala, S. M. (2001) Sphingosine-1-phosphate phosphatases. *Prostaglandins Other Lipid Mediat* **64**, 143-156
277. Pyne, S., Lee, S. C., Long, J., and Pyne, N. J. (2009) Role of sphingosine kinases and lipid phosphate phosphatases in regulating spatial sphingosine 1-phosphate signalling in health and disease. *Cell Signal* **21**, 14-21
278. Olivera, A., Kohama, T., Tu, Z., Milstien, S., and Spiegel, S. (1998) Purification and characterization of rat kidney sphingosine kinase. *J Biol Chem* **273**, 12576-12583
279. Kohama, T., Olivera, A., Edsall, L., Nagiec, M. M., Dickson, R., and Spiegel, S. (1998) Molecular cloning and functional characterization of murine sphingosine kinase. *J Biol Chem* **273**, 23722-23728
280. Pitson, S. M., D'Andrea R, J., Vandeleur, L., Moretti, P. A., Xia, P., Gamble, J. R., Vadas, M. A., and Wattenberg, B. W. (2000) Human sphingosine kinase: purification, molecular cloning and characterization of the native and recombinant enzymes. *Biochem J* **350 Pt 2**, 429-441
281. Liu, H., Sugiura, M., Nava, V. E., Edsall, L. C., Kono, K., Poulton, S., Milstien, S., Kohama, T., and Spiegel, S. (2000) Molecular cloning and functional characterization of a novel mammalian sphingosine kinase type 2 isoform. *J Biol Chem* **275**, 19513-19520
282. Labesse, G., Douguet, D., Assairi, L., and Gilles, A. M. (2002) Diacylglyceride kinases, sphingosine kinases and NAD kinases:

- distant relatives of 6-phosphofructokinases. *Trends Biochem Sci* **27**, 273-275
283. Wang, Z., Min, X., Xiao, S. H., Johnstone, S., Romanow, W., Meininger, D., Xu, H., Liu, J., Dai, J., An, S., Thibault, S., and Walker, N. (2013) Molecular basis of sphingosine kinase 1 substrate recognition and catalysis. *Structure* **21**, 798-809
  284. Pitson, S. M., Moretti, P. A., Zebol, J. R., Zareie, R., Derian, C. K., Darrow, A. L., Qi, J., D'Andrea, R. J., Bagley, C. J., Vadas, M. A., and Wattenberg, B. W. (2002) The nucleotide-binding site of human sphingosine kinase 1. *J Biol Chem* **277**, 49545-49553
  285. Shen, H., Giordano, F., Wu, Y., Chan, J., Zhu, C., Milosevic, I., Wu, X., Yao, K., Chen, B., Baumgart, T., Sieburth, D., and De Camilli, P. (2014) Coupling between endocytosis and sphingosine kinase 1 recruitment. *Nat Cell Biol* **16**, 652-662
  286. Olivera, A., and Spiegel, S. (1993) Sphingosine-1-phosphate as second messenger in cell proliferation induced by PDGF and FCS mitogens. *Nature* **365**, 557-560
  287. Hobson, J. P., Rosenfeldt, H. M., Barak, L. S., Olivera, A., Poulton, S., Caron, M. G., Milstien, S., and Spiegel, S. (2001) Role of the sphingosine-1-phosphate receptor EDG-1 in PDGF-induced cell motility. *Science* **291**, 1800-1803
  288. Yamanaka, M., Shegogue, D., Pei, H., Bu, S., Bielawska, A., Bielawski, J., Pettus, B., Hannun, Y. A., Obeid, L., and Trojanowska, M. (2004) Sphingosine kinase 1 (SPHK1) is induced by transforming growth factor-beta and mediates TIMP-1 up-regulation. *J Biol Chem* **279**, 53994-54001
  289. Edsall, L. C., Cuvillier, O., Twitty, S., Spiegel, S., and Milstien, S. (2001) Sphingosine kinase expression regulates apoptosis and caspase activation in PC12 cells. *J Neurochem* **76**, 1573-1584
  290. Doll, F., Pfeilschifter, J., and Huwiler, A. (2005) The epidermal growth factor stimulates sphingosine kinase-1 expression and activity in the human mammary carcinoma cell line MCF7. *Biochimica et biophysica acta* **1738**, 72-81
  291. Shu, X., Wu, W., Mosteller, R. D., and Broek, D. (2002) Sphingosine kinase mediates vascular endothelial growth factor-induced activation



- of ras and mitogen-activated protein kinases. *Mol Cell Biol* **22**, 7758-7768
292. Sukocheva, O. A., Wang, L., Albanese, N., Pitson, S. M., Vadas, M. A., and Xia, P. (2003) Sphingosine kinase transmits estrogen signaling in human breast cancer cells. *Mol Endocrinol* **17**, 2002-2012
293. Xia, P., Gamble, J. R., Rye, K. A., Wang, L., Hii, C. S., Cockerill, P., Khew-Goodall, Y., Bert, A. G., Barter, P. J., and Vadas, M. A. (1998) Tumor necrosis factor-alpha induces adhesion molecule expression through the sphingosine kinase pathway. *Proc Natl Acad Sci U S A* **95**, 14196-14201
294. Feistritzer, C., and Riewald, M. (2005) Endothelial barrier protection by activated protein C through PAR1-dependent sphingosine 1-phosphate receptor-1 crossactivation. *Blood* **105**, 3178-3184
295. van Koppen, C. J., Meyer zu Heringdorf, D., Alemany, R., and Jakobs, K. H. (2001) Sphingosine kinase-mediated calcium signaling by muscarinic acetylcholine receptors. *Life Sci* **68**, 2535-2540
296. Young, K. W., Willets, J. M., Parkinson, M. J., Bartlett, P., Spiegel, S., Nahorski, S. R., and Challiss, R. A. (2003) Ca<sup>2+</sup>/calmodulin-dependent translocation of sphingosine kinase: role in plasma membrane relocation but not activation. *Cell Calcium* **33**, 119-128
297. Meyer zu Heringdorf, D., Lass, H., Kuchar, I., Lipinski, M., Alemany, R., Rumenapp, U., and Jakobs, K. H. (2001) Stimulation of intracellular sphingosine-1-phosphate production by G-protein-coupled sphingosine-1-phosphate receptors. *Eur J Pharmacol* **414**, 145-154
298. Johnson, K. R., Becker, K. P., Facchinetti, M. M., Hannun, Y. A., and Obeid, L. M. (2002) PKC-dependent activation of sphingosine kinase 1 and translocation to the plasma membrane. Extracellular release of sphingosine-1-phosphate induced by phorbol 12-myristate 13-acetate (PMA). *J Biol Chem* **277**, 35257-35262
299. Auge, N., Nikolova-Karakashian, M., Carpentier, S., Parthasarathy, S., Negre-Salvayre, A., Salvayre, R., Merrill, A. H., Jr., and Levade, T. (1999) Role of sphingosine 1-phosphate in the mitogenesis induced by oxidized low density lipoprotein in smooth muscle cells via activation of sphingomyelinase, ceramidase, and sphingosine kinase. *J Biol Chem* **274**, 21533-21538

300. Kleuser, B., Cuvillier, O., and Spiegel, S. (1998) 1 $\alpha$ ,25-dihydroxyvitamin D3 inhibits programmed cell death in HL-60 cells by activation of sphingosine kinase. *Cancer Res* **58**, 1817-1824
301. Buehrer, B. M., Bardes, E. S., and Bell, R. M. (1996) Protein kinase C-dependent regulation of human erythroleukemia (HEL) cell sphingosine kinase activity. *Biochimica et biophysica acta* **1303**, 233-242
302. Doll, F., Pfeilschifter, J., and Huwiler, A. (2007) Prolactin upregulates sphingosine kinase-1 expression and activity in the human breast cancer cell line MCF7 and triggers enhanced proliferation and migration. *Endocr Relat Cancer* **14**, 325-335
303. Sobue, S., Hagiwara, K., Banno, Y., Tamiya-Koizumi, K., Suzuki, M., Takagi, A., Kojima, T., Asano, H., Nozawa, Y., and Murate, T. (2005) Transcription factor specificity protein 1 (Sp1) is the main regulator of nerve growth factor-induced sphingosine kinase 1 gene expression of the rat pheochromocytoma cell line, PC12. *J Neurochem* **95**, 940-949
304. Paugh, B. S., Bryan, L., Paugh, S. W., Wilczynska, K. M., Alvarez, S. M., Singh, S. K., Kapitonov, D., Rokita, H., Wright, S., Griswold-Prenner, I., Milstien, S., Spiegel, S., and Kordula, T. (2009) Interleukin-1 regulates the expression of sphingosine kinase 1 in glioblastoma cells. *J Biol Chem* **284**, 3408-3417
305. Sobue, S., Murakami, M., Banno, Y., Ito, H., Kimura, A., Gao, S., Furuhata, A., Takagi, A., Kojima, T., Suzuki, M., Nozawa, Y., and Murate, T. (2008) v-Src oncogene product increases sphingosine kinase 1 expression through mRNA stabilization: alteration of AU-rich element-binding proteins. *Oncogene* **27**, 6023-6033
306. Pitson, S. M., Moretti, P. A., Zebol, J. R., Lynn, H. E., Xia, P., Vadas, M. A., and Wattenberg, B. W. (2003) Activation of sphingosine kinase 1 by ERK1/2-mediated phosphorylation. *EMBO J* **22**, 5491-5500
307. Olivera, A., Edsall, L., Poulton, S., Kazlauskas, A., and Spiegel, S. (1999) Platelet-derived growth factor-induced activation of sphingosine kinase requires phosphorylation of the PDGF receptor tyrosine residue responsible for binding of PLCgamma. *FASEB J* **13**, 1593-1600
308. Jarman, K. E., Moretti, P. A., Zebol, J. R., and Pitson, S. M. (2010) Translocation of sphingosine kinase 1 to the plasma membrane is

- mediated by calcium- and integrin-binding protein 1. *J Biol Chem* **285**, 483-492
309. Hayashi, S., Okada, T., Igarashi, N., Fujita, T., Jahangeer, S., and Nakamura, S. (2002) Identification and characterization of RPK118, a novel sphingosine kinase-1-binding protein. *J Biol Chem* **277**, 33319-33324
  310. Ancellin, N., Colmont, C., Su, J., Li, Q., Mittereder, N., Chae, S. S., Stefansson, S., Liao, G., and Hla, T. (2002) Extracellular export of sphingosine kinase-1 enzyme. Sphingosine 1-phosphate generation and the induction of angiogenic vascular maturation. *J Biol Chem* **277**, 6667-6675
  311. Venkataraman, K., Thangada, S., Michaud, J., Oo, M. L., Ai, Y., Lee, Y. M., Wu, M., Parikh, N. S., Khan, F., Proia, R. L., and Hla, T. (2006) Extracellular export of sphingosine kinase-1a contributes to the vascular S1P gradient. *Biochem J* **397**, 461-471
  312. Pitson, S. M., Xia, P., Leclercq, T. M., Moretti, P. A., Zebol, J. R., Lynn, H. E., Wattenberg, B. W., and Vadas, M. A. (2005) Phosphorylation-dependent translocation of sphingosine kinase to the plasma membrane drives its oncogenic signalling. *J Exp Med* **201**, 49-54
  313. Barr, R. K., Lynn, H. E., Moretti, P. A., Khew-Goodall, Y., and Pitson, S. M. (2008) Deactivation of sphingosine kinase 1 by protein phosphatase 2A. *J Biol Chem* **283**, 34994-35002
  314. Xia, P., Wang, L., Moretti, P. A., Albanese, N., Chai, F., Pitson, S. M., D'Andrea, R. J., Gamble, J. R., and Vadas, M. A. (2002) Sphingosine kinase interacts with TRAF2 and dissects tumor necrosis factor- $\alpha$  signaling. *J Biol Chem* **277**, 7996-8003
  315. Olivera, A., Rosenthal, J., and Spiegel, S. (1996) Effect of acidic phospholipids on sphingosine kinase. *J Cell Biochem* **60**, 529-537
  316. Melendez, A., Floto, R. A., Gillooly, D. J., Harnett, M. M., and Allen, J. M. (1998) Fc $\gamma$ RI coupling to phospholipase D initiates sphingosine kinase-mediated calcium mobilization and vesicular trafficking. *J Biol Chem* **273**, 9393-9402
  317. Delon, C., Manifava, M., Wood, E., Thompson, D., Krugmann, S., Pyne, S., and Ktistakis, N. T. (2004) Sphingosine kinase 1 is an

- intracellular effector of phosphatidic acid. *J Biol Chem* **279**, 44763-44774
318. Stahelin, R. V., Hwang, J. H., Kim, J. H., Park, Z. Y., Johnson, K. R., Obeid, L. M., and Cho, W. (2005) The mechanism of membrane targeting of human sphingosine kinase 1. *J Biol Chem* **280**, 43030-43038
  319. Guo, L., Mishra, G., Taylor, K., and Wang, X. (2011) Phosphatidic acid binds and stimulates Arabidopsis sphingosine kinases. *J Biol Chem* **286**, 13336-13345
  320. Cazzolli, R., Shemon, A. N., Fang, M. Q., and Hughes, W. E. (2006) Phospholipid signalling through phospholipase D and phosphatidic acid. *IUBMB Life* **58**, 457-461
  321. Jang, J. H., Lee, C. S., Hwang, D., and Ryu, S. H. (2012) Understanding of the roles of phospholipase D and phosphatidic acid through their binding partners. *Prog Lipid Res* **51**, 71-81
  322. Hla, T., and Maciag, T. (1990) An abundant transcript induced in differentiating human endothelial cells encodes a polypeptide with structural similarities to G-protein-coupled receptors. *J Biol Chem* **265**, 9308-9313
  323. Liu, Y., Wada, R., Yamashita, T., Mi, Y., Deng, C. X., Hobson, J. P., Rosenfeldt, H. M., Nava, V. E., Chae, S. S., Lee, M. J., Liu, C. H., Hla, T., Spiegel, S., and Proia, R. L. (2000) Edg-1, the G protein-coupled receptor for sphingosine-1-phosphate, is essential for vascular maturation. *J Clin Invest* **106**, 951-961
  324. Kono, M., Mi, Y., Liu, Y., Sasaki, T., Allende, M. L., Wu, Y. P., Yamashita, T., and Proia, R. L. (2004) The sphingosine-1-phosphate receptors S1P1, S1P2, and S1P3 function coordinately during embryonic angiogenesis. *J Biol Chem* **279**, 29367-29373
  325. Kimura, T., Watanabe, T., Sato, K., Kon, J., Tomura, H., Tamama, K., Kuwabara, A., Kanda, T., Kobayashi, I., Ohta, H., Ui, M., and Okajima, F. (2000) Sphingosine 1-phosphate stimulates proliferation and migration of human endothelial cells possibly through the lipid receptors, Edg-1 and Edg-3. *Biochem J* **348 Pt 1**, 71-76
  326. Takashiro, Y., Nakamura, H., Koide, Y., Nishida, A., and Murayama, T. (2005) Involvement of p38 MAP kinase-mediated cytochrome c

release on sphingosine-1-phosphate (S1P)- and N-monomethyl-S1P-induced cell death of PC12 cells. *Biochem Pharmacol* **70**, 258-265

327. Banno, Y., Takuwa, Y., Akao, Y., Okamoto, H., Osawa, Y., Naganawa, T., Nakashima, S., Suh, P. G., and Nozawa, Y. (2001) Involvement of phospholipase D in sphingosine 1-phosphate-induced activation of phosphatidylinositol 3-kinase and Akt in Chinese hamster ovary cells overexpressing EDG3. *J Biol Chem* **276**, 35622-35628
328. Hanada, K., Kumagai, K., Yasuda, S., Miura, Y., Kawano, M., Fukasawa, M., and Nishijima, M. (2003) Molecular machinery for non-vesicular trafficking of ceramide. *Nature* **426**, 803-809
329. Bourquin, F., Riezman, H., Capitani, G., and Grutter, M. G. (2010) Structure and function of sphingosine-1-phosphate lyase, a key enzyme of sphingolipid metabolism. *Structure* **18**, 1054-1065
330. Sigal, Y. J., McDermott, M. I., and Morris, A. J. (2005) Integral membrane lipid phosphatases/phosphotransferases: common structure and diverse functions. *Biochem J* **387**, 281-293
331. Sato, K., Malchinkhuu, E., Horiuchi, Y., Mogi, C., Tomura, H., Tosaka, M., Yoshimoto, Y., Kuwabara, A., and Okajima, F. (2007) Critical role of ABCA1 transporter in sphingosine 1-phosphate release from astrocytes. *J Neurochem* **103**, 2610-2619
332. Mitra, P., Oskeritzian, C. A., Payne, S. G., Beaven, M. A., Milstien, S., and Spiegel, S. (2006) Role of ABCC1 in export of sphingosine-1-phosphate from mast cells. *Proc Natl Acad Sci U S A* **103**, 16394-16399
333. Takabe, K., Kim, R. H., Allegood, J. C., Mitra, P., Ramachandran, S., Nagahashi, M., Harikumar, K. B., Hait, N. C., Milstien, S., and Spiegel, S. (2010) Estradiol induces export of sphingosine 1-phosphate from breast cancer cells via ABCC1 and ABCG2. *J Biol Chem* **285**, 10477-10486
334. Kawahara, A., Nishi, T., Hisano, Y., Fukui, H., Yamaguchi, A., and Mochizuki, N. (2009) The sphingolipid transporter spns2 functions in migration of zebrafish myocardial precursors. *Science* **323**, 524-527
335. Fukuhara, S., Simmons, S., Kawamura, S., Inoue, A., Orba, Y., Tokudome, T., Sunden, Y., Arai, Y., Moriwaki, K., Ishida, J., Uemura, A., Kiyonari, H., Abe, T., Fukamizu, A., Hirashima, M., Sawa, H., Aoki, J., Ishii, M., and Mochizuki, N. (2012) The sphingosine-1-phosphate

- transporter Spns2 expressed on endothelial cells regulates lymphocyte trafficking in mice. *J Clin Invest* **122**, 1416-1426
336. Mendoza, A., Breart, B., Ramos-Perez, W. D., Pitt, L. A., Gobert, M., Sunkara, M., Lafaille, J. J., Morris, A. J., and Schwab, S. R. (2012) The transporter Spns2 is required for secretion of lymph but not plasma sphingosine-1-phosphate. *Cell Rep* **2**, 1104-1110
337. Yatomi, Y., Ozaki, Y., Ohmori, T., and Igarashi, Y. (2001) Sphingosine 1-phosphate: synthesis and release. *Prostaglandins Other Lipid Mediat* **64**, 107-122
338. Brinkmann, V., Cyster, J. G., and Hla, T. (2004) FTY720: sphingosine 1-phosphate receptor-1 in the control of lymphocyte egress and endothelial barrier function. *Am J Transplant* **4**, 1019-1025
339. Pappu, R., Schwab, S. R., Cornelissen, I., Pereira, J. P., Regard, J. B., Xu, Y., Camerer, E., Zheng, Y. W., Huang, Y., Cyster, J. G., and Coughlin, S. R. (2007) Promotion of lymphocyte egress into blood and lymph by distinct sources of sphingosine-1-phosphate. *Science* **316**, 295-298
340. Venkataraman, K., Lee, Y. M., Michaud, J., Thangada, S., Ai, Y., Bonkovsky, H. L., Parikh, N. S., Habrukowich, C., and Hla, T. (2008) Vascular endothelium as a contributor of plasma sphingosine 1-phosphate. *Circ Res* **102**, 669-676
341. Okajima, F. (2002) Plasma lipoproteins behave as carriers of extracellular sphingosine 1-phosphate: is this an atherogenic mediator or an anti-atherogenic mediator? *Biochimica et biophysica acta* **1582**, 132-137
342. Yatomi, Y. (2008) Plasma sphingosine 1-phosphate metabolism and analysis. *Biochimica et biophysica acta* **1780**, 606-611
343. Hanel, P., Andreani, P., and Graler, M. H. (2007) Erythrocytes store and release sphingosine 1-phosphate in blood. *FASEB J* **21**, 1202-1209
344. Alvarez, S. E., Harikumar, K. B., Hait, N. C., Allegood, J., Strub, G. M., Kim, E. Y., Maceyka, M., Jiang, H., Luo, C., Kordula, T., Milstien, S., and Spiegel, S. (2010) Sphingosine-1-phosphate is a missing cofactor for the E3 ubiquitin ligase TRAF2. *Nature* **465**, 1084-1088

345. Hait, N. C., Allegood, J., Maceyka, M., Strub, G. M., Harikumar, K. B., Singh, S. K., Luo, C., Marmorstein, R., Kordula, T., Milstien, S., and Spiegel, S. (2009) Regulation of histone acetylation in the nucleus by sphingosine-1-phosphate. *Science* **325**, 1254-1257
346. Hait, N. C., Wise, L. E., Allegood, J. C., O'Brien, M., Avni, D., Reeves, T. M., Knapp, P. E., Lu, J., Luo, C., Miles, M. F., Milstien, S., Lichtman, A. H., and Spiegel, S. (2014) Active, phosphorylated fingolimod inhibits histone deacetylases and facilitates fear extinction memory. *Nat Neurosci* **17**, 971-980
347. Kunkel, G. T., Maceyka, M., Milstien, S., and Spiegel, S. (2013) Targeting the sphingosine-1-phosphate axis in cancer, inflammation and beyond. *Nat Rev Drug Discov* **12**, 688-702
348. Yeh, E. A., and Weinstock-Guttman, B. (2011) Fingolimod: an oral disease-modifying therapy for relapsing multiple sclerosis. *Adv Ther* **28**, 270-278
349. Zhi, L., Kim, P., Thompson, B. D., Pitsillides, C., Bankovich, A. J., Yun, S. H., Lin, C. P., Cyster, J. G., and Wu, M. X. (2011) FTY720 blocks egress of T cells in part by abrogation of their adhesion on the lymph node sinus. *J Immunol* **187**, 2244-2251
350. Matloubian, M., Lo, C. G., Cinamon, G., Lesneski, M. J., Xu, Y., Brinkmann, V., Allende, M. L., Proia, R. L., and Cyster, J. G. (2004) Lymphocyte egress from thymus and peripheral lymphoid organs is dependent on S1P receptor 1. *Nature* **427**, 355-360
351. Schwab, S. R., Pereira, J. P., Matloubian, M., Xu, Y., Huang, Y., and Cyster, J. G. (2005) Lymphocyte sequestration through S1P lyase inhibition and disruption of S1P gradients. *Science* **309**, 1735-1739
352. Pham, T. H., Baluk, P., Xu, Y., Grigorova, I., Bankovich, A. J., Pappu, R., Coughlin, S. R., McDonald, D. M., Schwab, S. R., and Cyster, J. G. (2010) Lymphatic endothelial cell sphingosine kinase activity is required for lymphocyte egress and lymphatic patterning. *J Exp Med* **207**, 17-27
353. Lai, W. Q., Irwan, A. W., Goh, H. H., Howe, H. S., Yu, D. T., Valle-Onate, R., McInnes, I. B., Melendez, A. J., and Leung, B. P. (2008) Anti-inflammatory effects of sphingosine kinase modulation in inflammatory arthritis. *J Immunol* **181**, 8010-8017

354. Lan, T., Liu, W., Xie, X., Xu, S., Huang, K., Peng, J., Shen, X., Liu, P., Wang, L., Xia, P., and Huang, H. (2011) Sphingosine kinase-1 pathway mediates high glucose-induced fibronectin expression in glomerular mesangial cells. *Mol Endocrinol* **25**, 2094-2105
355. Milara, J., Navarro, R., Juan, G., Peiro, T., Serrano, A., Ramon, M., Morcillo, E., and Cortijo, J. (2012) Sphingosine-1-phosphate is increased in patients with idiopathic pulmonary fibrosis and mediates epithelial to mesenchymal transition. *Thorax* **67**, 147-156
356. Tokumura, A., Carbone, L. D., Yoshioka, Y., Morishige, J., Kikuchi, M., Postlethwaite, A., and Watsky, M. A. (2009) Elevated serum levels of arachidonoyl-lysophosphatidic acid and sphingosine 1-phosphate in systemic sclerosis. *Int J Med Sci* **6**, 168-176
357. Snider, A. J., Kawamori, T., Bradshaw, S. G., Orr, K. A., Gilkeson, G. S., Hannun, Y. A., and Obeid, L. M. (2009) A role for sphingosine kinase 1 in dextran sulfate sodium-induced colitis. *FASEB J* **23**, 143-152
358. Maines, L. W., Fitzpatrick, L. R., French, K. J., Zhuang, Y., Xia, Z., Keller, S. N., Upson, J. J., and Smith, C. D. (2008) Suppression of ulcerative colitis in mice by orally available inhibitors of sphingosine kinase. *Dig Dis Sci* **53**, 997-1012
359. Chumanevich, A. A., Poudyal, D., Cui, X., Davis, T., Wood, P. A., Smith, C. D., and Hofseth, L. J. (2010) Suppression of colitis-driven colon cancer in mice by a novel small molecule inhibitor of sphingosine kinase. *Carcinogenesis* **31**, 1787-1793
360. Shimizu, H., Takahashi, M., Kaneko, T., Murakami, T., Hakamata, Y., Kudou, S., Kishi, T., Fukuchi, K., Iwanami, S., Kuriyama, K., Yasue, T., Enosawa, S., Matsumoto, K., Takeyoshi, I., Morishita, Y., and Kobayashi, E. (2005) KRP-203, a novel synthetic immunosuppressant, prolongs graft survival and attenuates chronic rejection in rat skin and heart allografts. *Circulation* **111**, 222-229
361. Kawamori, T., Kaneshiro, T., Okumura, M., Maalouf, S., Uflacker, A., Bielawski, J., Hannun, Y. A., and Obeid, L. M. (2009) Role for sphingosine kinase 1 in colon carcinogenesis. *FASEB J* **23**, 405-414
362. Liang, J., Nagahashi, M., Kim, E. Y., Harikumar, K. B., Yamada, A., Huang, W. C., Hait, N. C., Allegood, J. C., Price, M. M., Avni, D., Takabe, K., Kordula, T., Milstien, S., and Spiegel, S. (2013) Sphingosine-1-phosphate links persistent STAT3 activation, chronic



intestinal inflammation, and development of colitis-associated cancer. *Cancer Cell* **23**, 107-120

363. Xia, P., Gamble, J. R., Wang, L., Pitson, S. M., Moretti, P. A., Wattenberg, B. W., D'Andrea, R. J., and Vadas, M. A. (2000) An oncogenic role of sphingosine kinase. *Curr Biol* **10**, 1527-1530
364. Guan, H., Liu, L., Cai, J., Liu, J., Ye, C., Li, M., and Li, Y. (2011) Sphingosine kinase 1 is overexpressed and promotes proliferation in human thyroid cancer. *Mol Endocrinol* **25**, 1858-1866
365. Watson, C., Long, J. S., Orange, C., Tannahill, C. L., Mallon, E., McGlynn, L. M., Pyne, S., Pyne, N. J., and Edwards, J. (2010) High expression of sphingosine 1-phosphate receptors, S1P1 and S1P3, sphingosine kinase 1, and extracellular signal-regulated kinase-1/2 is associated with development of tamoxifen resistance in estrogen receptor-positive breast cancer patients. *Am J Pathol* **177**, 2205-2215
366. Van Brocklyn, J. R., Jackson, C. A., Pearl, D. K., Kotur, M. S., Snyder, P. J., and Prior, T. W. (2005) Sphingosine kinase-1 expression correlates with poor survival of patients with glioblastoma multiforme: roles of sphingosine kinase isoforms in growth of glioblastoma cell lines. *J Neuropathol Exp Neurol* **64**, 695-705
367. Johnson, K. R., Johnson, K. Y., Crellin, H. G., Ogretmen, B., Boylan, A. M., Harley, R. A., and Obeid, L. M. (2005) Immunohistochemical distribution of sphingosine kinase 1 in normal and tumor lung tissue. *J Histochem Cytochem* **53**, 1159-1166
368. Nunes, J., Naymark, M., Sauer, L., Muhammad, A., Keun, H., Sturge, J., Stebbing, J., Waxman, J., and Pchejetski, D. (2012) Circulating sphingosine-1-phosphate and erythrocyte sphingosine kinase-1 activity as novel biomarkers for early prostate cancer detection. *Br J Cancer* **106**, 909-915
369. Nagahashi, M., Ramachandran, S., Kim, E. Y., Allegood, J. C., Rashid, O. M., Yamada, A., Zhao, R., Milstien, S., Zhou, H., Spiegel, S., and Takabe, K. (2012) Sphingosine-1-phosphate produced by sphingosine kinase 1 promotes breast cancer progression by stimulating angiogenesis and lymphangiogenesis. *Cancer Res* **72**, 726-735
370. Kapitonov, D., Allegood, J. C., Mitchell, C., Hait, N. C., Almenara, J. A., Adams, J. K., Zipkin, R. E., Dent, P., Kordula, T., Milstien, S., and Spiegel, S. (2009) Targeting sphingosine kinase 1 inhibits Akt

signaling, induces apoptosis, and suppresses growth of human glioblastoma cells and xenografts. *Cancer Res* **69**, 6915-6923

371. Paugh, S. W., Paugh, B. S., Rahmani, M., Kapitonov, D., Almenara, J. A., Kordula, T., Milstien, S., Adams, J. K., Zipkin, R. E., Grant, S., and Spiegel, S. (2008) A selective sphingosine kinase 1 inhibitor integrates multiple molecular therapeutic targets in human leukemia. *Blood* **112**, 1382-1391
372. Schnute, M. E., McReynolds, M. D., Kasten, T., Yates, M., Jerome, G., Rains, J. W., Hall, T., Chrencik, J., Kraus, M., Cronin, C. N., Saabye, M., Highkin, M. K., Broadus, R., Ogawa, S., Cukyne, K., Zawadzke, L. E., Peterkin, V., Iyanar, K., Scholten, J. A., Wendling, J., Fujiwara, H., Nemirovskiy, O., Wittwer, A. J., and Nagiec, M. M. (2012) Modulation of cellular S1P levels with a novel, potent and specific inhibitor of sphingosine kinase-1. *Biochem J* **444**, 79-88
373. Lim, K. G., Tonelli, F., Li, Z., Lu, X., Bittman, R., Pyne, S., and Pyne, N. J. (2011) FTY720 analogues as sphingosine kinase 1 inhibitors: enzyme inhibition kinetics, allostereism, proteasomal degradation, and actin rearrangement in MCF-7 breast cancer cells. *J Biol Chem* **286**, 18633-18640
374. Cuvillier, O., Pirianov, G., Kleuser, B., Vanek, P. G., Coso, O. A., Gutkind, S., and Spiegel, S. (1996) Suppression of ceramide-mediated programmed cell death by sphingosine-1-phosphate. *Nature* **381**, 800-803
375. Ogretmen, B., and Hannun, Y. A. (2004) Biologically active sphingolipids in cancer pathogenesis and treatment. *Nat Rev Cancer* **4**, 604-616
376. Sarkar, S., Maceyka, M., Hait, N. C., Paugh, S. W., Sankala, H., Milstien, S., and Spiegel, S. (2005) Sphingosine kinase 1 is required for migration, proliferation and survival of MCF-7 human breast cancer cells. *FEBS Lett* **579**, 5313-5317
377. Bonhoure, E., Pchejetski, D., Aouali, N., Morjani, H., Levade, T., Kohama, T., and Cuvillier, O. (2006) Overcoming MDR-associated chemoresistance in HL-60 acute myeloid leukemia cells by targeting sphingosine kinase-1. *Leukemia* **20**, 95-102
378. Baran, Y., Salas, A., Senkal, C. E., Gunduz, U., Bielawski, J., Obeid, L. M., and Ogretmen, B. (2007) Alterations of ceramide/sphingosine 1-phosphate rheostat involved in the regulation of resistance to

imatinib-induced apoptosis in K562 human chronic myeloid leukemia cells. *J Biol Chem* **282**, 10922-10934

379. Pchejetski, D., Golzio, M., Bonhoure, E., Calvet, C., Doumerc, N., Garcia, V., Mazerolles, C., Rischmann, P., Teissie, J., Malavaud, B., and Cuvillier, O. (2005) Sphingosine kinase-1 as a chemotherapy sensor in prostate adenocarcinoma cell and mouse models. *Cancer Res* **65**, 11667-11675
380. Sauer, L., Nunes, J., Salunkhe, V., Skalska, L., Kohama, T., Cuvillier, O., Waxman, J., and Pchejetski, D. (2009) Sphingosine kinase 1 inhibition sensitizes hormone-resistant prostate cancer to docetaxel. *Int J Cancer* **125**, 2728-2736
381. Min, J., Mesika, A., Sivaguru, M., Van Veldhoven, P. P., Alexander, H., Futerman, A. H., and Alexander, S. (2007) (Dihydro)ceramide synthase 1 regulated sensitivity to cisplatin is associated with the activation of p38 mitogen-activated protein kinase and is abrogated by sphingosine kinase 1. *Mol Cancer Res* **5**, 801-812
382. Sukocheva, O., Wang, L., Verrier, E., Vadas, M. A., and Xia, P. (2009) Restoring endocrine response in breast cancer cells by inhibition of the sphingosine kinase-1 signaling pathway. *Endocrinology* **150**, 4484-4492
383. Zhang, H., Li, W., Sun, S., Yu, S., Zhang, M., and Zou, F. (2012) Inhibition of sphingosine kinase 1 suppresses proliferation of glioma cells under hypoxia by attenuating activity of extracellular signal-regulated kinase. *Cell Prolif* **45**, 167-175
384. Riccitelli, E., Giussani, P., Di Vito, C., Condomitti, G., Tringali, C., Caroli, M., Galli, R., Viani, P., and Riboni, L. (2013) Extracellular sphingosine-1-phosphate: a novel actor in human glioblastoma stem cell survival. *PLoS One* **8**, e68229
385. Shirahama, T., Sweeney, E. A., Sakakura, C., Singhal, A. K., Nishiyama, K., Akiyama, S., Hakomori, S., and Igarashi, Y. (1997) In vitro and in vivo induction of apoptosis by sphingosine and N, N-dimethylsphingosine in human epidermoid carcinoma KB-3-1 and its multidrug-resistant cells. *Clin Cancer Res* **3**, 257-264
386. Sachs, C. W., Safa, A. R., Harrison, S. D., and Fine, R. L. (1995) Partial inhibition of multidrug resistance by safinolol is independent of modulation of P-glycoprotein substrate activities and correlated with inhibition of protein kinase C. *J Biol Chem* **270**, 26639-26648

387. Ling, L. U., Tan, K. B., and Chiu, G. N. (2011) Role of reactive oxygen species in the synergistic cytotoxicity of safinol-based combination regimens with conventional chemotherapeutics. *Oncol Lett* **2**, 905-910
388. Dickson, M. A., Carvajal, R. D., Merrill, A. H., Jr., Gonen, M., Cane, L. M., and Schwartz, G. K. (2011) A phase I clinical trial of safinol in combination with cisplatin in advanced solid tumors. *Clin Cancer Res* **17**, 2484-2492
389. French, K. J., Schrecengost, R. S., Lee, B. D., Zhuang, Y., Smith, S. N., Eberly, J. L., Yun, J. K., and Smith, C. D. (2003) Discovery and evaluation of inhibitors of human sphingosine kinase. *Cancer Res* **63**, 5962-5969
390. Colie, S., Van Veldhoven, P. P., Kedjouar, B., Bedia, C., Albinet, V., Sorli, S. C., Garcia, V., Djavaheri-Mergny, M., Bauvy, C., Codogno, P., Levade, T., and Andrieu-Abadie, N. (2009) Disruption of sphingosine 1-phosphate lyase confers resistance to chemotherapy and promotes oncogenesis through Bcl-2/Bcl-xL upregulation. *Cancer Res* **69**, 9346-9353
391. Huang, X., Taeb, S., Jahangiri, S., Emmenegger, U., Tran, E., Bruce, J., Mesci, A., Korpela, E., Vesprini, D., Wong, C. S., Bristow, R. G., Liu, F. F., and Liu, S. K. (2013) miRNA-95 mediates radioresistance in tumors by targeting the sphingolipid phosphatase SGPP1. *Cancer Res* **73**, 6972-6986
392. Senchenkov, A., Litvak, D. A., and Cabot, M. C. (2001) Targeting ceramide metabolism--a strategy for overcoming drug resistance. *J Natl Cancer Inst* **93**, 347-357
393. Bose, R., Verheij, M., Haimovitz-Friedman, A., Scotto, K., Fuks, Z., and Kolesnick, R. (1995) Ceramide synthase mediates daunorubicin-induced apoptosis: an alternative mechanism for generating death signals. *Cell* **82**, 405-414
394. Rath, G., Schneider, C., Langlois, B., Sartelet, H., Morjani, H., Btaouri, H. E., Dedieu, S., and Martiny, L. (2009) De novo ceramide synthesis is responsible for the anti-tumor properties of camptothecin and doxorubicin in follicular thyroid carcinoma. *Int J Biochem Cell Biol* **41**, 1165-1172
395. Charles, A. G., Han, T. Y., Liu, Y. Y., Hansen, N., Giuliano, A. E., and Cabot, M. C. (2001) Taxol-induced ceramide generation and

- apoptosis in human breast cancer cells. *Cancer Chemother Pharmacol* **47**, 444-450
396. Perry, D. K., Carton, J., Shah, A. K., Meredith, F., Uhlinger, D. J., and Hannun, Y. A. (2000) Serine palmitoyltransferase regulates de novo ceramide generation during etoposide-induced apoptosis. *J Biol Chem* **275**, 9078-9084
397. Garzotto, M., Haimovitz-Friedman, A., Liao, W. C., White-Jones, M., Huryk, R., Heston, W. D., Cardon-Cardo, C., Kolesnick, R., and Fuks, Z. (1999) Reversal of radiation resistance in LNCaP cells by targeting apoptosis through ceramide synthase. *Cancer Res* **59**, 5194-5201
398. Park, J. W., Park, W. J., and Futerman, A. H. (2014) Ceramide synthases as potential targets for therapeutic intervention in human diseases. *Biochimica et biophysica acta* **1841**, 671-681
399. Itoh, M., Kitano, T., Watanabe, M., Kondo, T., Yabu, T., Taguchi, Y., Iwai, K., Tashima, M., Uchiyama, T., and Okazaki, T. (2003) Possible role of ceramide as an indicator of chemoresistance: decrease of the ceramide content via activation of glucosylceramide synthase and sphingomyelin synthase in chemoresistant leukemia. *Clin Cancer Res* **9**, 415-423
400. Santana, P., Pena, L. A., Haimovitz-Friedman, A., Martin, S., Green, D., McLoughlin, M., Cordon-Cardo, C., Schuchman, E. H., Fuks, Z., and Kolesnick, R. (1996) Acid sphingomyelinase-deficient human lymphoblasts and mice are defective in radiation-induced apoptosis. *Cell* **86**, 189-199
401. Chmura, S. J., Nodzenski, E., Beckett, M. A., Kufe, D. W., Quintans, J., and Weichselbaum, R. R. (1997) Loss of ceramide production confers resistance to radiation-induced apoptosis. *Cancer Res* **57**, 1270-1275
402. Smith, E. L., and Schuchman, E. H. (2008) Acid sphingomyelinase overexpression enhances the antineoplastic effects of irradiation in vitro and in vivo. *Mol Ther* **16**, 1565-1571
403. Garcia-Barros, M., Paris, F., Cordon-Cardo, C., Lyden, D., Rafii, S., Haimovitz-Friedman, A., Fuks, Z., and Kolesnick, R. (2003) Tumor response to radiotherapy regulated by endothelial cell apoptosis. *Science* **300**, 1155-1159

404. Cai, Z., Bettaieb, A., Mahdani, N. E., Legres, L. G., Stancou, R., Masliah, J., and Chouaib, S. (1997) Alteration of the sphingomyelin/ceramide pathway is associated with resistance of human breast carcinoma MCF7 cells to tumor necrosis factor- $\alpha$ -mediated cytotoxicity. *J Biol Chem* **272**, 6918-6926
405. Alphonse, G., Bionda, C., Aloy, M. T., Ardail, D., Rousson, R., and Rodriguez-Lafrasse, C. (2004) Overcoming resistance to gamma-rays in squamous carcinoma cells by poly-drug elevation of ceramide levels. *Oncogene* **23**, 2703-2715
406. Lavie, Y., Cao, H., Bursten, S. L., Giuliano, A. E., and Cabot, M. C. (1996) Accumulation of glucosylceramides in multidrug-resistant cancer cells. *J Biol Chem* **271**, 19530-19536
407. Klappe, K., Hinrichs, J. W., Kroesen, B. J., Sietsma, H., and Kok, J. W. (2004) MRP1 and glucosylceramide are coordinately over expressed and enriched in rafts during multidrug resistance acquisition in colon cancer cells. *Int J Cancer* **110**, 511-522
408. Gouaze, V., Yu, J. Y., Bleicher, R. J., Han, T. Y., Liu, Y. Y., Wang, H., Gottesman, M. M., Bitterman, A., Giuliano, A. E., and Cabot, M. C. (2004) Overexpression of glucosylceramide synthase and P-glycoprotein in cancer cells selected for resistance to natural product chemotherapy. *Mol Cancer Ther* **3**, 633-639
409. Liu, Y. Y., Han, T. Y., Giuliano, A. E., and Cabot, M. C. (1999) Expression of glucosylceramide synthase, converting ceramide to glucosylceramide, confers adriamycin resistance in human breast cancer cells. *J Biol Chem* **274**, 1140-1146
410. Owczarek, T. B., Suchanski, J., Pula, B., Kmiecik, A. M., Chadalski, M., Jethon, A., Dziegiel, P., and Ugorski, M. (2013) Galactosylceramide affects tumorigenic and metastatic properties of breast cancer cells as an anti-apoptotic molecule. *PLoS One* **8**, e84191
411. Veldman, R. J., Mita, A., Cuvillier, O., Garcia, V., Klappe, K., Medin, J. A., Campbell, J. D., Carpentier, S., Kok, J. W., and Levade, T. (2003) The absence of functional glucosylceramide synthase does not sensitize melanoma cells for anticancer drugs. *FASEB J* **17**, 1144-1146
412. Cabot, M. C., Giuliano, A. E., Han, T. Y., and Liu, Y. Y. (1999) SDZ PSC 833, the cyclosporine A analogue and multidrug resistance

modulator, activates ceramide synthesis and increases vinblastine sensitivity in drug-sensitive and drug-resistant cancer cells. *Cancer Res* **59**, 880-885

413. Raggars, R. J., van Helvoort, A., Evers, R., and van Meer, G. (1999) The human multidrug resistance protein MRP1 translocates sphingolipid analogs across the plasma membrane. *J Cell Sci* **112 ( Pt 3)**, 415-422
414. Gillet, J. P., Calcagno, A. M., Varma, S., Marino, M., Green, L. J., Vora, M. I., Patel, C., Orina, J. N., Eliseeva, T. A., Singal, V., Padmanabhan, R., Davidson, B., Ganapathi, R., Sood, A. K., Rueda, B. R., Ambudkar, S. V., and Gottesman, M. M. (2011) Redefining the relevance of established cancer cell lines to the study of mechanisms of clinical anti-cancer drug resistance. *Proc Natl Acad Sci U S A* **108**, 18708-18713
415. Hooks, S. B., Santos, W. L., Im, D. S., Heise, C. E., Macdonald, T. L., and Lynch, K. R. (2001) Lysophosphatidic acid-induced mitogenesis is regulated by lipid phosphate phosphatases and is Edg-receptor independent. *J Biol Chem* **276**, 4611-4621
416. Pilquill, C., Dewald, J., Cherney, A., Gorshkova, I., Tigyi, G., English, D., Natarajan, V., and Brindley, D. N. (2006) Lipid phosphate phosphatase-1 regulates lysophosphatidate-induced fibroblast migration by controlling phospholipase D2-dependent phosphatidate generation. *Journal of Biological Chemistry* **281**, 38418-38429
417. Wang, X. J., Hayes, J. D., and Wolf, C. R. (2006) Generation of a stable antioxidant response element-driven reporter gene cell line and its use to show redox-dependent activation of nrf2 by cancer chemotherapeutic agents. *Cancer Res* **66**, 10983-10994
418. Wang, X., Tomso, D. J., Chorley, B. N., Cho, H. Y., Cheung, V. G., Kleeberger, S. R., and Bell, D. A. (2007) Identification of polymorphic antioxidant response elements in the human genome. *Hum Mol Genet* **16**, 1188-1200
419. Keum, Y. S., Yu, S., Chang, P. P., Yuan, X., Kim, J. H., Xu, C., Han, J., Agarwal, A., and Kong, A. N. (2006) Mechanism of action of sulforaphane: inhibition of p38 mitogen-activated protein kinase isoforms contributing to the induction of antioxidant response element-mediated heme oxygenase-1 in human hepatoma HepG2 cells. *Cancer Res* **66**, 8804-8813

420. Kurz, E. U., Cole, S. P., and Deeley, R. G. (2001) Identification of DNA-protein interactions in the 5' flanking and 5' untranslated regions of the human multidrug resistance protein (MRP1) gene: evaluation of a putative antioxidant response element/AP-1 binding site. *Biochem Biophys Res Commun* **285**, 981-990
421. Ji, L., Li, H., Gao, P., Shang, G., Zhang, D. D., Zhang, N., and Jiang, T. (2013) Nrf2 pathway regulates multidrug-resistance-associated protein 1 in small cell lung cancer. *PLoS One* **8**, e63404
422. Shen, G., and Kong, A. N. (2009) Nrf2 plays an important role in coordinated regulation of Phase II drug metabolism enzymes and Phase III drug transporters. *Biopharmaceutics & drug disposition* **30**, 345-355
423. Vollrath, V., Wielandt, A. M., Iruretagoyena, M., and Chianale, J. (2006) Role of Nrf2 in the regulation of the Mrp2 (ABCC2) gene. *Biochem J* **395**, 599-609
424. Hembruff, S. L., Laberge, M. L., Villeneuve, D. J., Guo, B., Veitch, Z., Cecchetto, M., and Parissenti, A. M. (2008) Role of drug transporters and drug accumulation in the temporal acquisition of drug resistance. *BMC Cancer* **8**, 318
425. Guo, B., Villeneuve, D. J., Hembruff, S. L., Kirwan, A. F., Blais, D. E., Bonin, M., and Parissenti, A. M. (2004) Cross-resistance studies of isogenic drug-resistant breast tumor cell lines support recent clinical evidence suggesting that sensitivity to paclitaxel may be strongly compromised by prior doxorubicin exposure. *Breast Cancer Res Treat* **85**, 31-51
426. Furukawa, M., and Xiong, Y. (2005) BTB protein Keap1 targets antioxidant transcription factor Nrf2 for ubiquitination by the Cullin 3-Roc1 ligase. *Mol Cell Biol* **25**, 162-171
427. He, T. C., Zhou, S., da Costa, L. T., Yu, J., Kinzler, K. W., and Vogelstein, B. (1998) A simplified system for generating recombinant adenoviruses. *Proc Natl Acad Sci U S A* **95**, 2509-2514
428. Du, G., Huang, P., Liang, B. T., and Frohman, M. A. (2004) Phospholipase D2 localizes to the plasma membrane and regulates angiotensin II receptor endocytosis. *Mol Biol Cell* **15**, 1024-1030
429. Johannessen, C. M., Boehm, J. S., Kim, S. Y., Thomas, S. R., Wardwell, L., Johnson, L. A., Emery, C. M., Stransky, N., Cogdill, A.



- P., Barretina, J., Caponigro, G., Hieronymus, H., Murray, R. R., Salehi-Ashtiani, K., Hill, D. E., Vidal, M., Zhao, J. J., Yang, X., Alkan, O., Kim, S., Harris, J. L., Wilson, C. J., Myer, V. E., Finan, P. M., Root, D. E., Roberts, T. M., Golub, T., Flaherty, K. T., Dummer, R., Weber, B. L., Sellers, W. R., Schlegel, R., Wargo, J. A., Hahn, W. C., and Garraway, L. A. (2010) COT drives resistance to RAF inhibition through MAP kinase pathway reactivation. *Nature* **468**, 968-972
430. Zhang, F., Wang, Z., Lu, M., Yonekubo, Y., Liang, X., Zhang, Y., Wu, P., Zhou, Y., Grinstein, S., Hancock, J. F., and Du, G. (2014) Temporal production of the signaling lipid phosphatidic acid by phospholipase D2 determines the output of extracellular signal-regulated kinase signaling in cancer cells. *Mol Cell Biol* **34**, 84-95
431. Mosmann, T. (1983) Rapid colorimetric assay for cellular growth and survival: application to proliferation and cytotoxicity assays. *J Immunol Methods* **65**, 55-63
432. Schmittgen, T. D., and Livak, K. J. (2008) Analyzing real-time PCR data by the comparative C(T) method. *Nature protocols* **3**, 1101-1108
433. Germain, D. R., Graham, K., Glubrecht, D. D., Hugh, J. C., Mackey, J. R., and Godbout, R. (2011) DEAD box 1: a novel and independent prognostic marker for early recurrence in breast cancer. *Breast Cancer Res Treat* **127**, 53-63
434. Liu, R. Z., Graham, K., Glubrecht, D. D., Germain, D. R., Mackey, J. R., and Godbout, R. (2011) Association of FABP5 expression with poor survival in triple-negative breast cancer: implication for retinoic acid therapy. *Am J Pathol* **178**, 997-1008
435. Trinkle-Mulcahy, L., Boulon, S., Lam, Y. W., Urcia, R., Boisvert, F. M., Vandermoere, F., Morrice, N. A., Swift, S., Rothbauer, U., Leonhardt, H., and Lamond, A. (2008) Identifying specific protein interaction partners using quantitative mass spectrometry and bead proteomes. *J Cell Biol* **183**, 223-239
436. Olivera, A., and Spiegel, S. (1998) Sphingosine kinase. Assay and product analysis. *Methods Mol Biol* **105**, 233-242
437. Pitman, M. R., Pham, D. H., and Pitson, S. M. (2012) Isoform-selective assays for sphingosine kinase activity. *Methods Mol Biol* **874**, 21-31

438. Cascales, C., Mangiapane, E. H., and Brindley, D. N. (1984) Oleic acid promotes the activation and translocation of phosphatidate phosphohydrolase from the cytosol to particulate fractions of isolated rat hepatocytes. *Biochem J* **219**, 911-916
439. Mitra, P., Payne, S. G., Milstien, S., and Spiegel, S. (2007) A rapid and sensitive method to measure secretion of sphingosine-1-phosphate. *Methods Enzymol* **434**, 257-264
440. Scherer, M., Leuthauser-Jaschinski, K., Ecker, J., Schmitz, G., and Liebisch, G. (2010) A rapid and quantitative LC-MS/MS method to profile sphingolipids. *J Lipid Res* **51**, 2001-2011
441. Nguyen, T., Sherratt, P. J., Huang, H. C., Yang, C. S., and Pickett, C. B. (2003) Increased protein stability as a mechanism that enhances Nrf2-mediated transcriptional activation of the antioxidant response element. Degradation of Nrf2 by the 26 S proteasome. *J Biol Chem* **278**, 4536-4541
442. Mitsuishi, Y., Taguchi, K., Kawatani, Y., Shibata, T., Nukiwa, T., Aburatani, H., Yamamoto, M., and Motohashi, H. (2012) Nrf2 redirects glucose and glutamine into anabolic pathways in metabolic reprogramming. *Cancer Cell* **22**, 66-79
443. Singh, A., Happel, C., Manna, S. K., Acquah-Mensah, G., Carrerero, J., Kumar, S., Nasipuri, P., Krausz, K. W., Wakabayashi, N., Dewi, R., Boros, L. G., Gonzalez, F. J., Gabrielson, E., Wong, K. K., Girnun, G., and Biswal, S. (2013) Transcription factor NRF2 regulates miR-1 and miR-206 to drive tumorigenesis. *J Clin Invest* **123**, 2921-2934
444. Shim, G. S., Manandhar, S., Shin, D. H., Kim, T. H., and Kwak, M. K. (2009) Acquisition of doxorubicin resistance in ovarian carcinoma cells accompanies activation of the NRF2 pathway. *Free Radic Biol Med* **47**, 1619-1631
445. DeNicola, G. M., Karreth, F. A., Humpton, T. J., Gopinathan, A., Wei, C., Frese, K., Mangal, D., Yu, K. H., Yeo, C. J., Calhoun, E. S., Scrimieri, F., Winter, J. M., Hruban, R. H., Iacobuzio-Donahue, C., Kern, S. E., Blair, I. A., and Tuveson, D. A. (2011) Oncogene-induced Nrf2 transcription promotes ROS detoxification and tumorigenesis. *Nature* **475**, 106-109
446. Hayashi, A., Suzuki, H., Itoh, K., Yamamoto, M., and Sugiyama, Y. (2003) Transcription factor Nrf2 is required for the constitutive and inducible expression of multidrug resistance-associated protein 1 in

mouse embryo fibroblasts. *Biochemical and biophysical research communications* **310**, 824-829

447. Lazebnik, Y. A., Kaufmann, S. H., Desnoyers, S., Poirier, G. G., and Earnshaw, W. C. (1994) Cleavage of poly(ADP-ribose) polymerase by a proteinase with properties like ICE. *Nature* **371**, 346-347
448. Kaufmann, S. H., Desnoyers, S., Ottaviano, Y., Davidson, N. E., and Poirier, G. G. (1993) Specific proteolytic cleavage of poly(ADP-ribose) polymerase: an early marker of chemotherapy-induced apoptosis. *Cancer Res* **53**, 3976-3985
449. Keane, M. M., Ettenberg, S. A., Nau, M. M., Russell, E. K., and Lipkowitz, S. (1999) Chemotherapy augments TRAIL-induced apoptosis in breast cell lines. *Cancer Res* **59**, 734-741
450. Durand, R. E., and Olive, P. L. (1981) Flow cytometry studies of intracellular adriamycin in single cells in vitro. *Cancer Res* **41**, 3489-3494
451. Qadir, M., O'Loughlin, K. L., Fricke, S. M., Williamson, N. A., Greco, W. R., Minderman, H., and Baer, M. R. (2005) Cyclosporin A is a broad-spectrum multidrug resistance modulator. *Clin Cancer Res* **11**, 2320-2326
452. Gollapudi, S., Kim, C. H., Tran, B. N., Sangha, S., and Gupta, S. (1997) Probenecid reverses multidrug resistance in multidrug resistance-associated protein-overexpressing HL60/AR and H69/AR cells but not in P-glycoprotein-overexpressing HL60/Tax and P388/ADR cells. *Cancer Chemother Pharmacol* **40**, 150-158
453. Homolya, L., Hollo, Z., Germann, U. A., Pastan, I., Gottesman, M. M., and Sarkadi, B. (1993) Fluorescent cellular indicators are extruded by the multidrug resistance protein. *J Biol Chem* **268**, 21493-21496
454. Hollo, Z., Homolya, L., Davis, C. W., and Sarkadi, B. (1994) Calcein accumulation as a fluorometric functional assay of the multidrug transporter. *Biochimica et biophysica acta* **1191**, 384-388
455. Lohoff, M., Prectl, S., Sommer, F., Roellinghoff, M., Schmitt, E., Gradehandt, G., Rohwer, P., Stride, B. D., Cole, S. P., and Deeley, R. G. (1998) A multidrug-resistance protein (MRP)-like transmembrane pump is highly expressed by resting murine T helper (Th) 2, but not Th1 cells, and is induced to equal expression levels in Th1 and Th2 cells after antigenic stimulation in vivo. *J Clin Invest* **101**, 703-710

456. Doyle, L., and Ross, D. D. (2003) Multidrug resistance mediated by the breast cancer resistance protein BCRP (ABCG2). *Oncogene* **22**, 7340-7358
457. Robillard, K. R., Hoque, T., and Bendayan, R. (2012) Expression of ATP-binding cassette membrane transporters in rodent and human sertoli cells: relevance to the permeability of antiretroviral therapy at the blood-testis barrier. *J Pharmacol Exp Ther* **340**, 96-108
458. Krech, T., Scheuerer, E., Geffers, R., Kreipe, H., Lehmann, U., and Christgen, M. (2012) ABCB1/MDR1 contributes to the anticancer drug-resistant phenotype of IPH-926 human lobular breast cancer cells. *Cancer Lett* **315**, 153-160
459. Manmontri, B., Sariahmetoglu, M., Donkor, J., Bou Khalil, M., Sundaram, M., Yao, Z., Reue, K., Lehner, R., and Brindley, D. N. (2008) Glucocorticoids and cyclic AMP selectively increase hepatic lipin-1 expression, and insulin acts antagonistically. *J Lipid Res* **49**, 1056-1067
460. Lau, A., Tian, W., Whitman, S. A., and Zhang, D. D. (2013) The predicted molecular weight of Nrf2: it is what it is not. *Antioxidants & redox signaling* **18**, 91-93
461. Rushmore, T. H., Morton, M. R., and Pickett, C. B. (1991) The antioxidant responsive element. Activation by oxidative stress and identification of the DNA consensus sequence required for functional activity. *J Biol Chem* **266**, 11632-11639
462. Gewirtz, D. A. (1999) A critical evaluation of the mechanisms of action proposed for the antitumor effects of the anthracycline antibiotics adriamycin and daunorubicin. *Biochem Pharmacol* **57**, 727-741
463. Kobuchi, H., Moriya, K., Ogino, T., Fujita, H., Inoue, K., Shuin, T., Yasuda, T., Utsumi, K., and Utsumi, T. (2012) Mitochondrial localization of ABC transporter ABCG2 and its function in 5-aminolevulinic acid-mediated protoporphyrin IX accumulation. *PLoS One* **7**, e50082
464. Westlake, C. J., Cole, S. P., and Deeley, R. G. (2005) Role of the NH2-terminal membrane spanning domain of multidrug resistance protein 1/ABCC1 in protein processing and trafficking. *Mol Biol Cell* **16**, 2483-2492

465. Aleksunes, L. M., Slitt, A. L., Maher, J. M., Augustine, L. M., Goedken, M. J., Chan, J. Y., Cherrington, N. J., Klaassen, C. D., and Manautou, J. E. (2008) Induction of Mrp3 and Mrp4 transporters during acetaminophen hepatotoxicity is dependent on Nrf2. *Toxicol Appl Pharmacol* **226**, 74-83
466. Lacroix, M., Toillon, R. A., and Leclercq, G. (2006) p53 and breast cancer, an update. *Endocr Relat Cancer* **13**, 293-325
467. Harrison, E. M., McNally, S. J., Devey, L., Garden, O. J., Ross, J. A., and Wigmore, S. J. (2006) Insulin induces heme oxygenase-1 through the phosphatidylinositol 3-kinase/Akt pathway and the Nrf2 transcription factor in renal cells. *The FEBS journal* **273**, 2345-2356
468. Yu, R., Chen, C., Mo, Y. Y., Hebbar, V., Owuor, E. D., Tan, T. H., and Kong, A. N. (2000) Activation of mitogen-activated protein kinase pathways induces antioxidant response element-mediated gene expression via a Nrf2-dependent mechanism. *J Biol Chem* **275**, 39907-39913
469. Sun, Z., Huang, Z., and Zhang, D. D. (2009) Phosphorylation of Nrf2 at multiple sites by MAP kinases has a limited contribution in modulating the Nrf2-dependent antioxidant response. *PLoS One* **4**, e6588
470. Huang, H. C., Nguyen, T., and Pickett, C. B. (2000) Regulation of the antioxidant response element by protein kinase C-mediated phosphorylation of NF-E2-related factor 2. *Proc Natl Acad Sci U S A* **97**, 12475-12480
471. Zhang, D. D., and Hannink, M. (2003) Distinct cysteine residues in Keap1 are required for Keap1-dependent ubiquitination of Nrf2 and for stabilization of Nrf2 by chemopreventive agents and oxidative stress. *Mol Cell Biol* **23**, 8137-8151
472. Lee, J. M., Hanson, J. M., Chu, W. A., and Johnson, J. A. (2001) Phosphatidylinositol 3-kinase, not extracellular signal-regulated kinase, regulates activation of the antioxidant-responsive element in IMR-32 human neuroblastoma cells. *J Biol Chem* **276**, 20011-20016
473. Martin, D., Rojo, A. I., Salinas, M., Diaz, R., Gallardo, G., Alam, J., De Galarreta, C. M., and Cuadrado, A. (2004) Regulation of heme oxygenase-1 expression through the phosphatidylinositol 3-kinase/Akt pathway and the Nrf2 transcription factor in response to the antioxidant phytochemical carnosol. *J Biol Chem* **279**, 8919-8929

474. Nakaso, K., Yano, H., Fukuhara, Y., Takeshima, T., Wada-Isoe, K., and Nakashima, K. (2003) PI3K is a key molecule in the Nrf2-mediated regulation of antioxidative proteins by hemin in human neuroblastoma cells. *FEBS Lett* **546**, 181-184
475. Apopa, P. L., He, X., and Ma, Q. (2008) Phosphorylation of Nrf2 in the transcription activation domain by casein kinase 2 (CK2) is critical for the nuclear translocation and transcription activation function of Nrf2 in IMR-32 neuroblastoma cells. *J Biochem Mol Toxicol* **22**, 63-76
476. Huang, H. C., Nguyen, T., and Pickett, C. B. (2002) Phosphorylation of Nrf2 at Ser-40 by protein kinase C regulates antioxidant response element-mediated transcription. *J Biol Chem* **277**, 42769-42774
477. Rada, P., Rojo, A. I., Chowdhry, S., McMahon, M., Hayes, J. D., and Cuadrado, A. (2011) SCF/ $\beta$ -TrCP promotes glycogen synthase kinase 3-dependent degradation of the Nrf2 transcription factor in a Keap1-independent manner. *Mol Cell Biol* **31**, 1121-1133
478. Rojo, A. I., Sagarra, M. R., and Cuadrado, A. (2008) GSK-3 $\beta$  down-regulates the transcription factor Nrf2 after oxidant damage: relevance to exposure of neuronal cells to oxidative stress. *J Neurochem* **105**, 192-202
479. Salazar, M., Rojo, A. I., Velasco, D., de Sagarra, R. M., and Cuadrado, A. (2006) Glycogen synthase kinase-3 $\beta$  inhibits the xenobiotic and antioxidant cell response by direct phosphorylation and nuclear exclusion of the transcription factor Nrf2. *J Biol Chem* **281**, 14841-14851
480. Chowdhry, S., Zhang, Y., McMahon, M., Sutherland, C., Cuadrado, A., and Hayes, J. D. (2013) Nrf2 is controlled by two distinct  $\beta$ -TrCP recognition motifs in its Neh6 domain, one of which can be modulated by GSK-3 activity. *Oncogene* **32**, 3765-3781
481. Lavi, O., Greene, J. M., Levy, D., and Gottesman, M. M. (2013) The role of cell density and intratumoral heterogeneity in multidrug resistance. *Cancer Res* **73**, 7168-7175
482. Pulaski, B. A., and Ostrand-Rosenberg, S. (1998) Reduction of established spontaneous mammary carcinoma metastases following immunotherapy with major histocompatibility complex class II and B7.1 cell-based tumor vaccines. *Cancer Res* **58**, 1486-1493

483. DuPre, S. A., Redelman, D., and Hunter, K. W., Jr. (2007) The mouse mammary carcinoma 4T1: characterization of the cellular landscape of primary tumours and metastatic tumour foci. *Int J Exp Pathol* **88**, 351-360
484. Ewens, A., Luo, L., Berleth, E., Alderfer, J., Wollman, R., Hafeez, B. B., Kanter, P., Mihich, E., and Ehrke, M. J. (2006) Doxorubicin plus interleukin-2 chemoimmunotherapy against breast cancer in mice. *Cancer Res* **66**, 5419-5426
485. Dexter, D. L., Kowalski, H. M., Blazar, B. A., Fligiel, Z., Vogel, R., and Heppner, G. H. (1978) Heterogeneity of tumor cells from a single mouse mammary tumor. *Cancer Res* **38**, 3174-3181
486. Heppner, G. H., Dexter, D. L., DeNucci, T., Miller, F. R., and Calabresi, P. (1978) Heterogeneity in drug sensitivity among tumor cell subpopulations of a single mammary tumor. *Cancer Res* **38**, 3758-3763
487. Tao, K., Fang, M., Alroy, J., and Sahagian, G. G. (2008) Imagable 4T1 model for the study of late stage breast cancer. *BMC Cancer* **8**, 228
488. Hiraga, T., Williams, P. J., Ueda, A., Tamura, D., and Yoneda, T. (2004) Zoledronic acid inhibits visceral metastases in the 4T1/luc mouse breast cancer model. *Clin Cancer Res* **10**, 4559-4567
489. Morecki, S., Yacovlev, L., and Slavin, S. (1998) Effect of indomethacin on tumorigenicity and immunity induction in a murine model of mammary carcinoma. *Int J Cancer* **75**, 894-899
490. Kurt, R. A., Baher, A., Wisner, K. P., Tackitt, S., and Urba, W. J. (2001) Chemokine receptor desensitization in tumor-bearing mice. *Cell Immunol* **207**, 81-88
491. Fantozzi, A., and Christofori, G. (2006) Mouse models of breast cancer metastasis. *Breast Cancer Res* **8**, 212
492. Pastore, A., Federici, G., Bertini, E., and Piemonte, F. (2003) Analysis of glutathione: implication in redox and detoxification. *Clin Chim Acta* **333**, 19-39
493. Rottenberg, S., Nygren, A. O., Pajic, M., van Leeuwen, F. W., van der Heijden, I., van de Wetering, K., Liu, X., de Visser, K. E., Gilhuijs, K. G., van Tellingen, O., Schouten, J. P., Jonkers, J., and Borst, P.

- (2007) Selective induction of chemotherapy resistance of mammary tumors in a conditional mouse model for hereditary breast cancer. *Proc Natl Acad Sci U S A* **104**, 12117-12122
494. Choi, J. W., Herr, D. R., Noguchi, K., Yung, Y. C., Lee, C. W., Mutoh, T., Lin, M. E., Teo, S. T., Park, K. E., Mosley, A. N., and Chun, J. (2010) LPA receptors: subtypes and biological actions. *Annu Rev Pharmacol Toxicol* **50**, 157-186
495. An, S., Bleu, T., Hallmark, O. G., and Goetzl, E. J. (1998) Characterization of a novel subtype of human G protein-coupled receptor for lysophosphatidic acid. *J Biol Chem* **273**, 7906-7910
496. Chu, F. F., Esworthy, R. S., Akman, S., and Doroshov, J. H. (1990) Modulation of glutathione peroxidase expression by selenium: effect on human MCF-7 breast cancer cell transfectants expressing a cellular glutathione peroxidase cDNA and doxorubicin-resistant MCF-7 cells. *Nucleic Acids Res* **18**, 1531-1539
497. Reuter, S., Gupta, S. C., Chaturvedi, M. M., and Aggarwal, B. B. (2010) Oxidative stress, inflammation, and cancer: how are they linked? *Free Radic Biol Med* **49**, 1603-1616
498. Gorrini, C., Gang, B. P., Bassi, C., Wakeham, A., Baniasadi, S. P., Hao, Z., Li, W. Y., Cescon, D. W., Li, Y. T., Molyneux, S., Penrod, N., Lupien, M., Schmidt, E. E., Stambolic, V., Gauthier, M. L., and Mak, T. W. (2014) Estrogen controls the survival of BRCA1-deficient cells via a PI3K-NRF2-regulated pathway. *Proc Natl Acad Sci U S A* **111**, 4472-4477
499. Prossnitz, E. R., Arterburn, J. B., and Sklar, L. A. (2007) GPR30: A G protein-coupled receptor for estrogen. *Mol Cell Endocrinol* **265-266**, 138-142
500. Hannun, Y. A., and Obeid, L. M. (2008) Principles of bioactive lipid signalling: lessons from sphingolipids. *Nat Rev Mol Cell Biol* **9**, 139-150
501. Bandhuvula, P., Fyrst, H., and Saba, J. D. (2007) A rapid fluorescence assay for sphingosine-1-phosphate lyase enzyme activity. *J Lipid Res* **48**, 2769-2778
502. Smyth, S. S., Sciorra, V. A., Sigal, Y. J., Pamuklar, Z., Wang, Z., Xu, Y., Prestwich, G. D., and Morris, A. J. (2003) Lipid phosphate phosphatases regulate lysophosphatidic acid production and signaling



in platelets: studies using chemical inhibitors of lipid phosphate phosphatase activity. *J Biol Chem* **278**, 43214-43223

503. Kihara, A., Anada, Y., and Igarashi, Y. (2006) Mouse sphingosine kinase isoforms SPHK1a and SPHK1b differ in enzymatic traits including stability, localization, modification, and oligomerization. *J Biol Chem* **281**, 4532-4539
504. Hu, R., Xu, C., Shen, G., Jain, M. R., Khor, T. O., Gopalkrishnan, A., Lin, W., Reddy, B., Chan, J. Y., and Kong, A. N. (2006) Identification of Nrf2-regulated genes induced by chemopreventive isothiocyanate PEITC by oligonucleotide microarray. *Life Sci* **79**, 1944-1955
505. Hu, R., Xu, C., Shen, G., Jain, M. R., Khor, T. O., Gopalkrishnan, A., Lin, W., Reddy, B., Chan, J. Y., and Kong, A. N. (2006) Gene expression profiles induced by cancer chemopreventive isothiocyanate sulforaphane in the liver of C57BL/6J mice and C57BL/6J/Nrf2 (-/-) mice. *Cancer Lett* **243**, 170-192
506. Mercado, N., Kizawa, Y., Ueda, K., Xiong, Y., Kimura, G., Moses, A., Curtis, J. M., Ito, K., and Barnes, P. J. (2014) Activation of transcription factor Nrf2 signalling by the sphingosine kinase inhibitor SKI-II is mediated by the formation of Keap1 dimers. *PLoS One* **9**, e88168
507. Henkels, K. M., Boivin, G. P., Dudley, E. S., Berberich, S. J., and Gomez-Cambronero, J. (2013) Phospholipase D (PLD) drives cell invasion, tumor growth and metastasis in a human breast cancer xenograph model. *Oncogene* **32**, 5551-5562
508. Heibein, A. D., Guo, B., Sprowl, J. A., Maclean, D. A., and Parissenti, A. M. (2012) Role of aldo-keto reductases and other doxorubicin pharmacokinetic genes in doxorubicin resistance, DNA binding, and subcellular localization. *BMC Cancer* **12**, 381
509. Renes, J., de Vries, E. G., Nienhuis, E. F., Jansen, P. L., and Muller, M. (1999) ATP- and glutathione-dependent transport of chemotherapeutic drugs by the multidrug resistance protein MRP1. *British journal of pharmacology* **126**, 681-688
510. Sognier, M. A., Zhang, Y., Eberle, R. L., Sweet, K. M., Altenberg, G. A., and Belli, J. A. (1994) Sequestration of doxorubicin in vesicles in a multidrug-resistant cell line (LZ-100). *Biochem Pharmacol* **48**, 391-401

511. Arnold, R. D., Slack, J. E., and Straubinger, R. M. (2004) Quantification of Doxorubicin and metabolites in rat plasma and small volume tissue samples by liquid chromatography/electrospray tandem mass spectroscopy. *J Chromatogr B Analyt Technol Biomed Life Sci* **808**, 141-152
512. Tigyi, G. (2010) Aiming drug discovery at lysophosphatidic acid targets. *British journal of pharmacology* **161**, 241-270
513. Niture, S. K., Jain, A. K., and Jaiswal, A. K. (2009) Antioxidant-induced modification of INrf2 cysteine 151 and PKC-delta-mediated phosphorylation of Nrf2 serine 40 are both required for stabilization and nuclear translocation of Nrf2 and increased drug resistance. *J Cell Sci* **122**, 4452-4464
514. Malloy, M. T., McIntosh, D. J., Walters, T. S., Flores, A., Goodwin, J. S., and Arinze, I. J. (2013) Trafficking of the transcription factor Nrf2 to promyelocytic leukemia-nuclear bodies: implications for degradation of NRF2 in the nucleus. *J Biol Chem* **288**, 14569-14583
515. Panupinthu, N., Lee, H. Y., and Mills, G. B. (2010) Lysophosphatidic acid production and action: critical new players in breast cancer initiation and progression. *Br J Cancer* **102**, 941-946
516. Gaetano, C. G., Samadi, N., Tomsig, J. L., Macdonald, T. L., Lynch, K. R., and Brindley, D. N. (2009) Inhibition of autotaxin production or activity blocks lysophosphatidylcholine-induced migration of human breast cancer and melanoma cells. *Molecular carcinogenesis* **48**, 801-809
517. Singh, A., Boldin-Adamsky, S., Thimmulappa, R. K., Rath, S. K., Ashush, H., Coulter, J., Blackford, A., Goodman, S. N., Bunz, F., Watson, W. H., Gabrielson, E., Feinstein, E., and Biswal, S. (2008) RNAi-mediated silencing of nuclear factor erythroid-2-related factor 2 gene expression in non-small cell lung cancer inhibits tumor growth and increases efficacy of chemotherapy. *Cancer Res* **68**, 7975-7984
518. Gouaze, V., Mirault, M. E., Carpentier, S., Salvayre, R., Levade, T., and Andrieu-Abadie, N. (2001) Glutathione peroxidase-1 overexpression prevents ceramide production and partially inhibits apoptosis in doxorubicin-treated human breast carcinoma cells. *Mol Pharmacol* **60**, 488-496
519. Sinha, B. K., Mimnaugh, E. G., Rajagopalan, S., and Myers, C. E. (1989) Adriamycin activation and oxygen free radical formation in

human breast tumor cells: protective role of glutathione peroxidase in adriamycin resistance. *Cancer Res* **49**, 3844-3848

520. Vibet, S., Goupille, C., Bougnoux, P., Steghens, J. P., Gore, J., and Maheo, K. (2008) Sensitization by docosahexaenoic acid (DHA) of breast cancer cells to anthracyclines through loss of glutathione peroxidase (GPx1) response. *Free Radic Biol Med* **44**, 1483-1491
521. Jardim, B. V., Moschetta, M. G., Leonel, C., Gelaleti, G. B., Regiani, V. R., Ferreira, L. C., Lopes, J. R., and Zuccari, D. A. (2013) Glutathione and glutathione peroxidase expression in breast cancer: an immunohistochemical and molecular study. *Oncol Rep* **30**, 1119-1128
522. Li, S., Wang, W., Niu, T., Wang, H., Li, B., Shao, L., Lai, Y., Li, H., Janicki, J. S., Wang, X. L., Tang, D., and Cui, T. (2014) Nrf2 deficiency exaggerates doxorubicin-induced cardiotoxicity and cardiac dysfunction. *Oxid Med Cell Longev* **2014**, 748524
523. Magesh, S., Chen, Y., and Hu, L. (2012) Small molecule modulators of Keap1-Nrf2-ARE pathway as potential preventive and therapeutic agents. *Med Res Rev* **32**, 687-726
524. Guo, S., and Dipietro, L. A. (2010) Factors affecting wound healing. *J Dent Res* **89**, 219-229
525. Gordon, C. R., Rojavin, Y., Patel, M., Zins, J. E., Grana, G., Kann, B., Simons, R., and Atabek, U. (2009) A review on bevacizumab and surgical wound healing: an important warning to all surgeons. *Ann Plast Surg* **62**, 707-709
526. de Visser, K. E., and Jonkers, J. (2009) Towards understanding the role of cancer-associated inflammation in chemoresistance. *Curr Pharm Des* **15**, 1844-1853
527. Holmes, E. W., Yong, S. L., Eiznhamer, D., and Keshavarzian, A. (1998) Glutathione content of colonic mucosa: evidence for oxidative damage in active ulcerative colitis. *Dig Dis Sci* **43**, 1088-1095
528. Calon, A., Espinet, E., Palomo-Ponce, S., Tauriello, D. V., Iglesias, M., Cespedes, M. V., Sevillano, M., Nadal, C., Jung, P., Zhang, X. H., Byrom, D., Riera, A., Rossell, D., Mangués, R., Massagué, J., Sancho, E., and Batlle, E. (2012) Dependency of colorectal cancer on a TGF-beta-driven program in stromal cells for metastasis initiation. *Cancer Cell* **22**, 571-584

529. Singh, A., Bodas, M., Wakabayashi, N., Bunz, F., and Biswal, S. (2010) Gain of Nrf2 function in non-small-cell lung cancer cells confers radioresistance. *Antioxidants & redox signaling* **13**, 1627-1637
530. Chen, W., Sun, Z., Wang, X. J., Jiang, T., Huang, Z., Fang, D., and Zhang, D. D. (2009) Direct interaction between Nrf2 and p21(Cip1/WAF1) upregulates the Nrf2-mediated antioxidant response. *Mol Cell* **34**, 663-673
531. Vaupel, P. (2004) Tumor microenvironmental physiology and its implications for radiation oncology. *Semin Radiat Oncol* **14**, 198-206
532. Jullien-Flores, V., Dorseuil, O., Romero, F., Letourneur, F., Saragosti, S., Berger, R., Tavitian, A., Gacon, G., and Camonis, J. H. (1995) Bridging Ral GTPase to Rho pathways. RLIP76, a Ral effector with CDC42/Rac GTPase-activating protein activity. *J Biol Chem* **270**, 22473-22477
533. Li, H., Zhao, Z., Wei, G., Yan, L., Wang, D., Zhang, H., Sandusky, G. E., Turk, J., and Xu, Y. (2010) Group VIA phospholipase A2 in both host and tumor cells is involved in ovarian cancer development. *FASEB J* **24**, 4103-4116
534. Maceyka, M., Milstien, S., and Spiegel, S. (2009) Sphingosine-1-phosphate: the Swiss army knife of sphingolipid signaling. *J Lipid Res* **50 Suppl**, S272-276
535. Scherer, M., Schmitz, G., and Liebisch, G. (2009) High-throughput analysis of sphingosine 1-phosphate, sphinganine 1-phosphate, and lysophosphatidic acid in plasma samples by liquid chromatography-tandem mass spectrometry. *Clin Chem* **55**, 1218-1222
536. <http://ClinicalTrials.gov/show/NCT01766817> Safety and Efficacy of a Lysophosphatidic Acid Receptor Antagonist in Idiopathic Pulmonary Fibrosis.
537. <http://ClinicalTrials.gov/show/NCT01651143> Proof of Biological Activity of SAR100842 in Systemic Sclerosis.
538. <http://ClinicalTrials.gov/show/NCT01762033> A Phase 2 Study of ASONEP™ to Treat Unresectable and Refractory Renal Cell Carcinoma.

539. <http://ClinicalTrials.gov/show/NCT01414153> Efficacy and Safety Study of iSONEP With & Without Lucentis/Avastin/Eylea to Treat Wet AMD.
540. Berndt, N., Hamilton, A. D., and Sebti, S. M. (2011) Targeting protein prenylation for cancer therapy. *Nat Rev Cancer* **11**, 775-791
541. Zhang, F. L., and Casey, P. J. (1996) Protein prenylation: molecular mechanisms and functional consequences. *Annu Rev Biochem* **65**, 241-269
542. Maurer-Stroh, S., Washietl, S., and Eisenhaber, F. (2003) Protein prenyltransferases. *Genome Biol* **4**, 212
543. Fukunaga, K., Arita, M., Takahashi, M., Morris, A. J., Pfeffer, M., and Levy, B. D. (2006) Identification and functional characterization of a presqualene diphosphate phosphatase. *J Biol Chem* **281**, 9490-9497
544. Faulkner, A., Chen, X., Rush, J., Horazdovsky, B., Waechter, C. J., Carman, G. M., and Sternweis, P. C. (1999) The LPP1 and DPP1 gene products account for most of the isoprenoid phosphate phosphatase activities in *Saccharomyces cerevisiae*. *J Biol Chem* **274**, 14831-14837
545. Barila, D., Plateroti, M., Nobili, F., Muda, A. O., Xie, Y., Morimoto, T., and Perozzi, G. (1996) The Dri 42 gene, whose expression is up-regulated during epithelial differentiation, encodes a novel endoplasmic reticulum resident transmembrane protein. *J Biol Chem* **271**, 29928-29936
546. Tong, H., Holstein, S. A., and Hohl, R. J. (2005) Simultaneous determination of farnesyl and geranylgeranyl pyrophosphate levels in cultured cells. *Anal Biochem* **336**, 51-59
547. Troutman, J. M., Roberts, M. J., Andres, D. A., and Spielmann, H. P. (2005) Tools to analyze protein farnesylation in cells. *Bioconjug Chem* **16**, 1209-1217
548. Escalante-Alcalde, D., Sanchez-Sanchez, R., and Stewart, C. L. (2007) Generation of a conditional Ppap2b/Lpp3 null allele. *Genesis* **45**, 465-469
549. Miriyala, S., Subramanian, T., Panchatcharam, M., Ren, H., McDermott, M. I., Sunkara, M., Drennan, T., Smyth, S. S., Spielmann, H. P., and Morris, A. J. (2010) Functional characterization of the

atypical integral membrane lipid phosphatase PDP1/PPAPDC2 identifies a pathway for interconversion of isoprenols and isoprenoid phosphates in mammalian cells. *J Biol Chem* **285**, 13918-13929

550. Onono, F., Subramanian, T., Sunkara, M., Subramanian, K. L., Spielmann, H. P., and Morris, A. J. (2013) Efficient use of exogenous isoprenols for protein isoprenylation by MDA-MB-231 cells is regulated independently of the mevalonate pathway. *J Biol Chem* **288**, 27444-27455

## **APPENDIX – Effects of lipid phosphate phosphatases on prenylation of proteins.**

### **A1. INTRODUCTION**

Prenylation of proteins is a common post-translational modification. Prenylation of proteins can result in profound effects such as increased cell migration, trafficking, survival and proliferation. Targeting protein prenylation has hence been suggested as a potential strategy in cancer-treatment (540). Prenylation occurs by addition of either a farnesyl- or geranylgeranyl- or both- functional groups to the protein. Prenyl-modifications occurs at the cysteine residue of proteins with a CAAX motif by the action of farnesyltransferase (FTase) or two geranylgeranyltransferases (GGTase1/2) (541). FTase adds a 15-carbon farnesyl group to the CAAX motif, where A is any aliphatic amino acid and X is C, S, Q, A, M, T, H, V, N, F, G, or I. GGTase 1 adds a 20-carbon geranylgeranyl group to the CAAX, where X is L, F, I, V, or M. GGTase 2, which is specific for the small GTPase Rab, does not have a stringent amino acid requirement like the other two prenyl transferases. However, it may require protein-protein interactions to access its motif (542).

Farnesyl pyrophosphate (FPP) is a major intermediate in the mevalonate pathway, which leads to synthesis of important cellular components such as cholesterol, dolicholpyrophosphate and steroid hormones. The mevalonate pathway generates isoprenoid precursors, which are then incorporated into proteins as farnesyl- or geranylgeranyl-modifications (Fig. A1). Statins are a broad class of compounds, which target this pathway by inhibiting the rate limiting step catalyzed by HMG-CoA reductase. Statins can thus decrease the synthesis of cholesterol and other complex derivatives of the

mevalonate pathway. Statins also decrease FPP and GGPP concentrations in cells resulting in decreased prenylation of proteins such as the small GTPases, Rho, Rac and Cdc42. Thus, statins have been suggested to have potentially beneficial effects in cancer (540).

A synthetic pathway for accumulation of isoprenoids in the cell involves the alcohol-derivates of the isoprenoids, farnesol (FOH) and geranylgeraniol (GGOH). Treatment of cells with FOH/GGOH results in conversion of these alcohols into FPP/GGPP and then incorporation into proteins. The existence of this pathway led to the search for potential kinases and phosphatases which regulate their inter-conversion in the cell. However, the biological relevance of this pathway has not been validated *in vivo* (Fig. A1).

LPPs are broad specificity lipid phosphatases, which were shown by our group to dephosphorylate FPP and GGPP in cell extracts (177). A previous study by our group found increased accumulation of monophosphates and alcohol-derivatives of FPP and GGPP by LPP1-overexpressing cellular fractions (Mataya C.M., unpublished). A presqualene diphosphate phosphatase, which shares consensus sequence with LPPs, showed phosphatase activity towards FPP *in vitro* (543). In yeast, the dolichol pyrophosphatase 1 (DPP1) and lipid phosphate phosphatase 1 (LPP1) account for most of the isoprenoid pyrophosphatase activity. A double knockout of LPP1 and DPP1 depletes cellular isoprenoids in yeast (544). However, there has been no direct demonstration of lipid phosphatase activity against FPP/GGPP in higher eukaryotes so far.

LPPs are localized with their catalytic site facing the lumen of ER or outside the plasma membrane based on predicted topology models (189) and experimental evidence



from the rat homolog Dri 42 (545) (Fig. A1.2). The predicted extracellular-facing catalytic site localization pattern may prevent it from accessing lipids such as FPP/GGPP. This discrepancy is usually explained by flipping of the lipid substrates spontaneously across the membranes. Alternately, these lipids could flip across the membranes by assistance from transporters. Several studies have demonstrated a role for LPPs in decreasing intracellular lipids such as S1P, LPA and PA (Reviewed in (189)). We hypothesized that LPP1 will decrease FPP/GGPP levels in the cell and decrease the isoprenylation of proteins.

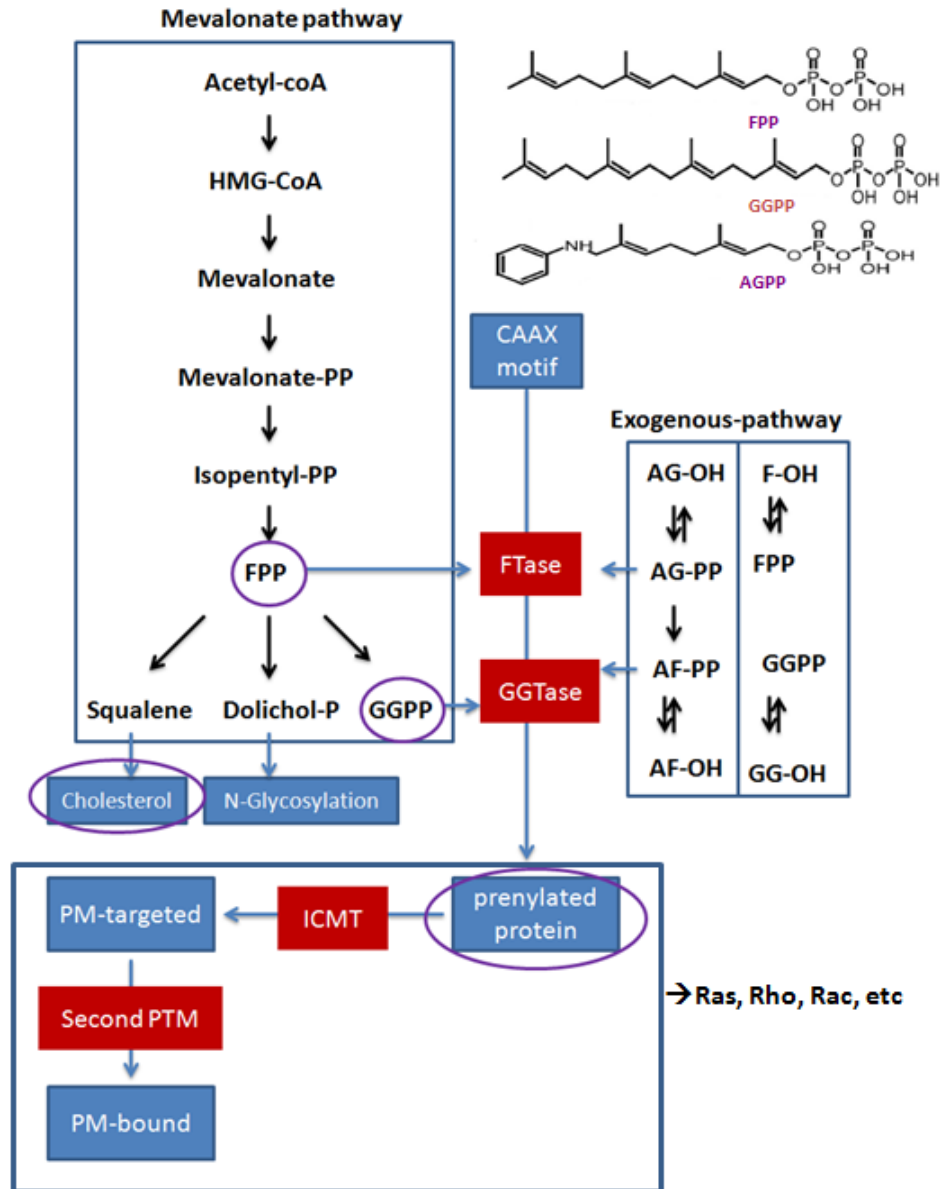


**Figure A1.1 - Illustration of the mevalonate pathway and exogenous pathway resulting in increased prenyl-modification of proteins:** The mevalonate pathway results in production of important lipids such as cholesterol, dolicholpyrophosphate or isoprenoid pyrophosphates, which have important structural and functional roles in the cell. FPP or synthetic AGPP can farnesylate proteins with the CAAX motif by the action of FTase. GGPP or the synthetic AFPP can geranylgeranilate proteins at the CAAX motif by the action of GGTases. Both forms of prenylation are found in proteins such as K-Ras. These proteins are then subject to isoprenylcysteinemethyltransferases (ICMT) before they can be targeted to the plasma membrane (PM) and sequestered by a second post-translational modification (PTM).

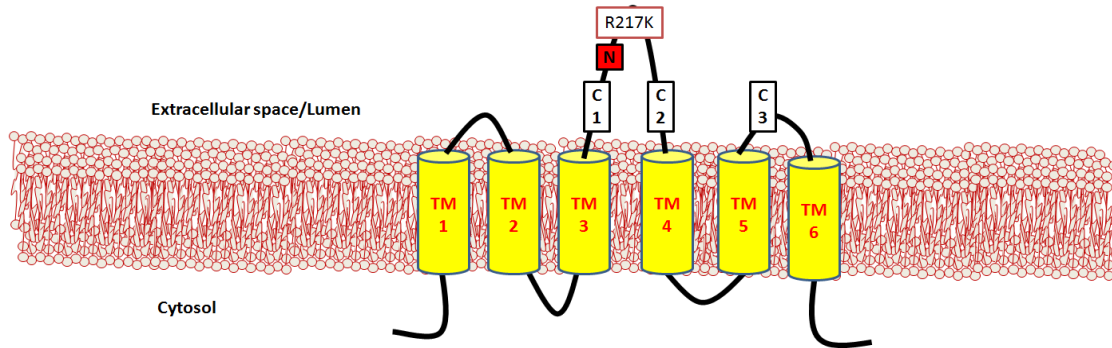


**Figure A1.2. Predicted membrane topology of LPP1 with active side facing the extracellular space/lumen** – The catalytically active site of the transmembrane protein, LPP1, is localized to the extracellular loops in the plasma membrane or ER lumen by predicted topology modeling and experimental evidence from the Rat homolog, Dri 42 (545). The glycosylation site (N), conserved domains (C1-C3) and the catalytically inactive mutant R217K are shown.

## A2. MATERIALS AND METHODS

### A2.1 Determination of FPP/GGPP levels in breast cancer cells

The estimation method for FPP/GGPP was developed based on a method previously described by Tong *et al.*, (546). It is based on detection of farnesyl/geranylgeranyl-peptides generated by the enzymes FTase and GGTase-1 *in vitro* from extracted lipids. Dansylated peptides, which mimic farnesylation (GCVLS) or geranylgeranylation (GCVLL) were made by Alberta Peptide Institute (University of Alberta). Cancer cells were grown to 40-50% confluence before being treated with adenoviruses expressing wild-type LPP1 or R217K LPP1. Alternatively, they were treated with 100 nM of pooled siRNA against LPP1 (GE Dharmacon, Ottawa, ON) for up to 48 h. Twenty  $\mu$ M lovastatin (Merck, Montréal, QC) was added to a control dish. The cells were trypsinized, spun down and the pellet was washed with HBS. The pellet was redissolved in 1.5 ml of butan-

1-ol: 75 mM ammonium hydroxide: ethanol (1:1.25:2.75). This was transferred to polypropylene eppendorf tubes. The isoprenoids were extracted by placing the tubes in heater bath at 70°C for 30 min. The samples were spun down at 13000 rpm for 30 min at 4°C. The pellets were extracted once more as before and the supernatants were combined from both extractions and dried down in a stream of nitrogen at 50°C. The lipids were re-suspended in Tris-HCl assay buffer (50 mM Tris- HCl pH 8, containing 5 mM DTT, 5 mM MgCl<sub>2</sub>, 10 μM ZnCl<sub>2</sub>, 1.1% octyl-β-D-glucopyranoside) by washing them down on the side of the tubes. This extract was used immediately (recommended) or stored at -80°C for later use. GCVLS and GCVLL were added at 0.125 nmol each (prepared in 1.1% octylglucoside). GGTase-1 (800-1000 ng) and FTase (61-100 ng) (Jena Biosciences, Jena, Germany) were added to the reaction in the supplied buffer. Standards were prepared from 0-10 pmol of FPP and GGPF. The total reaction volume for standards and samples was 100 μl. The reaction was stopped by the addition of 40 μL of acetonitrile and 2.5 μL 20% HCl. Denatured proteins were removed by centrifugation at 2000 rpm for 30 min and the supernatant was analyzed. The reaction products were analyzed by HPLC system (Beckman Coulter, Mississauga, ON) equipped with a fluorescence detector. The sample analysis was performed in a C18-reverse phase column with a two solvent system as described previously (546). To normalize the results, a phospholipid phosphate assay was performed was performed on 1/10 of the solvent extract. However, a direct phosphate analysis of the cell lysates was not possible due to the presence of inorganic phosphates. One ml of methanol, 1 ml of chloroform and 0.9 ml of double distilled water was added to the dried down extract. The samples were mixed and centrifuged at 2,800 rpm for 15 min. The upper phase was almost completely

removed using vacuum suction and the bottom phase was re-extracted with chloroform and methanol. The interface between chloroform and aqueous phases contained all of the cell debris and other contaminants, which was not disturbed. The chloroform phase was dried down and analyzed by the organic phosphate assay. Briefly, the samples were heated with 50  $\mu$ l of perchloric acid for approximately 30 min. They were then cooled down; 278  $\mu$ l of double distilled water and 55  $\mu$ l of 2.5% ammonium molybdate was added and the samples were mixed well. Finally, 55  $\mu$ l of 10% freshly prepared ascorbic acid was added, mixed and the samples were heated in a water bath at 80°C for 15 min. 180  $\mu$ l of the reaction mixture was added to each well of a multi-well plate and absorbance was measured at 700 nm. A standard was prepared using glycerol-3-phosphate to calculate the phospholipid phosphate content of the samples.

## **A2.2. Anilinogeraniol labeling and detection of labeled proteins in breast cancer cells**

The structure of the farnesol analog, AGOH, is shown in Fig. A1.1. Cells were plated in 10-cm dishes. The medium were changed to serum containing medium and 25, 50, 100  $\mu$ M AGOH were added for 18 h or 36 h before collecting the cells. Cell lysates were immunoblotted (as described before (547)) with a mouse monoclonal antibody raised against anilinogeraniol (A gift from Dr. Andrew Morris and Dr. Peter Spielmann, University of Kentucky). A 50  $\mu$ M concentration was used in experiments, where LPP1 expression has been modified.

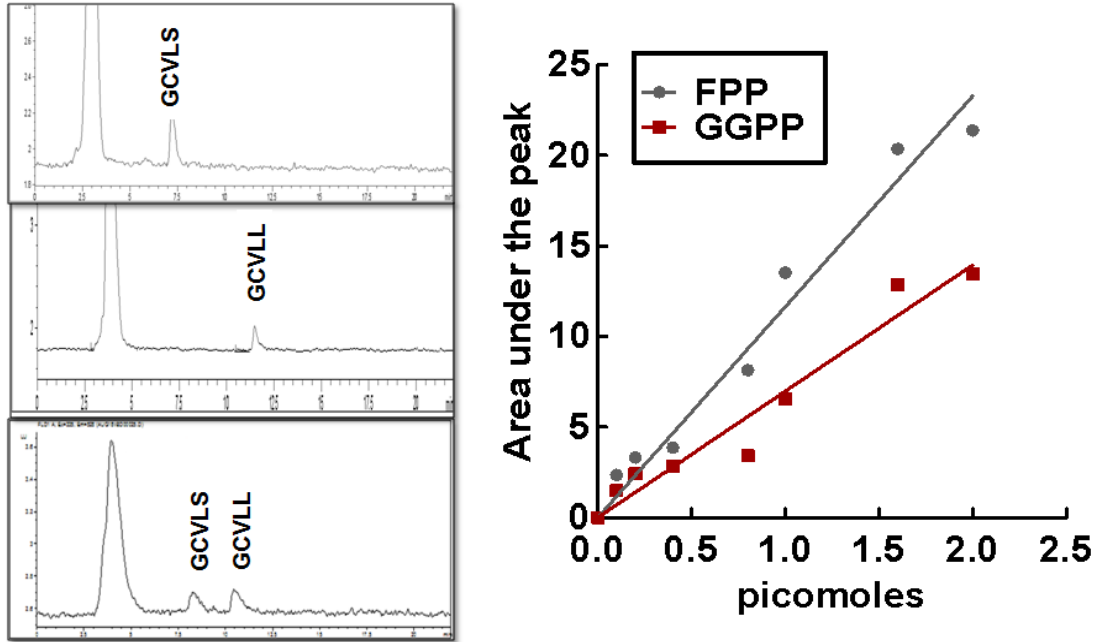


**Figure A2.1: Simultaneous detection of FPP and GGPP in breast cancer cells:** Representative histograms of HPLC showing detection of FPP (GCVLL) or GGPP (GCVLS) or simultaneously both. A standard peak of FPP/GGPP showing femtomolar detection was used to detect FPP/GGPP levels in breast cancer cells.

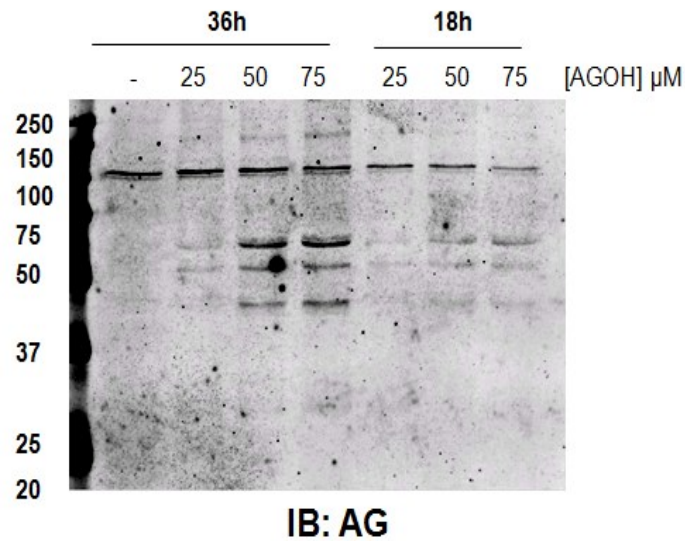


**Figure A2.2: Detection of AGOH incorporation in proteins by immunoblotting:** MDA-MB-231 cells were labeled with increasing concentrations of AGOH as described in the Materials and Methods. Fifty  $\mu\text{g}$  of lysate protein was immunoblotted with a mouse monoclonal antibody raised against anilinograninol (AG).

### **A2.3 Adenoviral overexpression, knockdown of LPP1 and determination of LPP activity**

To overexpress LPP1 using adenovirus, cells were plated in 10-cm dishes. When they were nearly 50% confluent they were treated with adenovirus expressing empty vector, R217K LPP1 or WT LPP1 in serum-containing medium (185). The MOI used for infections were 25, 50, and 100. The virus was diluted into 1 ml of serum-containing medium which is just enough to cover the 10-cm dish. Inoculums were left for 12 h and then dishes were washed free of capsid coats and fresh serum-containing medium was added and the dishes were incubated for further 36 h. 36-48 h incubation increased the gene expression significantly.

To knockdown LPP1 using siRNAs, cells were plated in 10-cm dishes and allowed to grow overnight. The medium in the dishes were then changed to antibiotic free medium and left for further 6-8 h. When the cells were nearly 50% confluent they were transfected with 100 nM of mixed smart pool siRNA against hLPP1 (Dharmacon GE). Cells were grown on OPTI-MEM medium containing siRNA–lipofectamine complex for 12 h. Now the medium was changed to serum-containing medium and the dishes containing cells were incubated for another 36 h before proceeding with subsequent analysis.

To determine LPP activity, cell lysates were sonicated on ice for 10-15 s. A 100 µl reaction was performed in 3 different protein concentrations with 60 µl diluted sample (protein concentration ranging from 0 – 10 µg), 20 µl of 5x Tris-buffer (500 mM Tris-

HCl pH 6.5, 10 mg/ml BSA, 30 mM N-ethylmaleimide) and 20  $\mu$ l of the LPP substrate (3 mM PA, 1.36  $\mu$ Ci/ml [ $^3$ H]PA in 2.5% TritonX-100). The samples were immediately mixed and placed in 37 $^{\circ}$ C incubator for 60 min while keeping the assay time constant among tubes. The reaction was stopped by adding 2.2 ml of chloroform/methanol (19:1 v/v) containing 0.08 % olive oil) and one scoop (~1 g) of dry aluminum oxide and the tubes were mixed well. The tubes were centrifuged at 2000 rpm for 5 min. One ml of supernatant was transferred to a scintillation vial, the chloroform was allowed to evaporate and 2 ml of scintillation fluid added. The samples were vortexed well and then radioactivity was determined in a scintillation counter.

#### **A2.4. Cholesterol estimation**

Cancer cells were grown in 10-cm dishes for up to 50% confluence before the medium was removed and replaced with starvation medium with or without 20  $\mu$ M lovastatin. The dishes were washed twice in HBS and the cells were collected twice in 1 ml methanol and extracted with 2 ml chloroform and 1.8 ml of 0.1 M HCl/ 2 M KCl in Fisher glass tubes. The samples were vortexed and centrifuged at 2,800 rpm for 15 min. The upper phase was removed and 1.6 ml of organic phase was dried under a stream of nitrogen. The samples were then resuspended in 200  $\mu$ l chloroform, which was washed down into the tubes, and dried again. Next, they were resuspended in 100  $\mu$ l of propan-1-ol. The total assay volume was 500  $\mu$ L in an Eppendorf tube (40  $\mu$ l sample/standard and 460  $\mu$ l color development solution), which was used to provide duplicates of 200  $\mu$ L in a 96-well plate. The assay is based on conversion of free and esterified cholesterol into its oxidized form and hydrogen peroxide. Hydrogen peroxide is then detected by a



colorimetric reaction at 700 nm. The samples were incubated until color was developed as described in the kit (Cholesterol C2 assay kit WAKO). Standard cholesterol solutions were prepared by diluting the cholesterol stock solution in propan-1-ol.

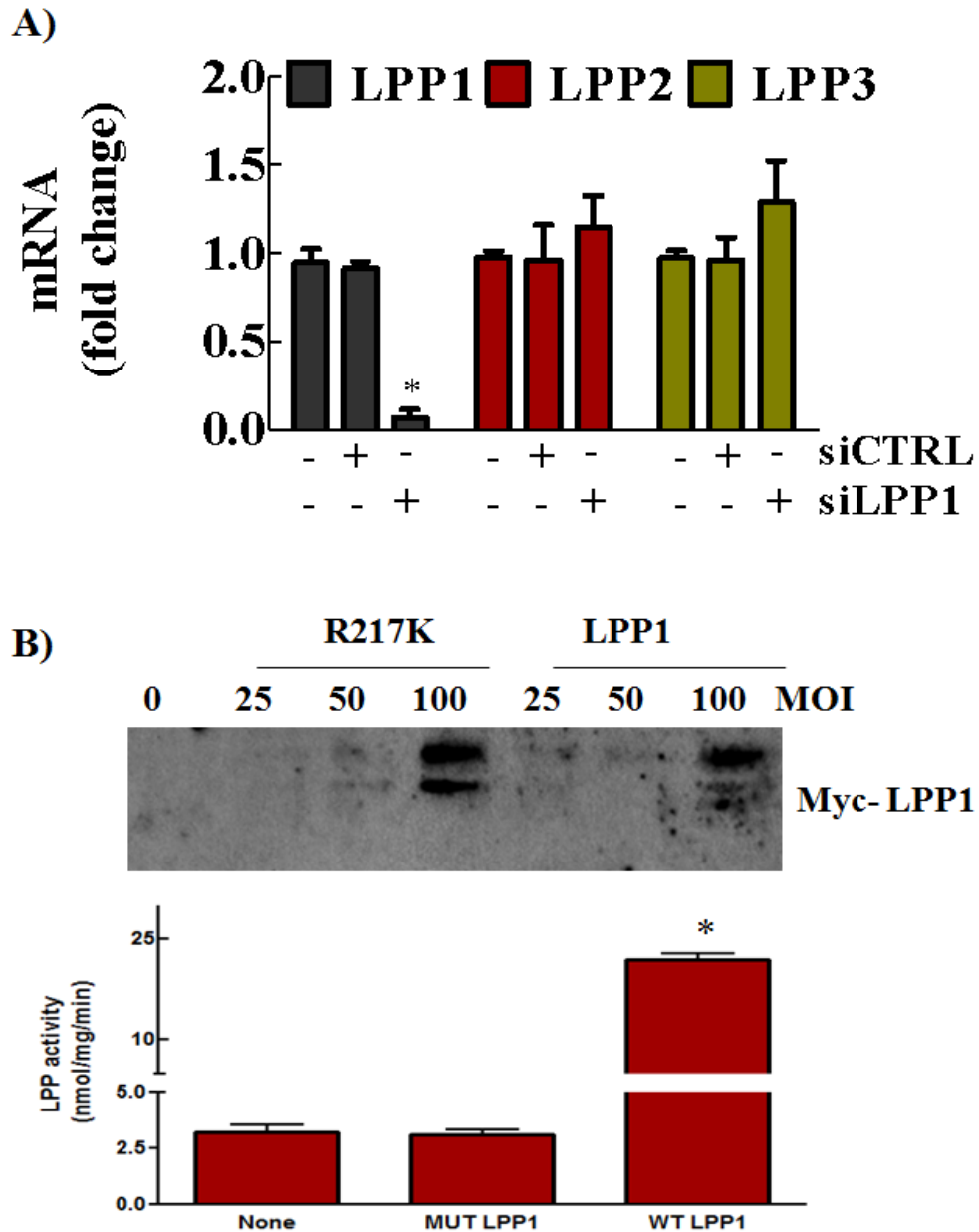


**Figure A2.3: LPP1 overexpression and knockdown:** A) siRNA knockdown of LPP1 in MDA-MB-231 cells, B) Adenoviral overexpression of LPP1 in MDA-MB-231 - Immunoblot showing adenoviral expression of R217K or WT LPP1 infected at 25, 50 and 100 MOI (top panel). Increase in total LPP activity from adenoviral overexpression of WT and not R217K LPP1 is shown below (bottom panel).

### **A2.5. Extraction of isoprenoids from cultured cells for estimation of prenylcysteines by LC-MS**

The isoprenoid extractions were performed as before with some modifications. Cells grown in 10-cm dishes were extracted with 5 ml of butan-1-ol: 75 mM ammonium hydroxide: ethanol (1:1.25:2.75). The extracts containing cell lysates were transferred to screw-capped 8 ml glass tubes containing 50 pmol of D5 AGPP and an additional 1 ml of butan-1-ol: 75 mM ammonium hydroxide: ethanol (1:1.25:2.75) was added. Samples were vortexed for 5 min; tubes were placed in heater block at 70°C for 20 min and vortexed again. The samples were centrifuged to pellet debris and the supernatant was transferred to another 8 ml glass tube. The pellet was then re-extracted in 5 ml of butan-1-ol: 75 mM ammonium hydroxide: ethanol (1:1.25:2.75) and the supernatant was transferred to the 8 ml glass tube with the original extract. At this point the samples were shipped in dry ice for LC-MS analysis. Briefly, the proteins were extracted from the samples by acetonitrile precipitation before sampling it in LC-MS. Subsequent analysis was performed by Dr. Frederick Onono in Dr. Andrew Morris's laboratory, University of Kentucky.

### **A3. RESULTS**

We initially estimated cholesterol levels in rat fibroblasts stably expressing R217K or WT LPP1 (185). LPP1 overexpression did not affect cholesterol synthesis. However, the HMG-CoA reductase inhibitor lovastatin decreased the cholesterol content by about 50% (Fig. A3.1).

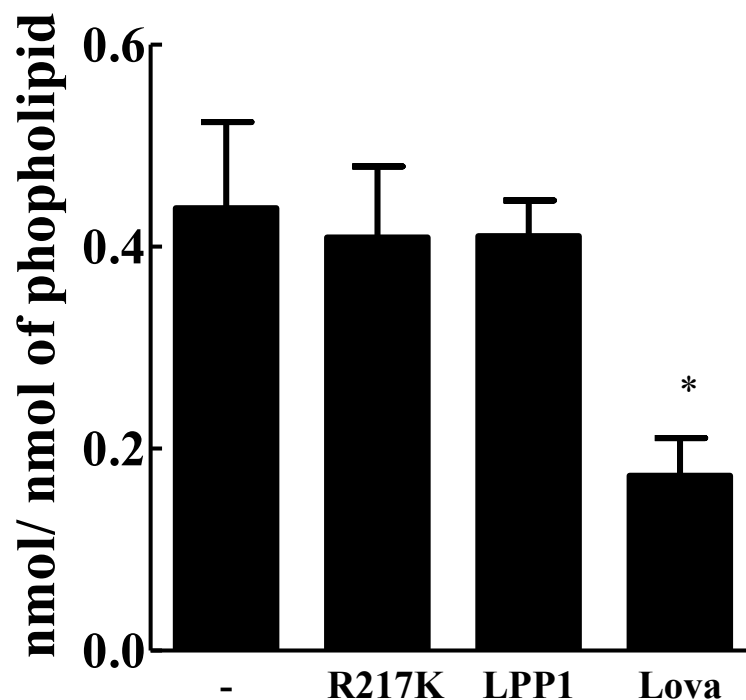


**Figure A3.1. LPP1 does not affect cellular cholesterol levels** – Cholesterol was estimated in MDA-MB-231 cells overexpressing catalytically active (LPP1) or inactive LPP1 (R217K) as described in the Materials and Methods Section. Lovastatin (Lova) decreased cholesterol accumulation in the cell. n=6. Results are expressed as mean  $\pm$  SEM. \* p<0.05.

We next estimated the effects of LPP1 directly on FPP/GGPP levels of breast cancer cells as described in the Materials and Methods Section (Fig. A2.1). Adenoviral overexpression of LPP1 increased the expression of LPP1 mRNA, protein and total LPP activity (Fig. A2.3). However, it did not affect the levels of FPP/GGPP in either MDA-MB-231 breast cancer or U87 glioblastoma cell line, which express higher FPP/GGPP levels (Fig. A3.2). We also assessed the levels of FPP/GGPP in mouse embryonic fibroblasts from LPP1<sup>-/-</sup> (139) or LPP3<sup>-/-</sup> (548) mice (Gifts from Dr. Kevin Lynch and Dr. Diana Escalante-Alcalde, respectively). Here again, there was no differences in the expression of FPP/GGPP between WT and KO MEFs (Fig. A3.3).

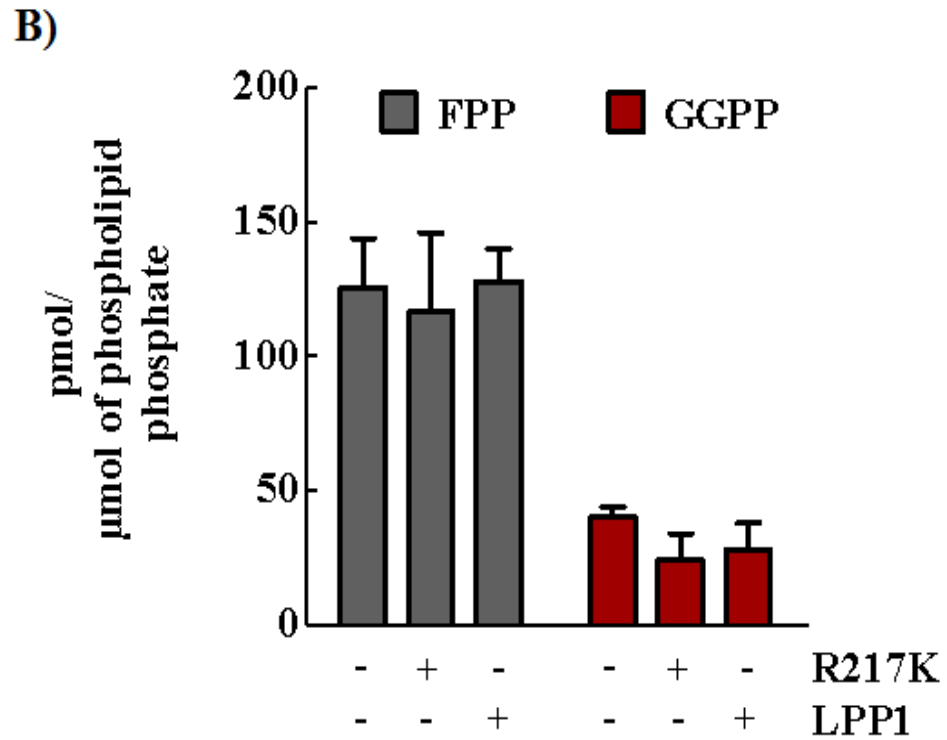
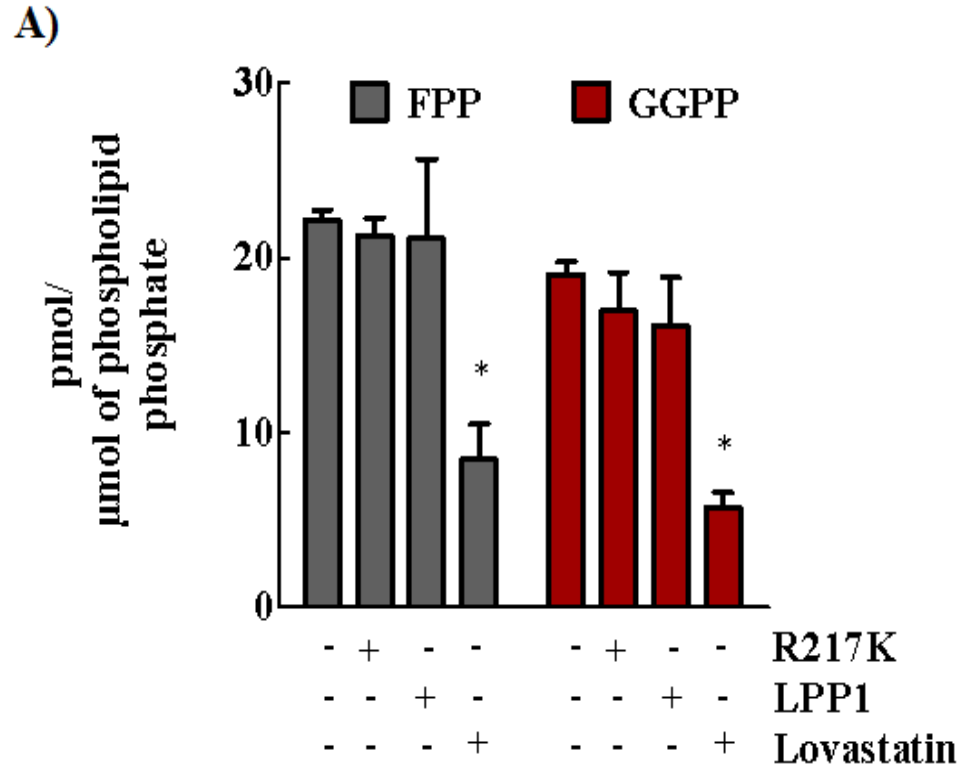


**Figure A3.2. LPP1 does not affect FPP/GGPP levels in breast cancer or glioblastoma –** FPP/GGPP levels were estimated as described in the Materials and Methods in MDA-MB-231 (A) and U87 cells (B). n=3. Results are expressed as mean  $\pm$  SEM. \* p<0.05.

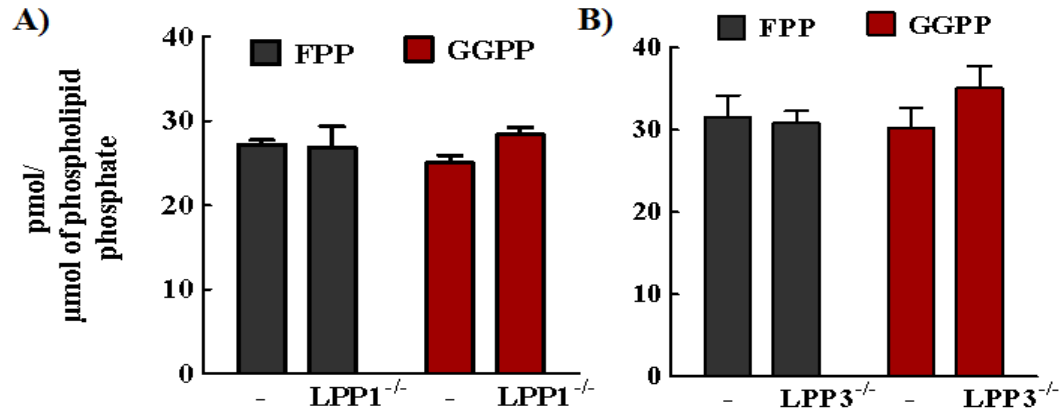


**Figure A3.3. Genetic ablation of LPP1 or LPP3 does not affect FPP/GGPP levels in the cell** – FPP/GGPP levels were estimated as described in Materials and Methods in HET or LPP1<sup>-/-</sup> MEFs (A) or in PMEF E1A<sup>tr/tr</sup> or PMEF LPP3<sup>-/-</sup> (B).

We next measured the effect of LPPs on prenylation of proteins indirectly by labeling the cells with a farnesol analog, anilino geraniol (AGO) (Fig. A2.2). LPP1 overexpression only marginally increased the incorporation of AGPP in proteins as detected by immunoblotting with an antibody raised against the synthetic analog (Fig. A3.4). However, we did not detect the low molecular proteins, such as the small GTPases, by this method.

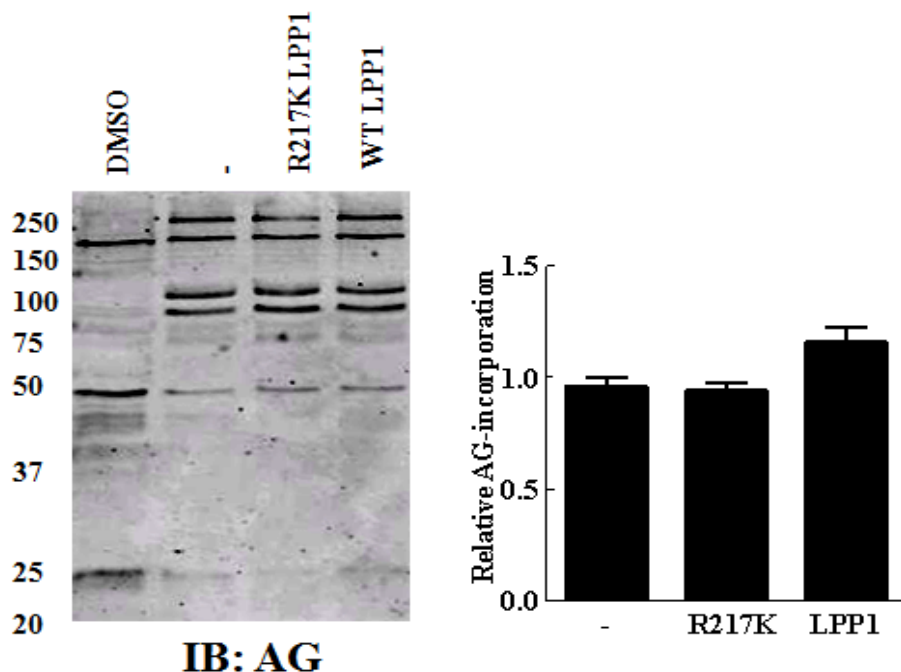


**Figure A3.4. LPP1 does not affect anilino geraniol incorporation into proteins** – MDA-MB-231 cells labeled with AGOH were immunoblotted for proteins incorporating the farnesyl-analog with an AG antibody as described in the Materials and Methods Section. The quantification of total changes in protein-labeling is shown in the right panel.

Next, we decided to employ a sensitive LC-MS method to detect prenylcysteines directly. In LPP1 overexpressing fibroblasts, prenylcysteines were slightly elevated. In LPP1<sup>-/-</sup> or LPP3<sup>-/-</sup> MEFs prenylcysteines were low or undetectable compared to their controls (Fig. A3.5).

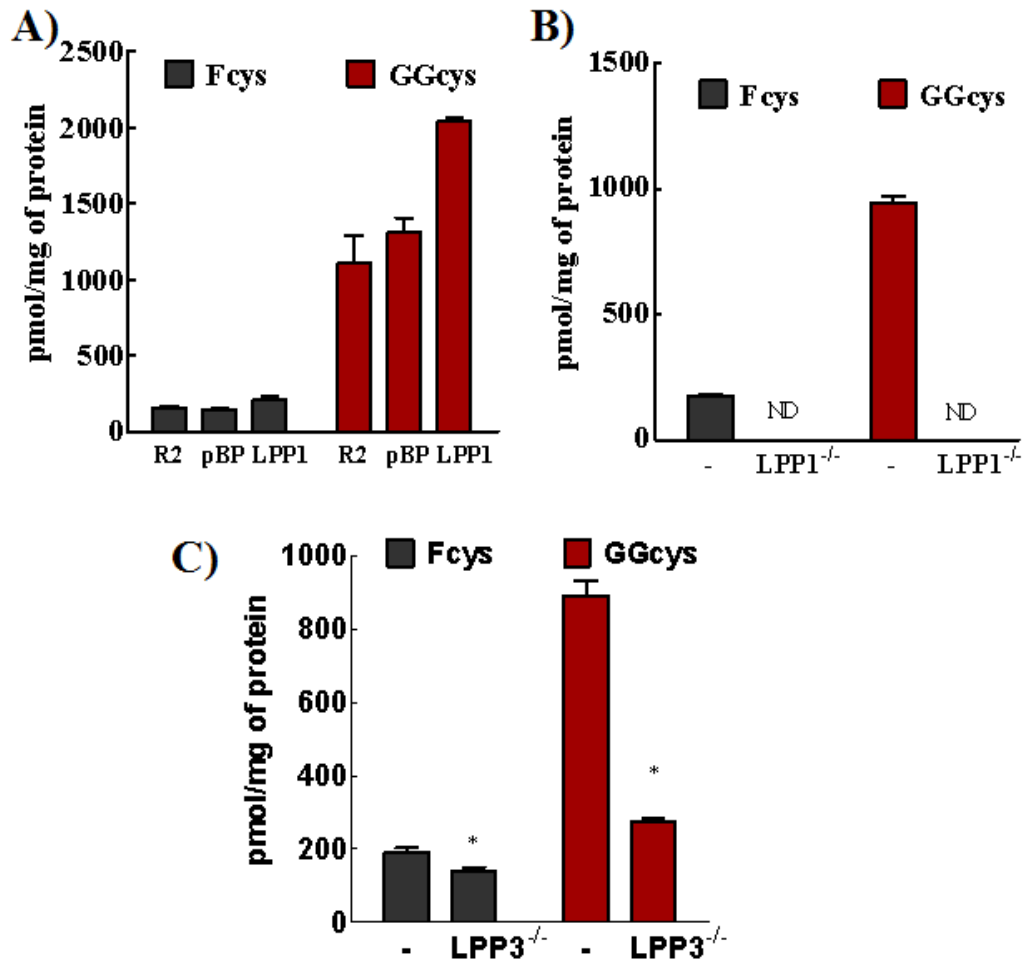


**Figure A3.5. LPP1<sup>-/-</sup> or LPP3<sup>-/-</sup> MEFs show decreased levels of prenylcysteines** – Prenyl cysteine extractions were performed in Rat2 fibroblasts overexpressing LPP1 (A) or in LPP1<sup>-/-</sup> (B) and LPP3<sup>-/-</sup> MEFs (C) as described in the Materials and Methods Section. The levels of prenylcysteines were determined by Dr. Frederick Onono in Dr. Andrew Morris's laboratory, University of Kentucky by LC-MS using D5-AGPP as internal standard (Method described in (549)).

#### **A4. DISCUSSION AND FUTURE DIRECTIONS**

I devoted a lot of time in my training to develop a successful and sensitive method to study the levels of FPP/GGPP in breast cancer cells. The technique is robust enough to determine the levels of isoprenoids simultaneously in a large sample set relatively quickly. We modified LPP1 activity to determine if LPP1 could act as a cellular isoprenoids phosphatase. Unfortunately, modifying LPP1 activity did not affect the cellular isoprenoid levels or the incorporation of synthetic analogs into proteins. However, the HMG-CoA reductase inhibitor decreased FPP/GGPP levels in serum starved cells. One possibility is that our levels of overexpression/knockdown were not sufficient or not active but we demonstrate a near complete knockdown of LPP1 and 8-fold increases in total LPP activity suggesting that this is unlikely. We could not detect low molecular weight farnesylated proteins by labeling with synthetic analog of FPP. We collaborated with another group in University of Kentucky to determine if LPPs could regulate isoprenylation of proteins by directly determining the isoprenylcysteines extracted from cells. Here, unexpectedly LPP1<sup>-/-</sup> or LPP3<sup>-/-</sup> MEFs show decreased levels of protein prenylation. This could be an adaptation of LPP1/3<sup>-/-</sup> MEFs to regulate growth factor signaling in the absence of LPPs.

Studies done since we began this work has suggested another lipid phosphatase with homology to LPP1, the atypical PDP1/PPPAPDC2, can dephosphorylate isoprenoids in cells. This was suggested based on their deleterious effects of PDP1 overexpression in the cell, predicted topology facing cytosol and indirect demonstration of phosphatase activity based on reduced levels of accumulation of the synthetic analog of FPP (549). It is not clear if these effects were simply due to decreased cellular



accumulation of AGOH since AG-modified proteins could not be detected even at 48 h in PDP1-expressing cells. The contribution of PDP1 to cholesterol synthesis and presqualenediphosphate synthase on the cellular effects was not determined. Further the expression levels and the relevance of PDP1 in higher eukaryotes needs to be demonstrated. Incorporation of prenyl-analogs by the exogenous pathway was shown to suppress the cellular mevalonate pathway of prenylation (550). This suggests that there are significant differences in the way such artificial substrates are utilized by the cell, which may not represent actual cellular modification of isoprenoids. In the future, we will need to establish if LPP1 and LPP3 are involved in prenylation of proteins. Also the role of LPP2 needs to be determined. Finally, the PPPAPDC family members need to be investigated to determine if they are physiological regulators of prenylation.